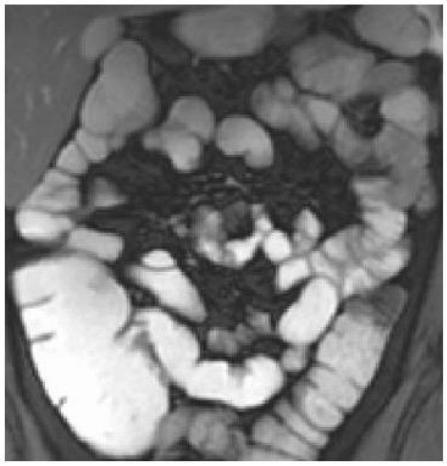

# Small bowel motility Quantitation using MRI and its relationship to gastrointestinal symptoms

Ruaridh M Gollifer

Centre for Medical Imaging

University College London (UCL)

A thesis submitted to University College London for the degree of Doctor of Philosophy.

2019

I, Ruaridh Gollifer, confirm that the work presented in this thesis is my own. Where information has been derived from other sources, I confirm that this has been indicated in the thesis.

# Abstract

The small bowel is difficult to analyse due to its deep anatomical location and the large variation seen in individuals, in regard to both anatomy and function including motility.

Dynamic MRI allows small bowel motility to be captured and visually assessed by radiologists, but there is often large inter-observer variation and a lack of complicated motility patterns being investigated. This thesis aims to explore the link between abnormal motility and gastrointestinal (GI) symptoms in Crohn's disease (CD) and irritable bowel syndrome (IBS) using MRI.

Firstly, a scan duration of 15 seconds and a temporal resolution of 1 image per second were shown to be sufficient for robust small bowel MRI motility measurements. Next, a validation study confirmed an association between aberrant motility and CD patient symptoms, particularly diarrhoeal stools (rho = -0.29). The strongest association was in patients with higher symptom severity (rho = -0.633).

Building on this work, more complex motility metrics were developed and compared to subjective radiological scoring. Spatial and temporal variation were found to be associated with CD patient symptoms and were also particularly difficult to visually assess.

The motility metrics were applied in clinical IBS data to explore differences in IBS subgroups. Significantly reduced temporal variation of motility ($P < 0.001$) and area of motile bowel ($P < 0.001$) was found in IBS-C (constipation-predominant) compared to IBS-M (mixed constipation and diarrhoea).

Finally, texture analysis (TA) terminal ileum (TI) to colon ratios were found to be higher for TA contrast ($P = 0.005$) and lower for TA energy ($P = 0.03$) in IBS-C compared to healthy controls (HCs). Ascending colon diameter was shown to be significantly larger in IBS-C than HCs ($P = 0.005$).

# Impact Statement

Crohn's disease (CD) is a lifelong chronic inflammatory bowel disease, affecting around 1 in 30,000 people. It often occurs relatively early in life, leading to lifelong medication, surgery and a decreased quality of life. Irritable bowel syndrome (IBS) is a condition characterised by a range of gastrointestinal (GI) symptoms such as abdominal pain or discomfort, bloating, constipation and diarrhoea. The prevalence of IBS is up to 20% of the population in many western countries and makes up to a third of the gastroenterologists' clinical workload in the UK.

In both conditions, quality of life is a major issue. In CD symptoms often persist even when there are only low levels of inflammation present while in IBS, conventional tests are normal, and it is a diagnosis of exclusion. The work in this thesis has been presented in conferences and several papers have been published which has increased the interest and the awareness of quantitative dynamic MRI as a technique for assessing motility. MRI offers advantages over traditional motility analysis techniques with improved patient acceptability and potentially more easily interpreted results.

The impact of this work is yet to translate fully into the clinic, however there are many interesting findings which could be investigated further. The underlying software being utilised is a major component of a healthcare start-up company, Motilent. One of the company's aim is to integrate the technology into the clinical workflow. They will start the first prospective use of the product in the clinical setting in patients who have undergone small bowel motility MRI over the next 12 months. In the clinic, radiologists subjectively grade motility in a binary "on" or "off" fashion. Building on the work of Motilent, quantitative metrics have been developed here for motility patterns which are difficult to visually assess. These metrics have shown improvements over visual scoring of motility as they are repeatable and have been shown to be associated with abdominal symptoms in

Crohn’s disease and IBS. Therefore, it is possible that a non-invasive MRI assessment of motility will enhance the understanding of the underlying physiology of symptoms, in many different GI conditions, and this will impact clinical decision making. There is the potential for future drug development and therapy for treatment and management of GI symptoms.

Within academia, there has been interest in the initial MRI findings with both motility and texture analysis used to demonstrate differences between IBS patients and healthy controls. This work was awarded with the summa cum laude award at the largest international MRI conference, International Society for Magnetic Resonance in Medicine (ISMRM). This shows the high level of interest in this work in terms of technical analysis within a clinical context. In the future, for the IBS work, a larger repeatability study is necessary to give insight into how clinically applicable these motility and texture analysis measures would be in multiple sites. If successful, it could potentially lead to an explanation for the link between abnormal motility patterns and symptoms in IBS to guide future clinical treatment.

# Acknowledgements

First, I would like to thank David Atkinson, who has provided me with constant guidance and support throughout this project. He has greatly helped me develop as a researcher, through providing crucial technical input, always presented in a balanced and thoughtful way, as well as invaluable career development advice. I would also like to thank Stuart Taylor, who has been supportive throughout and has provided vital clinical insight, which has provided a strong clinical direction for the project and has enhanced my understanding of the clinical issues that need to be addressed in the field.

I would also like to give a special mention to my work colleague and collaborator, Alex Menys who has been a driving force in the area of bowel motility research, both as a researcher and through his company Motilent.  He has been invaluable in sharing his knowledge with me and has greatly supported me with this project. I had the opportunity to do paid work for Motilent, to gain experience outside of my PhD, and Motilent has also funded me to attend the Federation of Neurogastroenterology and Motility conference in Amsterdam in 2018. David, Stuart and Alex have constantly been available to respond to email queries, provide feedback on analysis and help with the editing of papers. I am grateful to all of them and could not have asked for better mentors.

Alex has also been instrumental in facilitating collaborations with clinicians and researchers in the field of bowel motility research, especially Sofieke de Jonge who I worked closely with for the work in chapter 3. Her enthusiasm and dedication made the collaboration extremely productive and enjoyable. I would like to thank the collaborators who have helped me throughout my PhD, including Aart Nederveen, Jaap Stoker, Natalia Zarate-Lopez, Dave Chatoor, Anton Emmanuel and Sven Månsson. I would especially like to thank Andrew Plumb, who along with Stuart Taylor, visually graded bowel motility in over one hundred datasets, which was a key component of

the work in chapter 5 and the thesis overall, and Bodil Ohlsson, who funded a visit to Malmö for our collaboration which led to the work in chapter 6.

This work has been supported by the EPSRC-funded UCL Centre for Doctoral Training (CDT) in Medical Imaging (EP/L016478/1) and the Department of Health's NIHR-funded Biomedical Research Centre at (University College London Hospital). I would like to thank my friends from the CDT and from my department, CMI (Centre for Medical Imaging) for sharing the experience with me, particularly Lebina Kakkar, Rafat Chowdhury, Will Devine and Tim Bray, who have been encouraging throughout my time at CMI. I would also like to thank João Ramalhinho and Kyriaki (Rica) Mengoudi who I shared a flat with for the majority of my PhD. They were supportive of me and my work and an important part of the journey. Rica was also extremely helpful with her input on statistical design and as a co author for the work in chapter 5.

Finally, I am extremely grateful to my wonderful family (Mum, Dad and Kirsty), who have constantly supported me throughout my studies and have ensured the process has been as enjoyable as possible.

# Contents

# List of Figures

# List of Tables

# Thesis Overview

This thesis consists of eight chapters grouped into five sections outlined below. Each original research chapter (chapters 3-7) will contain an author declaration stating the contribution of the thesis author and collaborators and whether the work is published.

***Section A*** provides a literature review including the clinical background to the gastrointestinal (GI) tract, and the techniques involved in addressing the clinical problems presented in this field. In **Chapter 1**, the clinical aspect of Crohn's disease (CD) and irritable bowel syndrome (IBS) are described as well as the role of small bowel motility, in both health and disease, and the use of patient questionnaires used to record GI symptoms. Assessment of motility is described for techniques other than magnetic resonance imaging (MRI). In **Chapter 2**, the acquisition of dynamic MRI is described and there is a review of the techniques currently used to quantify small bowel motility using MR enterography, especially post-processing techniques involving dynamic MRI. Texture analysis measures used to analyse anatomical small bowel images are also described.

***Section B*** focuses on validating and testing previous assumptions related to dynamic MRI motility data. **Chapter 3** involves defining the optimum dynamic MRI protocol with joint research carried out with a collaborator from Academic Medical Center (AMC) in Amsterdam, which addresses questions about the necessary acquisition time and temporal resolution. **Chapter 4** looks at validating the inverse correlation, previously found in a single-centre study, between spatial variation of small bowel motility and symptoms in Crohn's disease patients. In this chapter, this observation is assessed in a larger, two-centre study.

***Section C*** builds on the work in section B and investigates the association of motility and distension features from dynamic MRI images with Crohn's disease symptoms. **Chapter 5** presents work testing the association between several motility metrics and abdominal symptoms in Crohn's disease using both radiologist subjective grading of motility and automated computer-based motility metrics. The intra- and inter-observer agreement for two radiologists subjectively grading dynamic MRI datasets is assessed.

***Section D*** explores the utility of the motility metrics, described in section C, and texture analysis summary measures, when applied to IBS patients. **Chapter 6** follows on from the CD work in chapter 5 by using the motility measures to explore differences in different IBS subgroups; constipation-predominant (IBS-C), diarrhoea-predominant (IBS-D) and mixed IBS (IBS-M), and healthy controls. Additionally, an association between several motility features and abdominal symptoms, recorded using IBS-Symptom Severity Score (IBS-SSS) questionnaires, was tested. **Chapter 7** investigates whether MRI can demonstrate differences in terminal ileum content and motility between constipation-predominant IBS (IBS-C) patients with bloating and healthy controls. Specifically, using computer-based motility metrics and texture analysis measures.

***Section E*** concludes the thesis with **Chapter 8** summarising key findings and outlining future potential research topics in the field.

## Peer-reviewed Journal Articles

CS de Jonge*, **RM Gollifer***, AJ Nederveen, D Atkinson, SA Taylor, J Stoker, A Menys. **"Dynamic MRI For Bowel Motility Imaging – How Fast And How Long?"** The British Journal of Radiology 2018 91:1088

*joint first co-authors

**RM Gollifer**, A Menys, J Makanyanga, CAJ Puylaert, FM Vos, J Stoker, D Atkinson, SA Taylor. **"Relationship between MRI quantified small bowel motility and abdominal symptoms in Crohn's disease patients—a validation study."** The British Journal of Radiology 2018 91:1089

**RM Gollifer**, A Menys, A Plumb, K Mengoudi, CAJ Puylaert, JAW Tielbeek, J Makanyanga CY Ponsioen, FM Vos, J Stoker, SA Taylor, D Atkinson. **"Automated vs Subjective assessment of spatial and temporal MRI small bowel motility in Crohn's disease."** Clinical Radiology 2019

## Peer-Reviewed Conference Abstracts

**R Gollifer**, A Menys, J Makanyanga, C Puylaert, F Vos, J Stoker, D Atkinson, S Taylor. **"Analysis of Motility in Apparently Normal Small Bowel–Relationship to Crohn's Symptoms."** Proceedings of the 25th meeting of the International Society for Magnetic Resonance in Medicine (ISMRM), Hawaii, USA (2017).

CS de Jonge*, **RM Gollifer***, AJ Nederveen, D Atkinson, SA Taylor, J Stoker, A Menys. **"Dynamic MRI For Bowel Motility Imaging – How Fast And How Long?"** Proceedings of the 25$^{th}$ meeting of ISMRM, Hawaii, USA (2017).

*joint first co-authors

**R Gollifer**, A Menys, A Plumb, FM Vos, J Stoker, SA Taylor, D Atkinson. **"Magnetic resonance imaging assessed small bowel dysmotility and its relationship with patient reported symptoms: An exploration of automated vs subjective assessment techniques."** The European Society of Neurogastroenterology and Motility (ESNM), Cork, Ireland (2017). Oral presentation (10-15 minutes Free Presentation).

**R Gollifer**, A Menys, A Plumb, F Vos, J Stoker, S Taylor, D Atkinson. **"MRI assessed small bowel dysmotility and its relationship with patient reported symptoms: An exploration of automated vs subjective assessment techniques."** Proceedings of the 26th meeting of ISMRM, Paris, France (2018).

**RM Gollifer**, A Menys, A Plumb, F Vos, J Stoker, D Atkinson, S Taylor. **"Intra- and inter-observer variability in visually graded small bowel motility features from dynamic MRI of Crohn's disease patients."** 29th Annual Meeting of European Society of Gastrointestinal Abdominal Radiology (ESGAR), Dublin, Ireland (2018). Oral presentation (6-8 minutes presentation).

**RM Gollifer**, A Menys, F Vos, J Stoker, D Atkinson, S Taylor. **"Slice-by-slice comparison of quantitative small bowel motility metrics from dynamic MRI in Crohn's disease patients with a range of symptom severities."** ESGAR, Dublin, Ireland (2018). Moderated poster session (5 minutes presentation)

**R Gollifer**, A Menys, N Zarate-Lopez, D Chatoor, A Emmanuel, S Taylor, D Atkinson. **"MRI assessed dysmotility and texture analysis in the terminal ileum and small bowel: A pilot study comparison between Irritable Bowel Syndrome (IBS) patients with bloating and healthy controls."** Proceedings of the 27th meeting of ISMRM, Montreal, Canada (2019). Oral presentation (Power Pitch)

**R Gollifer**, A Menys, S Månsson, P Leander, O Ekberg, S Taylor, D Atkinson, B Ohlsson. **"Comparison of MRI assessed small bowel dysmotility in Irritable Bowel Syndrome (IBS) and healthy controls."** ESNM, Lisbon, Portugal (2019).

# Section A: Background to small bowel motility and quantitative assessment using MRI

Small bowel motility is a series of coordinated contractile actions which facilitate the absorption of nutrients from food. The food has been ingested via the mouth and turned into chyme (a mixture of food and gastric juices), within the stomach, before entering the small bowel. Motility is controlled by the myenteric plexus (or so called “gut brain”), which acts in response to hormonal, dietary and neurological factors. This enables the chyme to move through the small bowel (due to peristalsis) to pass into the colon, while being broken down further during transit (due to segmentation).

Dynamic Magnetic Resonance Imaging (‘cine’ or dynamic MRI) allows visualisation and analysis of gastrointestinal (GI) tract motility. Several studies have demonstrated potential clinical applications of dynamic MRI in Crohn’s disease (CD) as well as in GI motility disorders and functional bowel disorders such as chronic intestinal pseudo-obstruction (CIPO), Ehlers-Danlos syndrome (Hypermobility type), functional constipation, postoperative ileus and irritable bowel syndrome (IBS), where motility is abnormal and altered compared to healthy subjects. The gut is also secondarily involved in Parkinson’s disease where altered motility precedes neurological symptoms by 10 years. The main advantages of MRI over other techniques such as manometry and scintigraphy are that dynamic MRI not only allows visualisation of the GI tract (both locally and globally), but is also non-invasive and does not impart ionising radiation.

Patients with dysmotility often experience GI symptoms such as pain, bloating, constipation and/or diarrhoea. Although such symptoms are subjective, there are several validated patient questionnaires which

are used to assess the severity of these symptoms. For example, the Harvey-Bradshaw Index (HBI) commonly used in Crohn's disease and specialised IBS symptom questionnaires such as IBS-SSS (SSS = Symptom Severity Score) and VAS-IBS (VAS = Visual Analogue Score) have been developed.

**Chapter 1** introduces the clinical background to Crohn's disease and irritable bowel syndrome as well as the role of motility of the small bowel, in both health and disease. The current usage and limitations of the non-MRI techniques used to assess motility are discussed. CD and IBS will be the focus of this thesis, specifically how motility is related to GI symptoms in these conditions. A brief summary of the patient questionnaires used to assess symptom severity are described.

**Chapter 2** introduces the principles of dynamic MRI acquisition followed by the post-processing techniques used to quantify small bowel motility. The focus is on the optic-flow registration of a 2D time series of images, used to generate an objective measure of motility, which is the basis of the majority of the analysis throughout this thesis. Finally, a brief overview of texture analysis is provided in the context of MRI as background for chapter 7.

# Chapter 1: Background and literature review of small bowel anatomy and physiology, non-MRI assessment of motility and symptoms questionnaires

## 1.1 Anatomy and Physiology

### 1.1.1 Anatomy of Small bowel and Colon in Health

The digestive or gastrointestinal (GI) tract consists of a series of hollow tubes/organs where ingested food travels from the mouth to the anus via the oesophagus, stomach, small intestine (or small bowel) and large intestine (or colon) [1].

The focus of this thesis will be the small bowel (SB) in the context of Crohn's disease (CD) and Irritable Bowel Syndrome (IBS), with the colon also briefly described in a study involving the ileocolic junction (chapter 7). The small bowel is on average 7m in length (but can range from 3-9m) and consists of three main parts starting with the **duodenum**, where food enters the SB from the stomach. The food bolus or chyme, i.e. the mixture of food and gastric juices from the stomach, then travels through the **jejunum** and lastly through the **ileum** (including terminal ileum) before entering the colon [1].

The terminal ileum is an important region of the small bowel as it is where Crohn's disease occurs most frequently (45% of CD located in the terminal ileum with 32% in the colon, 19% in the ileocolon and

4% in the upper gastrointestinal tract [2]) and where the food bolus is stored while the ileocecal sphincter is closed. The opening of the ileocecal sphincter is coordinated with contractions (wave-like peristalsis described in more detail below) in the terminal ileum, which propel the bolus into the caecum [2].

The colon consists of several parts; the caecum (a small pouch at the entrance of the large intestine), the ascending colon (in normal anatomy located on the right), the transverse colon, the descending colon (in normal anatomy located on the left), the sigmoid colon and the rectum [1].

There are four tissue layers in the small bowel and colon wall; serosa, muscularis, submucosa and mucosa. The innermost layer, the mucosa surrounds the hollow lumen and comes in direct contact with the food bolus.

The small bowel has the main function of absorbing nutrients from food, already partially broken up by the stomach. Intestinal motility aids this digestive process through propulsion (or peristalsis) and mixing (or segmentation) which involves contraction of smooth muscle cells aligned in circular and longitudinal layers within the muscularis propria in the bowel wall [1] (figure 1).

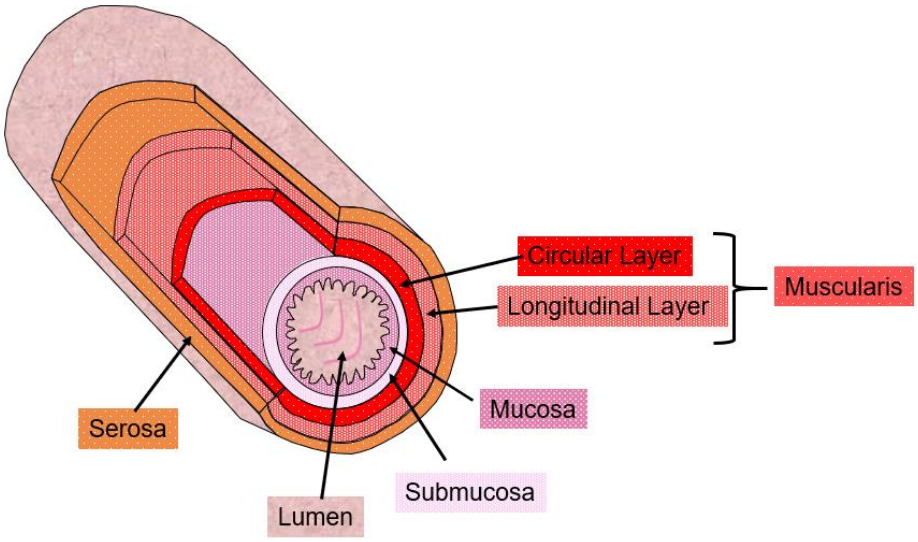


**Figure 1: The tissue layers of mucosa, submucosa, muscularis (circular and longitudinal layers) and serosa surrounding the lumen of the gastrointestinal tract.**

### 1.1.2 Motility

The importance of motility coordination in the bowel is analogous to the importance of contractions in the heart, they need to be synchronised to move food at the correct rate and perform the correct amount of mixing [3], [4].

The interstitial cells of cajal serve as a pacemaker to control the contractions of smooth muscle [5] through the myenteric plexus. Motility patterns are influenced by three factors; hormonal, dietary and neurological which act via the myenteric plexus.

Enteroendocrine cells (EEC), located in the gut wall, regulate secretions into the gut and motor function through sensing intraluminal nutrients and releasing peptides and amines in response. Enteroendocrine cells are also stimulated by mechanical, physiochemical stimuli, internal secretion, microorganisms and toxic compounds. EEC cells consist of a variety of receptors and chemical transmitters, allowing detection of luminal contents and the appropriate response through secretion of hormones or release of neurotransmitters to the nervous system [6]. Gastric emptying is delayed by cholecystokinin (CCK) [7] or glucagon-like peptide-1 (GLP-1)-mediated mechanisms in response to meal stimulation (intraduodenal perfusion of lipid or glucose) in healthy individuals. When fatty acids are introduced into the ileum, SB motility is decreased by the release of polypeptide YY (PYY) [8], gastric emptying is delayed by parenteral PYY [9] and food intake is reduced [10].

This control can result in the complete inhibition of contractions or in a range of contractile actions which can be described broadly according to two states; fed (i.e. postprandial actions) and fasted (mainly via the migrating motor complex [MMC]) [4], [11]–[14].

The fasted state, which occurs between digestive periods, involves the MMC which originates in the stomach and migrates downstream to push undigested food into the colon. The MMC consists of three phases which each occur over a longer period of time than motility activity in the fed state; a period of quiescence where contractions are rare (phase I), followed by a longer period of irregular and short contractions (phase II) and a short period where there are strong, regular, peristaltic contractions (phase III) [15].

The fed state occurs after food is ingested and involves postprandial actions such as peristalsis and segmentation which are both short in duration, but have different roles in digestion.

Peristalsis is a type of motility which pushes the food bolus along the small bowel through wave-like and rhythmic movements. The smooth muscle walls contract behind the bolus causing constriction of the lumen while relaxing in front of the bolus, causing distension which allows smooth transit. Additionally, peristalsis also facilitates the mixing of the chyme with digestive juices.

However, the main mechanism of mixing is through another type of motility called segmentation. This involves segmental contraction and relaxation of the longitudinal muscles, so the bolus is in contact with the bowel wall, where nutrients are absorbed. The bolus is further broken up and therefore there is a larger surface area of the overall bolus exposed to the mucosa for absorption [4], [11]–[14].

Generally in the fasted state, there are 9-12 contractions per minute in the small bowel [16]. Transit time through the small bowel is about 30-60 minutes for liquids and 4-5 hours for solids [17]–[19]. Colonic motility consists of either segmental mixing with around 3 contractions per minute or low-amplitude propagated contractions

(occur 60 times daily) [20] and high-amplitude propagated contractions (occur less frequently at around 6 times a day) [21].

Beyond this, more detailed knowledge of intestinal motility is sparse. Part of this is due to investigational techniques which involve the insertion of pressure sensors into the bowel, only giving a clear view of the distal and proximal regions. As a result, evaluation of motility has been largely omitted from routine clinical practice outside of specialist physiology clinics, and even here, results can be challenging to interpret and utilise [22].

Despite the challenges, the range of clinical conditions identified as seemingly associated with gut dysmotility has driven several advancements in methods to measure motility. The next section describes the main non-MRI based techniques used for quantifying bowel motility.

## 1.2 Non-MRI based techniques for motility

The ideal method for motility assessment is a test that can explore both global and segmental motility patterns under physiological conditions. This is difficult to achieve, and a diverse array of tests have been developed to explore the different aspects of gut motility.

The ‘biomarker roadmap’, described by O’Connor et al., involves discovery (domain 1), validation (domain 2) and qualification and ongoing technical validation (domain 3). For domain 1/discovery, a single centre conceives of the idea of an imaging biomarker to address an unmet clinical need or to improve an existing biomarker. For domain 2/validation, phantom, preclinical and/or clinical datasets are initially used in a single or a small number of expert centres before being developed and/or researched further in multiple centres. The two main types of validation are technical validation as well as biological and clinical validation. Technical validation consists of

precision (repeatability and reproducibility), bias and availability (software, hardware, ethics, regulation IP and licencing) of an imaging biomarker. Biological and clinical validation includes a relationship to intervention and comparison of imaging to biological markers such as histology or in the context of this field, inflammatory markers. For domain 3, prospective large trials are undertaken and finally implemented in healthcare systems.

Emerging non-MRI techniques for motility assessment include 3D-Transit system and high-resolution manometry. The uses, advantages and disadvantages of techniques are summarised in table 1.

| **Motility assessment techniques** | **Location and use** | **Advantages** | **Disadvantages** |
|---|---|---|---|
| Antro-duodenal Manometry | Proximal bowel – to measure motility patterns | It is reliable and there is no radiation exposure. | It is highly invasive and can only be performed at specialised centres due to the technical complexity of acquiring and interpreting the data. |
| Hydrogen breath test | Small bowel – to measure oro-caecal transit times | It is a cheap, non-invasive method with no radiation exposure. | Abdominal bloating and distension are common side effects and the data interpretation is |

| | | | |
|---|---|---|---|
| | | | distorted by small bowel bacteria overgrowth and lactulose causing osmotic activity, accelerating small bowel transit. The method therefore has poor sensitivity. |
| Radiopaque markers | Whole gut – to measure regional and whole transit times | It is simple and inexpensive with low invasiveness as well as being highly standardised. | The method is time consuming with markers ingested on consecutive days before an X-ray is acquired and therefore there is exposure to radiation. |
| Scintigraphy | Whole gut – to measure regional and whole transit times | It is a validated method for colonic transit time and is non-invasive. | It is costly, there is a lack of standardisation especially for small bowel transit time and there is radiation exposure. It is also time consuming and the data |

| | | | |
|---|---|---|---|
| | | | interpretation is difficult. |
| Wireless motility capsule | Whole gut – to measure regional and whole transit times and motility patterns [23] | It is a non-invasive technique with no radiation exposure and high standardisation. It allows the patient to walk while the capsule collects the data. | It provides indirect measures of motility through pressure measurements and therefore coughs, hiccups etc. causing changes in intraluminal pressure can be misclassified as motility making data interpretation difficult.<br><br>It also cannot provide segmental colonic transit times with only whole colonic transit measured. It is expensive and not widely available and cannot be used in cases where obstruction of the bowel poses a risk. |

| | | | |
|---|---|---|---|
| 3D-Transit system* (electro-magnetic pills which can be tracked in space and time) | Whole gut – to measure regional and whole transit times and motility patterns with direction, velocity and length of bowel contractions captured | It is non-radioactive and non-invasive and allows the patient to walk while the capsules collect the data. | Intense physical activity may cause external noise which makes the data difficult to interpret. Localised motility patterns are difficult to capture due to the movement of the capsules. There is also a risk of obstruction of the bowel. |
| High-resolution manometry* | Colon – to measure motility patterns | It offers high spatio-temporal resolution compared to conventional manometry and there is limited radiation exposure. | It is costly and highly invasive with difficult data interpretation. |

**Table 1: Summary of the current motility techniques (* highlights emerging techniques)** [24]**.**

### 1.2.1 Antro-duodenal manometry

Antro-duodenal manometry involves the insertion of catheters which allow contractions and motor patterns to be studied in the gut through pressure measurements within the lumen of the bowel [25].

A contraction is therefore recorded by a change in pressure being measured at the location within the bowel where the manometry sensor has been placed. Measurements can be recorded from the stomach and duodenum, if the catheters are inserted through the mouth, and from the other end, contractions of the terminal/distal ileum and colon can be measured via insertion through the anus. Therefore, the measurement of motility within the small bowel is limited.

The frequency, length and amplitude of a contraction can be measured due to the catheter consisting of several sensors positioned at regular intervals, which capture a contraction propagating along the gut due to the detection of pressure changes by multiple sensors.

The procedure is highly invasive, with the placement of catheters under the guidance of endoscopy sometimes necessary, and can only be performed at specialised centres due to the complexity of acquiring the data. The data is also difficult to interpret with a large range of pressure changes, representing contractions, seen in health and disease, potentially due to motion other than motility present in the abdomen [26].

### 1.2.2 Hydrogen breath-testing

Hydrogen breath testing involves a dose of unabsorbed carbohydrates, such as lactulose, being ingested, which produces hydrogen gas through fermentation by gut bacteria. The oro-caecal

transit time is measured as the time between lactulose ingestion and a rise in the level of hydrogen measured by the breath test [26], [27].

This is a simple, non-invasive test which has been validated and has been used in research and the clinic to demonstrate associations between the ora-caecal transit time and several dysmotility related diseases. Bacterial overgrowth in certain patients causes an increase in small bowel motility, leading to inaccurate transit time measurements [28]–[30]. Transit time is also not a direct measurement of motility.

### 1.2.3 Radiopaque markers

Radiopaque markers are ingested on consecutive days, followed by an abdominal x-ray to track the markers. This gives information on small bowel and colonic transit time, as the markers in the bowel can be located since each marker is a different shape, allowing easy identification on the X-ray [31], [32].

This technique is widely used since it is cheap with low invasiveness and easy data interpretation. However, ionising radiation is being used, it is time consuming and motility is not being measured directly, with transit time often not correlating with motility [24].

### 1.2.4 Scintigraphy

Scintigraphy involves radio-labelled solid and/or liquid foods being ingested to measure gastric emptying (GE), by acquiring repeat images over 1-4 hours. Transit time for the whole gut, small bowel or colon is calculated using gamma camera images [33].

This technique is non-invasive and widely used for colonic transit time (the location and volume of radio-labelled material is assessed at 24, 48 and 72 hours post meal) in IBS as well as functional

diarrhoea and constipation [34]. Similarly, to the limitations of radiopaque markers, it is time consuming, there is radiation exposure and a lack of direct motility measurement. Additional disadvantages are that the low spatial resolution from gamma camera images makes the identification of precise anatomical locations difficult, and therefore data interpretation is difficult [24].

### 1.2.5 Wireless Motility Capsule

There are two commercially available wireless motility capsules with the PillCam [35], [36] and Smartpill® (Givin Imaging, Yokneam, Israel) [36], [37]. In both cases, the capsule is ambulatory with no radiation exposure, but they cannot be used in cases where bowel obstruction is a risk for patients e.g. in CD patients with strictures.

Firstly, the PillCam is capable of 'video capsule endoscopy', where a camera with a light records a video of the interior of the entire GI tract. This can be used to find and assess bleeds and mucosal damage in Inflammatory Bowel Disease (IBD) as well as measuring the regional (by visualising the stomach, small bowel and colon from the video) and total transit time. Additionally, contractile actions in the gut can be studied, but are limited in scope since the direction the camera is facing at any given point biases the motility assessment. Therefore, the whole gut is not being captured throughout the transit [38]–[40].

Smartpill® (Givin Imaging, Yokneam, Israel) involves a wireless motility capsule being ingested, which measures intraluminal pressure, pH and temperature of the gut as it passes through the GI tract over several days. This information is transmitted to an external data receiver where it can be analysed through software. Transit time can be measured based on the changes of pH at specific locations [41], [42], with validation against radiopaque markers demonstrating good performance for colonic transit times [43]. Additionally, motility can be measured based on the presence or absence of contractions at certain points along the GI tract [41], [42].

These techniques are highly expensive and data interpretation is again difficult, especially in the context of motility, where contractions are only detected at certain locations at a specific time, with no global motility pattern being detected [24].

### 1.2.6 3D-Transit system

Capsules are ingested and tracked as with the wireless capsules described above. The 3D transit system (Motilis Medica, SA, Lausanne, Switzerland) involves a receiver plate carried on the abdomen which allows the exact position of the electromagnetic pill to be tracked in space and time. Regional transit times as well as the direction, velocity and length of bowel contractions can be captured by 3D-Transit [44].

The 3D-Transit system has been used in several studies including examining GI transit times in healthy subjects after taking oxycodone and the relationship between GI function and sleep. Fast transit in diarrhoea and slower transit in severe ulcerative colitis patients have also been demonstrated [45]–[48].

The system is ambulatory like Smartpill® with low invasiveness and no radiation exposure. The use of electromagnetic pill makes the potential future use of the system in conjunction with MRI an interesting prospect. The technique is expensive and currently not available clinically with bowel obstruction from capsule retention again a risk. The data interpretation is difficult with standard ranges of values for healthy individuals and GI patients not yet established [24].

### 1.2.7 High-Resolution Manometry

High-resolution catheters are inserted, with several sensors closely spaced together, to give better resolution than conventional

manometry, and allowing the identification of small migrating motor complexes [24].

High-resolution manometry improves on the resolution of conventional manometry, where the sensors are spaced over 10cm apart, by reducing the distance between sensors to the scale of 10-40mm intervals. It has been used in studies for establishing the normal ranges of motor patterns in the colons of healthy subjects as well as in patients with constipation and in patients with faecal incontinence [49]–[51].

The technique is highly expensive and highly invasive, with complex data acquisition and analysis. These limitations mean this technique is only available in specialised centres able to carry out the procedure. High-resolution manometry is still largely experimental, however the improved spatio-temporal resolution of the pressure measurements offers an improvement, over antro-duodenal manometry, which could see the technique being utilised more readily [24].

The next section describes how motility is affected in GI diseases and conditions such as Crohn's disease and irritable bowel syndrome.

## 1.3 Small Bowel Motility in disease

Abnormal motility is associated with several common gastrointestinal (GI) conditions and diseases such as Crohn's disease (CD), irritable bowel syndrome (IBS), ulcerative colitis (UC) [52], functional constipation [53], Ehlers-Danlos syndrome (Hypermobility type) [54], chronic intestinal pseudo obstruction (CIPO) [55]–[59] and postoperative ileus [60]. Furthermore, aberrant motility has been found to precede neurological symptoms in Parkinson's disease by 10 years [61]–[64].

The focus of this thesis will be Crohn's disease and irritable bowel syndrome. In CD, symptoms often persist even when inflammation has been resolved. A previously established association [65] between motility and symptoms is explored further in this thesis. In IBS, there is often no physical evidence of structural damage present so alternatively functional motility has been postulated as a possible cause of symptoms (see section 1.3.5).

### 1.3.1 Crohn's disease – an inflammatory bowel disease

Crohn's disease is a lifelong, chronic inflammatory bowel disease which often occurs relatively early in life, often leading to surgery and a decreased quality of life [2]. European prevalence and incidence is 322 per 100, 000 persons and 12.7 per 100, 000 person-years, respectively [66]. CD fluctuates between periods of disease activity (manifesting as inflammation of the bowel) and remission. However, only 10% of patients have prolonged clinical remission. The Lémann score was developed to assess intestinal damage in CD through the assessment of irreversible bowel damage, stricturing lesions, penetrating lesions and surgical resections. Often areas of inflammation caused by the disease are interspersed with normal bowel, so called "skip lesions" [2]. The disease can affect anywhere from the mouth to the anus, but typically affects the small bowel and colon. The disease is particularly predisposed to affecting the terminal ileum of the small bowel [2]. As discussed in section 1.4, symptoms tend not to correlate strongly with clinically important observations including endoscopy, blood tests and structural imaging.

Treatment of CD involves managing inflammatory activity and aims to move patients from the active phase of the disease into remission i.e. without ongoing inflammation [67]. Powerful anti-inflammatory drugs, such as anti-TNF alpha antibodies (TNF = tumour necrosis

factor) e.g. infliximab and adalimumab or corticosteroids, are fast acting so are used to control inflammation rapidly and for alleviating symptoms. Immunosuppressants such as thiopurines or methotrexate are more commonly used for long-term maintenance of the disease. Other biologics such as ustekinumab and vedolizumab provide an alternative for patients where anti-TNF therapy is unsuccessful [68]. Generally, a combination of therapies has been shown to be more beneficial than only using a single drug therapy [69], [70].

There is a need clinically to determine when to start these therapies, especially powerful anti-inflammatory drugs, and to monitor whether the treatment is working. Anti-TNFs cost £2,500 per patient year and in 2013 cost the UK's NHS £300 million [71]. These drugs fail after 12 months in 23-46% patients [72] so determining ongoing underlying disease activity is vital so treatment can be stopped or altered if there is no benefit to the patient from continuing the drug [73].

50% of CD patients require surgery within 10 years of their diagnosis, with bowel resection. This is often due to a lack of response to drug therapy, strictures with bowel obstruction or high grade dysplasia/cancer [2], [74].

The key to optimally managing Crohn's disease is accurate evaluation of the underlying inflammatory burden, so treatment can be tailored as appropriate. There are several tests for assessing inflammation with no single test being optimal. Therefore, a combined approach is normally undertaken using blood and stool markers, imaging and endoscopy, along with indices of patient symptoms [2].

Inflammatory markers such as C-reactive protein (CRP) and faecal calprotectin (fCP) are non-specific global measurements of inflammation, and cannot provide information on the severity or location of the disease [75], [76].

Endoscopy allows direct inspection of the bowel lining and histopathological assessment through biopsies of the mucosa, but is invasive and requires full bowel purgation. It also can only visualise the last few centimetres of the terminal ileum at best [75].

Capsule endoscopy, mentioned in section 1.2.5, is an emerging technology which makes it possible to view the whole GI tract including the areas of small bowel that are difficult to reach with traditional endoscopy/colonoscopy [77].

Imaging offers several complementary benefits when used in combination with other techniques in the assessment of Crohn's disease.

Cross-sectional imaging such as CT, MRI and ultrasound are essentially non-invasive and can give information about the location, extent and severity of bowel inflammation. They can also help monitor drug treatments in a non-invasive way [75].

Clinically, radiologists use enteric MR to assess bowel wall structure, and anatomical observations such as wall thickening and signal and pattern of contrast enhancement are used to assess the amount of active disease [78]. Inflamed small bowel typically exhibits increased wall thickness, increased T2 signal (on MRI), increased contrast enhancement on CT and MRI, (or increased Doppler signal on US) and perimural mesenteric changes [78]. These observations are based on bowel wall structure and form the bedrock of interpretation of cross-sectional imaging in Crohn's disease.

The work in this thesis concentrates on the use of cine MRI to capture bowel motility (see chapter 2), particularly in apparently normal bowel and explores the link with patient symptoms, which are not always directly related to inflammation [79], [80].

### 1.3.2 Motility in Crohn's disease

Abnormal motility has been previously associated with abdominal symptoms in CD patients with both active and inactive inflammation and in the context of MRI will be discussed in more detail in chapter 2.

Previous research suggests enteric motility is abnormal in CD, although the volume of data is relatively small.

For example, delayed gastric emptying has been demonstrated using $^{13}$C-octanoic acid breath test in conjunction with the ingestion of a solid meal [81], and with scintigraphy (see section 1.2.4) [82]. It has been postulated that excessive CCK release may be partly responsible for the $^{13}$C-octanoic acid breath test [83].

Additionally, reduced oro-caecal transit time on hydrogen breath testing (see section 1.2.2) has been seen in CD patients [84], [85]. Furthermore, a combination of reduction in small bowel contractions and an increase in the frequency of single or clustered propagated contractions has been measured in CD patients using conventional manometry [86].

Inflammation, even at low levels, may underlie this dysmotility, although the exact mechanisms by which distal CD inflammation affects motility and induces symptoms is unknown. As described previously in section 1.1.2, enteroendocrine cells regulate motor function and secretion of peptides and amines into the gut, in response to the presence of intraluminal nutrients. An important location for EEC expression is in the terminal ileum [87]. GLP-1 and PYY are satiety (or fullness) signals which are affected by inflammation in symptomatic CD patients and increased levels of these gut peptides results in reduced appetite [87], [88].

In terminal ileal CD, where inflammation is present, there is disruption of the normal function of enteroendocrine cells (EEC) with

increases in ileal expression of GLP-1 (2.5 fold) [87] and PYY (2.2 fold) [88] compared to healthy controls. Asymptomatic patients in remission have normal EEC peptide levels whereas nausea and bloating in CD patients are associated with an increase in plasma peptide levels in the small bowel [88]. CD patients also displayed reduced appetite before and after eating due to the increased PYY [88].

The ability of magnetic resonance enterography (MRE) to capture abnormal motility patterns in structurally normal bowel could prove a powerful tool in improving the understanding of gastrointestinal motility in health and disease. This PhD aims to explore further the observation that abnormal motility is associated with patient symptoms.

### 1.3.3 Irritable bowel syndrome and GI symptoms

Irritable bowel syndrome is a condition characterised by a range of GI symptoms such as abdominal pain or discomfort, bloating, constipation and diarrhoea [89]. The prevalence of IBS is up to 20% of the population in many western countries and makes up to a third of the gastroenterologists' clinical work load in the UK [90].

The aetiology of IBS remains unknown with patients often having structurally normal bowel, on standard investigations such as cross-sectional imaging and endoscopy. As such, it is usually a clinical diagnosis following exclusion of structural disorders such as Crohn's disease which can cause similar symptoms [91], [92].

Clinically, IBS can be subclassified into constipation-predominant (IBS-C), diarrhoea-predominant (IBS-D) and mixed IBS (IBS-M) based on validated patient questionnaires (see section 1.4.2 and chapter 6) [89], [93], [94].

The diagnosis of IBS is based on the Rome criteria with abdominal pain and bloating dominant symptoms of IBS [89], [95]–[98].

Bloated patients often present in clinic with a large, distended abdomen which could potentially be caused by colonic distension. Abdominal bloating is defined, subjectively by the patient, as a sensation of fullness. When this subjective sensation is associated with visible objective distension then it is referred to as abdominal distension (figure 2).

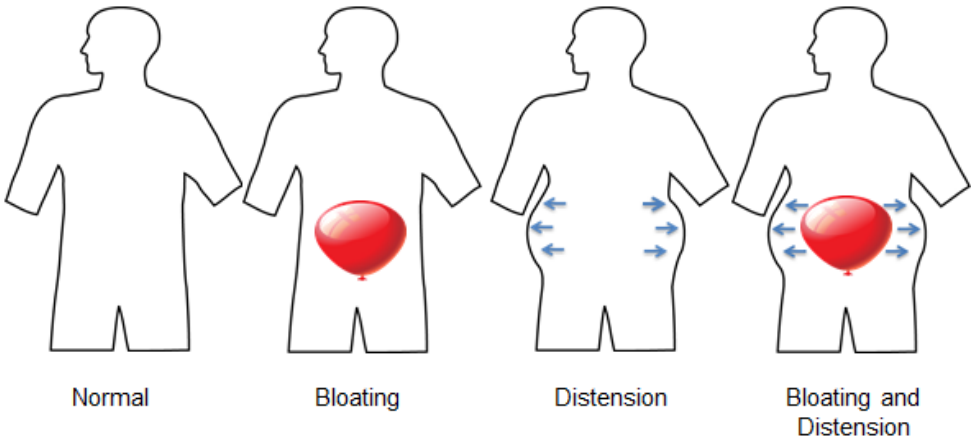


**Figure 2: Bloating is a subjective sensation of fullness whereas abdominal distension is an objective increase in abdominal girth with a large, distended abdomen. Bloated patients often experience both bloating and distension simultaneously.**

Bloating and distension is frequently reported in patients with IBS, particularly in those with IBS-C and those with associated slow colonic transit [99].

Previously, differences between IBS-D patients and healthy controls have been found for the ascending colon diameter with a decreased diameter in IBS-D [100]. In chapter 7, the ascending colon diameter will be compared between IBS-C patients and healthy controls.

An increased perception to the feeling of bloating is associated with gas retention and increased abdominal girth with visceral hypersensitivity postulated to be the cause [101]. Visceral

hypersensitivity, i.e. an increase in pain sensitivity when the gut is stimulated experimentally, is considered to be a key cause of pain and discomfort in IBS patients [102]–[104]. Increases in peripheral [105]–[108] and central [109]–[111] nervous system sensitivity are thought to cause this visceral hypersensitivity. An increased perception to the feeling of bloating is associated with increased abdominal girth.

### 1.3.4 Low-grade inflammation, increased permeability and altered gut microbiota

There is evidence that some IBS patients have an increased number of inflammatory cells, such as mast cells, eosinophils and T cells in the colonic and ileal mucosa, compared to healthy controls [112]. This low-grade inflammation has been demonstrated mainly in IBS-D patients. It should be noted that this inflammatory response is much lower than the inflammation seen in CD [113], [114].

Altered gut microbiota, food allergy, and increased intestinal permeability (which can be increased by bile acid malabsorption) have all been postulated as potential factors that lead to low-grade inflammation in IBS [115].

An increase in intestinal permeability has been shown in IBS-D patients and post-infectious IBS i.e. the onset of IBS following infectious gastroenteritis [116]–[119].

It has been suggested that tight junction dysfunction or adherence proteins are responsible for increased permeability in IBS [117].

IBS also has an important psychological component with patients reporting a worsening of symptoms in relation to life events such as

stress which is another potential contributary factor to increased permeability [120].

Altered gut microbiota is another factor considered important in IBS [117], [121], [122]. Wireless motility capsule studies suggest that there is altered microbiota at the TI-caecum level, with a lower caecal pH (suggesting higher colonic fermentation), in patients with bloating and distension [123] and in IBS patients irrespective of subgroup, compared to controls [124].

### 1.3.5 Small bowel motility in IBS

Abnormal enteric motility patterns have been hypothesised as a potential cause of IBS symptoms. Regular phasic contractions in the small bowel have been recorded with manometry, at around 1Hz in some patients, with the onset of pain, which may or may not be specific for IBS [125]. In the colon, the frequency of low-amplitude propagated contractions and high-amplitude propagated contractions can be varied. These contractions are often linked with pain and the patient having IBS-D or IBS-C [126], [127].

Previously, it has been shown that the duration of postprandial motor activity was shorter in IBS patients, compared to HCs, and migrating motor complex intervals were shorter in IBS-D than in IBS-C. Clustered contractions with a mean duration of 46 minutes were detected and often associated with transient abdominal pain and discomfort [128].

Abnormal small bowel motility has been associated with small intestinal bacterial overgrowth (SIBO), with a reduced frequency of MMC, which is responsible for cleaning the bowel and therefore keeping it bacteria free [129], [130]. SIBO is thought to contribute to

bloating in IBS with abnormal lactulose breath tests found in 84% of patients, and symptom improvement observed once SIBO has been resolved [129].

The reduction in MMC is thought to lead to responses, such as impaired intestinal gas propulsion, that lead to pain and/or changes in bowel habit [131].

Colonic transit time has been shown to be abnormal in IBS patients with faster transit in IBS-D and slower transit in IBS-C, both compared to healthy controls based on scintigraphy [132]. Altered motility, total and segmental colonic transit time assessed by radiopaque markers, was also shown to be linked to IBS symptoms, specifically altered bowel habits [133].

In chapter 7, abnormal motility in IBS-C patients is investigated. Anecdotally, radiologists report “faecalisation” of terminal ileum luminal content on MRI performed in patients with IBS-C (S Taylor, personal communication). This is hypothesised to be reflux of caecal contents back into the terminal ileum with altered motility postulated as a potential cause. If the involvement of abnormal motility could be established in IBS-C patients, then this could indicate the contribution of motility to symptoms in this IBS subgroup.

Due to the lack of knowledge about the association, or lack thereof, between IBS symptoms and dysmotility, these patients are often continually undergoing gastroenterological examinations, with a variety of drug treatments attempted before eventually being treated with psychotherapy.

Since IBS is a heterogenous patient group it is important to determine whether altered motility is present in a high proportion of IBS patients, regardless of symptoms classification, or if it is more prevalent in association with particular IBS subgroups.

### 1.3.6 Summary of CD and IBS

It is thought that abnormal small bowel motility may be linked to patient symptom burden. Therefore, an improved understanding of what constitutes abnormal small bowel motility might help the appropriate treatment choices to be selected and could help in the management of both CD and IBS. Another important aspect of research in this field is the quantification of symptoms that characterise these GI conditions/diseases. An easy and standardised method of measuring the severity of symptoms is vital. The next section will describe the questionnaires used to record patient symptoms.

## 1.4 Symptoms and questionnaires

Self-reporting of patients' symptoms is highly variable and subjective. In CD, abnormalities on endoscopy, blood tests and structural imaging correlate poorly with symptoms. For example, faecal calprotectin levels and MRI features of bowel inflammation often show poor correlation with the HBI score [134]. Even when the CD treatment manages to successfully control inflammation, with endoscopic mucosal healing and low levels of inflammatory markers present such as C-reactive protein (CRP), CD can still cause debilitating symptoms e.g. diarrhoea and abdominal pain, with a profound effect on quality on life. For example, 31% of 48 patients with very low faecal calprotectin had symptoms [79], [135], [136]

Similarly, in IBS, the origin of symptoms is unclear with many potential factors contributing such as altered gut microbiota, altered motility, visceral hypersensitivity, gut permeability and low-grade inflammation. [137]. In an attempt to standardise quantification of patient symptoms, various questionnaires have been developed for both CD and IBS. These are summarised below.

### 1.4.1 Harvey-Bradshaw Index (HBI) in CD

The HBI consists of five components including general wellbeing, abdominal pain, number of liquid stools per day, abdominal mass and complications. Wellbeing, pain and abdominal mass (evident on physical examination) are graded on a scale. The number of stools per day and the number of complications add directly to the total HBI score which classifies the patients' disease activity [138].

The questionnaire is generally completed based on symptoms within the preceding 24 to 48-hour period. The abdominal mass is scored by the doctor or advanced nurse practitioner after a physical examination, but the other components are completed by the patients themselves. The number of liquid stools are recorded with formed or slightly loose stools excluded from the total number [139]. The HBI components are shown in table 2.

| **HBI Component** | **Description** |
|---|---|
| General Wellbeing | 0=very well<br>1=slightly below par<br>2=poor<br>3=very poor<br>4=terrible |
| Abdominal Pain | 0=none<br>1=mild<br>2=moderate<br>3=severe |

| | |
|---|---|
| Number of liquid stools per day (day of scan or day before) | This value adds directly to the HBI score |
| Abdominal mass | 0=none<br>1=dubious<br>2=definite<br>3=definite and tender |
| Complications (score 1 per item) | Arthralgia<br>Uveitis<br>Erythema nodosum<br>Apthous<br>Ulcers<br>Pyoderma gangrenosum<br>Anal fissure<br>New fistula abscess |

**Table 2: HBI Component breakdown with description** [138]**.**

A CD patient with a HBI score of less than 5 is considered likely to be in remission i.e. have little or no underlying gut inflammation and minimal symptoms. Mild disease is classified as an HBI score between 5 and 7 with moderate disease classified as between 8 and 16 HBI score and severe active disease classified as over 16 HBI score [138].

### 1.4.2 Irritable Bowel Syndrome-Symptom Severity Score (IBS-SSS) and Visual Analog Scale for IBS (VAS-IBS)

An attempt to rectify the lack of standardisation in defining IBS and assessing the severity of the condition led to the development of the Irritable Bowel Syndrome-Symptom Severity Score (IBS-SSS) [140]. Two important aspects of symptoms questionnaires are their ease of use through simplification of the scoring method, with a smaller number of the most relevant symptom components being considered, and the ability to assess symptom severity.

IBS-SSS includes components such as pain intensity, pain frequency, bloating, dissatisfaction with bowel habits and interference in daily life which are each scored on a scale of 0-100, giving a maximum score of 500 [140]. IBS-SSS is recorded based on the 10 days preceding the questionnaire being completed (table 3).

| **IBS-SSS Component** | **Description** |
|---|---|
| Pain Intensity | 0% = no pain<br>25% = not very severe<br>50% = quite severe<br>75% = severe<br>100% = very severe |
| Pain Frequency | Enter the number of days that you get pain in every 10 days (score multiplied by 10 to provide a score out of 100) |
| Bloating severity | 0% = no distension<br>25% = not very severe |

| | |
|---|---|
| | 50% = quite severe<br><br>75% = severe<br><br>100% = very severe |
| Bowel habits satisfaction/dissatisfaction | 0% = very happy<br><br>25% = quite happy<br><br>75% = unhappy<br><br>100% = very unhappy |
| Interference in daily life | 0% = not at all<br><br>25% = not much<br><br>75% = quite a lot<br><br>100% = completely |

**Table 3: IBS-SSS Component breakdown with description** [140]**.**

Another IBS questionnaire called the Visual Analog Scale for IBS (VAS-IBS) was developed to be used in clinical practice with the aim to measure the treatment responses of symptoms and well-being in IBS patients as well as being user friendly for both the patient and the healthy professional [93], [94].

VAS-IBS includes components such as abdominal pain, diarrhoea, constipation, bloating & flatulence, vomiting & nausea, perception of mental well-being and intestinal symptoms' effect on daily life. Each component was scored on a scale of 0-100 (very severe discomfort = 0 to no discomfort at all = 100) based on the previous week. This is because the Gastrointestinal Symptom Rating Scale (GSRS) and the Psychological General Well-Being Index (PGWB), which were used to test the criterion validity of VAS-IBS, use the same time window [93], [94].

## 1.5 Chapter Summary

Motility patterns are complex with a great variation in both disease and health. It is important to develop methods to assess both localised and global motility that are accurate, cost effective and non-invasive. The deep anatomical location of the small bowel makes this especially difficult.

In summary, abnormal motility has been postulated as a potential cause of symptoms in CD and IBS.

In CD, delayed gastric emptying ($^{13}$C-octanoic acid breath test and scintigraphy data) and reduced orocaecal transit time (hydrogen breath test data) has been demonstrated. Additionally, a combination of a reduction in small bowel contractions and an increase in the frequency of single or clustered propagated contractions has been measured using manometry.

In IBS, the duration of postprandial motor activity has been shown to be shorter in IBS patients compared to HCs and migrating motor complex intervals were shorter in IBS-D than in IBS-C (manometry data). Reduced frequency of MMC has been associated with small intestinal bacterial overgrowth. Colonic transit time has been shown to be faster in IBS-D and slower in IBS-C, compared to HCs (scintigraphy data). IBS symptoms have been associated with abnormal motility and colonic transit time (radiopaque markers).

Having discussed non-MRI techniques, the next section introduces MRI which has potential as a powerful diagnostic tool. Interestingly, MRI has arrived as a means of assessing motility via Crohn's disease, a condition where dysmotility was not considered particularly important until recently.

# Chapter 2: Background and literature review of motility and texture analysis using MRI

## 2.1 Magnetic Resonance Imaging Enterography

Magnetic Resonance Imaging (MRI) is a technique which achieves high spatial resolution and provides good soft tissue visualisation while having the advantage of being non-invasive and non-ionising. It is flexible in terms of the different contrasts that can be achieved when imaging a range of organs and can provide both anatomical/structural and functional information [141].

This section provides a description of the basic principles behind MRI, T1 and T2 relaxation processes, image formation and pulse sequences. There is a particular focus on balanced steady-state free precession sequences which can be used to acquire both static (anatomical) and dynamic (or 'cine') MRI data. For the purposes of this thesis, the term balanced steady-state free precession is interchangeable with True FISP (Fast Imaging with Steady-state Precession), balanced-FFE (Fast Field Echo) and BTFE (balanced turbo field echo).

### 2.1.1 Physical Principles of MRI

The MRI signal comes primarily from protons, i.e. hydrogen nuclei within water and fat molecules, which have resonance frequencies determined by the strength of their local magnetic field. The protons

are placed in a strong, uniform magnetic field called the main magnetic field ($B_0$). Later, a radiofrequency (RF) pulse ($B_1$) is applied at the resonance frequency (of water) which excites the protons, causing the emission of signals that can be detected and converted into an image through a series of processing steps.

Protons can be considered to have the intrinsic quantum mechanical property of spin i.e. the angular momentum carried by particles spinning on their own axis. Nuclei with spin also possess a magnetic moment. The classical description of the magnetic moment is a spinning charged particle with the nuclear magnetic moment defined by the gyromagnetic ratio i.e. the ratio of its magnetic moment to its angular momentum.

When an external magnetic field, $B_0$ is applied to a magnetic moment a torque is produced which causes the proton to “precess” around $B_0$. Therefore, the proton spins on its own axis and this axis itself rotates about $B_0$ at the angular frequency of precession, which is known as the Larmor frequency. The equation for the Larmor frequency is $\omega_0 = \gamma B_0$, where $\gamma$ is the gyromagnetic ratio, an intrinsic property of the nuclei, and $B_0$ is the magnetic field strength.

There are two available states for a hydrogen nucleus, “spin up” and “spin down”. Spin up occurs when protons are aligned with the field in a lower energy level and spin down occurs when protons are antiparallel to the field in a higher energy level. In the absence of a magnetic field, there is no difference in energy between the two energy levels.

However, in the presence of a static magnetic field there are two energy states with a small excess in spin up. This excess of spins means there is a bulk magnetic moment for the tissue and therefore a small net magnetisation (from all the nuclear magnetic moments). This net magnetisation vector, $M_0$, is therefore aligned with the main

magnetic field and, therefore, there is a net positive magnetisation in the direction parallel to the main $B_0$ axis.

Transitions between the two energy levels occur when a radiofrequency pulse is applied. The frequency of the energy level difference is at the Larmor or resonant frequency at which the nuclei are precessing.

The direction of the main magnetic field, $B_0$, defines the coordinate system used to describe magnetisation excitation and relaxation, based on the MRI coils which are physically fixed in position in the scanner. The longitudinal axis parallel to $B_0$ is designated as the z-axis and the transverse plane perpendicular to $B_0$, where the signal is collected, is designated as the x-y plane, by convention. The effect of the RF pulse is that the net magnetisation vector, $M_0$, is tipped away from $B_0$, along, the z-axis, towards the x-y plane, perpendicular to the main field, where a signal can be detected.

The angle of the RF pulse which flips the $M_0$ magnetisation vector away from the $B_0$ field is called the flip angle and can be chosen to be any value, typically this is between 0-180$^o$.

After excitation of the net magnetisation vector, through application of the RF pulse, and signal detection in the x-y plane, through RF receiver coils, the magnetisation dephases and slowly returns to alignment with $B_0$, causing signal decay. The rate at which excited nuclei dephase and return to equilibrium is the basis of contrast between different tissues [141].

Magnetisation over time in the x, y and z direction is described by the Bloch equations [142].

### 2.1.2 T1 and T2 Relaxation

There are two relaxation processes that occur simultaneously, at different rates, which are important for MRI image contrast. These are spin-lattice (T1) relaxation, where the magnetisation vector, $M_Z$, recovers along the **longitudinal** z-axis and spin-spin (T2) relaxation where there is a decay of the net magnetisation vector, $M_{XY}$, in the **transverse** x-y plane.

Spin-lattice, or T1, relaxation occurs because the spins lose their magnetic energy to the surrounding tissue (the lattice). As the energy is transferred back to the tissue, the net magnetisation returns to equilibrium i.e. alignment with Bo. Spin-lattice relaxation is always slower (typically in the order seconds) than spin-spin relaxation (in the order of tens to hundreds of milliseconds).

Spin-spin, or T2, relaxation occurs due to interactions between adjacent spins causing exchange of energy. Local magnetic fields produced by neighbouring spins alter spin precession frequencies, leading to **dephasing** and loss of phase coherence.

In addition to spin-spin relaxation, T2* decay, which is visible in gradient echo sequences, is caused by dephasing due to different chemical shifts of nuclei and field inhomogeneities in the main magnetic field. The T2 or T2* signal decays exponentially. Spin-spin relaxation is an irreversible process, however dephasings due to chemical shifts and field inhomogeneities are reversible processes which can be accounted for using spin echo sequences.

This is mentioned later with the description of balanced sequences in section 2.1.6.

### 2.1.3 How an Image is formed

In addition to the main static Bo field, magnetic field gradients are applied in three orthogonal axes in order to obtain spatial information by generating and measuring the MRI signal. The gradients cause nuclei in different positions to experience different magnetic fields.

These gradients are slice select, phase encoding and frequency encoding (or readout) and are applied, typically in the z, y and x direction respectively, by convention. However, it should be made clear that these three gradients can point in any direction as long as they are orthogonal i.e. slice select can also be applied in the x and y direction or a combination of gradients can be used so that slices are angled away from being aligned directly with the scanner x-y-z coordinate system.

Slice selection involves selectively exciting spins in a defined slice (2D plane) or slab (3D block) of tissue. A RF pulse with a specified range of frequencies is applied simultaneously with a slice select gradient ($G_Z$). The slice thickness is determined by the RF pulse bandwidth and the strength of the $G_Z$ gradient, and therefore only spins within this slice are tipped through $90^o$ into the x-y plane. The thickness of the slice can be decreased by increasing the $G_Z$ gradient or reducing the bandwidth. Slice position can be varied by changing the carrier frequency of the RF pulse. Slice selection is shown in figure 3.

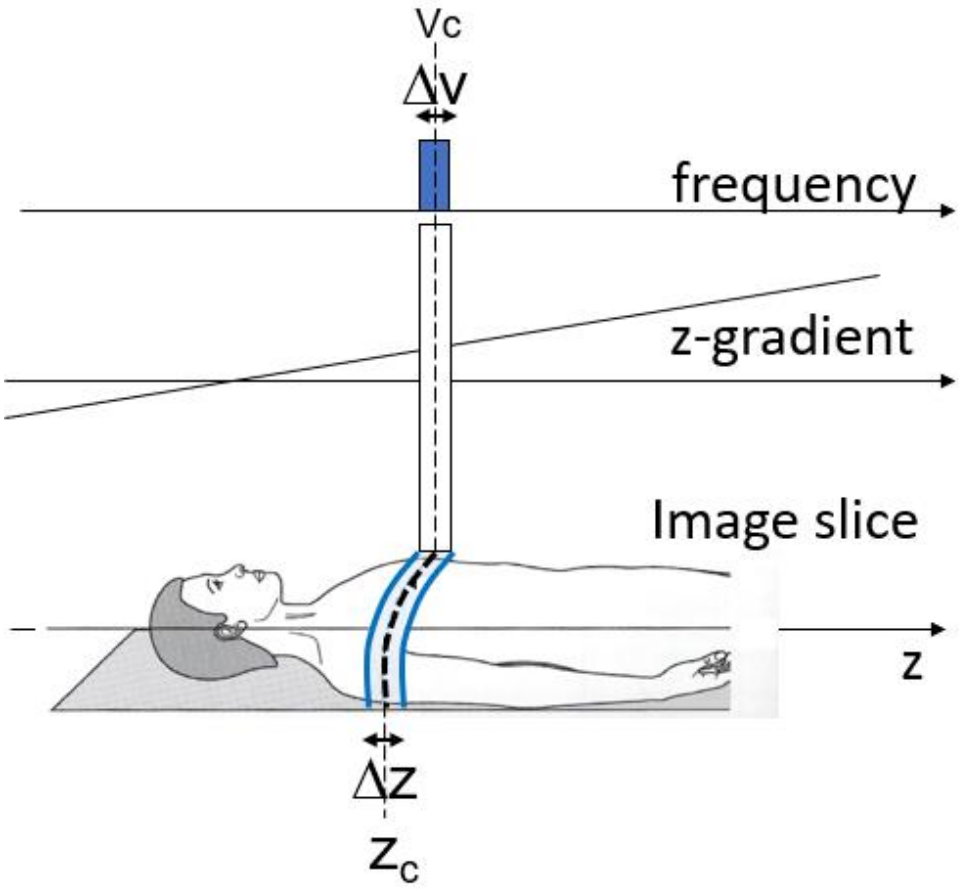


**Figure 3: Slice select gradient, Gz (z-gradient) is applied simultaneously with a RF pulse with a bandwidth of Δv and carrier frequency of $v_c$. The slice thickness Δz is determined by the RF bandwidth Δv and the strength of Gz, while the slice position $z_c$ is determined by $v_c$** [143]**.**

The phase encoding gradient, $G_Y$, is applied before the readout gradient and signal acquisition. The $G_Y$ gradient is switched on so protons are spatially encoded based on higher and lower resonant frequencies in the y-direction. However, the protons revert to the original Larmor frequency when the $G_Y$ gradient is switched off, but crucially they retain their phase, with a higher frequency corresponding to a larger phase change. A number of phase encoding steps need to be applied with different, unique gradient amplitudes and this is one of the main limiting factors in terms of acquisition time in MRI.

The frequency encoding gradient, $G_X$, also known as the readout gradient, is applied during signal acquisition. Protons in the higher parts of the field gradient will resonate at a higher frequency than protons in the lower parts of the field. Therefore, the range of frequencies acquired correspond to known spatial locations i.e. $G_X$ has encoded spatial information in the x-direction.

As will be discussed in more detail in section 2.1.7, there is a trade-off between spatial and temporal resolution in dynamic motility imaging, since more phase encoding steps provide a higher spatial resolution, but take longer to acquire and vice-versa.

The spatial frequency information is stored in a k-space matrix, acquired using the frequency and phase-encoding gradients. Each phase-encoding step with a readout gradient fills a single row of k-space (see figure 4). The inverse Fourier transform of the k-space matrix is used to create the image, if the data is fully sampled. A more complicated reconstruction is necessary if the data is undersampled i.e. SENSE (see section 2.1.7) which is often used in acquiring balanced sequences for the purpose of faster acquisition in small bowel imaging.

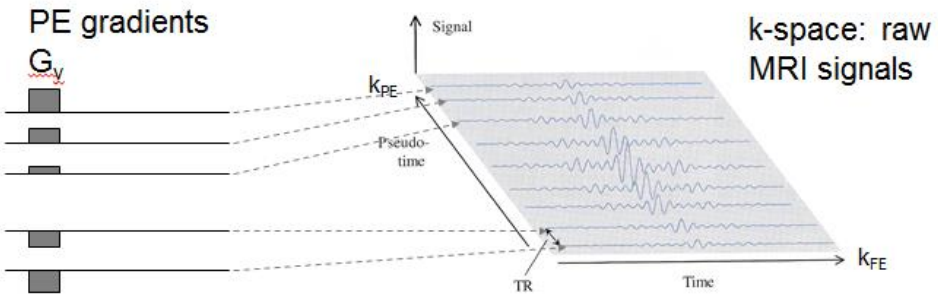


**Figure 4: Phase-encoding (PE) gradients, $G_Y$ applied at each repetition of the pulse sequence for multiple k-space lines or phase encoding steps ($k_{PE}$). Each phase-encoding step is applied with a readout gradient in the frequency encoding direction ($k_{FE}$) to fill a single row of k-space** [143]**.**

## 2.1.4 Pulse Sequences

Pulse sequences are a series of RF pulses and gradients which are applied in a predefined order to generate the MRI signal i.e. the echo. Gradient echoes (GE) and spin echoes (SE) are the main types of echo. Additionally, there are stimulated echoes (STE) which will be explained in more detail when discussing balanced sequences (see section 2.1.6).

A spin echo sequence involves a 90$^{o}$ RF pulse to flip the net magnetisation vector into the transverse plane, followed by a 180$^{o}$ RF pulse. Conversely, a gradient echo sequence generally uses smaller flip angles than 90$^{o}$ for the initial RF pulse and does not include a 180$^{o}$ RF pulse.

The echo time (TE) is the time between the initial RF pulse applied and the centre of the echo signal being collected. The repetition time (TR) is the time between corresponding points in a repeated sequence of pulses and gradients. For instance, between successive 90$^{o}$ pulses in spin echo.

For ease of explanation, the rotating reference frame will be used when describing the pulse sequences. This frame of reference ignores the spin caused by the static field, $B_0$, by defining the x and y axes as rotating around the z axis at a frequency which matches the precession frequency. This allows the initial net magnetisation vector to appear static in the longitudinal plane and simplifies the explanation of the magnetisation after application of RF pulses and gradient.

A spin echo sequence involves the application of a 90$^{o}$ RF pulse to flip the net magnetisation vector into the transverse plane where the spins begin to dephase. A 180$^{o}$ pulse is then applied at TE/2 after the

initial 90º pulse to reverse the phase angles of the spins so they refocus and form a spin echo at TE (see figure 5A).

The basic spin echo pulse sequence is shown alongside the generation of the spin echo from the 90º and 180º RF pulses in figure 5.

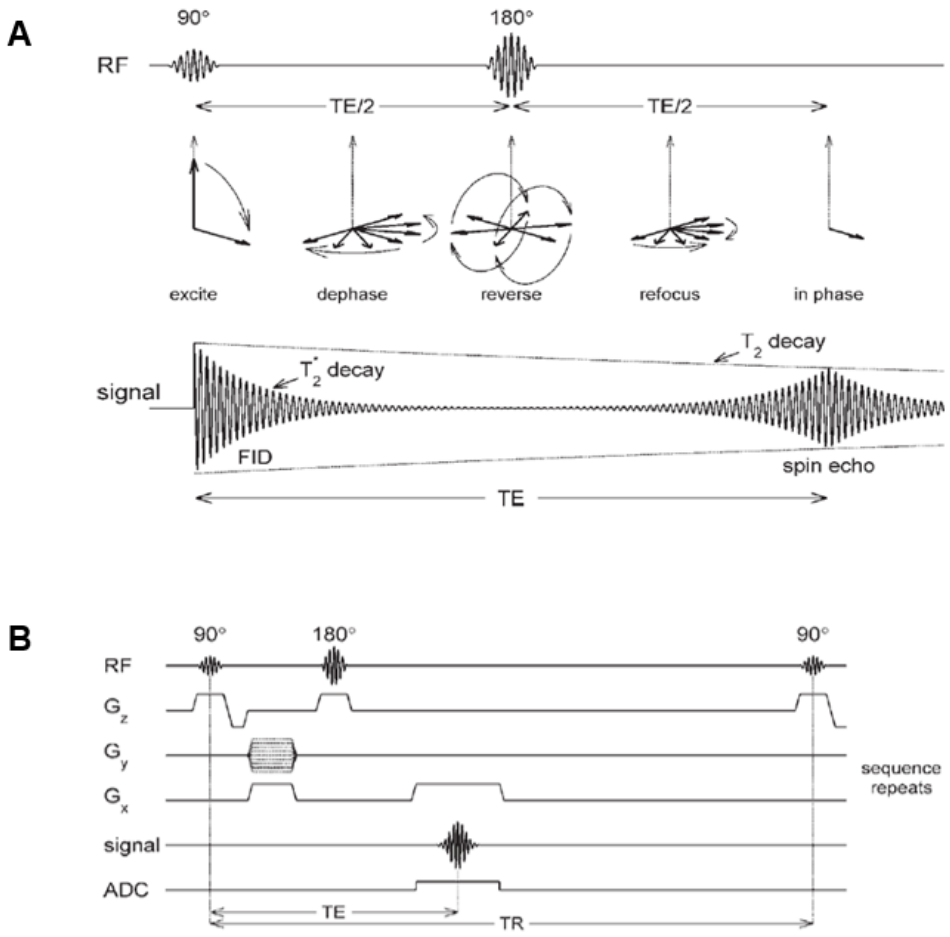


**Figure 5: Generation of a spin echo with excitation from 90º RF pulse which produces the free induction decay (FID) signal which is not collected. There is then dephasing which is reversed by 180º RF pulse. Finally, the spins are refocussed and a spin echo signal is collected when the spins are in phase (A). A typical spin-echo pulse sequence with 90º and 180º RF pulses is shown (B)** [143]**.**

A gradient echo sequence involves the application of a RF pulse (90º or lower) to flip a proportion of the net magnetisation vector into the transverse plane. A negative readout gradient lobe is then applied causing rapid dephasing of the transverse magnetisation. A gradient

of opposite polarity is applied with this positive readout gradient causing the spins to rephase and form a gradient echo (figure 6).

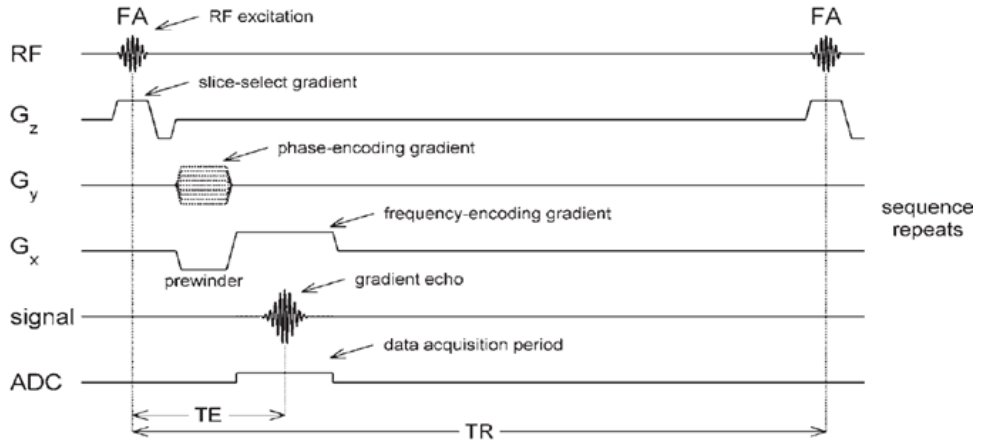


**Figure 6: Typical gradient-echo pulse sequence. RF = Radiofrequency, FA = flip angle, ADC = analogue to digital conversion, TE = echo time, TR = repetition time** [143]**.**

One of the main differences between spin echo and gradient echo is that the signal at TE has decayed by the T2* process in gradient echo and by the T2 process in spin echo. The T2* process in GE occurs through irreversible spin-spin relaxation and reversible dephasing from magnetic field inhomogeneity and local inhomogeneities from tissue susceptibility. The T2 process in SE occurs only through spin-spin relaxation since the 180$^{o}$ pulse removes the effect of the Bo field inhomogeneity (magnetic field inhomogeneity and local inhomogeneities from tissue susceptibility) by rephasing any dephasing that does not vary with time.

## 2.1.5 Conventional T1 and T2 weighting

TE and TR are scan parameters which can be set to provide T1-weighted or T2-weighted (or T2*-weighted) contrast in MRI.

A short TR (and a short TE) will provide T1-weighted imaging if TR << T1 since the net magnetisation vector will not have had enough time to recover fully during the TR interval. The next repeated

application of pulses and gradients will therefore be affected by the T1 values within the tissue being imaged and the next signal will be reduced since there will be less magnetisation available to flip into the transverse plane.

A long TR and a long TE will allow tissues with different T2 values to undergo relaxation, providing T2-weighted (for spin echo) or T2*-weighted (for gradient echo) contrast. In an idealised conventional T2-weighted pulse sequence with a long TR, the net magnetisation vector fully recovers along the z-axis ($M_Z$) to a maximum magnetisation level ($M_0$), leaving no magnetisation in the transverse plane ($M_{XY}$). When the next TR interval starts and the initial excitation RF pulse is again applied, there is the maximum amount of magnetisation ($M_0$) available to flip into the transverse plane. If TR >> T1 then the sensitivity to T1 will be removed from the image contrast.

In balanced sequences, the image contrast obtained is from a combination of T1 and T2 weighting as described in section 2.1.6 below.

### 2.1.6 Balanced Steady-State Free Precession Sequences

Dynamic or ‘cine’ MRI allows small bowel motility to be captured. There are many important factors to consider with bowel motility imaging such as the scan protocol; breath-hold or free breathing, choice of oral contrast, choice of fast imaging sequence/scan parameters, field strength and image post-processing methods. There is a trade-off between spatial and temporal resolution as well as the signal-to-noise ratio (SNR).

Since the acquisition to image bowel motility needs to be fast with low motion sensitivity, rapid sequences such as the balanced steady-state free precession gradient echo, True FISP are acquired which help make the technique reliable even in cases where patients have difficulty holding their breath [144]–[146].

The main reason for these sequences to be used, in the context of bowel motility imaging, is the SNR efficiency (providing good SNR while being quick). Additionally, the image contrast comes from a combination of both T2 and T1 weighting which highlights fluid so oral contrast solution appears very bright on the images, an important feature of bowel imaging. In practice, since low flip angles are used to limit the specific absorption rate (SAR) then some of this balanced contrast benefit is diminished, but it is still adequate with oral contrast.

The disadvantage of True FISP is that banding artifacts are common due to the sensitivity to local inhomogeneities in the magnetic field. This causes dark stripes/black bands to appear in the image, due to off-resonance effects which cause variations in signal intensities. Therefore, TR is set to be as short as possible and shimming, i.e. the application of fields to try to get the field in the body as uniform as possible, should be performed prior to the acquisition. However, in most images this banding artifact can be limited to the edges of the field of view, i.e. outside or at the edges of the body away from the bowel, which is mainly located in the central portions of the image.

If the TR is set to be extremely short (TR << T1 and TR <<T2), which is desirable for fast imaging, then the transverse magnetisation, $M_{XY}$, will not have completely disappeared and the longitudinal magnetisation, $M_Z$, will not have completely recovered. Therefore, when the next excitation RF pulse is applied the signal generated will be reduced, since there is less magnetisation being flipped into the transverse plane.

However, after the application of several RF pulses, typically at least four, with a very short TR interval, a steady-state level of transverse magnetisation ($M_{SS}$) is reached. The aim is to reach the steady-state quickly (to achieve this, the first RF pulse applied may have half the flip angle of the other RF pulses).

The $M_{XY}$ signal fluctuates between $M_{SS}$ and a minimum magnetisation where the signal in the transverse plane does not decay to zero. This is because the TR is short enough that the signal from the free induction decay (FID) never fully disappears before a spin echo and/or stimulated echo is starting to be generated.

FID refers to the exponential decay which occurs immediately after the RF excitation and is not usually measured (although in balanced sequences it contributes to the signal collected at TE).

A spin echo (SE) is produced from a pair of consecutive RF pulses whereas a stimulated echo (STE) is produced from a minimum of three RF pulses, with the STE appearing at the same time as the SE when the sequence is balanced. A steady-state free precession-like sequence demonstrates that if the initial 90º and subsequent 180º refocussing RF pulses in a classic Carr-Purcell-Meiboom-Gill (CPMG) are replaced by identical RF pulses (timed to coincide with each subsequent spin echo), then every pulse is followed by a FID-like signal and an echo-like signal reforms before each pulse (consisting of SE and STE) (figure 7A). This results in steady-state free precession (figure 7B) [147]–[149].

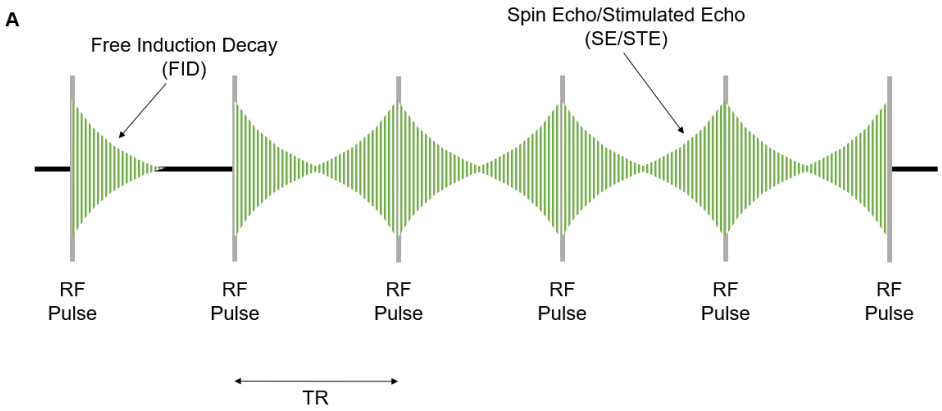

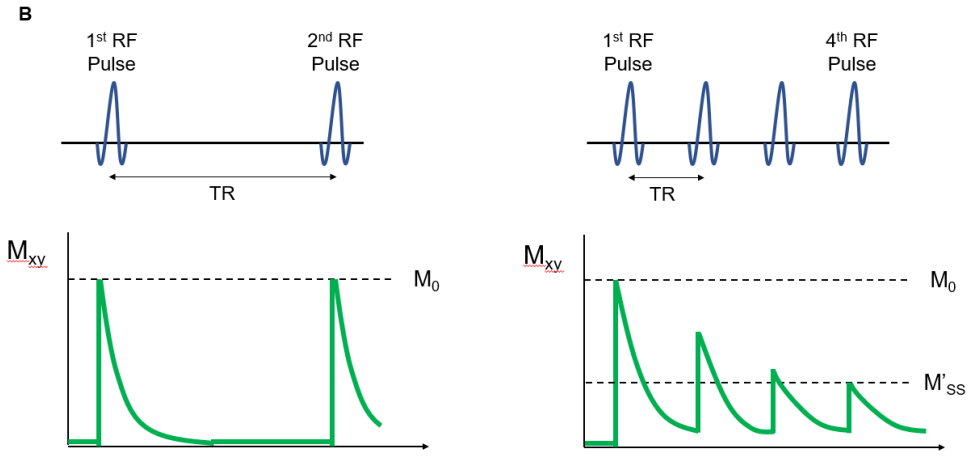


**Figure 7: Steady-state free precession-like sequence where initial 90° and subsequent 180° RF pulses are replaced with identical RF pulses (A) and development of steady-state transverse magnetisation M'$_{ss}$ (B).**

Balanced sequences such as TrueFISP (also known as Balanced-Fast Field Echo or BFFE) therefore utilise FID and SE/STE together. The net dephasing of spins due to gradients over each TR interval is zero, i.e. "balanced" gradients are applied which refocus FID, spin echo and stimulated echo components as a single echo at the centre of the pulse sequence, hence TE = TR/2. Balanced gradients are applied along all three axes as shown in figure 8.

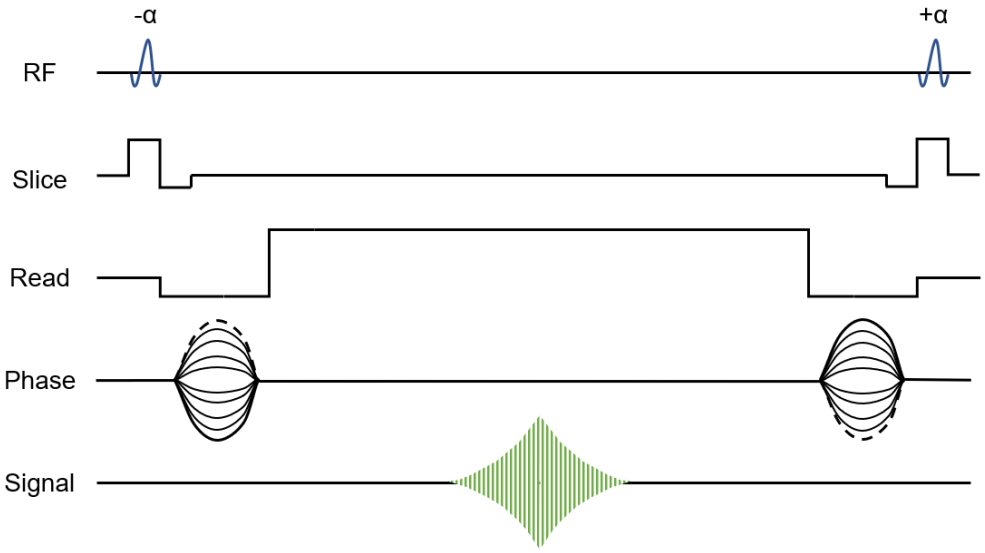


**Figure 8: Balanced Steady-State gradient echo True FISP pulse sequence.**

The acquired signal intensity, $S_{Bal}$, for True FISP relies on both T1 and T2 weighting. If the signal is acquired in the middle of the interval, i.e. TE = TR/2, then there is a dependence on T2 rather than T2* decay:

$$S_{Bal} = k \sin\alpha \frac{1 - e^{-TR/T1}}{1 - (e^{-TR/T1} - e^{-TR/T2})\cos\alpha - (e^{-TR/T1})(e^{-TR/T2})} e^{-TE/T2}$$

**Equation 1: The signal intensity, $S_{Bal}$ for the balanced sequence, True FISP.**

Since TR is much shorter than T1 or T2, then the exponential terms containing TR can be omitted and the signal intensity equation can be simplified to:

$$S_{Bal} = k \sin\alpha \frac{1}{1 + \cos\alpha + (1 - \cos\alpha)(T1/T2)} e^{-TE/T2}$$

**Equation 2: Shorted version of the signal intensity, $S_{Bal}$ for the balanced sequence, True FISP. The signal intensity is related to the T2/T1 ratio.**

The signal intensity is therefore directly related to the T2/T1 ratio. Since the T2/T1 ratio is small for most solid tissues, it means that fat (0.3) and fluids (0.7) are highlighted on these images.

True FISP can be used for both functional (dynamic motility scans) and structural (static anatomical scans) bowel imaging, with a higher spatial resolution achievable in anatomical images, since there does not need to be a trade-off between spatial and temporal resolution. In both cases, oral contrast solution is administered which fills the bowel and appears bright on the images. The main purpose of the contrast is to allow visualisation of the bowel wall, but it may also stimulate motility and be considered as the small bowel equivalent of a cardiac stress test, where the response to a stimulant is measured [150] i.e. the motility response to oral contrast ingestion [151].

### 2.1.7 Subject preparation and scan protocol

Data acquisition is normally performed after ingestion of an oral contrast agent such as mannitol solution or locust bean gum with mannitol solution. If water is used as an oral contrast there is inconsistent distension since it is rapidly absorbed. Since the chemical structure of mannitol prevents intestinal absorption, it remains in the bowel lumen [152].

Ingestion of mannitol is most commonly used in clinical MR enterography since it distends the bowel and allows the bowel wall to examined by radiologists [153]. In the context of this thesis, it also provides contrast to help characterise motility and is useful for texture analysis measures because it appears bright in images. Although the solution has almost no caloric component and therefore should not, in theory, drive fed motion patterns, a marked increase in motility is often seen in the prepared bowel and one might infer that they are seeing segmentation and peristalsis [54]. The mannitol load appears to mimic the postprandial state seen after ingestion of a meal and this can be subjectively assessed [151].

Whilst “stimulating” motility with mannitol has advantages, facilitating quantification over shorter time periods and exaggerating differences between normal and abnormal bowel, it may be desirable in future studies to acquire scans without bowel preparation. This would allow examination of the fasting state, including the migrating motor complex, as well as motility responses to food and drug treatments. However, bowel visualisation would be more difficult without oral contrast due to poor distension.

The two main protocols for acquiring motility data are breath-hold (BH) and free-breathing (FB). BH is commonly used clinically with short scan times of normally 15 to 20 seconds. BH has the

advantage that respiratory motion correction is not needed, but the short scan time may not allow enough time for representative motility patterns to be captured. Additionally, it is more challenging for the patients with recovery time needed between BHs and with multiple BHs there are inconsistences in the positioning of the bowel. FB allows for longer motility datasets to be acquired, but respiratory motion, which has a large effect on abdominal regions, would need to be corrected for, especially with post-processing techniques.

There is always a trade-off between temporal and spatial resolution and coverage in motility imaging, with all parameters important. Currently, multiple 2D slices are acquired in the supine or prone position for most studies, because although 3D motility imaging offers greater bowel volume coverage, there are still challenges with acquisition and post-processing to overcome in order to achieve sufficient temporal and spatial resolution. Clinically, slices are generally acquired in 2D which leads to temporal incoherence between slices.

In this thesis, 2D data is used with the scan duration and temporal resolution necessary for motility analysis explored in chapter 3.

One approach to decreasing the acquisition time is through undersampling k-space to achieve adequate temporal resolution. Parallel imaging methods such as SENSE (SENSitivity Encoding), often used in dynamic imaging, and GRAPPA are commonly used as acceleration techniques.

In GRAPPA (GeneRalized Autocalibrating Partial Parallel Acquisition), partial k-space data is acquired with many phase-encoding steps or k-space lines skipped. Lines through the centre of k-space are fully sampled with this region containing the autocalibration signal (ACS). Global weighting factors are calculated for each coil based on the known data from the ACS. The weighting

factors from all the coils are used, in combination with local known data for each small region, to estimate the missing k-space lines. Fourier transformation is then performed to create individual images from each coil and these images are combined using a sum of squares method to create the final magnitude image [154].

In SENSE, collecting data from multiple, receiver coils to calculate coil sensitivity maps allows the number of phase-encoding steps or k-space lines required for image reconstruction to be lower. A SENSE factor of 2 therefore means that half the k-space lines are acquired i.e. only one out of every two k-space lines are acquired [155].

Another technique for image acceleration is compressed sensing (CS). However, implementation of CS is complicated. CS also did not show any advantages over SENSE for use in bowel motility imaging with diagnostic quality of the scans graded higher in SENSE [156].

Simultaneous multislice (SMS) imaging excites two or more slices simultaneously and this greatly accelerates the acquisition. It is a rapidly developing field and is being adopted by major vendors, but has not yet been applied in dynamic imaging, with challenges to overcome such as noise and phase-encoding artifacts [157].

MRI data used in this thesis is acquired from different scanners at both 1.5T and 3T. At higher field strengths the nuclei precess faster about the $B_0$ axis, which provides more signal and therefore the SNR is generally better at 3T. The differences in contrast between 1.5T and 3T are due to the T1 and T2 changing with field strength. This may have an effect on the appearance of bowel contents and the texture analysis measures calculated in chapter 7.

As previously mentioned, shimming is used to get the magnetic field within the body as uniform as possible. Additionally, ‘dual transmit’ of RF pulses is useful in body imaging, especially at 3T, as an attempt to get the B1 excitation more uniform across the body.

## 2.2 Motility analysis using MRI

Having considered, in the previous chapter, the role of motility in diseases and ways of measuring it using non-imaging or non-MRI techniques, the use of MRI in motility analysis is discussed here. Visual assessment is the simplest evaluation method of dynamic MR motility images. Radiologists view images displayed consecutively as a movie and subjectively grade the contractile activity [158]. In routine clinical practice, radiologists classify the bowel as a binary assessment of either motile or 'hypo-motile'. However, the bowel must be distended with oral contrast to aid the assessment and inter- and intra-observer variation is unknown [159]. Such limitations are potentially surmountable by software quantification of motility.

### 2.2.1 Quantitative motility assessment

Beyond visual radiological assessment, there are several MRI motility quantitative (and semi-quantitative) methods with diameter measurements, displacement mapping and GI tagging summarised in table 4.

| **Motility assessment techniques** | **Advantages** | **Disadvantages** |
|---|---|---|
| Visual radiological assessment | Simple, allows for both local and global motility assessment and can easily be used in the clinic. | Time consuming and training required with large inter- and intra-observer variation (see chapter 5) [160].<br><br>Through-plane motion causes false |

| | | |
|---|---|---|
| | | contractions to be captured. |
| Diameter measurements | Simple and provides quantification of contractions. Can be implemented using either semi-automatic software which provides fast and highly standardised measurements or manually which can be used easily in the clinic. | Cannot provide global assessment since only local contractions are measured and is time consuming if implemented manually.<br>Through-plane motion causes false contractions to be captured. |
| Displacement mapping | Allows for both local and global motility assessment which can be displayed in easily readable motility maps. | Motility is provided as a surrogate measure and only provides the amplitude of contractions, but not the frequency. |
| GI tagging | Allow fully automated analysis of both breath-hold and longer free breathing data. | Long scan durations are necessary to calculate the contraction frequency. |

**Table 4: Summary of the MRI Motility Quantification (and qualitative radiological scoring)** [158]**.**

Visual assessment of motility is simple and easy to implement in the clinic without the need for specialised software for post-processing of MR data. However, it is a time consuming task requiring radiological training and grading of motility can be subject to observer bias. Therefore, there are several quantitative MR motility assessment methods including diameter measurements, displacement mapping and GI tagging, which aim to produce repeatable and reproducible quantitative measurements with a reduction in analysis time.

Diameter measurements are simple and easy to implement if analysing a specific location in the small bowel i.e. the TI. The manual placing of line ROIs in all frames of the motility data can be time consuming and subject to observer bias. Semi-automated analysis through 'Motasso' software (see section 2.2.3) or non-rigid registration (described in section 2.3) provide higher reliability and are faster than manual measurements. However, global diameter measurements are difficult to implement in the small bowel.

Therefore, displacement mapping or GI tagging are preferable for whole bowel motility assessment. Displacement mapping has been shown to provide repeatable global motility measurements [161]. In theory, the motility from displacement mapping is also reproducible since it is unaffected by the variation in intensity changes between scanners i.e. between 1.5T and 3T, assuming the bowel wall is in the same position. The SD Jacobian metric, described in section 2.3.3, calculated from displacement mapping is less intuitive than diameter changes making interpretation of results difficult and the amplitude, but not the frequency, of contractions is capture. Another metric (temporal variation of motility) is developed in chapter 5 to incorporate temporal information into the motility measurement.

GI tagging provides fully automated motility assessment including frequency analysis. It is also more suitable to capture the flow of chyme, than displacement mapping, with laminar flow velocity and direction previously being quantified [162]. However, currently the motion is only measured in one orientation and the MR data is not readily available clinically. The taglines are also particularly obtrusive

for small structures, like the small bowel, so are more suitable for analysing colonic motility.

Texture analysis, described in section 2.4, can be used to capture differences in intensity changes between specific regions of the small bowel and the colon within the same patient. Although not directly a measure of motility, texture analysis can provide information on the contents of the lumen i.e. whether the TI has homogeneous contents or heterogeneous contents (see chapter 7) which results from the flow of chyme. However, texture measures between patients cannot be directly compared since the measures are based on the intensity values from the MR images.

### 2.2.2 Visual radiological assessment

Visual radiological assessment is the simplest method for assessing motility and involves a radiologist scoring a dynamic MRI series that can be played as a “movie” with all consecutive frames being viewed. The radiologist assesses contractions present in the small bowel and the direction of travel of the oral contrast solution. Segmental small bowel motility can be graded on a 5-point scale [160], [163] or through a classification system [164], [165].

The ability of radiologists to subjectively assess more complicated motility patterns is studied through inter- and intra-observer analysis in chapter 5.

### 2.2.3 Diameter measurements

Small bowel diameter measurements allow for simple analysis, but provide only local motility assessment and through-plane motion can be falsely interpreted as a contraction. Changes in the diameter of the lumen over time can be measured by manually drawing a line in all frames of the motility data [166] or in a semi-automated way through ‘Motasso’ software [167], [168] or non-rigid registration

(figure 9). For ‘Motasso’ software, the SB segment is selected by mouseclick in the centre of the lumen. The SB walls are then detected automatically by the software with a line drawn over the selected segment orthogonal to the luminal long axis. The software automatically measures the diameter between the midpoints of the SB wall [169].

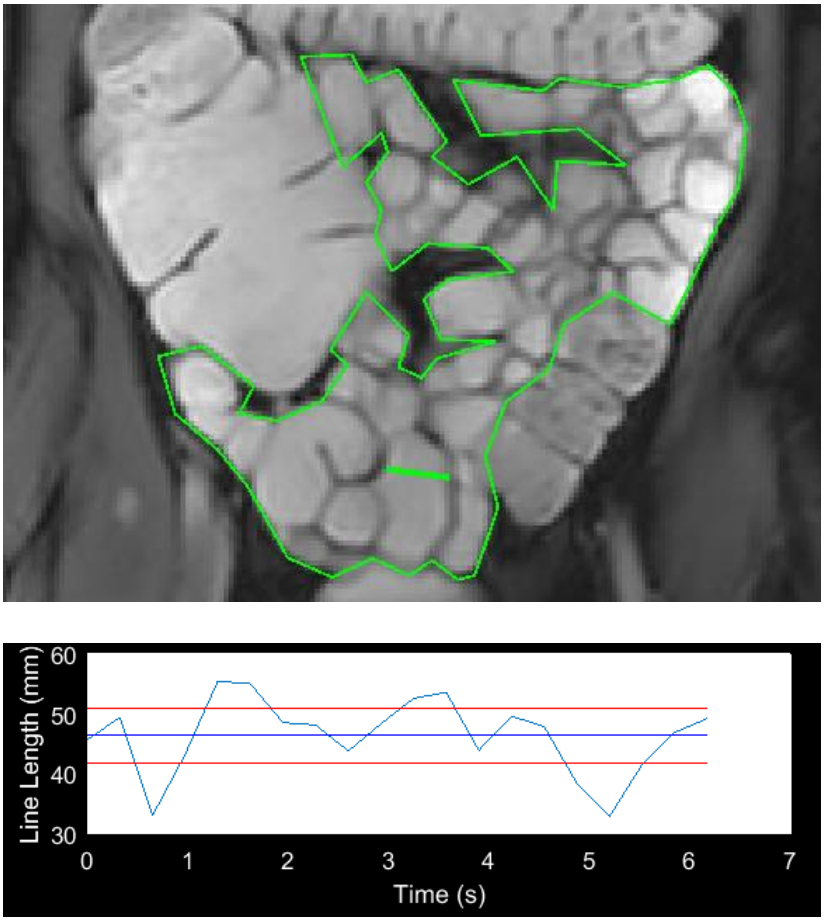


**Figure 9: The line ROI is placed across the diameter of a small bowel loop. A polygon ROI encompasses the whole of the small bowel in the MRI (top image). The measurement of the lumen diameter (line ROI) of a small bowel loop allows tracking of the diameter changes over time frames (bottom image).**

In Crohn’s disease (CD), diameter measurements of small bowel motility have been correlated with inflammatory markers, C-reactive protein and calprotectin [169], and histopathology in the terminal ileum [170], as well as differentiating between CD patients with and without histologically proven acute inflammatory changes [171]. The mean diameter of inflammatory small bowel lesions have also been correlated with the dilatation of non-CD affected segments [172].

A decrease in motility, measured by the contraction ratio [(maximum extension of luminal diameter – maximum contraction of luminal diameter)/maximum extension] in MRI, was found in CIPO patients which was validated by the equivalent findings from manometry [58], [59]. Several studies have measured gastric diameter [173]–[175] and in the colon MR and manometry measurements have been simultaneously acquired [176].

Contractions per minute (CPM) allows contractility frequency to be calculated as a diameter change of more than 10% of the mean luminal diameter, but requires longer scans [177], [178].

One of the main drawbacks of diameter measurements are that they can only assess motility locally (although if only analysing a specific location e.g. the TI in CD then this is sufficient) and they are subject to bias and potentially poor inter-reader agreement. However, subtle non-occlusive contractions seen in MRI [159] are not always picked up by manometry.

Therefore, a technique that assesses motility both locally and globally and is sensitive to smaller contractions is desired. Recently, a move towards a global lumen diameter measurement was demonstrated in the stomach and colon. This involves manually drawing lines in the centre of the lumen and the walls either side of the lumen. Several measurements of diameter can be obtained perpendicular to the central line drawn in the lumen (see figure 10) [179]. However, this is more difficult to implement in the small bowel due to through-plane motion of bowel segments causing the disappearance of the bowel wall in some frames and therefore the diameter measurement would fail in these cases.

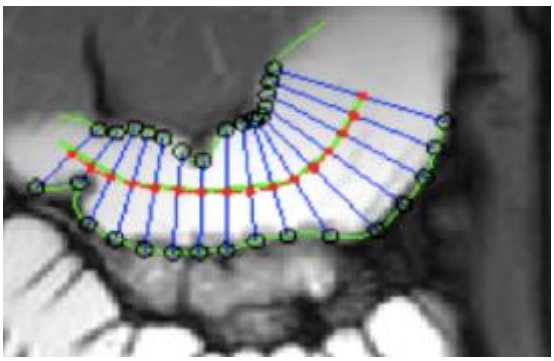

**Figure 10: Lines are manually drawn in the centre of the lumen and the two walls either side of the lumen (green lines). Nodes (red dots) are automatically placed along the central lumen line with spacing defined by the user. Lines connecting the two bowel walls through the nodes are generated perpendicular to the central lumen line (blue lines) which allows the diameter and position of each line to be recorded for each time point in a cine MRI series** [179]**.**

## 2.2.4 GI Tagging

SPAMM (SPatial Modulation of the Magnetisation) was developed initially for assessing myocardial wall motion. Taglines are applied to body tissue by saturating the magnetisation. There is then a delay, allowing movement of the tagged tissue, before the readout gradient is applied. These lines therefore deform due to motion caused by motility (see figure 11). Quantification techniques have allowed tracking of taglines in the frequency domain [180] and the measurement of laminar flow velocity and direction [162].

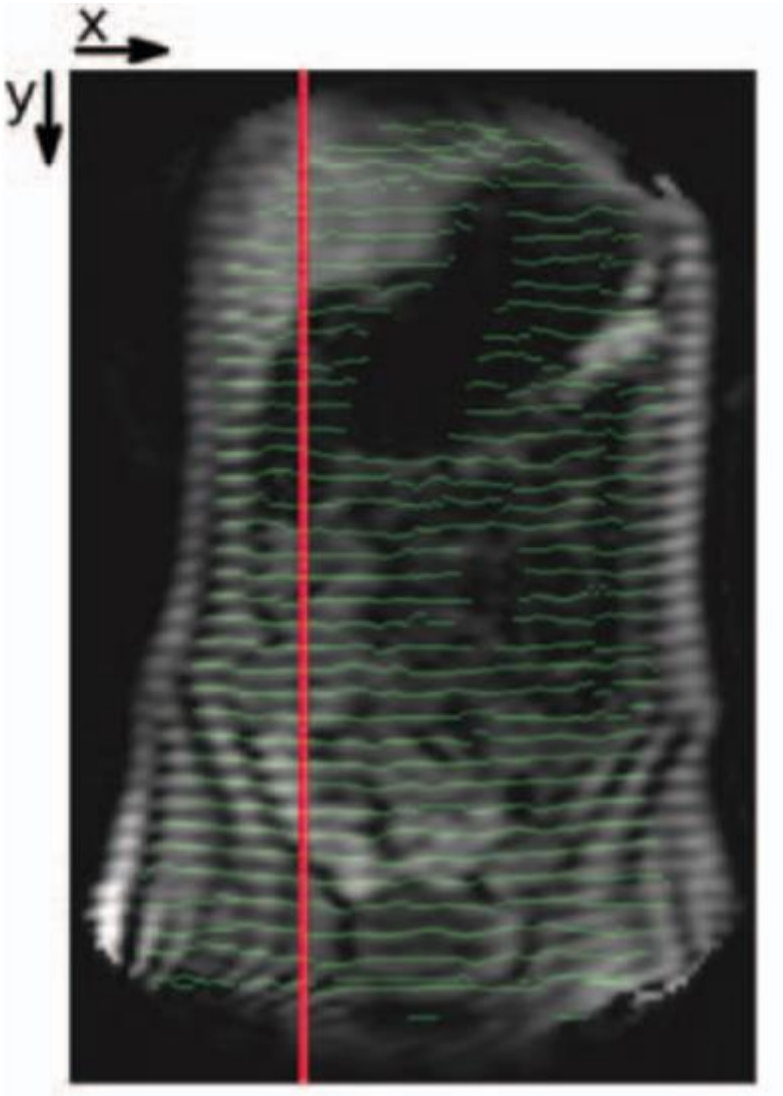


**Figure 11: Example of a coronal tagged MRI image. ROIs can be placed along the dark taglines (green horizontal lines) and deformation of these taglines can be tracked through time by analysis in the y-direction (red vertical line)** [180]**.**

Good coverage of the bowel with a high temporal resolution can be achieved during longer free-breathing acquisitions since the technique can perform well with lower spatial resolution than is needed for diameter measurements and displacement mapping. Pharmacologically induced changes in motility have been detected following quantification [181].

The clinical utility is limited by the complexity of the technique generally. Additionally, longer scan durations of the order of minutes are required for GI tagging/SPAMM colon measurements where contractions are not frequent enough for BH.

### 2.2.5 Displacement mapping

Motility maps generated from non-rigid optic-flow based registration allow for rapid assessment of GI motility (see section 2.3). The aim is to address the need for a global measure of motility and to tackle this problem with a quantitative solution. Additionally, motility can be measured locally with this technique. The benefits are repeatable motility measurements and sensitivity to motility differences in health and disease as well as pharmacologically induced motility changes.

The main limitations are that the local area change captured in this metric is less intuitive than diameter changes in mm making it difficult to interpret since it is a surrogate measure of motility and the information about the frequency of contractions is lost.

## 2.3 Image registration for motility quantitation

In this PhD, dynamic or cine MRI data has been collected as a time series of images or frames displaying bowel motion, following ingestion of mannitol as the oral contrast agent. In this section, image registration will be described briefly in the context of quantitative assessment of motility. Firstly, there will be a background overview of registration [182]–[184].

### 2.3.1 Registration Background

Image registration is used to line up the same anatomy in the same image position throughout all the images or frames. Generally, corresponding pixel intensity values or features are used to match the images and bring them into spatial alignment. Registration is an iterative process involving three main steps:

- Transformation model
- Cost Function (similarity measure and regularisation)
- Optimisation scheme

Using the simplest case of registering one image (the floating or source image) to another image (the reference or target image), the first step is to apply a transformation model. For each pixel with coordinate (i, j) in the reference image, the corresponding anatomy is at point (i', j') in the floating image. The floating image is transformed or deformed by computing the displacement vector to transform the coordinates of each pixel in the floating image, so they are in anatomical alignment with the reference image, resulting in a transformed floating image. For our method, multiple images are individually registered to a single reference frame (see section 2.3.3).

The simplest transformation models are rigid-body transformations, which involve only translation and/or rotation, and affine transformations, which combine a rigid-body transformation with a shear and scaling transformation to stretch/compress the entire image. Non-rigid transformations are more complex with individual pixels in the floating image able to undergo displacement to match the corresponding reference image pixels.

Rigid registration only needs 6 parameters to describe motion i.e. translation in 3 directions and rotation in 3 directions. Non-rigid registration requires more parameters with a **displacement or deformation field** consisting of all the pixel displacements across the whole image i.e. typically a vector field with a resolution similar to the underlying image [185].

A cost function is used to quantify the alignment of the two images, typically including a similarity measure and regularisation. The simplest and most computationally efficient measure of similarity is sum of squares difference (SSD). This compares intensity

differences between floating and reference images directly through subtracting the corresponding pixel intensity values and then summing the square of these values.

This is most commonly used in monomodal problems where the images being registered were acquired using the same sequence e.g. all the frames in a dynamic MRI time series dataset. Monomodal in this context refers not only to data acquired from the same type of scanner, i.e. registering MRI to MRI or registering CT to CT, but specifically registering two MRI images acquired using the same type of sequence and therefore with a similar image intensity contrast i.e. registering two T1 MRI images together, rather than a T1 MRI image being registered to a T2 MRI image. SSD works best when the image intensity contrasts are similar.

Other examples of similarity measures are normalised cross correlation, where a linear relationship between image intensities is assumed, and information theoretic measures based on image entropy, such as mutual information and normalised mutual information, where the amount of information (entropy) is quantified by using probability distributions [186]–[188].

Regularisation is another feature of the cost function, which is intended to act as a penalty or a restraint, so the deformations are physically realistic. For instance, there is a need to stretch the floating image to match the reference image while restricting the deformation, so the resulting deformed image is still biological plausible. If only the constraint was applied, then the image would not be deformed at all whereas if only the measure of similarity is applied then there would be no regularisation and there is the potential for image folding i.e. where tissue within the image disappears due to overfitting. The regularisation can be implicit, i.e. embedded within the transformation model, or explicit i.e. adding a penalty term to the cost function which will limit the deformation.

Finally, an optimisation scheme is employed to maximise the alignment between two images through numerical maximisation of the measure of the cost function. Common numerical optimisation schemes include gradient descent, conjugate gradient and Gauss-Newton schemes.

### 2.3.2 Non-rigid registration and modelling of intensity changes algorithm

There are two main families of non-rigid registration algorithms characterised by parametric, e.g. free form deformation, and non-parametric, e.g. optical flow. Rigid registration is not suitable for the small bowel since motility cannot be captured by translation and rotational movement only.

Parametric algorithms involve a mathematical formulation to obtain the deformed transformation with the deformation parameterised e.g. using B-splines. Free form deformation involves a deformation field generated from a grid of control points with gross movement around each grid point. The control point grid may be less dense than the underlying pixels [189].

In non-parametric algorithms such as optical-flow, a dense deformation field, with every pixel having its own degree of freedom (DoF), can be implemented. This has the advantage of being sensitive at a small scale and allows estimation of accurate, high resolution displacements characterised by large local motion as seen in bowel motility [190].

The implementation used in this thesis involves a coarse-to-fine approach by initially using a coarse resolution i.e. a 256x256 image is downsampled to 16x16 for speed and gross large-scale motions before increasingly fine resolutions are used until every pixel has a DoF.

An existing non-rigid optic-flow based registration technique [191] has been adapted for quantitative assessment of motility [192]. It has the benefit of being quantitative and repeatable and is therefore the basis of the motility analysis in this thesis. The development and use of the registration algorithm by Odille et al. (2012) was an important advance for two reasons:

1. The time taken for assessment of bowel motility could be rapidly reduced through the automation of the registration.
2. The deformation fields themselves could be used as a surrogate measure of motility and provide an entirely novel method of global bowel motility assessment.

Odille et al. (2012) combined joint registration of local deformations, i.e. bowel motility generated by bowel wall motion, and modelling of intensity changes over time, caused by movement of luminal content through the bowel.

The incorporation of modelling of intensity changes was to account for local intensity changes due to through-plane motion i.e. segments of bowel 'disappearing' out of the slice during the time series. Breath-hold protocols are often used to limit this through-plane motion. Additionally, there are intensity changes both in-plane and through-plane caused by the flow of chyme within the bowel. Without accounting for these intensity changes, which can be substantial from time frame to time frame, registration algorithms can struggle to differentiate between intensity change, due to structures moving, from a change in the underlying intensity. Assumptions of similarity measures are violated or less favourable when localised intensity changes occur [193]–[197].

Therefore, an explicit model of intensity changes is optimised simultaneously with the deformation fields in the registration. In a dynamic MRI dataset, there are $N_t$ frames which contain $N_x$ x $N_y$ pixels so the images can be represented by a vector ρ of length

$N=N_x*N_y*N_x$ and the intensity changes over time are expressed as follows:

$$c = \rho_{ref} - T_{ux,\,uy} * \rho$$

**Equation 3: The intensity changes model, c is calculating from the difference between ρref i.e. an N-length vector of the reference frame intensities replicated $N_t$ times and the transformation, Tux, uy applied to all the images in N-length vector ρ. Tux, uy is a sparse matrix which interpolates image intensity values at the locations pointed by the deformation fields.**

The cost function consists of the similarity measure, SSD and an additional constraint or regularisation term, R, which imposes a spatial smoothness on the displacement vectors in the x and y direction ($u_x$ and $u_y$ respectively) and the model of all the intensity changes not due to in-plane bowel wall motion (c), to ensure plausible biological deformations occur.

$$C(u_x, u_y, c) = SSD(u_x, u_y, c) + R(u_x, u_y, c)$$

**Equation 4: The cost function to be minimised with respect to the displacement vectors, $u_x$ and $u_y$ and the model of intensity changes, c.**

The weights given to the spatial smoothness of the displacement fields and maps of intensity changes can be tuned. These weights were not changed for the research in this PhD due to this being a validated technique used in multiple previous studies with baseline measures for healthy controls [151], [161], [198] and Crohn's disease patients (see section 2.2) based on a standardised measure of motility which will be discussed in detail below.

A Gauss-Newton optimisation scheme was implemented by Odille et al. (2012) to minimise the cost function with respect to $u_x$, $u_y$ and c. This is a nonlinear least-squares optimisation problem which is solved iteratively by solving a series of easier linear least-squares problems as follows:

$$\begin{bmatrix} \delta u_x^{opt} \\ \delta u_y^{opt} \\ \delta c^{opt} \end{bmatrix} = \left( \begin{bmatrix} diag(\partial_x \rho\,^2) & diag(\partial_x \rho\,.\,\partial_y \rho\,) & diag(\partial_x \rho) \\ diag(\partial_x \rho\,.\,\partial_y \rho\,) & diag(\partial_y \rho\,^2) & diag(\partial_y \rho) \\ diag(\partial_x \rho) & diag(\partial_y \rho) & I \end{bmatrix} + \begin{bmatrix} \lambda_u H^T H & 0 & 0 \\ 0 & \lambda_u H^T H & 0 \\ 0 & 0 & \lambda_c H^T H \end{bmatrix} \right)^{\tau} * \left( \begin{bmatrix} diag(\partial_x \rho)\, \rho_{res} \\ diag(\partial_y \rho)\, \rho_{res} \\ \rho_{res} \end{bmatrix} - \begin{bmatrix} \lambda_u H^T H\, u_x^{(k)} \\ \lambda_u H^T H\, u_y^{(k)} \\ \lambda_c H^T H\, c^{(k)} \end{bmatrix} \right)$$

**Equation 5: At each iteration, k an optimal update to the displacement fields is calculated through optimisation of the cost function with respect to $u_x$, $u_y$ and c. I is a NxN identity matrix, diag(∂x ρ) and diag(∂y ρ) are NxN diagonal matrices containing diagonal elements of the partial derivatives of the images ∂x and ∂y respectively, λu and λc are the weights given to the spatial smoothness of the displacement fields and intensity changes respectively, H is the Hessian matrix and $\rho_{res}$ is the residual registration error. The superscript, T is the transpose and the superscript, τ is the estimated inverse.**

### 2.3.3 Deformation fields used to summarise motility

In the algorithm used throughout this thesis, the reference image was selected as the image or frame within the time series which most closely matched the median image of the series, based on the minimal Euclidian distance between images. The algorithm searches for deformation fields and intensity changes over time, that best match each frame from the time series onto the selected reference frame. After registration, the frames are in spatial alignment and there is one deformation field per frame.

The deformation fields were used to automatically generate motility maps to quantify small bowel motility (figure 12). Since the registration was non-rigid, this allowed local deformations to be captured since pixels/voxels would be able to change in both size and shape.

The Jacobian determinant was calculated from the deformation fields acquired during registration and provided a single scalar value per pixel in every frame. In a 2D image, this represents the area change that each individual pixel in an image undergoes when being transformed to the equivalent pixel in the reference image.

The Jacobian determinant of the deformation fields can be used to check for folding, with a Jacobian determinant < 0 indicating folding and an error in the registration due to the lack of an appropriate constraint.

If the Jacobian determinant is 1 this represents no area change (but the pixel can still move in the image as long as the area is the same). A pixel being compressed with the pixel area decreasing (and no folding) gives a Jacobian determinant value between 0-1 and Jacobian determinant values over 1 means the pixel area has increased.

The standard deviation (SD) of the Jacobian determinant of the deformation fields with respect to time is calculated and will henceforth be referred to as the SD Jacobian in this thesis. This summarises the variations in time of the local expansion and contraction on a per pixel basis and is displayed on the reference frame (or motility map). The motility map therefore essentially displays the SD Jacobian over time, which represents the area change of each pixel in the image.

The SD Jacobian is now a well tested motility metric and should, in theory, be robust to rigid movements that are independent of true motility, since the Jacobian determinant for a rigid transformation (no local area change) is 1. The SD Jacobian would be approaching zero in regions which only move rigidly, such as organs where an imperfect breath-hold leads to translation, but not a change in shape of that region. It would also have a near zero value in regions which do not move, with higher SD Jacobian values occurring when there are large local contractions and expansions as seen in normal bowel motility. The SD Jacobian should represent the amplitude of contractions, but not the frequency as summarisation by taking the SD leaves it ‘blind’ to time. Regions of interest (ROIs) can be manually drawn on this SD Jacobian map, allowing direct analysis of the deformation fields.

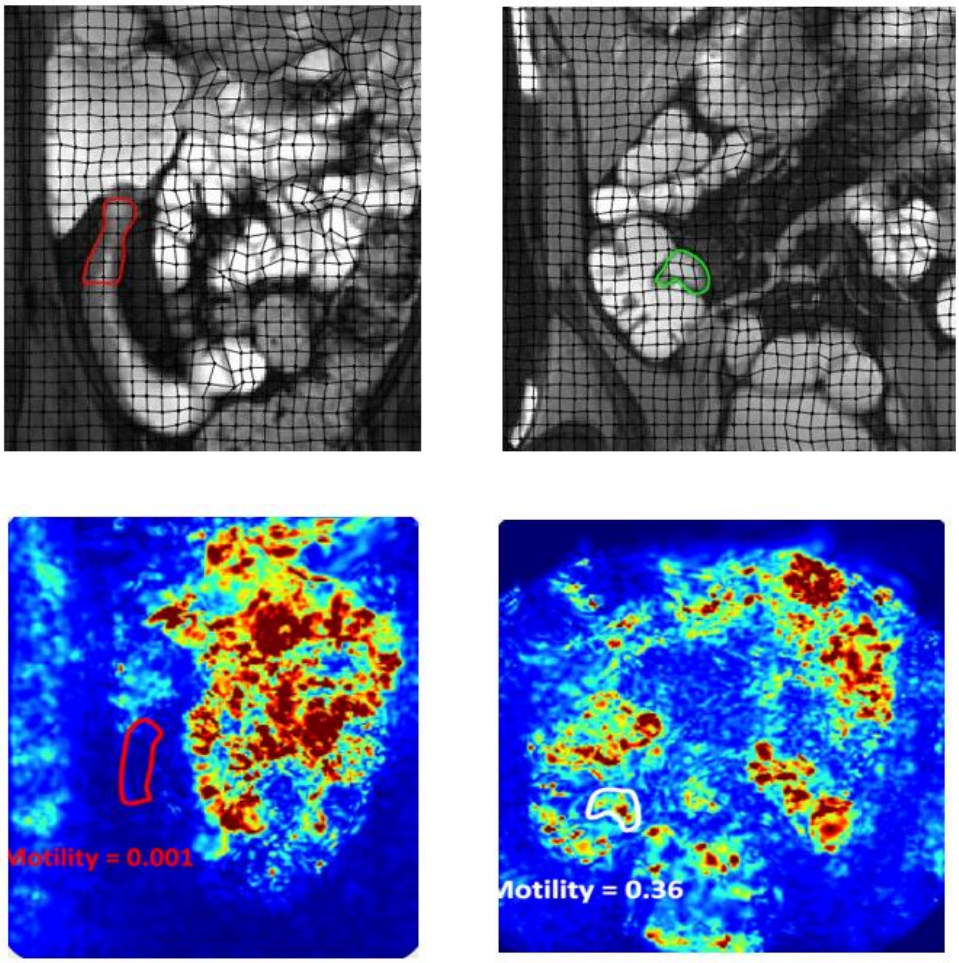


**Figure 12: A deformation grid used in the displacement mapping is overlaying a coronal dynamic MRI image to represent the deformation field (top images). The motility maps generated from these deformation fields are displayed (bottom images). For low motility (red ROIs), the pixels do not deform greatly (top left) and this corresponds to a low mean motility of 0.001 on the motility map (bottom left). Conversely, for high motility (green and white ROIs), the pixels are deformed to a greater extent (top right), providing a higher mean motility of 0.36 (bottom right).**

Several metrics have been derived from this SD Jacobian map, with new metrics developed as described in chapter 5. The most commonly used metric in the literature is the mean SD Jacobian within an ROI (it is often referred to as the motility index in the literature, although this term has also been used to describe other motility measures), which in healthy bowel usually has a value around 0.3, in diseased bowel <0.015 and in extreme cases can get as high as 0.7 [161], [199].

This thesis will focus on the use of these metrics in relating motility to symptoms in Crohn's disease and irritable bowel syndrome. Additionally, texture analysis measures, which will be described in the next section, will be used in chapter 7 to compare IBS-C patients with healthy controls.

## 2.4 Texture Analysis

Balanced sequences are not only used for the acquisition of dynamic MRI, but are used to acquire anatomical data with higher spatial resolution. As described in section 2.1.6, these sequences provide T2/T1 image intensity contrast which highlights fluids and fat, since they have a much higher T2/T1 ratio compared to most solid tissues. Therefore, an oral contrast agent such as mannitol, which is ingested prior to MRI data acquisition, will fill the bowel and appear bright on the images. In theory, for healthy individuals, there should be smooth transit of mannitol through the whole small bowel and into the colon, with the luminal contents appearing bright throughout the small bowel and in most of the colon (depending on the transit time of the individual).

However, anecdotally, radiologists have reported a "faecalisation" of terminal ileum luminal content on MRI performed in IBS-C patients. This is hypothesised to be reflux of caecal contents from the ascending colon and caecum back into the terminal ileum. (see figure 13).

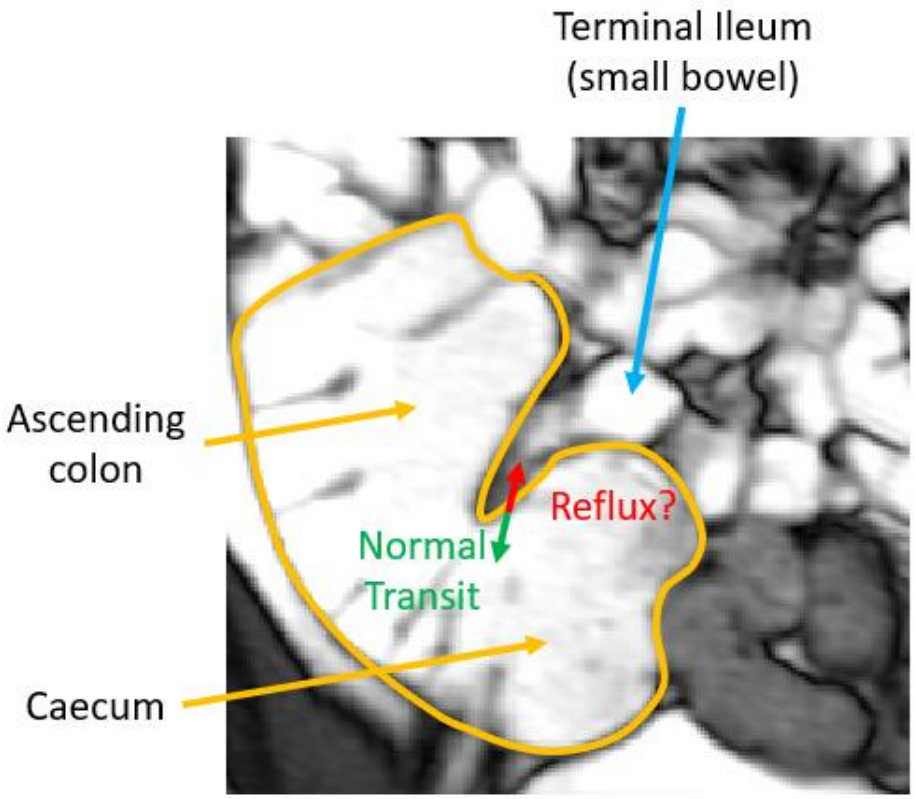


**Figure 13: Normal transit (in green) from terminal ileum (blue) into caecum (orange) and potential abnormal reflux (in red) from caecum back into the terminal ileum.**

### 2.4.1 Texture Analysis Medical Imaging Applications

Texture Analysis uses statistical measures to characterise the texture of an image. The texture is the appearance of a ROI i.e. the grey level differences between neighbouring pixels. Texture analysis methods have been used in medical imaging for segmentation of a particular anatomical region of interest [200], [201], but are most commonly used to differentiate between healthy and diseased tissues [202].

Applications in MRI include the improvement in the diagnosis of skeletal muscle dystrophy using texture analysis [203], spinal cord MR differences in multiple sclerosis and healthy controls [204], differentiation between healthy and pathological MR brain images, e.g. in Alzheimer's disease [205], [206], brain tumour grading in T1-weighted MRI [207], segmentation of diffuse brain lesions [208] and

lesions of focal cortical dysplasia in T1-weighted MR images [209]–[211], which has potential uses in epilepsy [211]. Several studies used texture analysis to distinguish pathological hippocampal tissue from healthy tissue to identify epilepsy patients suitable for surgery [212]–[215].

In other imaging modalities, other than MRI, colposcopic images were used to characterise cervical lesions [216] and CT lung images were used to differentiate between a range of obstructive lung diseases and healthy subjects [217].

In this PhD, texture analysis will be used for examining texture differences in small bowel and colon luminal content in IBS patients and healthy controls (figure 13 above). Common texture analysis methods will be briefly described, with more detail on the use of the grey level co-occurrence matrix (GLCM) which is the most appropriate method for the application in chapter 7.

### 2.4.2 Texture Analysis methods including GLCM

There are several statistical texture analysis methods; histogram, absolute gradient, run-length matrix and grey level co-occurrence matrix (GLCM) [202].

Histogram analysis can be considered as “first order” since measures such as mean, variance, entropy, kurtosis and percentiles consider all the pixels in the ROI independent of their local neighbourhood and therefore they are non-spatially dependent measures [202], [218].

“Second order” texture measures consider relationships between pairs of pixels [218]. Absolute gradient calculates variations from pixel to pixel, e.g. if there is an abrupt change from a pixel of low intensity to a pixel of high intensity, then the absolute gradient will be high. Conversely, if the two neighbouring pixels have a similar

intensity level, i.e. both pixels are low intensity or both pixels are high intensity, then the absolute gradient will be low. This is useful for edge detection and can therefore be utilised in segmentation methods [202].

Run-length matrices are calculated based on the run size, which is the number of consecutively adjacent pixels with the same grey-level value, and the direction to search for this run of pixels. Generally, four matrices are calculated for horizontal, vertical and two diagonal (north-west to south-east and north-east to south-west) directions. For example, if there are 8 grey levels and runs are calculated for four run sizes from 2-5 pixels then the size of the run-length matrix for each direction will be 8x4. Measures that can be derived from these matrices are “short-run emphasis”, which represents the proportion of runs in the image that have a short length e.g. less than 3 pixels in a row with the same grey level, and “fraction of images in run”, which is the percentage of image pixels that are part of any of the runs calculated in the matrix computation [202], [219].

The focus in this thesis will be the texture measures derived from the GLCM since the aim is to capture the textural appearance of bowel contents where relationships between neighbouring pixels are important (i.e. not histogram analysis) and there is no concern about the directionality of the texture (i.e. not run-length matrices) or edge detection (i.e. not absolute gradient measures). It should be noted that in the context of texture analysis (TA), TA contrast refers to a summary measure of the GLCM which is different from mannitol being referred to as an oral contrast solution. Image contrast refers generally to differences between tissues in the MR image.

GLCMs are calculated based on the pixel distance/spacing i.e. the distance between the pixel of interest and its neighbour, the number of grey levels in the image and the direction of analysis [202], [218], [220].

The size of the GLCM is also dependent on the number of grey levels, e.g. if 32 grey levels are chosen for creating the “scaled” image then the size of the GLCM calculated will be 32x32, since the calculation is based on counts between pairs of pixels.

Once the scaled image has been created, the calculation of a GLCM involves selecting a direction (0º, 45º, 90º, 135º) and a distance between the pixel of interest and its neighbour (1 pixel, 2 pixel, 3 pixel, 4 pixel distance) to be analysed (figure 14). A count is then made between pairs of pixels separated by this defined distance in the given direction for the distribution of grey level values.

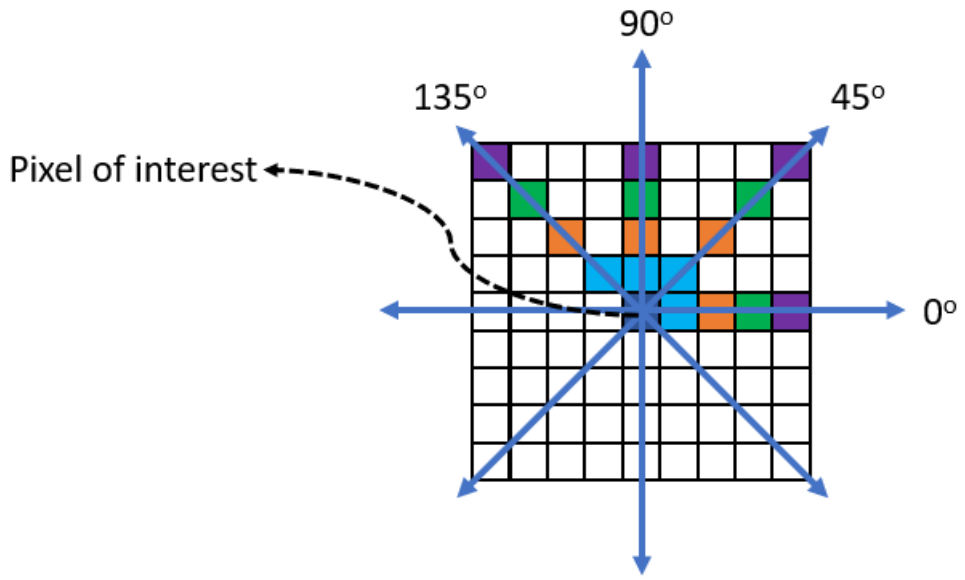


**Figure 14: Calculation of a grey level co-occurrence matrix (GLCM) involves selecting a direction (0º, 45º, 90º, 135º) and a distance between the pixel of interest (dark blue) and its neighbour (1 pixel = light blue, 2 pixels = orange, 3 pixels = green, 4 pixels = purple).**

## 2.4.3 GLCM Summary Measures

Texture analysis summary measures; contrast (texture analysis contrast, not to be confused with oral contrast), energy and homogeneity can be derived from the GLCM. Since the directionality

in regards to the texture is not a concern, the summary measures would be averaged for the 4 directions [221].

Texture analysis contrast (TA contrast) is a measure of local image variations, i.e. the measure of the intensity contrast between a pixel and its neighbour with a range of values from 0 (for a constant image) to 961 [ (number of grey levels – 1)$^2$ ] [220], [222].

$$\sum_{i,j} |i-j|^2 \, p(i,j)$$

**Equation 6: TA contrast equation where i is the row position, j is the column position and p(i,j) is the (i,j)th value in the GLCM.**

Texture analysis energy (TA energy) has a range of values from 0 to 1 (for a constant image) so, therefore, a higher TA energy image will be more homogenous and the TA contrast will be lower [220], [222].

$$\sum_{i,j} p(i,j)^2$$

**Equation 7: TA energy equation where p(i,j) is the (i,j)th value in the GLCM.**

Texture analysis homogeneity (TA homogeneity) has a range of values from 0 to 1 and gives a measure of the closeness of the distribution of the elements in the GLCM to the GLCM diagonal. Therefore, a homogenous image with pixel pairs containing similar grey levels i.e. counts along or near the diagonal will return a higher TA homogeneity value [220], [222].

$$\sum_{i,j} \frac{p(i,j)}{1+|i-j|}$$

**Equation 8: TA homogeneity equation where i is the row position, j is the column position and p(i,j) is the (i,j)th value in the GLCM.**

Therefore, a heterogenous ROI will have a high TA contrast, a low TA energy (nearer to 0) and a low TA homogeneity (nearer to 0) and vice-versa for a more homogenous ROI. In the example below the chosen pixel spacing for calculating the GLCM has a large effect on the TA contrast whereas the effect of pixel spacing on TA energy and TA homogeneity is less pronounced (figure 15).

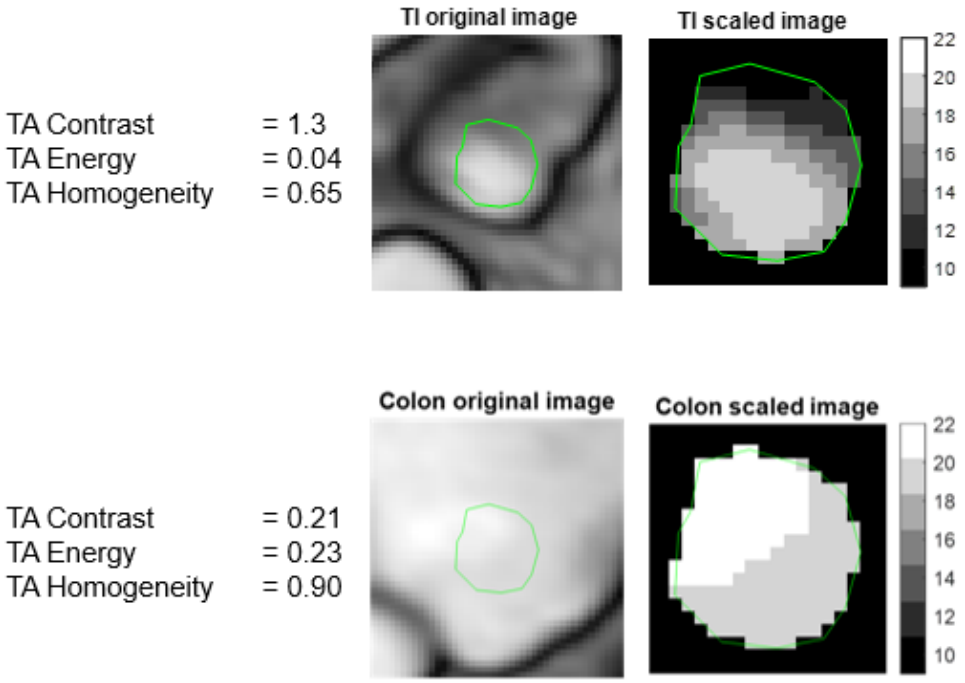


**Figure 15: The heterogeneous texture in the TI ROI is represented well by the scaled texture image (top) where there is a range of grey level values seen. Conversely, the homogenous texture in the colon ROI is represented by a homogenous scaled texture image (bottom) with much fewer grey level values. The summary measures accurately represent the heterogeneity/homogeneity of the texture seen in the image with over a fivefold increase in TA contrast for the heterogeneous ROI (0.21 to 1.3) and over a fivefold increase in TA energy for the homogeneous ROI (0.04 to 0.21).**

## 2.4.4 Texture Analysis GLCM summary

In summary, GLCMs allow comparison of pixel pairs; similar grey levels within an ROI indicating smooth, homogenous texture whereas several different grey levels within the ROI would indicate rough, heterogeneous texture.

In chapter 7, ratios between the TI and the SB (TI/SB ratio) and between the TI and colon (TI/colon ratio) will be calculated. In healthy controls, it is expected that both of these ratios will be around 1 since the luminal contents should be homogenous in the small bowel and the colon. However, in IBS-C patients it would be expected that the ratios would be either above (TA contrast) or below (TA energy) 1, due to the heterogenous texture within the TI.

## 2.5 Chapter Summary

This chapter has given a summary of MRI acquisition using balanced sequences to acquire static/anatomical and dynamic MRI and the current post-processing techniques used in the quantitative MRI assessment of motility. In particular, dynamic MRI with quantification using a non-rigid registration algorithm provides an excellent non-invasive method for assessing motility. Additionally, texture analysis will be used to examine luminal contents within the small bowel and colon in chapter 7. The main drawback with these analyses is the lack of standardisation in the data acquisition and analysis with different options to consider when designing the study protocol, which could affect the analysis.

The next chapters (chapters 3-7) in this thesis aim to address some of the current unknowns. Specifically:

- **Scan parameters** – the minimum requirements in terms of temporal resolution and scan duration (**discussed in chapter 3**)
- **Motility metrics** – is motility being adequately captured with the appropriate metrics and can quantitative motility measurements offer improvements over subjective radiological assessment in certain cases (**discussed in chapters 4 and 5**)?
- **Symptom scoring** – which questionnaires are better clinical outcome measures for testing the relationship between motility and symptoms in GI conditions (**discussed in chapters 4, 5 and 6**)?
- **ROI selection** – do segmental or global measures of motility correlate better with symptoms in CD and IBS (**discussed in chapters 4, 5, 6 and 7**)?
- **Texture Analysis** – can texture analysis measures in anatomical data be used to find differences between IBS-C patients and healthy controls (**discussed in chapter 7**)?

# Section B: Validating and testing assumptions of dynamic MRI acquisition and small bowel motility analysis

**Section B** presents work testing and validating previous assumptions for quantitative analysis in small bowel motility studies.

In **Chapter 3**, the imaging protocols for dynamic MRI acquisition are examined in six healthy volunteers as part of a joint research study carried out with a collaborator from Academic Medical Center (AMC), Amsterdam (see author declaration in chapter 3). The required scan duration and temporal resolution are studied in dynamic MRI within the context of quantitative motility assessment of the small bowel. There has been limited data to guide imaging protocols with respect to quantitative analysis. This chapter suggests the minimum temporal resolution and scan duration required in breath-hold scans to obtain robust measurements of small bowel motility from dynamic MRI.

In **Chapter 4**, a previous single-centre study suggesting an inverse correlation between normal small bowel spatial variation of motility and abdominal symptoms in 53 CD patients [65] is validated here in a larger, two-centre study of 82 CD patients.

# Chapter 3: Dynamic MRI for bowel motility imaging – how fast and how long?

## Author Declaration

The work presented here was jointly led by the thesis author (2 years of experience at time of publication) and Sofieke De Jonge (3 years of experience at time of publication) working in collaboration on performing the literature review, analysis of the scan duration (main focus of the thesis author) and temporal resolution (main focus of De Jonge), under the supervision of Alex Menys, Stuart Taylor, David Atkinson, Aart Nederveen and Jaap Stoker.

Data was collected at Amsterdam (AMC) by Sofieke De Jonge. Alex Menys and Freddy Odille developed the registration algorithm and the graphical user interface (GUI) displaying the dynamic MRI data and motility maps. The thesis author enhanced the functionality of the GUI for data analysis. This included exporting a matrix of the Jacobian determinants for the full length of the datasets prior to undersampling in the final analysis of scan duration and temporal resolution and for extracting the cross-section in the temporal direction of the datasets to test for an upward trend in SD Jacobian for the scan duration analysis (figure 21).

This research appears in the PhD thesis titled “Functional MRI of the small bowel” by CS de Jonge and has been published in: CS de Jonge*, RM Gollifer*, AJ Nederveen, D Atkinson, SA Taylor, J

Stoker, A Menys. “Dynamic MRI For Bowel Motility Imaging – How Fast And How Long?” The British Journal of Radiology 2018 91:1088

*joint first co-authors

The key components of my work here were:

- Enhancing the functionality of the GUI for both temporal resolution and scan duration analysis as described above.
- Designing the study including ROI placement and statistical analysis to assess both scan parameters, in collaboration with Sofieke de Jonge (Methods section 3.2.3)
- Data analysis of the scan duration, including performing additional tests to explain the findings (Results section 3.3.2) and the control ROIs (Results section 3.3.3), and providing the Jacobian determinant matrix for the temporal resolution analysis to be carried out by Sofieke de Jonge with assistance from the thesis author (Results section 3.3.1).

## 3.1 Introduction

As discussed in chapter 2, the use of MRI to explore intestinal dysmotility has rapidly expanded, in part driven by increased clinical uptake of MRI enterography in evaluating small bowel disorders coupled with advances in post-processing technologies enabling rapid and reliable quantification. Indeed, MRI-quantified bowel motility is providing new insights into the importance of aberrant gut motility in disease.

Most of the research to date involving bowel motility quantification using dynamic MRI has made assumptions regarding acquisition protocols which have not been rigorously tested such as:

1) temporal resolution of the cine series (typically acquired by many researchers at one image per second)

2) scan duration of the acquisition (typically acquired using a breath-hold protocol of around 20 seconds)

Regarding temporal resolution, the literature suggests that the small bowel undergoes between 9 and 12 contractions per minute (see section 1.1.2), and this so called slow wave activity is described to be continuous and regular in the fasted state [16]. However, Menys et al. (2014) [159] using 20 second breath-hold dynamic MRI data showed regions of bowel that were almost static even in healthy subjects. It is assumed that acquiring images at 1 image per second is sufficient to resolve small bowel contractions, although the implications of inadvertently undersampling contractions are significant.

A 20 second scan duration is usually chosen for pragmatic reasons i.e. the amount of time a patient is able to hold their breath during scanning (see section 2.1.7). However, due to a lack of periodicity in contractions, this could lead to inconsistent results and inaccurate conclusions drawn from bowel motility measures. Importantly for clinical practice, 20 seconds might be too much time for the patients (see section 2.1.7), and a reduction in scan duration could potentially make dynamic MRI imaging a more efficient addition to clinical workflows and be more comfortable for patients.

In this study, an accelerated 10 images per second two-dimensional MRI sequence was acquired during a breath-hold. This protocol was chosen to “over-sample” bowel motility and quantify the small bowel motility using the registration based technique, described in section 2.3, to provide guidance on the required temporal resolution and scan duration for consistent small bowel motility assessment.

## 3.2 Methods

Ethical permission was obtained from the relevant Medical Ethics Committee and all subjects gave full written informed consent.

### 3.2.1 Volunteer recruitment

Six healthy subjects (median age, 22 years, range, 21–25 years, 3 females) were recruited prospectively by advertisement and interview for an ongoing concurrent study and therefore the number of subjects was based on the data available at the time of the analysis. Inclusion criteria included healthy volunteers who were willing to undergo minimal bowel preparation and MRI, were non-smokers and fasted overnight (including abstaining from the use of toothpaste and caffeinated and alcoholic drinks on the day of the scan). Exclusion criteria were contraindications to undergo MRI, age younger than 18 years or older than 45 years (a research policy in the Netherlands), history of abdominal surgery, gastrointestinal diseases or current gastrointestinal symptoms and use of medication with known direct effects on motility such as prokinetic agents (e.g. neostigmine) and anti-spasmodics (e.g. buscopan).

### 3.2.2 MRI protocol

All volunteers fasted overnight (on average 8.7 hours, ranging from 7.3 to 10.1 hours) before the MRI scan. During the 30 minutes prior to the MRI scan, they ingested 1 litre of 2.5% mannitol solution at regular intervals of 10 minutes.

Scans were acquired with a 3T Philips Ingenia MRI scanner (Philips, Best, Netherlands) in supine position, with subjects positioning their

arms at their sides, using a combination of a posterior coil located in the table and an anterior torsocoil covering the entire abdominal region. After initial survey sequences, a coronal single slice two-dimensional balanced fast field echo motility sequence of the bowel was acquired.

The slice was positioned to include the terminal ileum if this was visible, together with a good volume of small bowel. The motility scan was acquired during an expiration breath-hold with the volunteers instructed to hold their breath for approximately 20 seconds.

The scan parameters were: echo time/repetition time: 0.98/1.90 ms, flip angle: 20°, field of view: 400 × 400 $mm^2$ [FH (Foot-Head) x LR (Left-Right)], spatial resolution: 2.5 × 2.5 × 10 mm, SENSE factor: 3.1 [RL(Right-Left)], resulting in a temporal resolution of 10 frames per second (fps) or images per second.

### 3.2.3 Motility Assessment

Motility data visualisation and secondary analysis were performed in MATLAB 2016 (The MathWorks, Natick, MA). This included a graphical user interface (GUI), where anonymised datasets are displayed, as both a static reference image and as a “cine” movie. This allowed for inspection of all the MRI data (as well as ROI placement and automated MRI metric measurement).

*Step 1: Dataset creation*

For the assessment of the optimal **temporal resolution**, all datasets at 10 images per second were used and were then retrospectively undersampled to create new datasets at 5, 4, 2, 1, 0.5, 0.25, 0.2, 0.1 fps (0.1 fps = 1 image every 10 seconds used in analysis).

For the assessment of the optimal **scan duration** for data acquisition, every cine series, acquired at a temporal resolution of 10 images per second, was undersampled to create datasets at a temporal resolution of 1 image per second, consistent with the temporal resolution used in published literature. Figure 16 illustrates the data processing workflow for the two components of the study:

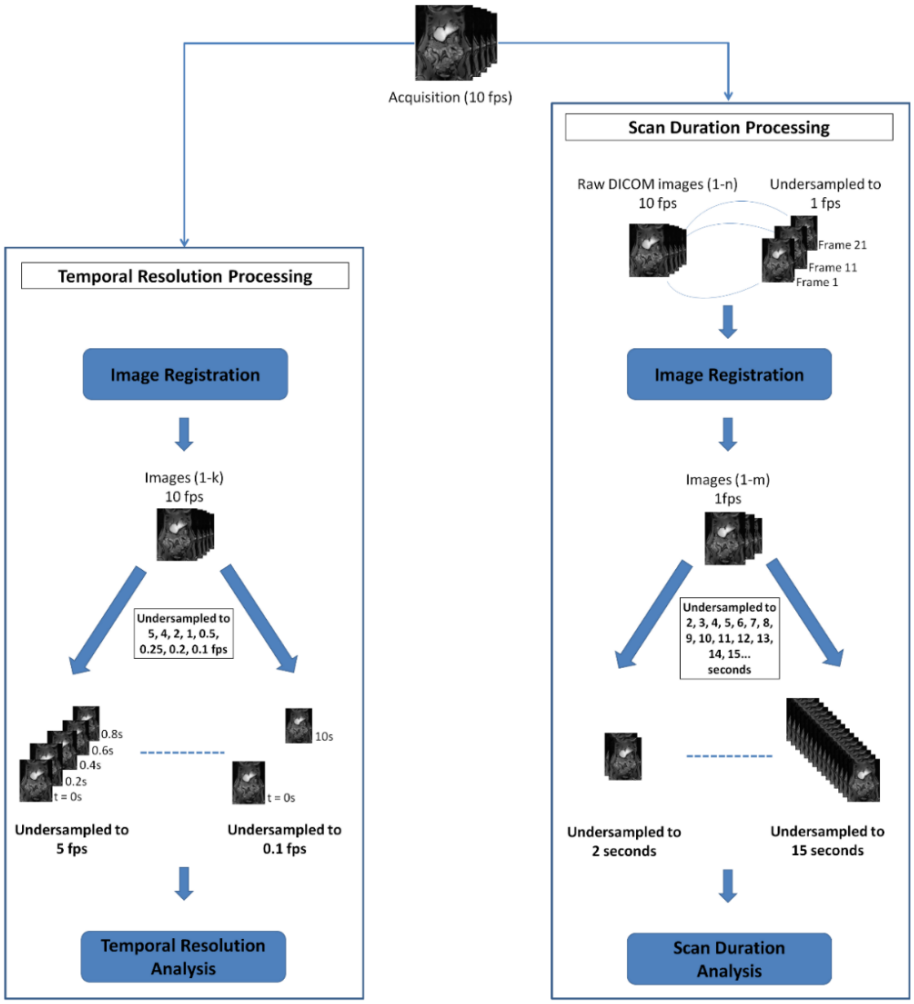


**Figure 16: Flow chart of data processing workflow prior to analysis. For the temporal resolution part of the study, the 10 fps dynamic series were registered before being undersampled to 5, 4, 2, 1, 0.5, 0.25, 0.2 and 0.1 fps. For the scan duration part of the study, the 10 fps dynamic series firstly had to be undersampled to 1 fps before being registered. After registration, the datasets were undersampled at 1 second intervals from 2 seconds to the duration of the dataset, e.g. 15 seconds. The effects of varying temporal resolution are not fully modelled in this work due to the constraint of data being captured in a single acquisition as opposed to several independent acquisitions with different temporal resolutions. fps, frames per second.**

*Step 2: Image Registration and calculating the SD Jacobian (Bowel motility assessment)*

As described in sections 2.3.2 and 2.3.3, each created cine series from step 1 was registered to a single reference frame using a previously validated optic flow based technique [191], [192]. The SD Jacobian was calculated on a per pixel basis, for different temporal resolutions and scan durations, and for each dataset was displayed on the reference frame as a motility map (figure 17).

*Step 3: Regions of interest (ROIs)*

Seven ROIs were drawn for each subject (figure 17) by the thesis author in consensus with De Jonge in all the created datasets:

- Global ROI including all visible small bowel (ROI 1)
- Four smaller local small bowel ROIs (ROI 2-5)
- Two reference or control ROIs in the hip muscle (ROI 6) and the liver (ROI 7)

The local ROIs were drawn in four quadrants with upper left, upper right, lower left and lower right of the small bowel (figure 17). ROIs were placed in these four quadrants according to the individual anatomy of the volunteer's bowel. The ROI for the lower right quadrant was placed in either the ileum or the terminal ileum (TI) if the TI was visible. The other local ROIs were placed in the jejunum.

The control ROIs were drawn in liver and hip muscle since the pixels in these locations should not change shape or size and therefore the SD Jacobian should be consistent at different temporal resolutions and scan durations (see section 2.3.3).

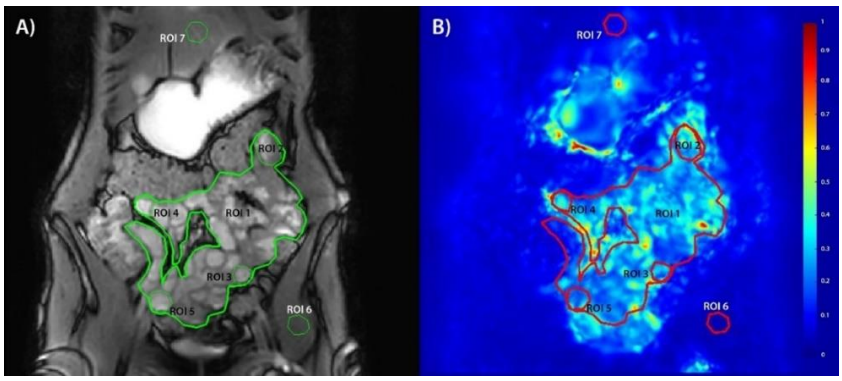


**Figure 17: The 7 different types of ROIs used in this study; Global small bowel (ROI 1), top left quadrant of the abdomen (ROI 2), bottom left quadrant (ROI 3), top right quadrant (ROI 4), bottom right quadrant (ROI 5), hip muscle reference (ROI 6) and liver reference (ROI 7). The reference image used for the ROI placement (A) with the motility map (B) where red = high motility and blue = low motility.**

*Step 4: Motility analysis*

The mean SD Jacobian within each ROI was calculated and plotted against the temporal resolution and scan duration for visualisation of the robustness of the motility measure. All data were initially plotted and assessed visually by the thesis author and De Jonge.

The observers visually assessed at 5 second intervals when the mean SD Jacobian appeared to be stabilising for both the plots of temporal resolution and scan duration. Stabilisation was defined as the point where there was little change in mean SD Jacobian in data points beyond.

The difference between the mean SD Jacobian at the point of stabilisation and the last data point (i.e. the longest scan duration or fastest temporal resolution) was expressed as an absolute percentage change. This change indicates the degree of stabilisation of the mean SD Jacobian and therefore the robustness of the SD Jacobian after a certain scan duration time and at a particular temporal resolution.

In case of no apparent stabilisation, the protocol for assessing the datasets was to triplicate the dataset (copy and paste a 20 second dataset to create a 60 second dataset with repeated data every 20

seconds), recalculate the SD Jacobian and visually inspect the datasets to look for an explanation.

## 3.3 Results

No adverse effects were observed in the six healthy volunteers. The acquisition resulted in breath-holds ranging from 15 to 21 seconds depending on the subject's ability to hold their breath.

### 3.3.1 Assessment of optimal temporal resolution

Visual inspection of the plot of mean SD Jacobian values for each ROI against different temporal resolutions suggested the SD Jacobian stabilised at a temporal resolution of 1 fps for both global (figure 18A) and local ROIs (figure 18B).

Temporal resolutions of 1 fps and 2 fps were therefore selected to assess the stabilisation of the mean SD Jacobian in comparison to the 10 fps data point (figure 18).

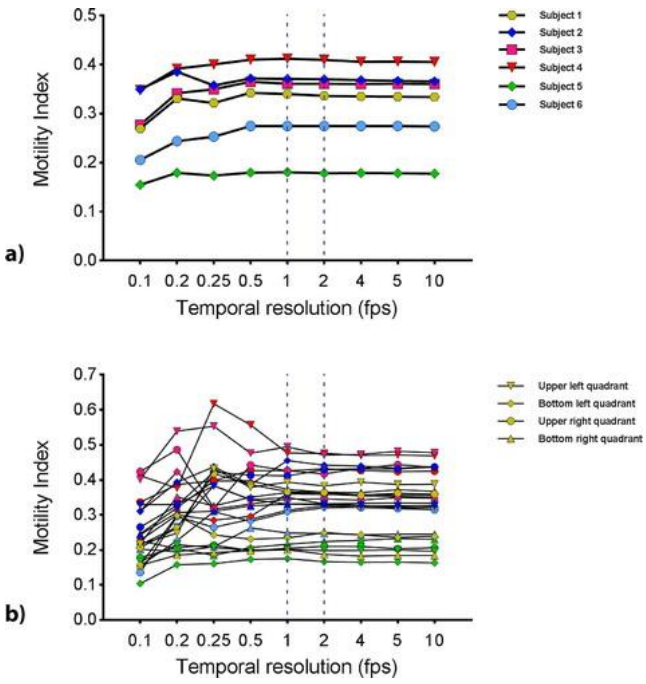


**Figure 18: Mean SD Jacobian from breath-hold scans for A) the global small bowel ROI at different temporal resolutions and B) the quadrant ROIs (ROIs 2 - 5) calculated at different temporal resolutions. The dotted lines mark 1fps and 2fps where the mean SD Jacobian appears to be stabilising and are therefore the temporal resolutions selected for further analysis. This figure appears in the PhD thesis titled "Functional MRI of the small bowel" by CS de Jonge.**

Table 5 shows the median and range of absolute percentage changes across all subjects for the SD Jacobian at temporal resolutions of 1 and 2 fps, in comparison to 10 fps. Global ROI median percentage changes were generally smaller than for the local (quadrant) ROIs.

| | **Global (% change)** | | | **Local (% change)** | | |
|---|---|---|---|---|---|---|
| | Median (%) | Range (%) | | Median (%) | Range (%) | |
| | | Min. | Max. | | Min. | Max. |
| 1 fps | 1.4 | 0.1 | 1.8 | 1.9 | 0.3 | 8.0 |
| 2 fps | 0.6 | 0.2 | 1.2 | 1.4 | 0.1 | 4.5 |

**Table 5: Median and range of the mean SD Jacobian absolute percentage change of both global and local ROIs based on selected temporal resolution in breath-hold at 1 fps and 2 fps, fps = frames per second.**

### 3.3.2 Assessment of optimal duration of data acquisition (scan duration)

Visual inspection of the plot of mean SD Jacobian values for each ROI against scan duration during breath-hold suggested the SD Jacobian stabilised at a scan duration of 10 seconds or more for both global (figure 19A) and local ROIs (figure 19B).

Based on visual assessment of the breath-hold data, scan duration times at 5 second intervals (10 and 15 seconds) were selected to assess the stabilisation of the mean SD Jacobian against the full breath-hold (figure 19). A scan duration of 5 seconds was not selected because there was no apparent stabilisation in the first 5 seconds.

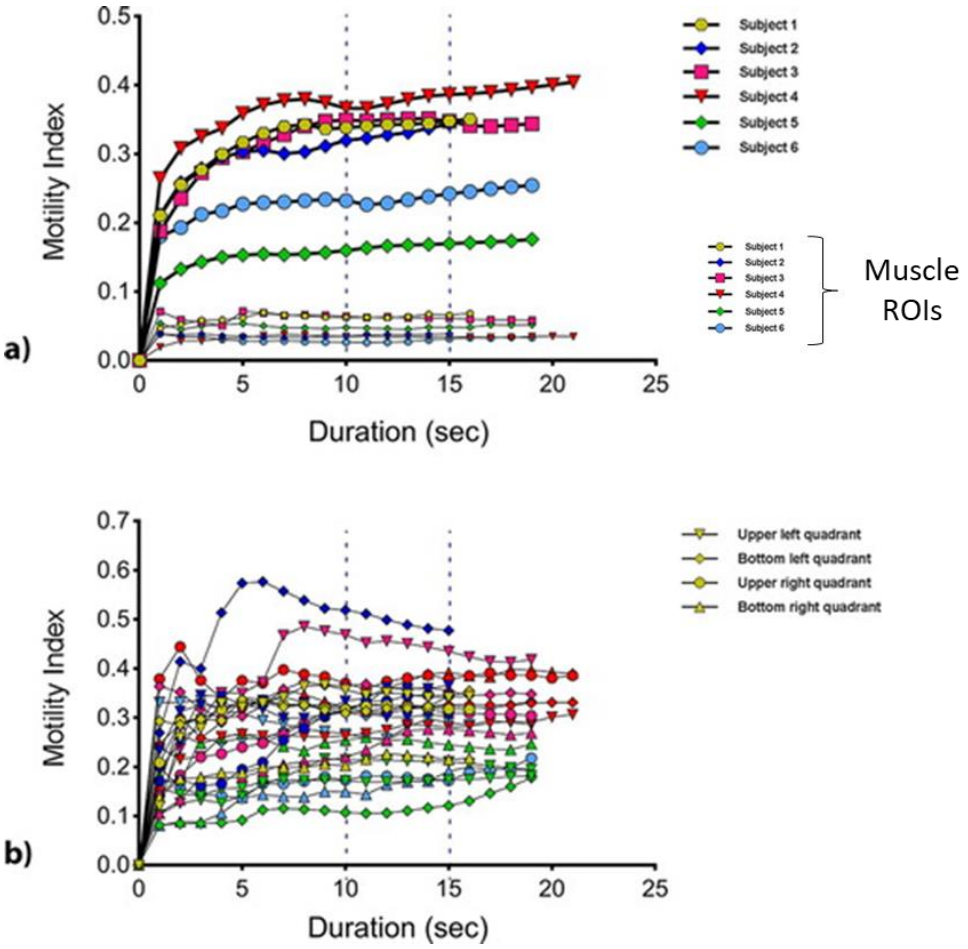


**Figure 19: Mean SD Jacobian from breath-hold scans for (a) the global ROI and the control ROIs in muscle at different scan durations and (b) the quadrant ROIs (ROIs 2–5) calculated at different durations. The dotted lines mark 10 and 15 s, where the mean SD Jacobian appears to be stabilising and are therefore, the scan durations selected for further analysis.**

Table 6 shows the median and range of absolute percentage changes across all subjects for the SD Jacobian at scan durations of 10 and 15 seconds, in comparison to the full breath-hold durations.

| | Global (% change) | | | Local (% change) | | |
|---|---|---|---|---|---|---|
| | Median (%) | Range (%) | | Median (%) | Range (%) | |
| | | Min | Max. | | Min | Max. |
| 10 sec. | 8.6 | 1.6 | 10.3 | 7.9 | 0 | 65.5 |
| 15 sec. | 2.8 | 0.8 | 5.1 | 1.7 | 0.2 | 47.1 |

**Table 6: Median and range of the mean SD Jacobian absolute percentage change of both global and local ROIs based on selected time points in breath-hold (10 and 15 seconds).**

The stabilisation of the SD Jacobian in this assessment demonstrated less stabilisation than for temporal resolution, with some datasets characterised by a gradual increase in the mean SD Jacobian. Two further tests were performed to understand the source of this climbing mean SD Jacobian over time:

1) By triplicating the breath-hold dataset (i.e. using a 20 second dataset to create a 60 second dataset where the same data is used 1-20s, 21-40s and 41-60s) and registering and recalculating the global ROIs, the registration algorithm was evaluated as a potential source of the rising mean SD Jacobian. Figure 20 visualises this additional test and shows that the mean SD Jacobian stabilises as expected and provides evidence against the algorithm itself as the source of this trend.

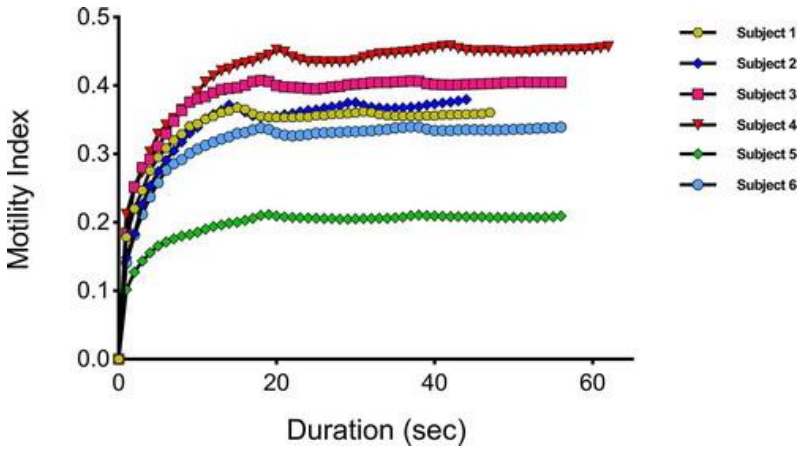


**Figure 20: Mean SD Jacobian from tripled breath-hold datasets for the global small bowel ROI calculated at different temporal resolutions.**

2) The dynamic datasets were visually re-assessed with a view to establishing a physiological cause of the increasing motility score. Here three imperfect breath-holds were identified in these datasets, showing a slight upwards trend in the positioning of the small bowel over time (figure 21) despite the breath-hold acquisition. Datasets where this was not present did not show the rising mean SD Jacobian suggesting that more movement was present in the dynamic dataset aside from the bowel motility, producing this artifact.

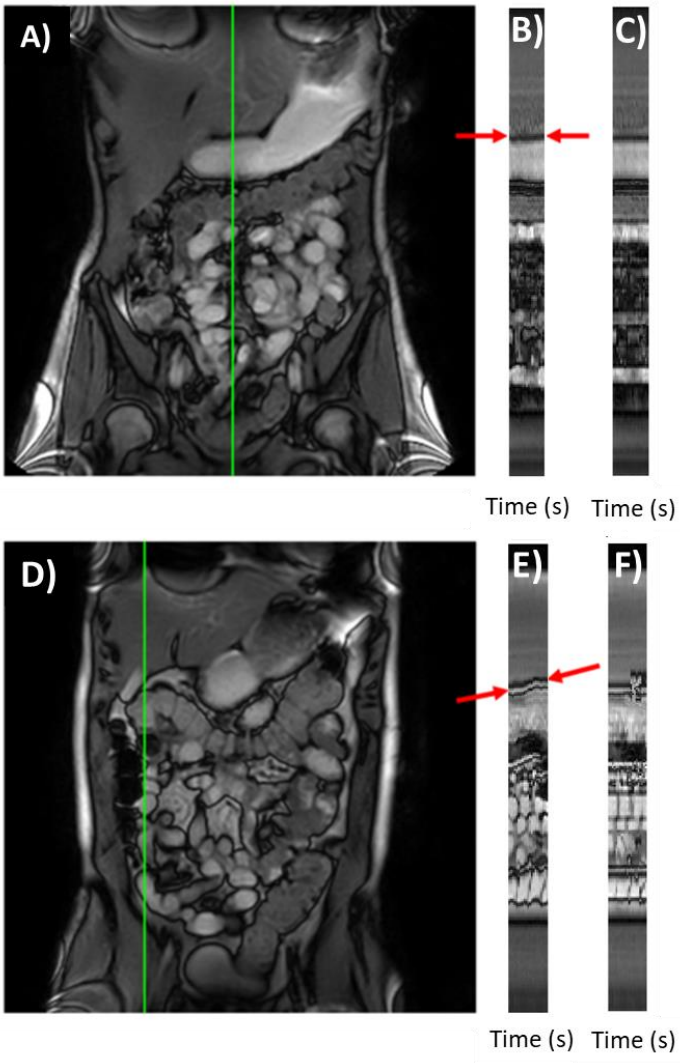


**Figure 21: Reference frame from a dynamic dataset of a good (A) and an imperfect (D) breath-hold. Images B and E show a cross-section along the temporal direction located at the vertical green line indicated in the reference frames A and D. The cross-section (E) shows an upwards trend in the positioning of the small bowel (see red arrows). The cross-sections in the same locations after registration are displayed in images C and F. It can be seen in the good breath-hold that registration works well with steady positioning of the small bowel (C) whereas although the registration can be seen to improve the imperfect breath-hold, there are some parts of the small bowel where the positioning is not perfectly steady and this could have an effect on the SD Jacobian (F).**

### 3.3.3 Control ROI

Additionally, the control ROIs in the liver and hip muscle exhibited very low motility with a mean SD Jacobian value below 0.1 and 0.2 respectively indicating very low or no motility occurring at these locations over the duration of an acquisition (figure 19A).

## 3.4 Discussion

The purpose of this prospective study was to provide evidence to define the required minimum temporal resolution (see section 3.4.1) and scan duration (see section 3.4.2) for consistent, quantitative measurements of small bowel motility with dynamic MRI using the SD Jacobian.

### 3.4.1 Temporal resolution

The first question addressed with this study was: at what temporal resolution are consistent motility, i.e. mean SD Jacobian values, observed in the small bowel? Acquiring the data too quickly and it could be oversampled resulting largely in practical inconveniences, e.g. creating an unnecessarily large amount of data for calculations, causing longer post-processing times and with cost implications for data storage. Furthermore, to achieve a higher temporal resolution there would be a potentially unnecessary compromise on spatial resolution. More concerning is acquiring data too slowly leading to undersampling or aliasing motility and potentially generating spurious motility values with no true physiological meaning.

The temporal resolution of dynamic sequences used in previous research largely ranges around 1 image per second due to adaption of sequences available on clinical systems [57]–[59], [159], [163], [167], [170], [181], [198], [223]–[225]. These images have a good signal to noise ratio, can be performed rapidly and are practicable for clinical use. From gastrointestinal physiology data, there is a suggestion that the small bowel routinely contracts between 9 and 12 times per minute [16] (0.15–0.2 Hz) suggesting that the typical temporal resolution of 1 image per second (equivalent to 1 Hz) should adequately capture the peristaltic cycle, therefore supporting the practical advantages of the dynamic sequences used in previous research. Reassuringly, by iteratively undersampling a high temporal resolution sequence (10 images per second), it was demonstrated in this study that quantification of bowel motility stabilises at a temporal resolution of 1 fps, with little change at temporal resolutions greater than this.

In support, the median absolute percentage change in motility across a range of ROIs size and positions remained below 2%, when comparing values from 1 fps to much higher temporal resolutions. Such data are welcome, as image acquisition at 1 fps is easily achievable on most 1.5–3 T MRI platforms, with most vendors supplying dynamic sequences as standard. Indeed, acquisition at 2 fps is also possible with only minor sequence modifications. To place this variance in context, a motility study comparing a placebo and a neostigmine stimulant, showed a 22% increase and comparing a placebo and butylscopolamine showed 57% decrease in the mean SD Jacobian [161]. In a Crohn’s disease study comparing inflamed to non-inflamed terminal ileum, an increase of 95% was observed [199].

In this study for quadrant ROIs, the median percentage change fell from 1.9% at 1 fps to 1.4% at 2 fps. For global ROIs, the median percentage fell from 1.4% at 1 fps to 0.6% at 2 fps. This difference is likely insignificant compared to the differences observed in previous studies however it might be important to consider if the potential effect size of future investigations is small.

It should be acknowledged that the effects of varying temporal resolution are not fully modelled in this work. Undersampling 10 fps datasets (200 frames in a 20 second dataset) to lower temporal resolutions was performed by discarding frames e.g. 20 frames in a 20 second dataset for 1 fps. Alternatively, several datasets with differing temporal resolutions could have been acquired. For instance, images acquired at 1 fps would be more blurred with a higher SNR than the equivalent images acquired at 10 fps and undersampled to 1 fps. However, in this study there was a constraint on the data being acquired in one acquisition. Due to movement of the small bowel in and out of plane and manual slice positioning then independent acquisitions would result in different areas of small bowel appearing in the acquired slice for different temporal resolutions within the same patient so would not be able to directly compare the exact same area of small bowel.

A different approach to modelling temporal resolution could be to use the 10 fps datasets to mimic the blurring seen at lower temporal resolutions through calculating the moving average. For example, it would be possible to calculate the 11 frame average so that each image in a 1 fps modelled dataset would consist of an average from the 5 previous frames, the frame used in the undersampling technique used in this study and the next 5 frames. The undersampling used here is useful for this study, but it is recognised that a more complete approach to modelling temporal resolution could be implemented.

### 3.4.2 Scan duration

The second, and perhaps more difficult question addressed in this study is the duration of the scan. Similarly, to the chosen values of temporal resolution, most researchers to date have been guided by clinical practicalities when choosing their scan duration. Prolonged acquisitions of 5 minutes or greater are impractical in most busy

clinical departments and breath-hold imaging is rapid, practical and limits through plane motion artifacts.

In this study, the effect of adding additional images to breath-hold data series was investigated by modelling prolonging of acquisition protocols ranging from 2 to 22 seconds. Specifically, the change in mean SD Jacobian as new data were added to the series was evaluated. Reassuringly, it was found that for most breath-hold datasets, acquisitions of less than 20 seconds were adequate and stabilisation in the SD Jacobian was visualised although a persistent “creep” was observed in several cases. For small local ROIs, the motility did seem more variable, the median percentage change fell below 10% at 10 seconds in breath-hold (7.9%), likely due to inherent variation in bowel contractility in smaller bowel regions. Data were more consistent for the larger global ROIs, the median percentage falls below 10% at 10 seconds in breath-hold (8.6%), likely due to averaging of motility over the full bowel volume. The size of the ROIs clearly had an effect on the SD Jacobian as the maximum percentage for local ROIs was 65.5% (10 seconds) and 47.1% (15 seconds) compared to 10.3% (10 seconds) and 5.1% (15 seconds) for global ROIs. For both global and local ROIs, the median percentage change falls below 5% at 15 seconds in breath-hold (global = 2.8%, local = 1.7%).

As reported in the results, a general, positive trend in the mean SD Jacobian with the increasing number of time points was observed. The concerns were that either there might be a systematic bias in the algorithm or that inherent physiological variation was leading to an evolution of the motility score and that, a 20 seconds observation was insufficient to observe small bowel motility. Two further experiments to resolve the potential cause of this effect were performed. The same breath-hold motility data for each subject was triplicated before recalculating the mean SD Jacobian. Reassuringly, it was found that the mean SD Jacobian plot stabilised. This ruled out the registration algorithm itself being the source of this upward mean

SD Jacobian trend. Had there been a cumulative error, an increasing value over the 60 time points would have been seen.

Second, it was noticed there was a slight upwards trend in the positioning of the small bowel between the first and last frame in the dynamic series when reviewed as a cine loop. This “jump” was particularly pronounced where the upward inflection in the mean SD Jacobian plot was seen and absent where the mean SD Jacobian values flattened out. This result suggests that the quality of the breath-hold is important as well beyond the simple use of breath-hold. Going forward, the presence of the upwards trend is relatively simple to check for and potentially avoid with careful communication with the subject. Alternatively, this bias can be potentially corrected during post processing. Although this artifact subtly alters the mean SD Jacobian value, this change is below the effect size seen in clinical studies and therefore it does not appear to impact existing published research. It will be useful to examine this phenomenon in free-breathing examinations to assure that there is no bias introduced in the mean SD Jacobian by the breathing in these datasets. However, since a different registration algorithm is used to calculate the SD Jacobian in free-breathing datasets [226], [227] breath-hold and free-breathing cannot be directly compared in this study. In future, it may still be more desirable to acquire longer free breathing datasets. This would reduce patient discomfort compared to breath-holding and potentially capture a more complete picture of motility. Software has already been developed which can correct for respiratory motion [226].

### 3.4.3 General Discussion

The sequence used in this study, a single-slice rapid acquisition with a flip angle of 20°, is similar to the acquisitions used in previous work imaging multiple slices at a lower temporal resolution [57], [159], [226]. The image quality was adequate for registration and the quality of the registration was assessed visually by playing the frames as a movie. The movie displayed the propagation of the ROIs drawn on the reference frame through all the frames, with the correct registration evident from the alignment of the bowel walls in each of the frames.

It would be interesting to investigate whether the SD Jacobian, as a surrogate for motility, relates to transit time measured by the 3D-Transit system (with transit an indirect measure of motility). However, there is no previous data examining this relationship and since the 3D-Transit system involves ingestion of an electromagnetic pill then transit data cannot be captured simultaneously with MRI due to the risks associated with an electromagnetic pill within the body being placed within the MRI scanner.

This study does have limitations. It is important to interpret the data in the context of the registration algorithm used to generate the SD Jacobian. As discussed in section 2.3, although well validated in healthy volunteers and patient groups [57], [159], [161], [192], [198] the metric, described as the standard deviation of the deformation fields' Jacobian determinant, is a surrogate measure of motility only, rather than a measure of a defined, physiological action (i.e. peristalsis).

The metric captures information on how the bowel deforms and, by taking the standard deviation, temporal information on the frequency of contractions is lost. That is, if a bowel loop underwent multiple rapid contractions of equal amplitude, the same SD Jacobian would be recorded as if it only underwent one large contraction. There was little gain in accelerating the acquisition to faster than 1 image per

second, although this may be useful for small ROIs. The literature currently reports a range of diameter based measurements (e.g. contractions per minute), [58], [65], [166], [167] (see section 2.2.3). Since the datasets were relatively short in terms of minutes, it was not possible to do a thorough investigation of such metrics here. This study only explored one motility metric, conversely, using a frequency metric like “contractions per minute” may not, by definition, be robust under these circumstances.

Additionally, the sample size of six subjects is relatively small. Nevertheless, these data are still representative of subjects seen in the clinical setting, given the known heterogeneity in bowel motility described previously by Menys et al. [159] collected in a cohort of 20 patients (four ROIs per patient).

Another consideration is the underlying bowel physiology in terms of fed and fasted motility patterns. Clinically, patients are required to fast prior to small bowel enterography and then ingest up to 2 litres of a contrast solution to distend the bowel for visualisation purposes. As discussed in section 2.1.7, mannitol appears to mimic the postprandial state and this likely prokinetic effect of mannitol seems to drive and elevate motility homogeneously along the bowel resulting in relatively clustered data. Mannitol is a hyperosmotic, low calorie stimulant and it differs significantly from usual food stuffs which can provoke symptoms in patients. It is however useful for identifying areas of low motility [161]. Alternate sources of preparation should also be considered [228]. Furthermore, the scan duration may need to be longer in cases where motility is not stimulated and this has been investigated in several studies [228], [229]. In unprepared bowel, the bowel wall is less well defined and after ingestion of food, chyme can be seen to move through the small bowel. The model of intensity changes, described in section 2.3.2, is a parameter in the registration algorithm which is not used as a motility measure in this chapter due to the bowel being in fed state (after mannitol ingestion) and therefore motility is better captured by studying the movement of the bowel wall using the deformation

fields. However, when comparing the fasted state (unprepared bowel) and the fed state (such as a food challenge i.e. soup being ingested) changes in signal intensity in the small bowel have been observed and therefore this registration parameter can be used as a motility measure for this type of analysis [228], [230].

It should be noted that the data in this study was acquired in the supine position. Scanning subjects in the prone position where the bowel is flattened out, for better visualisation, may also have an effect on the SD Jacobian.

## 3.5 Summary

In summary, this study shows that a temporal resolution of 1 image per second over a scan duration of 15 seconds in breath-hold is sufficient to obtain robust measurements of small bowel motility from MRI when quantified using optic flow registration techniques. These assumptions regarding the acquisition protocol were tested in healthy volunteers to establish a standard MRI protocol necessary for motility assessment in future research studies. The rest of this thesis will assess the utility of quantified motility measurements generated by registering dynamic MRI data, in gastrointestinal (GI) conditions such as Crohn's disease (CD) (chapters 4 and 5) and IBS (chapters 6 and 7). In the next chapter, a validation study is detailed which examines a previous association found between abnormal small bowel motility and CD patient symptoms.

# Chapter 4: Relationship between MRI quantified small bowel motility and abdominal symptoms in Crohn's disease patients—a validation study

## Author Declaration

The work presented here was led by the thesis author (2 years of experience at the time of publication) including performing the literature review, downloading, anonymising and segmenting the datasets, and performing the motility and statistical analysis, under the supervision of Alex Menys, David Atkinson and Stuart Taylor.

Alex Menys and Freddy Odille developed the registration algorithm and graphical user interface (GUI) displaying the dynamic MRI data and motility maps. The thesis author enhanced the functionality of the GUI for data analysis.

Data was collected by the VIGOR++ consortium to develop a computer aided diagnosis framework for CD. The VIGOR++ study recruited patients from Amsterdam (AMC) and UCLH to undergo MR enterography, colonoscopy and patient symptoms scoring in order to develop software to measure structural MRI markers of disease activity, notably bowel wall thickness and contrast enhancement. Motility sequences of the whole small bowel volume were acquired as part of the MRI protocol.

This research has been published in: RM Gollifer, A Menys, J Makanyanga, CAJ Puylaert, FM Vos, J Stoker, D Atkinson, SA Taylor. “Relationship between MRI quantified small bowel motility and abdominal symptoms in Crohn’s disease patients—a validation study.” The British Journal of Radiology 2018 91:1089

The key components of my work here were:

- Enhancing the functionality of the GUI for extracting the two motility metrics (mean motility and spatial variation of motility) from the motility maps
- Designing the study including statistical analysis to validate the previous single-centre study and performing an additional analysis restricted to those patients with a symptom score above certain thresholds when correlating symptoms with the spatial variation of motility.

## 4.1 Introduction

As discussed in section 1.3.1, Crohn’s disease (CD) is a lifelong chronic inflammatory bowel disease characterised by periods of disease activity and remission. Current treatments, typified by biological agents, are directed at effectively managing inflammatory activity with the aim of both treating patients’ symptoms and reducing long-term bowel damage.

However, as discussed in section 1.4, it is clear that symptoms are not always directly related to inflammation. The aetiology of abdominal symptoms and their link to disease activity therefore remains obscure. Clinical and endoscopic indices, such as those mentioned in section 1.3.1, give an indication of disease activity and the severity of CD at the time they are measured. Furthermore, disease burden refers to the impact of a health problem measured by rate of surgical resections, hospitalisations and mortality [231].

Indeed, recent single-site data in 53 patients suggests that aberrant motility (notably a decreased spatial variability measured using MRI) in apparently healthy bowel may be linked to patient symptoms in CD [65]. If this observation could be validated, MRI quantified bowel motility could provide new insights into the aetiology of abdominal symptoms in CD.

The purpose of this study was to validate the previously observed apparent link between reduced small bowel spatial variation of motility, seen in dynamic MRI, and patient abdominal symptoms in CD (recorded using HBI symptom questionnaires as described in section 1.4.1) as part of a prospective multicentre study. Alternative outcome measures such as PRO2 (number of liquid stools and abdominal pain) could have been used, but HBI showed the same utility in clinical practice as PRO2 (both 3 out of 8) and better utility in clinical trials (2 out of 5) than PRO2 (1 out of 5).

## 4.2 Methods

The current study was retrospective and has been approved by both centres' ethics committees (Hampstead REC, London and the ethics committee of the Academic Medical Center). The patients provided written informed consent for the original research studies and the requirement for consent was waived for the retrospective analysis in this study.

### 4.2.1 Patient selection

The current study included a subset of patients recruited to the VIGOR++ study, a prospective trial which developed novel software

metrics to quantify CD activity using MRI in comparison to an endoscopic reference [232]. In brief, patients with known or suspected CD underwent contemporaneous (within 2 weeks) MR enterography and colonoscopy at two centres (Academic Medical Centre, AMC and University College London Hospital, UCLH) between October 2011 and September 2014.

As part of the trials, patients completed a HBI symptom questionnaire the day prior to scanning [138] (see table 2 in section 1.4.1). Demographic data pertaining to age, sex, current medication, disease duration and surgical history was also collected.

Inclusion criteria for the current study were patients who had a final diagnosis of CD based on clinical, biochemical, endoscopic, imaging and histopathological data and the availability of associated dynamic MRI and HBI data.

Exclusion criteria were contraindications to undergo MRI, patients who had a stoma, and the use of medication with known direct effects on motility such as prokinetic agents (e.g. neostigmine), anti-spasmodics (e.g. buscopan) and opioid analgesics.

Patients were also excluded from the current study if they had either failed to undergo an adequate dynamic MRI cine sequence through the whole small bowel volume (greater than three slices and complete time series - see MRI protocol details below or failed to complete a HBI questionnaire. Exclusions were confirmed a priori and before data analysis.

### 4.2.2 MRI protocol

Patients fasted for 4 hours before ingesting 800 ml of 2.5% mannitol, 3 hours prior to the start of the scan to distend the colon. A further 1600 ml of 2.5% mannitol was provided 1 hour before the scan start time to distend the small bowel.

Patients were scanned in the supine position on 3T systems (Ingenia/Achieva; Philips, Best, Netherlands) using the manufacturer's torso array coil. In addition to standard anatomical sequences (T2 single-shot fast spin echo and T1 spoiled gradient echo) a dynamic "cine motility" sequence was acquired during a 22 second breath-hold prior to spasmolytic administration using a two-dimensional (2D), coronal, balanced steady-state free precession sequence.

The parameters were as follows: flip angle 45$^{o}$, repetition time = 2 ms, echo time = 1 ms, 256 × 200 matrix filling, zero-filling to 512 × 512 and 1 × 1 mm in-plane resolution, temporal resolution = 1.1 images per second, slice thickness = 10 mm.

The MRI radiographer/technician repeated these coronal blocks to encompass the whole small bowel volume, the number of acquisitions ranging from 5 to 14 depending on the size of the patient.

### 4.2.3 Motility assessment

Motility data visualisation and analysis were performed in MATLAB 2016 (The MathWorks, Natick, MA). This included a graphical user interface (described previously in section 3.2.3), where anonymised datasets are displayed, as both a static reference image and as a "cine" movie. This allowed for inspection of all the MRI data (as well as ROI placement and automated MRI metric measurement).

*Step 1: Generation of the SD Jacobian*

As described in sections 2.3.2 and 2.3.3, frames from each subject's 2D cine motility series were registered to a single reference frame using a previously validated optic flow based technique. The SD

Jacobian was calculated on a per pixel basis and displayed on the reference frame as a motility map.

*Step 2: Motility analysis and ROI placement*

For each patient, the thesis author used the GUI to place ROIs on the reference image (without motility map displayed), blinded to the HBI score. The ROIs were validated by a research fellow with over 5 years MRE experience (Menys).

The ROIs were deliberately placed in morphological normal small bowel only, excluding small bowel affected by CD [65]. In addition, morphological normal small bowel directly adjacent to the diseased area, which may exhibit abnormal motility due to the proximity to disease, was not included in the ROIs. In such cases, a gap of several bowel segments was left between the ROI and the diseased area. The observers had access to both cine motility loops and anatomical small bowel images to aid ROI placement. Specifically, small bowel demonstrating the typical stigmata of CD (such as wall thickening, abnormal T2 signal hyper enhancement etc. described in section 1.3.1) [78] was excluded from the ROI, as was the small bowel mesentery. ROIs were placed in each of the individual cine motility blocks acquired for each patient so as to include all morphologically normal bowel as far as possible.

Based on the previous derivation study [65], two motility metrics were derived from the ROIs and summed across the whole patient volume: (1) mean motility and (2) spatial variation of motility. The two motility metrics here provide summaries over the ROIs of their spatial distribution.

The mean motility metric i.e. the mean SD Jacobian (introduced in chapter 2) gives an indication of the overall motility of the segmented bowel with a high value suggesting high motility (figure 22).

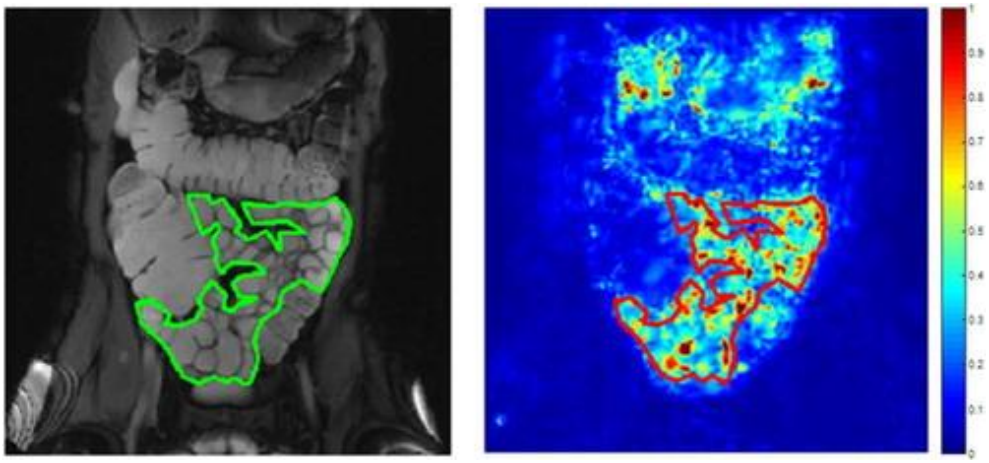

**Figure 22: An example of a coronal reference frame displaying a SB ROI (left) with the corresponding motility map of the whole small bowel volume (right), based on the SD of the Jacobian determinant with low (blue) to high (red) motility. This is an example of high homogeneous motility where the small bowel in the ROI is predominantly motile.**

The spatial variation of motility metric i.e. the variance of the SD Jacobian gives an indication of the spatial variability of motility e.g. high motility variance corresponds to a wide range of SD Jacobian values across the small bowel with areas of both high and low motility, independent of the overall motility level (figure 23).

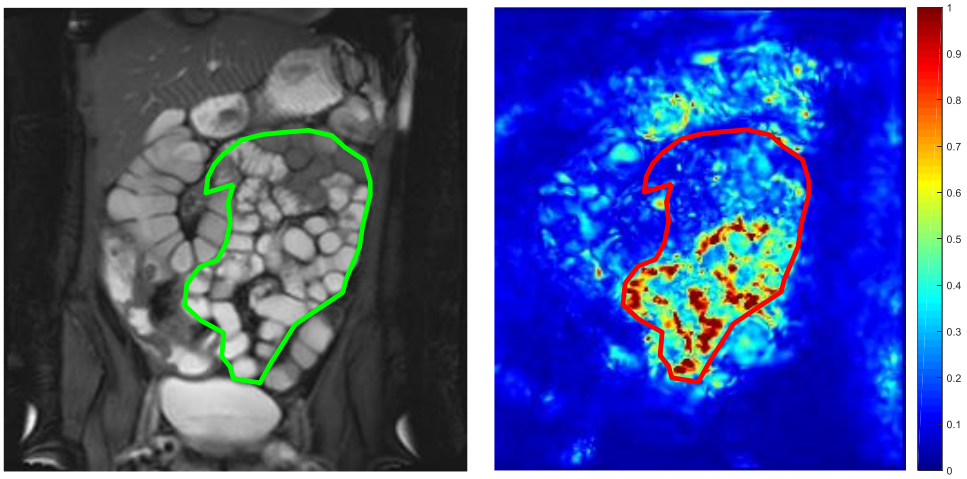


**Figure 23: An example of heterogenous motility where there are areas of active (red) and inactive (dark blue) in the small bowel ROI.**

Conversely a low spatial variation of motility corresponds to more homogeneous motility with less variation in the range of SD Jacobian values. For example, a patient with low spatial variation of motility could have either homogenously high (figure 22) or homogeneously low motility (figure 24).

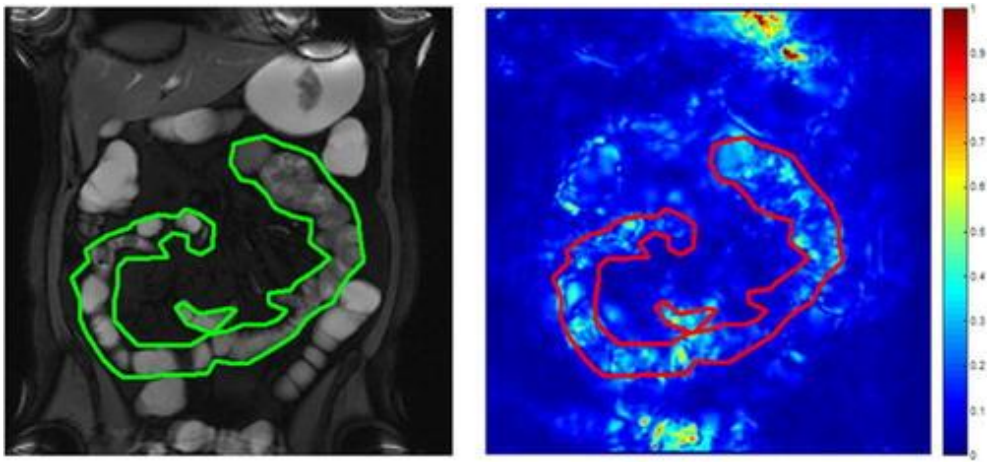

**Figure 24: An example of low homogeneous motility where the small bowel in the ROI is predominantly immotile.**

### 4.2.4 Statistical analysis

All statistical analysis was performed using MATLAB 2016 (The MathWorks, Natick, MA).

All data were checked for normality using Shapiro-Wilk test (alpha = 0.05); non-parametric statistics were used in cases where data were non-normally distributed.

Correlation was performed between the two motility metrics and the total HBI symptoms score using Spearman's correlation statistics, with $p < 0.05$ being taken as statistically significant.

*MATLAB function used: [rho p] = corr(HBI, Motility metric, 'type', 'Spearman');*

The best performing metric was then correlated with each of the HBI subcomponents of well-being, pain and liquid stools, again using correlative statistics.

Correlation was also performed between the two motility metrics and the inflammatory biomarker, CRP.

## 4.3 Results

### 4.3.1 Cohort demographics

The full VIGOR++ study cohort consisted of 158 patients (89 AMC, 69 UCLH).

For the current study, a total of 76 patients were excluded for the following reasons; diagnosis other than CD (n = 18), >14 days between MRI and colonoscopy (n = 7), failure to comply with oral contrast protocol (n = 6), cancelled or aborted ileocolonoscopy (n = 5), missing motility sequences or inadequate small bowel coverage (n = 14), acquired motility sequences data was not available for analysis (n = 24), insufficient bowel cleansing (n = 1) and non-compliance to breathing commands due to a language barrier (n = 1). The demographics for the remaining 82 patients (41 AMC, 41 UCLH) included in the current study are shown in table 7.

| **Parameter** | **AMC** | | **UCLH** | |
|---|---|---|---|---|
| Age | 19-68 Years Old (median age 35) | | 16-63 Years Old (median age 29) | |
| Males (%) | 22 (54%) | | 16 (39%) | |
| Disease Duration (years) | <1<br>1-5<br>5-10<br>>10<br>Unknown | 4<br>4<br>11<br>21<br>1 | <1<br>1-5<br>5-10<br>>10<br>Unknown | 4<br>8<br>16<br>12<br>1 |

| | | | | |
|---|---|---|---|---|
| Disease Location | Ileal | 22 | Ileal | 6 |
| | Colonic | 6 | Colonic | 7 |
| | Ileocolonic | 13 | Ileocolonic | 28 |
| Disease Behaviour | B1 (Non-stricturing, non-penetrating) | 18 | B1 (Non-stricturing, non-penetrating) | 28 |
| | B2 (Stricturing) | 10 | B2 (Stricturing) | 6 |
| | B3 (Penetrating) | 1 | B3 (Penetrating) | 5 |
| | B1+peri-anal | 0 | B1+peri-anal | 0 |
| | B2+peri-anal | 4 | B2+peri-anal | 0 |
| | B3+peri-anal | 2 | B3+peri-anal | 0 |
| | Other | 6 | Other | 2 |
| Medications | None | 7 | None | 10 |
| | 5-ASA | 3 | 5-ASA | 18 |
| | Immuno-modulators | 15 | Immuno-modulators | 14 |
| | Biological Agents | 16 | Biological Agents | 9 |
| Surgical History | None | 22 | None | 31 |
| | 1 operation | 13 | 1 operation | 10 |
| | 2 operations | 6 | 2 operations | 0 |

**Table 7: Patient Demographics with 82 patients in study cohort.**

### 4.3.2 HBI and motility metrics

The range and median values of the two motility metrics and HBI score is shown in table 8. Median total HBI score for the cohort was 5, ranging from 0 to 38. For patients recruited from UCLH, the median was 4, ranging from 0 to 10 and for patients recruited from AMC, the median was 7, ranging from 0 to 38.

| | Median | Range | |
|---|---|---|---|
| | | Minimum | Maximum |
| **Mean motility** | 0.34 | 0.16 | 0.51 |
| **Spatial variation of motility** | 0.038 | 0.012 | 0.085 |
| **HBI** | 5 | 0 | 38 |
| *Well-being* | 1 | 0 | 4 |
| *Abdominal Pain* | 1 | 0 | 3 |
| *Liquid stool* | 2 | 0 | 30 |

**Table 8: Median, minimum and maximum motility and HBI values.**

There was a negative correlation between the spatial variation of motility metric and total HBI score, although this did not reach statistical significance ($r = -0.17$, $p = 0.12$) (figure 25). There was no evidence of any correlation between the mean motility metric and total HBI score ($r = -0.02$, $p = 0.84$). The spatial variation of motility metric was therefore the best performing metric.

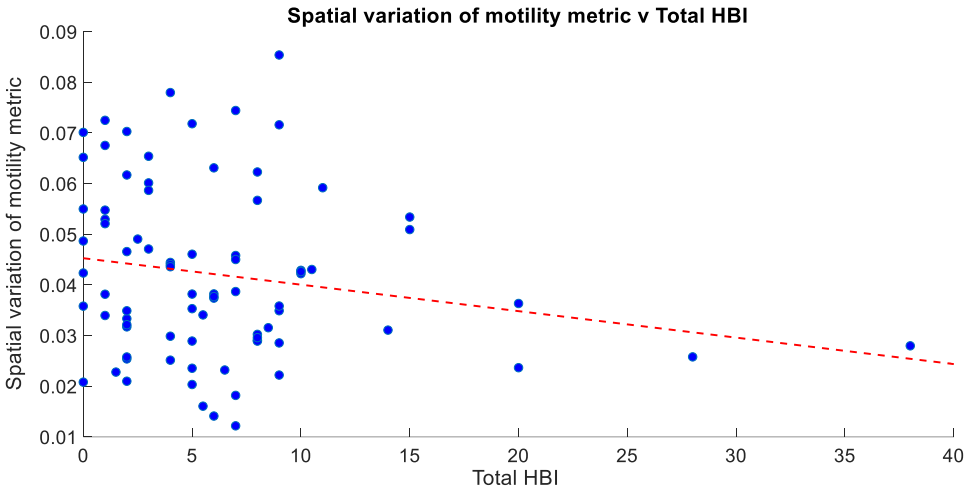


**Figure 25: The spatial variation of motility metric vs total HBI. There was some evidence of an inverse association between spatial variation of motility metric and the total HBI (r = −0.17, p = 0.12).**

## 4.3.3 CRP and motility metrics

No significant correlation was found between CRP and both mean motility (rho = -0.16, P =0.15) and spatial variation (rho = -0.21, P = 0.06

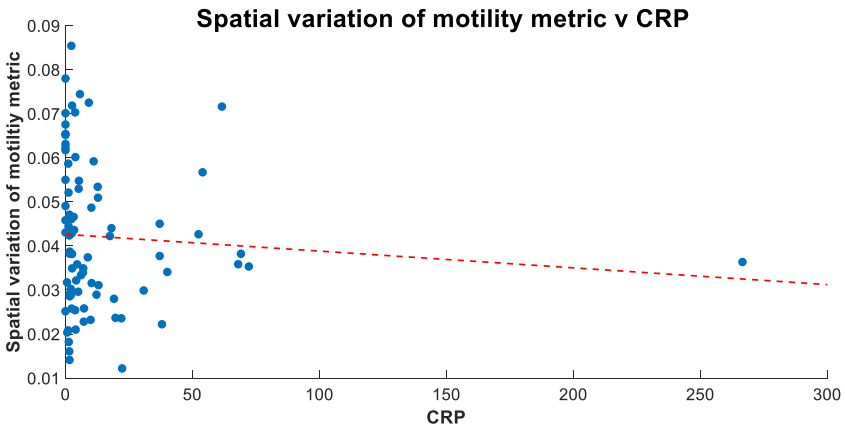


**Figure 26: The spatial variation of motility metric vs CRP. There was no significant correlation between spatial variation of motility metric and CRP (r = -0.21, p = 0.06).**

### 4.3.4 Spatial variation of motility metric against HBI components

There was also a significant negative correlation between the spatial variation of motility metric and the number of diarrhoeal stools ($r = -0.29$, $p < 0.01$) (figure 27).

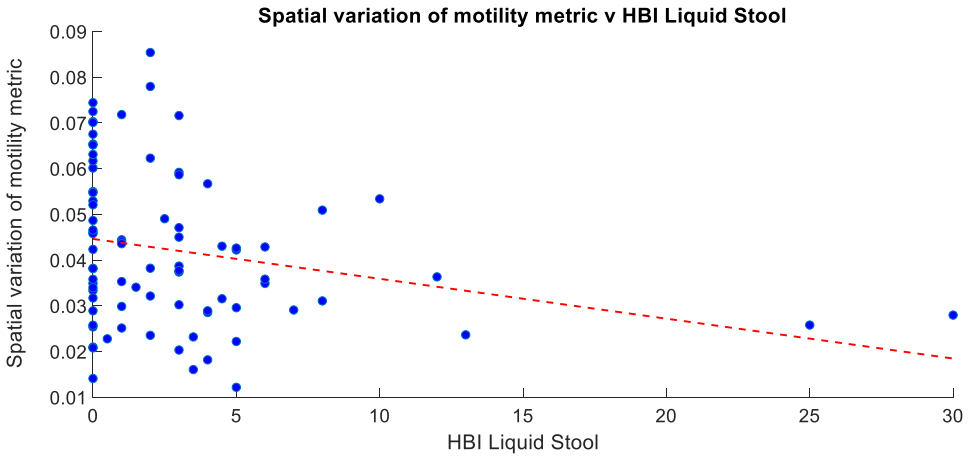


**Figure 27: Spatial variation of motility metric vs HBI liquid stools. There was a significant inverse association between the spatial variation of motility metric and the HBI liquid stools ($r = -0.29$, $p < 0.01$).**

Conversely there was no correlation between the spatial variation of motility metric and the other HBI components of pain and well-being (table 9).

| HBI Component | r value (correlation against spatial variation of motility metric) | P value (correlation against spatial variation of motility metric) |
|---|---|---|
| **Diarrhoeal Stools** | -0.29* | <0.01* |
| **Pain** | -0.022 | 0.85 |
| **Well-being** | 0.023 | 0.84 |

**Table 9: Correlation of HBI components (diarrhoeal stools, pain and well-being) against motility variance metric. *Significant result**

## 4.4 Discussion

The data in this study, demonstrates an inverse association between motility variance in morphologically normal small bowel and diarrhoea in CD. No correlation was found with mean motility, indicating that absolute levels of motility are not a significant driver of patient reported symptoms.

Previously, using a single-centre study design in 53 Crohn's disease subjects, Menys et al. [65] reported a significant inverse correlation between spatial variation of motility and HBI ($r = –0.45$, $p < 0.001$). There was also a significant inverse correlation between spatial variation of motility and the HBI symptom components of well-being, abdominal pain and number of liquid stools ($r = −0.4$, $p < 0.01$).

A correlation between spatial variation of motility and total HBI was again found, but this was not significant. There was an inverse association between the spatial variation of motility and the symptom of diarrhoea in this study, but no correlation with symptoms of well-being or abdominal pain was found. Therefore, the current validation study only reproduces the association between spatial variation of motility and the number of liquid stools. Indeed, it seems that the symptom of diarrhoea is the major contributor to the observed inverse correlation between spatial variation of motility and HBI (no associations with the individual scores of pain and well-being were found). The HBI is heavily weighted by stool frequency so it would appear that the total HBI score did not reach significance due to the additional HBI components of pain and well-being. In post-operative state, it would be expected that the stool frequency would be abnormal, depending on the extent of the surgery. If a large amount of bowel has been removed then the frequency of liquid stools would likely be higher than if minimal i.e. a small stricture, or no surgery was performed. Just over a third of the patients in this study underwent surgery prior to being scanned which could explain the proportion of patients at the higher end of stool frequency.

The reason for this apparent inverse association between the spatial variation of motility and patient symptoms is unclear with this explored further in chapter 5. A possible explanation is that impaired coordination of bowel motility rather than changes in absolute levels of motility leads to worsening of patient symptoms, particularly diarrhoea. Variation in small bowel motility is a normal finding in healthy individuals [12], [13], [128], [233], [234] and appears to be a marker of gut well-being. A reduction in this variability in turn may lead to abdominal symptoms. The postprandial state involves peristalsis and segmentation to facilitate the mixing of food ingested and absorption of nutrients. In this state however, variability is induced across the bowel volume, with episodes of peristalsis movement interspersed with periods of inactivity which prolongs transit time to aid absorption [13], [235], [236]. The mannitol administered prior to MR enterography seems to mimic the post-prandial state [151], [159] allowing us to capture the complexities of gut motility in a controlled and reproducible way [161]. Since mean motility scores were not correlated to the number of diarrhoeal stools, it can be surmised that absolute levels of motility are unlikely to be a driver for symptoms.

It is interesting to note that validated MRI CD activity scores which are based on structural observations such as bowel wall thickening, T2 signal and contrast enhancement etc. in the main show no association with clinical indices to assess symptoms such as HBI.

For example, the CD activity score has been developed and validated against a histological standard of reference [237] and has recently been extended to provide a global MRI activity score (MRI enterography global score) [134]. However, in previous work no significant correlation was found between the MRI enterography global score and HBI ($r = 0.102$, $p = 0.40$) in a cohort of 71 patients [134]. In the same study, Makanyanga et al. [134] reported no

correlation between a CD activity score and HBI ($r = 0.045$, $p = 0.630$). Indeed, HBI also correlates poorly with objective measures of inflammation such as faecal calprotectin (fCP). Sipponen et al. [238] for example showed no correlation between HBI and fCP ($p > 0.05$).

In this study, no correlation was found between either of the motility metrics and inflammation, measured by CRP.

This suggests the HBI score reflects more than simply underlying CD inflammatory activity and there are alternative drivers behind patient symptoms, potentially including aberrant motility [134], [239]. It also suggests that anatomical or structural MRI observations show little correlation with patient symptoms as captured by HBI. It has been acknowledged however that this lack of association has not been reconfirmed as part of the design of the current study.

It should also be acknowledged that although HBI is a validated patient symptom score, it is relatively simplistic and has limitations as a method to capture patient symptoms. More complex CD questionnaires such as the Inflammatory Bowel Disease Questionnaire have been developed [240]. However, HBI is easier to implement clinically and the three symptoms encompassed by the HBI are clearly of great importance to patients. Of course, whatever tool is used to capture symptoms, they are by their very nature subjective. In the context of HBI, two patients experiencing a similar level of pain could class this symptom as mild to severe depending on their individual perception. This could explain why this study does not fully validate the relationship between motility and total HBI. There may be differences in how the two different cohorts assessed their own symptoms, leading to discrepancies in the total HBI scores (generally the AMC cohort scored symptoms more highly than the UCLH cohort).

To attract a high HBI score of 10 or above, patients usually need to record a high level of diarrhoeal stools, which is arguably a more objective measure of patient symptomatology compared to the more subjective pain or well-being scores. It would perhaps be expected

that CD patients with mild symptoms would be much more likely to exhibit heterogeneous motility (with high motility variance) since they are presumably closer to having “healthy bowel”.

The utility of motility metrics in future mechanistic research may therefore be greatest in patients with moderate and severe abdominal symptoms. Future research will investigate the effects of Crohn’s disease medication on motility metrics and patient symptoms. The group of patients who retain a high symptom scores despite apparently being in clinical remission are of particular interest, as it may be that aberrant motility, if present, could be a target for pharmacological intervention.

This study does have limitations. Only morphologically normal bowel on MRI criteria was analysed. It is acknowledged that in the absence of capsule endoscopy or histological sampling, subtle CD could be present.

The motility data was only acquired over a 20 second breath-hold which may not be sufficient to capture the true complex nature of bowel motility. However, as discussed in chapter 3, a scan duration of 15 seconds has been shown to be sufficient for robust global small bowel motility measurements using the registration based motility assessment. However, longer free breathing datasets potentially may capture a more complete picture of motility (see section 3.4.2).

The MRI motility protocol involved acquiring multiple 2D slices, each consisting of a time series, to obtain full coverage of the bowel. However, these were acquired at different times so there was a temporal incoherence between slices which were acquired 30 seconds apart.

It should be noted that a reasonable proportion of the original 158 datasets were excluded (n = 76 excluded). However, only 14 of these were due to an incomplete MRI protocol (e.g. missing sequences or

inadequate small bowel coverage) and the rest was due to HBI or MRI data not being available. Therefore, only a small proportion of the excluded datasets were caused by the difficulty of acquiring dynamic MRI or poor image quality.

## 4.5 Summary

In summary, this study has demonstrated an inverse relationship between normal small bowel spatial variation of motility and patient abdominal symptoms in CD, specifically diarrhoeal stools.

Motility patterns are complex and therefore a combination of metrics, rather than a single metric, may provide better insight into aberrant motility and correlate better with symptoms in CD. Therefore, in chapter 5, new motility metrics are developed and tested in combination against symptoms, in a larger dataset of 105 CD patients. The performance of these computer-based metrics is compared to subjective radiological scoring of the equivalent motility features. Inter- and intra-observer variation is assessed between the two radiologists to determine whether complex motility patterns can be visually assessed, or if computer-based quantitative motility metrics are needed.

# Section C: Heterogeneity of motility patterns with the development of quantitative motility metrics and their relationship to Crohn's disease symptoms

**Section C** investigates the association between small bowel motility and distension from dynamic MRI images and Crohn's disease symptoms. **Chapter 5** presents work for testing the association between several new motility features, derived from dynamic MRI data, and abdominal symptoms from Harvey-Bradshaw Index (HBI) questionnaires, in 105 Crohn's disease patients, through both radiologist-based grading of motility and the development of computer-based motility image metrics. Multivariable linear regression was performed using generalised linear regression models to assess motility features (independent variables) individually or in combination against HBI symptom scores (dependent variable or outcome measure).

Quantitative motility assessment has been performed in several studies for Crohn's disease, but the global motility metrics described here have either been newly developed and/or have not been compared to the equivalent radiologist visual grading of motility. The intra- and inter-observer agreement for two radiologists subjectively grading dynamic MRI datasets is assessed for the first time in this study.

# Chapter 5: Automated versus subjective assessment of spatial and temporal MRI small bowel motility in Crohn's disease (CD)

## Author Declaration

The work presented here was led by the thesis author (3 years of experience at time of publication) including performing the literature review, downloading, anonymising and segmenting the datasets, designing the study for radiologist visual scoring, and performing the motility and statistical analysis, under the supervision of Alex Menys, David Atkinson and Stuart Taylor.

Alex Menys and Freddy Odille developed the registration algorithm and graphical user interface (GUI) displaying the dynamic MRI data and motility maps. The thesis author enhanced the functionality of the main GUI for data analysis, including the development of new motility metrics and a distension metric, and created a separate radiologist GUI for visual scoring of motility datasets.

Stuart Taylor and Andrew Plumb visually analysed the datasets for the radiological scoring.

Data was collected by the VIGOR++ consortium to develop a computer aided diagnosis framework for CD (see more details in author declaration and section 4.2.1 in chapter 4). Additional data included in this study was collected at UCLH as part of another study

[134]. Motility sequences of the whole small bowel volume were acquired as part of the MRI protocol.

This research has been published in: RM Gollifer, A Menys, A Plumb, K Mengoudi, CAJ Puylaert, JAW Tielbeek, J Makanyanga CY Ponsioen, FM Vos, J Stoker, SA Taylor, D Atkinson. “Automated vs Subjective assessment of spatial and temporal MRI small bowel motility in Crohn’s disease.” Clinical Radiology 2019.

The key components of my work here were:

- Development of new computer-based motility metrics (for the automated assessment part of the study) for single slice analysis.
- New functionality written into the main motility analysis GUI to select the slice containing the largest amount of small bowel and extract the motility metrics for that slice.
- Development of a new, separate radiologist GUI to allow the datasets to be viewed and visually graded by the radiologists.
- Designing the study to present the datasets to the radiologists in a methodologically sound manner, allowing for inter- and intra-observer variability analysis at a later stage.
- Performing statistical analysis using multivariable linear regression to test combinations of motility features against HBI symptoms and therefore compare the performance of automated motility metrics and the equivalent radiological graded motility features.

## 5.1 Introduction

As discussed previously in chapter 4, the ability of dynamic MRI to capture motility patterns in structurally normal bowel could prove a powerful tool in improving the understanding of gastrointestinal (GI) motility in health and diseases such as CD.

To date, most researchers have examined only a small number of motility metrics. For example, Bickelhaupt et al. (2013) [171] suggested that contraction frequencies are altered in the bowel distal to segments with inflammatory activity.

The findings in chapter 4 partly validated the previously found association between reduced global spatial variation of motility in normal appearing bowel and patients symptoms in CD, particularly diarrhoeal stools [65]. The association was strongest in patients with higher symptom scores (HBI scores greater than 10), but there was no significance when spatial variation of motility was tested against symptoms for all the patients. In both the original study and the validation study in chapter 4, no association was found between mean motility and patient symptoms.

Therefore, there remain many unknowns. For example, it is unclear which metrics, or combination thereof, best capture aberrant motility, and whether radiologists can reliably detect abnormal motility without the need for specialised software. In this study, new motility metrics have been developed, building on the work in chapter 4.

There has been no previous research into the ability of radiologists to detect abnormal motility patterns as part of their conventional reporting of Magnetic Resonance Enterography (MRE) datasets, providing added value without the need for additional software. Conversely, a computer-based metric could be developed to reliably capture motility patterns, which are difficult to visually assess. If a link could be established between abnormal motility, quantified by

software, and symptoms, then this could improve the efficiency of the clinical workflow.

The purpose of the current study was twofold.

Firstly, both established [65] (described in Chapter 4) and newly proposed computer-based metrics were investigated to derive the best combination associated with abdominal symptoms in CD patients.

Secondly, subjective grading of bowel motility by experienced radiologists was compared with automated measurement. This was done through evaluating the performance of the two methods of motility assessment when tested against symptoms. Inter- and intra-observer variation was also investigated.

## 5.2 Methods

The current study was retrospective and has been approved by both centres' ethics committees (Hampstead REC, London and the ethics committee of the Academic Medical Center). The patients provided written informed consent for the original research studies and the requirement for consent was waived for the retrospective analysis in this study.

### 5.2.1 Patient Selection

Data was collated from two previous studies:

1. VIGOR++ study (study 1), a prospective trial developing automated measurements of bowel wall thickness and contrast enhancement to quantify CD activity [232]
2. a prospective single-centre study (study 2) developing a global MRI CD activity score [134]

Patients recruited to both these studies completed a HBI symptom questionnaire (see section 1.4.1) on the day of an MRE examination, which included a motility sequence.

Inclusion criteria for the current study were patients who had a final diagnosis of CD based on clinical, biochemical, endoscopic, imaging and histopathological data and the availability of associated dynamic MRI and HBI.

A total of 185 datasets across the two parent studies were potentially available for inclusion in the current study. Exclusion criteria were contraindications to undergo MRI, patients who had a stoma, and the use of medication with known direct effects on motility such as prokinetic agents (e.g. neostigmine), anti-spasmodics (e.g. buscopan) and opioid analgesics. Datasets were also excluded if the dynamic MRI sequences were inadequate (e.g. less than 3 slices, incomplete time series or motility data unavailable to this study), a HBI score was not collected or the patient had a final diagnosis other than Crohn's disease.

A proportion of patient data (n=28) used in the current study was also used in previous work in chapter 4 investigating the relationship between two motility metrics (mean motility and spatial variation of motility) and abdominal symptoms [65], [241].

Demographic data pertaining to age, sex, current medication, disease duration and surgical history of the selected patients was collected.

### 5.2.2 MRI Protocol

Patients fasted for 4 hours before ingesting oral contrast prior to undergoing MRI in the supine position on either 1.5T (Avanto, Siemens, Medical Systems, Erlangen, Germany) or 3T (Achieva: Philips, Best, the Netherlands) units.

The MRI protocol included a dynamic “cine motility” sequence acquired during a 20 second breath-hold, and prior to administration of anti-spasmodics for anatomical images. Specifically, a multi-slice 2D, coronal, balanced steady-state free precession sequence with a temporal resolution of 1 image/second and a slice thickness of 10mm was acquired coronally.

Repeat coronal block acquisitions were performed to encompass the whole small bowel volume, the number of acquisitions ranging from 5 to 16 depending on the size of the patient (table 10).

| **Parameter** | **Donor study 1 (VIGOR)** | **Donor study 2** | |
|---|---|---|---|
| Scan dates | October 2011-July 2014 | February 2010-October 2011 | |
| Scan preparation | • Fasted for 4 hours<br>• 800ml of 2.5% mannitol ingested (3 hours prior to start of scan to distend colon)<br>• 1600ml of 2.5% mannitol ingested (1 hour prior to start of scan to distend small bowel) | • Fasted for 4 hours<br>• 1-1.5 litres of 0.2% locus bean gum/2.5% mannitol solution over 45 minutes | |
| MRI scanner | 3T systems (Ingenia/Achieva; Philips, Best, the Netherlands) | 1.5T (Avanto, Siemens, Medical Systems, Erlangen, Germany) | 3T (Achieva: Philips, Best, the Netherlands) |
| Repetition time (ms)* | 2-2.1 | 3.85 | 1.96 |

| | | | |
|---|---|---|---|
| Echo time (ms)* | 1 | 1.91 | 0.98 |
| Field of view (mm) | 380x380mm | Variable | Variable |
| Image matrix (Acquired matrix)* | 200x167 | 256x184 | 200x167 |
| Flip angle | 45 | 61 | 45 |

**Table 10: Motility balanced sequence parameters for donor site 1 and 2. * Representative parameters since actual values vary between scans and patients.**

### 5.2.3 Motility Assessment

Motility data visualisation and analysis were performed in MATLAB 2017 (The MathWorks, Natick, MA).

For the current study, two graphical user interfaces (GUIs) or viewers were developed. Within the main motility analysis viewer (described previously in sections 3.2.3 and 4.2.3), anonymised datasets are displayed, as both a static reference image and as a “cine” movie. This allowed for inspection of all the MRI data (as well as ROI placement and automated MRI metric measurement).

A second “radiologist viewer” which presented data in a blinded and pre-set order and facilitated subjective scoring of metrics by the study radiologists. This viewer displayed the “cine” movie only and was used for radiologist subjective grading of motility described below in section 5.2.5 (Appendix 1 in section 9.1).

*Step 1: Generation of the SD Jacobian*

As described in sections 2.3.2 and 2.3.3, frames from each subject’s 2D cine motility series were registered to a single reference frame

using a previously validated optic flow based technique. The SD Jacobian was calculated on a per pixel basis and displayed on the reference frame as a motility map.

Furthermore, in this chapter, the deformation fields' Jacobian determinant were used to derive additional automated motility metrics (temporal variation of motility and area of motile bowel) and the reference frame was used for ROI placement and derivation of the distension metric.

The process of implementing the registration and generating the motility metrics for each patient is summarised in figure 28, and each metric is described in more detail in section 5.2.4.

*Step 2: ROI placement and slice selection*

For each patient, the thesis author blinded to the HBI score used the main motility analysis viewer to place ROIs over the small bowel on the reference image, with the cine motility movies available to aid ROI placement. The ROIs were validated by a research fellow with over 5 years MRE experience (Menys).

In detail, for each of the motility datasets, ROIs were placed in morphologically normally appearing small bowel on all the coronal motility acquisition slices. The single coronal slice containing the largest area of small bowel was then objectively selected based on the largest number of "small bowel" pixels that could be encompassed by a single ROI.

The ROIs excluded small bowel mesentery and Crohn's disease affected small bowel (SB) i.e. SB demonstrating wall thickening, abnormal T2 signal hyper enhancement etc. (described in sections 1.3.1 and 4.2.3) [78]. CD affected SB has been previously been shown to be hypomotile [87]. However, in this study the association between motility in morphologically normal SB and CD symptoms was investigated to test the hypothesis that in the absence of inflammation, motility can still become aberrant in CD and give rise to symptoms.

### 5.2.4 Automated Assessment: motility metric measurements

The automated metrics were developed to capture motility features in a single acquisition slice. Five metrics were derived from the ROIs within the selected slice:

1. mean motility (previously introduced in chapters 2, 3 and 4)
2. spatial variation (previously introduced in chapter 4)
3. temporal variation (newly developed in this chapter)
4. area of motile bowel (newly developed in this chapter)
5. intestinal distension (newly developed in this chapter)

Metrics 1, 2 and 4 were derived from the motility map (described previously in sections 2.3.2 and 2.3.3) Metric 3 was derived from a temporal variation map and metric 5 was derived from the reference frame (figure 28).

In detail, **metric 1** and **metric 2** were derived by calculating the mean and the variance, respectively, of the SD Jacobian values. Similarly, mean motility and spatial variation of motility metrics have been derived in the previous study detailed in chapter 4, but across multiple slices [65]. Metrics 1 and 2 in the current chapter were applied to a single slice.

**Metric 4**, the area of motile bowel was defined as the percentage of pixels with an SD Jacobian above a threshold of 0.11. The cut-off of 0.11 was selected based on the work of Odille et al. (2012) suggesting bowel with a SD Jacobian<0.11 is classified as immotile [192] (figure 29G-H).

**Metric 3**, the temporal variation metric was derived by firstly calculating the standard deviation of the deformation fields' Jacobian determinant in multiple 5 second (or 5 frame) sliding windows, henceforth referred to as the Sliding SD Jacobian Value. For example, in a 20 second time series there would be 16 sliding windows i.e. 1-5 seconds (window 1) to 16-20 seconds (window 16). Each Sliding SD Jacobian Value is a per pixel measure of bowel expansion and contraction within a 5 second time period.

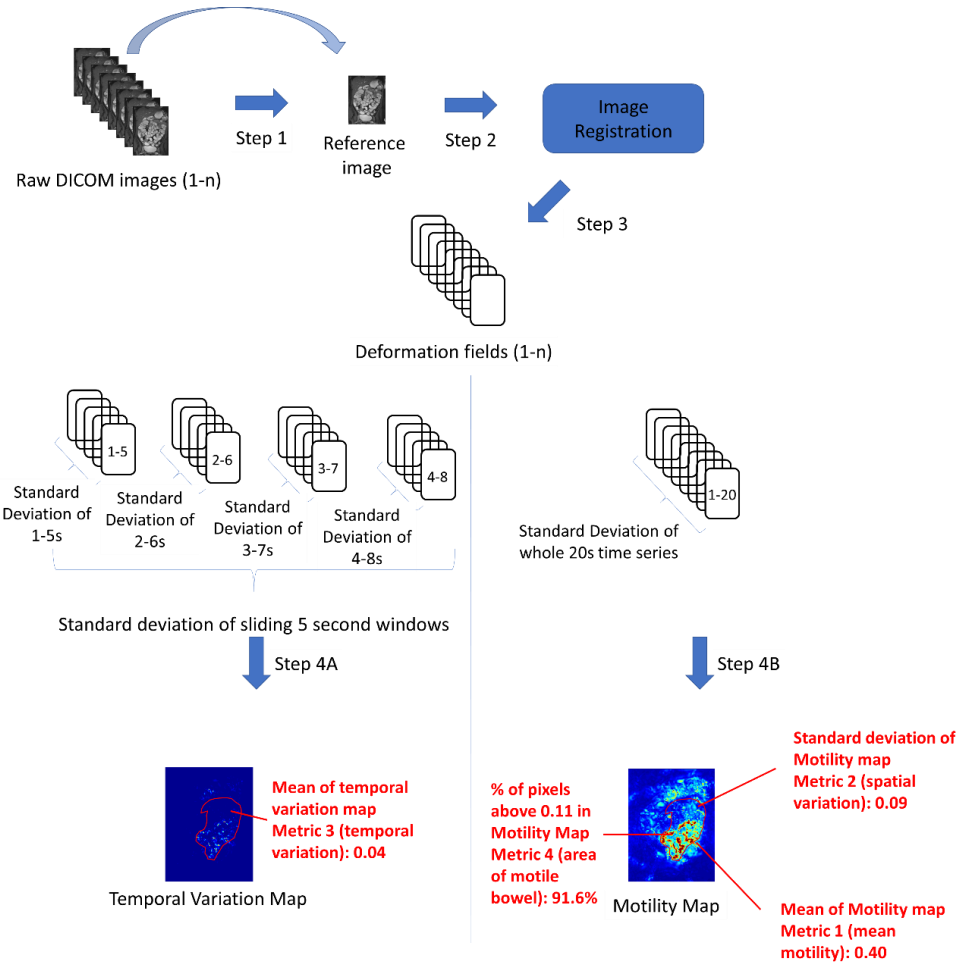


**Figure 28: A reference image was selected automatically from the stack of dynamic MRI images or frames (step 1). Each frame was registered to the reference image (step 2) to produce a set of deformation fields (step 3). The SD Jacobian was calculated to create a motility map (step 4B). Mean motility (metric 1), spatial variation of motility (metric 2) and area of motile bowel (metric 4) were calculated from this motility map. A temporal variation map was created by calculating the variance of the sliding SD Jacobian values map (step 4A). The temporal variation of motility (metric 3) was calculated from the temporal variation map and the intestinal distension (metric 5) was calculated from the reference frame by thresholding intensities based on 50% of the median intensity within the ROI.**

The temporal variation map was generated by calculating the variance of these Sliding SD Jacobian Values which captures the difference in motility between the sliding windows for each pixel. This temporal variation metric gives an indication of variability of motility over time e.g. low temporal variation corresponds to consistent motility (either constantly high motility or constantly low motility) throughout the entire scan time while high temporal variation corresponds to a wide range of Sliding SD Jacobian Values suggesting a higher proportion of the small bowel with fluctuating motility, between low and high (figure 29E-F).

**Metric 5**, the intestinal distension metric was developed based on the intensity of the pixels within the ROIs, and their neighbours, in the reference frame. A binary mask was created with each pixel assigned a value of 1 if the signal intensities of 6 out of 9 of their neighbouring pixels (8 neighbours and the pixel being analysed) were above a threshold of 50% of the median intensity within the ROIs. The value of intestinal distension was indicated by the percentage of pixels assigned a value of 1 (a high value representing higher signal, suggesting good distension with mannitol, and a low value indicating lower signal, presumed due to small bowel collapse) (figure 29I-J).

The intensities in most MR images are not comparable across subjects so a threshold has to be chosen based on the data itself. In this study, the small bowel ROI was used as a basis for the distension threshold and would therefore not be sensitive to tissue intensities in other regions, which might differ between patients, such as fat and artefacts. The connected criterium of a pixel and its neighbours was used to exclude small pockets of fluid and therefore only ‘count’ regions of genuine distension.

An important feature of distension, the diameter of the lumen, could be incorporated into the metric. However, this is difficult to measure throughout the small bowel as it would be time consuming and more automated methods would be challenging to implement due to through-plane motion. An alternative threshold was investigated,

using the liver as a normalised threshold across datasets, but this did not give results consistent with visual inspection of distension.

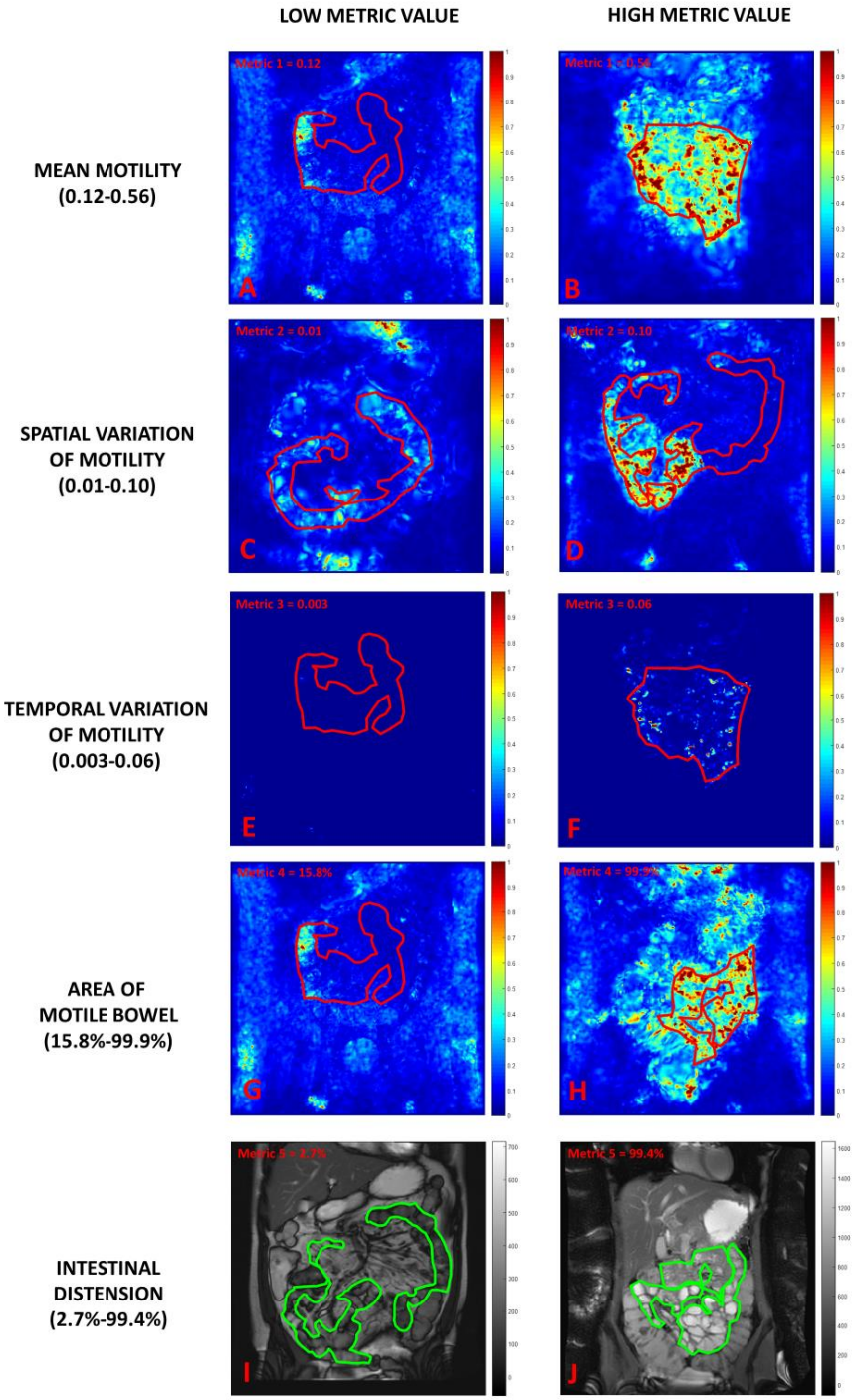


**Figure 29: Examples of low (first column) and high values (second column) displayed for the five metrics of mean motility (A-B), spatial variation of motility (C-D), temporal variation of motility (E-F), area of motile bowel (G-H) and intestinal distension (I-J).**

### 5.2.5 Subjective Radiological Assessment

The same five features were visually assessed using the cine motility time series for the chosen slice.

The thesis author conducted a training session with two experienced radiologists (Plumb and Taylor; 10 and 12 years of experience of MRE respectively) to explain the five metrics and what they represented in terms of different motility patterns.

For example, for metric 1 (mean motility), the radiologists were asked to subjectively grade the average motility of the small bowel across the slice. For metric 2 (spatial variation), they were asked to grade how variable motility was within the area of the ROI, and for metric 3 (temporal variation) they were asked to grade how the motility of the bowel changed over the 20 second time series. Fifteen datasets outside of the main study dataset were selected to demonstrate examples of different combinations of low, medium and high scores for metrics 1, 2, 3, 4 and 5. During the training session, these datasets were visually assessed firstly by each radiologist blinded to each other and then in consensus to agree upon a scoring scheme.

To record their grading, the radiologists would view the “cine” movie for each dataset and visually grade each of the five metrics on a sliding 0-10 scale (or % scale for area of motile bowel) discretised in increments of 0.1 using the radiologist viewer (Appendix 1). The two radiologists both scored all study datasets, blinded to the scores of the other. The datasets were presented in random order. Reading sessions typically included 15 or 30 datasets and were performed at 1 or 2 weekly intervals, respectively. One in every five datasets presented was a duplicate dataset. For example, in a 15-dataset scoring session, 12 would be original data and 3 would be duplicate data, previously scored. The 3 duplicate datasets were randomly selected and presented to the radiologists at least 2 weeks after they were originally scored. Radiologist 1 graded the datasets in the reverse order from radiologist 2 to account for learning effect bias.

### 5.2.6 Statistical analysis

All statistical analysis was performed using MATLAB 2017 (The MathWorks, Natick, MA). All data was checked for normality using a Shapiro-Wilk test (alpha = 0.05).

Intra-observer and inter-observer variability between radiologist observers was assessed using Bland-Altman plots. Mean absolute differences, 95% limits of agreement (LOA) and coefficient of variation (CV) were calculated. A low CV would be considered good and a high CV considered poor. The area of motile bowel metric was graded as a percentage and then converted to a 0-10 scale.

Mean absolute differences give an idea of the systematic bias between scoring either between 2 observers or repeat scoring for the same observer.

LOA gives an indication of the repeatability of the scoring and is calculated by 1.96 times the standard deviation of the measurements.

CV assesses the variability of scoring and is calculated by the ratio of the standard deviation between measurements to the overall mean of measurements.

Univariate and multivariable regression models were tested to assess the relationship between HBI patient symptoms scores and 1) Automated motility metrics, and 2) Subjective radiological motility features (based on the mean score of radiologist 1 and 2).

*MATLAB function used: mdl_glm = fitglm (currentPredictorsMatrix, HBI, 'linear', 'Distribution', 'gamma', 'Link', 'identity', 'PredictorVars', [firstvar,secondvar]);*

In both cases, thirty combinations of the five independent variables (metric 1 – mean motility, metric 2 – spatial variation, metric 3 – temporal variation, metric 4 – area of motile bowel, metric 5 –

intestinal distension) were tested against the dependent variable of HBI.

All variables in the models and the HBI were standardised so that the estimated coefficients between metrics of different scales could be directly compared. The larger the absolute value of the standardised coefficient estimate, the higher the importance of the variable in predicting HBI.

The goodness of fit in the regression analysis is reported as R2 (adjusted) to account for the varying number of independent variables being tested each time. Note that for a perfect fit, the R2 (adjusted) value would be 1.

Multicollinearity, i.e. variables are correlated with other variables within the model, was tested to rule out models containing high collinearity between independent variables with variance inflation factor (VIF) > 5 indicating a highly collinear variable [242]. Multicollinearity increases the standard errors of the coefficient estimates and therefore causes some of the coefficients estimates to be statistically insignificant when they potentially should be significant. If any of the standardised coefficient estimates within a model were insignificant, then the model was rejected.

Models were also excluded if the F-statistic was insignificant at the 5% significance level ($P > 0.05$) or if the R2 (adjusted) value was negative. Both these conditions indicate that the model poorly fits the data and is inferior to a simple intercept only i.e. fitting a horizontal line.

The best accepted models met the following criteria:

1. Low multicollinearity i.e. all variables in the model had a low variance inflation factor (VIF < 5) [243]
2. F-statistic for the model was significant ($P < 0.05$)
3. R2 (adjusted) value for the model was positive ($R2 > 0$)
4. Standardised coefficient estimates for all variables in the model were significant ($P < 0.05$)

The following covariates: Age, sex, history of surgery (yes/no) and disease duration were added as independent variables to the accepted models to see if the standardised coefficient estimates for the metrics retained significance.

# 5.3 Results

## 5.3.1 Cohort Demographics

185 datasets were available from the 2 donor studies (124 donor study 1, 61 donor study 2) and 15 patients were selected for the radiologist training session (figure 30).

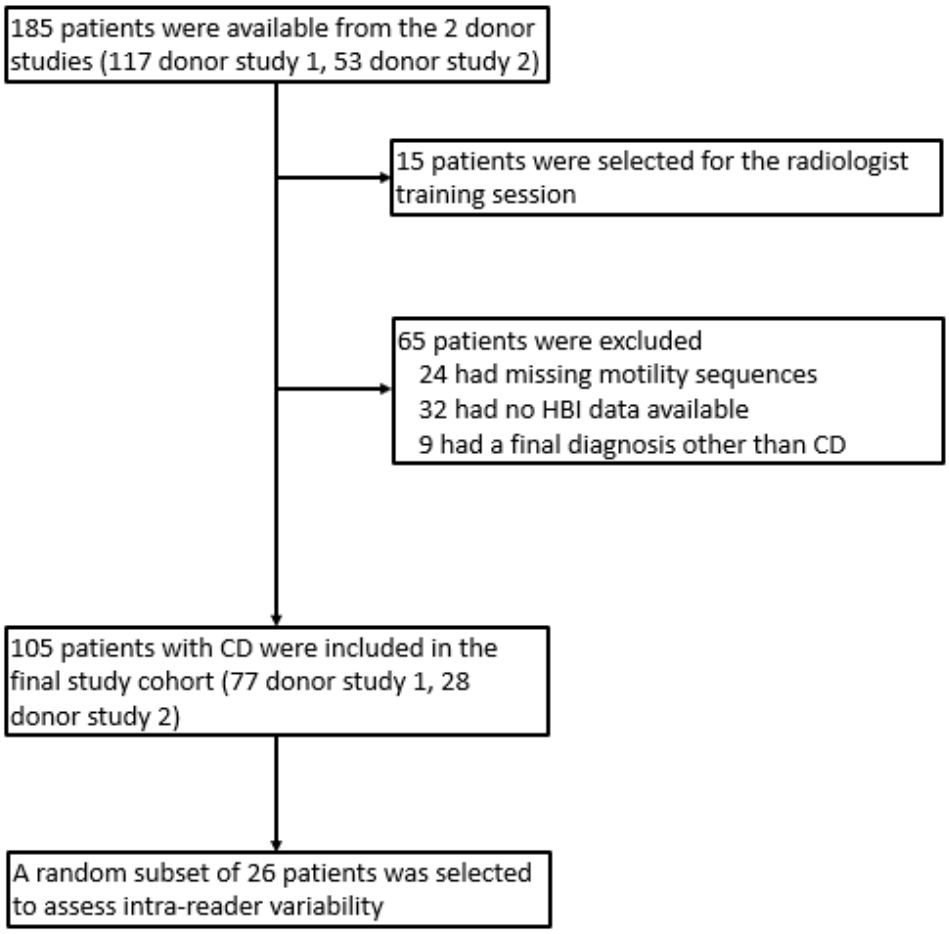


**Figure 30: Flow chart demonstrating patient inclusions and exclusions.**

65 patients were excluded for the following reasons; missing motility sequences (n=24) HBI data unavailable (n=32) and non-Crohn's disease final diagnosis (n=9).

The remaining 105 patients (77 donor study 1, 28 donor study 2) formed the final study cohort (table 11).

| **Parameter** | | **Donor study 1 (VIGOR)** | **Donor study 2** |
|---|---|---|---|
| Age (range and median, years) | | 16-68; 32 | 16-67; 32 |
| Males (%) | | 36 (47%) | 16 (57%) |
| Disease Duration (years) | <1 | 8 | 3 |
| | 1-5 | 10 | 7 |
| | 5-10 | 24 | 11 |
| | >10 | 33 | 7 |
| | Unknown | 2 | 0 |
| Disease Location | Ileal | 28 | 9 |
| | Colonic | 11 | 6 |
| | Ileocolonic | 38 | 13 |
| Medications | None | 16 | 3 |
| | 5-ASA | 17 | 11 |
| | Immuno-modulators | 27 | 22 |
| | Biological Agents | 25 | 5 |
| Small Bowel Surgical History | None | 50 | 16 |
| | 1 operation | 21 | 6 |
| | 2 operations | 6 | 6 |

**Table 11: Patient Demographics with 105 patients in study cohort.**

### 5.3.2 HBI and Motility Metrics

A summary of automated motility metrics and HBI scores is shown in table 12.

| | Median | Range | |
|---|---|---|---|
| | | Minimum | Maximum |
| **HBI** | 5 | 0 | 38 |
| **Mean motility** | 0.346 | 0.123 | 0.563 |
| **Spatial variation** | 0.038 | 0.008 | 0.098 |
| **Temporal variation** | 0.024 | 0.003 | 0.063 |
| **Area of motile bowel (% of ROI)** | 95.0 | 34.2 | 100.0 |
| **Intestinal distension (% of ROI)** | 82.3 | 66.4 | 98.6 |

**Table 12: Median, minimum and maximum HBI scores and automated motility metric values.**

### 5.3.3 Automated Assessment

The demographics did not have an effect on the model effectiveness and therefore the following results discuss the models without the addition of these demographic covariates (table 13).

The highest R2 adjusted value for a univariate model was 0.034 and consisted of standardised spatial variation of motility, which was negatively associated with standardised HBI (Coefficient estimate = -0.21, P < 0.05) (table 13).

The highest R2 adjusted value for a multivariable model was 0.036 and included standardised temporal variation, which was negatively associated with HBI, (Coefficient estimate = -0.23, P < 0.05) and standardised area of motile bowel, which was positively associated with standardised HBI (Coefficient estimate = +0.16, P < 0.05) (table 13).

| Metrics in Model | Coefficient Estimate | Confidence Intervals | | P value | R2 (Adjusted) |
|---|---|---|---|---|---|
| | | Min | Max | | |
| Intercept | 1.0 | 0.82 | 1.20 | P<0.001 | 0.034 |
| Spatial variation (Metric 2) | -0.21 | -0.37 | -0.06 | 0.006 | |
| Intercept | 1.0 | 0.82 | 1.19 | P<0.001 | 0.036 |
| Temporal variation (metric 3) | -0.23 | -0.39 | -0.07 | 0.005 | |
| Area of motile bowel (metric 4) | 0.16 | 0.03 | 0.29 | 0.010 | |

**Table 13: The coefficient estimates (with confidence intervals and p values) and associated R2 (adjusted) values for the two best automated models i.e. a univariate model containing the intercept and spatial variation (metric 2) and a multivariable model containing the intercept, temporal variation (metric 3) and area of motile bowel (metric 4).**

The regression models with the original units i.e. without standardising the independent variables and the HBI showed that for 0.01 unit increase in spatial variation, there was an associated 0.61 unit (95% confidence interval [CI], 0.18-1.03) decrease in HBI.

Assuming all other variables were kept constant, for each 0.01 unit increase in temporal variation there was an associated 0.97 (95% CI, 0.30–1.63) decrease in HBI and for each 10 percent increase in area of motile bowel there was an associated 0.88 (95% CI, 0.18-1.58) unit increase in HBI.

The fitted HBI generated from each of the two models was plotted against the actual HBI as shown in figure 31.

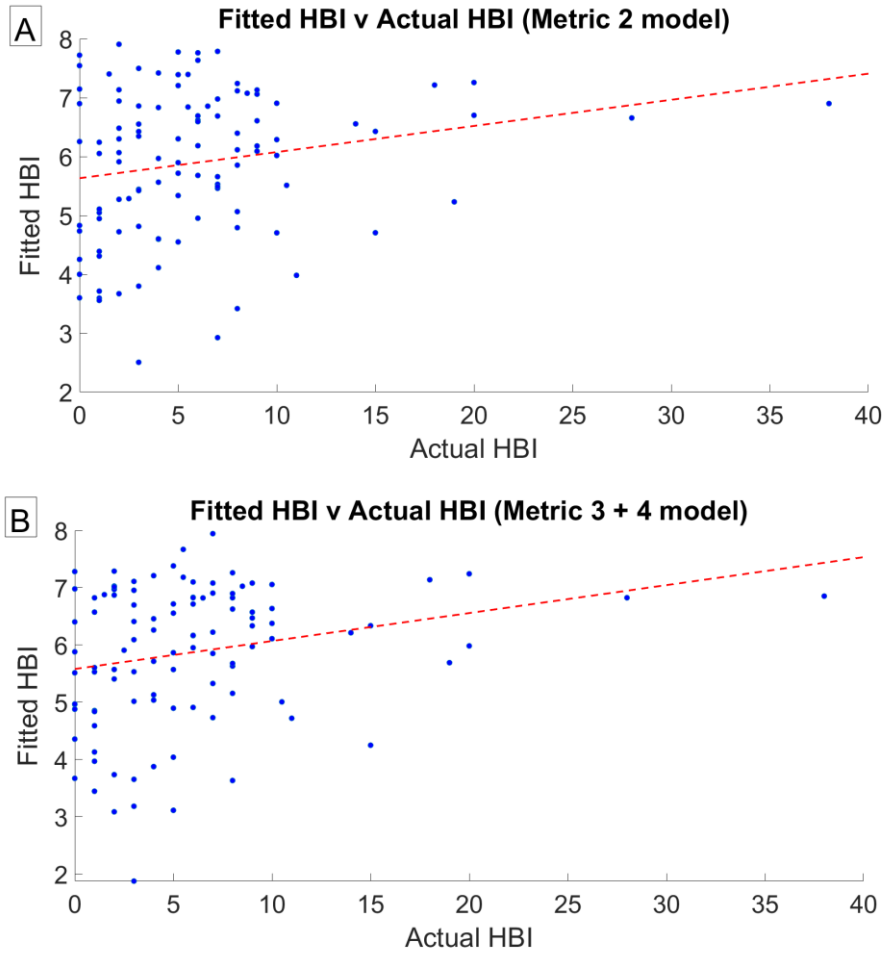


**Figure 31: Fitted HBI model data vs. Actual HBI data for the best automated models with A: negative association of metric 2 (spatial variation) and B: negative association of metric 3 (temporal variation) + positive association of metric 4 (area of motile bowel).**

## 5.3.4 Subjective Radiological Assessment

*Inter-observer variability*

Inter-observer variability for visually assessed motility features was poor (table 14).

| Comparison | Motility Feature | Mean difference (bias) | 95% LOA | CV |
|---|---|---|---|---|
| Radiologist 1 v Radiologist 2 (Inter-observer variability) | Mean motility | 1.1 (P<0.05) | -2.7-4.9 | 37% |
| | Spatial variation | -0.76 (P<0.05) | -5.8-4.3 | 55% |
| | Temporal variation | 1.3 (P<0.05) | -2.1-4.8 | 71% |
| | Area of motile bowel* | 0.19 (P=0.28) | -3.3-3.7 | 26% |
| | Intestinal distension | 0.45 (P=0.02) | -3.5-4.4 | 34% |

**Table 14: Mean difference, 95% LOA and CV for inter-observer variability (Radiologist 1 v Radiologist 2) in 5 visual assessed motility metrics (*converted to from a scale of 0-100 to 0-10 scale).**

The lowest coefficient of variation (CV) was 26% for area of motile bowel and the highest CV was 71% for temporal variation of motility. The absolute mean difference ranged from 0.19 for area of motile bowel to 1.3 for temporal variation of motility. The narrowest 95% limits of agreement (LOA) was for temporal variation of motility and

the widest 95% LOA was spatial variation of motility. The highest agreement was for area of motile bowel (figure 32A) and the lowest agreement was for spatial or temporal variation of motility (figure 32B).

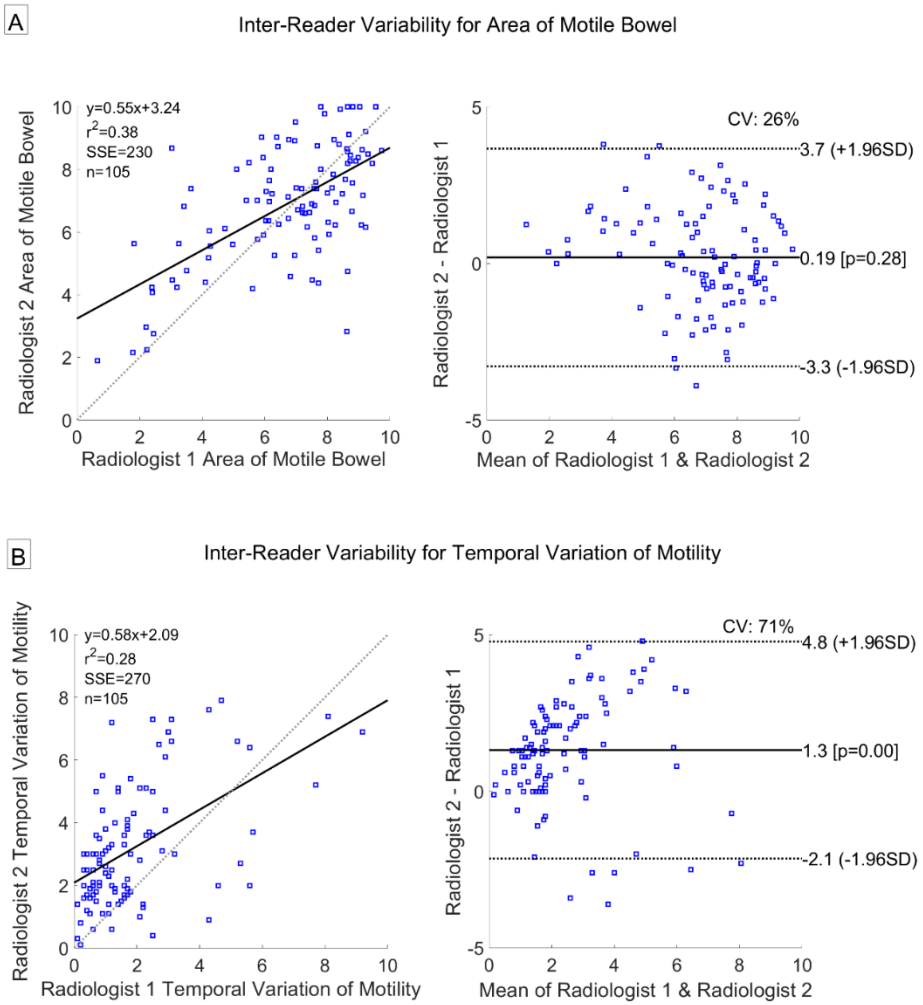


**Figure 32: The visual scoring for the area of motile bowel (A - top) and for temporal variation of motility (B - bottom) are displayed on simple correlation plots (left) and Bland-Altman plots (right). The highest inter-observer agreement is seen for the area of motile bowel visual scoring (top right) where the coefficient of variation (CV) is 26% on the Bland-Altman plot. The lowest inter-observer agreement is seen for the temporal variation of motility visual scoring (bottom right) where the CV is 71%.**

*Intra-observer variability*

Generally, intra-observer variability was better than inter-observer variability, with lower mean differences, narrower 95% LOAs and lower CVs (table 15) for radiologist 1 and for radiologist 2.

| Comparison | Motility Feature | Mean difference (bias) | 95% LOA | CV |
|---|---|---|---|---|
| Radiologist 1 (Intra-observer variability) | Mean motility | 0.06 (P=0.88) | -3.7-3.8 | 42% |
| | Spatial variation | 0.37 (P=0.39) | -3.9-4.6 | 39% |
| | Temporal variation | 0.08 (P=0.75) | -2.3-2.5 | 81% |
| | Area of motile bowel* | 0.23 (P=0.31) | -2-2.4 | 18% |
| | Intestinal distension | 0.05 (P=0.85) | -2.8-2.9 | 24% |
| Radiologist 2 (Intra-observer variability) | Mean motility | 0.11 (P=0.54) | -1.7-1.9 | 16% |
| | Spatial variation | 0.11 (P=0.37) | -4.1-3.9 | 45% |
| | Temporal variation | 0.11 (P=0.78) | -3.9-3.7 | 66% |
| | Area of motile bowel* | 0.32 (P=0.29) | -2.6-3.3 | 23% |
| | Intestinal distension | 0.27 (P=0.32) | -2.3-2.9 | 22% |

**Table 15: Mean difference, 95% LOA and CV for intra-observer variability (for both Radiologist 1 and Radiologist 2) in 5 visual assessed motility metrics (*converted to from a scale of 0-100 to 0-10 scale).**

The lowest CV was 16% for mean motility (radiologist 2) and the highest CV was 81% for temporal variation of motility (radiologist 1). The absolute mean difference ranged from 0.05 for intestinal distension (radiologist 1) to 0.37 for spatial variation of motility (radiologist 1). The narrowest 95% LOA was for mean motility (radiologist 2) and the widest 95% LOA was for spatial variation of motility (radiologist 1). The best intra-observer agreement was for radiologist 2 scoring of mean motility (figure 33A) and the worst intra-observer agreement was for radiologist 1 scoring of spatial or temporal variation of motility (figure 33B).

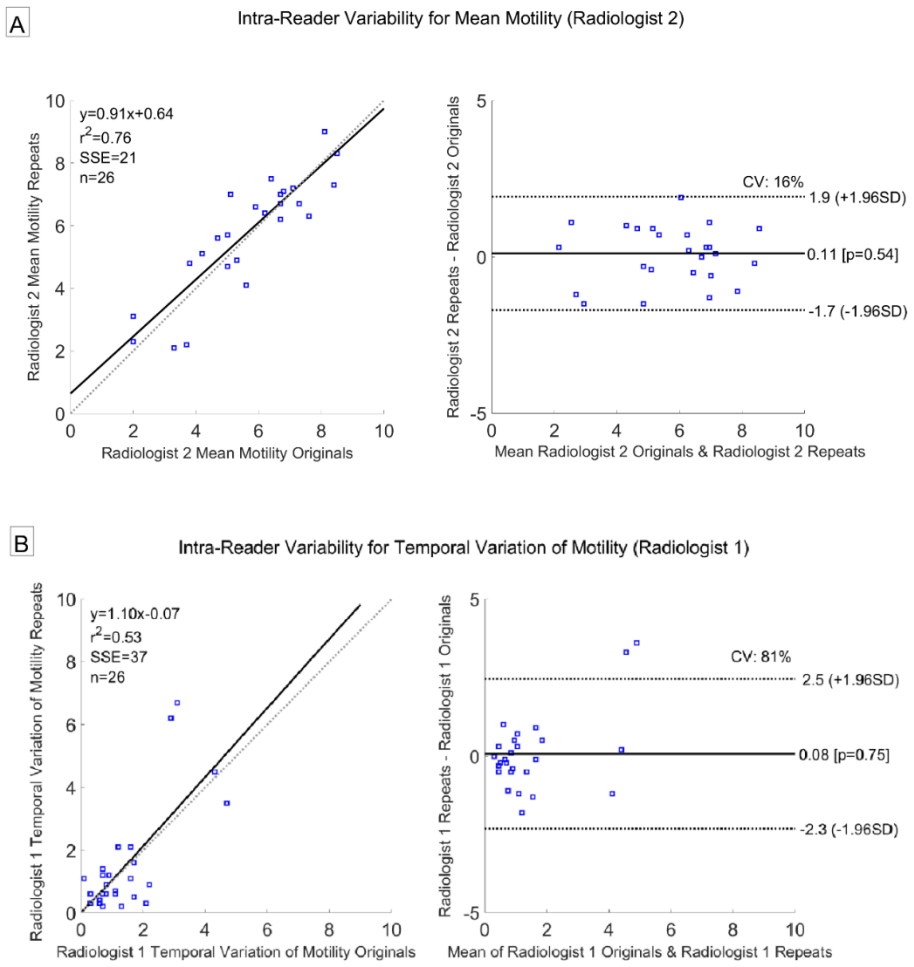


**Figure 33: The visual scoring for the mean motility from radiologist 2 (A - top) and for temporal variation of motility from radiologist 1 (B - bottom) are displayed on simple correlation plots (left) and Bland-Altman plots (right). The best intra-observer agreement is seen for the mean motility visual scoring from radiologist 2 (top right) where the coefficient of variation (CV) is 16% on the Bland-Altman plot. The worst intra-observer agreement is seen for the temporal variation of motility visual scoring from radiologist 2 (bottom right) where the CV is 81%.**

*Subjective models for combined observer motility scores v HBI*

None of the univariate or multivariable combined models using radiologist grading of motility metrics demonstrated an association with the HBI score. The F-statistic was insignificant ($P > 0.05$) for all models (Appendix 2 in section 9.2).

## 5.4 Discussion

The present study confirms there is an association between motility metrics in morphologically normal-appearing small bowel captured using cine MRI and the severity of patient symptoms in CD, which was also found in chapter 4. Radiologists cannot adequately grade these motility features by simple subjective evaluation, and software-based quantification is likely required to capture this relationship.

To date, the ability of radiologists to subjectively assess motility has not been investigated beyond “active” and “inactive” motility. As would be expected, intra-observer variation was lower than inter-observer variation. Visual grading for the area of motile bowel had the lowest inter- and intra-observer variability, with lower intra-observer variability also found in the visual grading for intestinal distension and the mean motility grading by radiologist 2. Conversely, grading of spatial variation and temporal variation were highly variable. Overall, the present data show that even between experienced radiologists inter-observer variation is poor suggesting that subjective grading of motility features is unlikely to be clinically useful. Indeed, neither univariate nor multivariable linear regression revealed any association between radiologist grading and HBI score.

Automated motility metrics therefore would have clear advantages over subjective assessment and provide a more consistent

assessment of motility. Automated measures have already been shown to be repeatable [161], and in this chapter they performed better than radiological scoring when tested against patient symptoms, with several automated motility models showing a relationship with HBI. This suggests they at least in part capture the likely aberrant small bowel motility in apparently normal bowel in patients with Crohn's disease.

Variation in spatial and temporal motility are clearly the most difficult motility features to visually assess yet they seem to have the strongest relationship to symptoms. For example, in a single centre study of 53 CD subjects, Menys et al. (2016) [65] have previously reported a significant inverse correlation between global bowel motility variance and HBI ($r = -0.45$, $P<0.001$) which was validated in chapter 4.

In the current study, utilising a larger dataset of 105 CD subjects collated from 2 recruitment sites a univariate model again suggested a negative association between spatial variation and HBI ($R2$ adjusted = 0.034) ($r = -0.21$, $P = 0.03$). Some overlap in the datasets between the current study and that of the previous work in chapter 4 must however be acknowledged with 28 patients used in both studies.

The reason why decreased spatial variation, which represents more homogenous motility over the bowel (either high or low), is associated with increased symptoms is not yet certain. The best performing model was a combination of decreased temporal variation and an increased area of motile bowel. This suggests bowel health is reflected by heterogenous and patchy motility with areas of low and high motility in different segments, presumably reflecting the different roles of the proximal and distal small bowel in transit of intestinal content and nutrient absorption. It would appear that "switching off" this heterogeneity (perhaps in response to small bowel inflammation in CD) is associated with increased abdominal symptoms. Low motility (hypomotility) can be induced by IL-1 and TNF during intestinal inflammation as shown in murine models [244] whereas

conversely IL-10 increases motility [245]. In terminal ileal CD, GLP-1 and PYY (fullness signals) are increased where inflammation is present [87], [88]. The release of PYY (as discussed in section 1.1.2) decreases SB motility so considering the high proportion of patients with ileal or ilocolonic CD (88 out of 105 patients) it is possible that localised inflammation in the TI has influenced motility globally for those patients with active inflammation.

A range of putative metrics which reflect the absolute level of small bowel motility as well as spatial and temporal variation were tested. Without a “gold standard” to define patterns of global small bowel motility in health and disease, it is possible that the metrics do not fully reflect the motility phenomena they aim to capture. Indeed, it should be noted that the association between motility metrics and abdominal symptoms was not particularly strong; the best performing model had a modest R2 adjusted of 0.036. Aberrant motility in CD is complex and although some of the tested metrics show definite promise, it is likely further refinements will be needed in the future. For example, the temporal variation metric was calculated using 5 second sliding windows, and the size of the time window could easily be modified.

As discussed previously in chapter 4 (section 4.4), although HBI is a validated patient symptom score, it is relatively simplistic and this represents a limitation in this study.

It would be interesting to test the motility metrics against more complex questionnaires to see if associations are stronger. However, all measures of patient symptoms, by their very nature, are subjective to some degree but remain the clinically important endpoint against which to develop new methods.

Another limitation to consider is the MRE protocol for capturing motility, specifically the preparation, scan duration and the slice selection.

The scan duration has already been discussed in chapters 3 and 4, with a minimum scan duration of 15 seconds shown to be sufficient for robust bowel motility measurements.

As discussed in chapters 2 (section 2.1.7) and 3 (section 3.4.3), mannitol mimics the postprandial state, but it differs from usual food stuffs. It is however useful for identifying areas of low motility [161], which has been demonstrated in inflamed TI in CD patients [246], [247].

The single slice chosen in this study was objectively based on encompassing the largest areas of small bowel within a single ROI. This avoids the problem, in chapter 4, of temporal incoherence in multi-slice analysis which occurs since slices in different acquisition blocks are acquired around several seconds apart. However, it should be noted that the motility varies depending on the bowel segment [159] (and by inference slice position). Further work is needed to determine if single slice analysis is sufficient or whether multi-slice protocols are preferable. Ultimately 3D acquisitions would eliminate the temporal incoherence limitation, although they are technically challenging to acquire at an adequate temporal resolution.

## 5.5 Summary

In summary, it has been shown that subjective grading of MRI motility cannot reliably capture motility, through visual scoring, and that objective computer-based quantification is required. Spatial and temporal variation are particularly difficult to assess visually. An association between automated, objective motility metrics and patient symptoms is again demonstrated suggesting the metrics are at least in part capturing the likely aberrant small bowel motility presence in

CD patients and have potential as a powerful non-invasive tool to interrogate bowel motility in health and disease.

In chapter 6, the relationship between small bowel motility and symptoms is explored in another GI condition, IBS, where symptoms are present in patients with structurally normal bowel seen on standard investigations. IBS is a heterogenous disease with several subgroups (see sections 1.3.3 and 1.4.2). The motility metrics developed in this chapter will be applied in this patient group to determine whether there are characteristic abnormal motility patterns associated with different IBS subgroups. HBI was originally designed to assess overall disease activity in CD, and contains several components which are not directly related to symptoms. Therefore, it is not appropriate as a questionnaire to assess IBS symptoms. Alternatively, in chapter 6, the IBS-SSS questionnaire will be used as an outcome measure to test the motility metrics against.

# Section D: Utility of small bowel motility metrics and enteric texture analysis in irritable bowel syndrome

**Section D** explores the utility of the motility metrics, described previously in section C, and texture analysis summary measures, using clinical data; comparing irritable bowel syndrome (IBS) patients to healthy controls.

**Chapter 6** follows on from the Crohn's disease (CD) work by applying the quantitative motility metrics developed in chapter 5, in IBS patients. IBS-VAS symptom questionnaires were used to classify patients into IBS-C, IBS-D or IBS-M. Data from 34 IBS patients, acquired using a standard Magnetic Resonance Enterography (MRE) protocol in a cohort of patients representative of those seen in clinical practice, and 20 healthy controls were analysed to investigate whether global motility patterns are different between IBS patients and healthy controls, and between subtypes of IBS patients. Additionally, an association between motility patterns and symptoms from the IBS-SSS questionnaire was tested.

In **Chapter 7**, data from 18 IBS-C patients and 20 healthy controls was analysed to investigate whether MRI can demonstrate differences in enteric motility and terminal ileum content through texture analysis, colon diameter and computer-based motility metrics. Gastrointestinal symptoms in IBS occur without any obvious structural gut abnormality so this pilot study aims to explore a potential abnormal function, with reflux of caecal contents back into the terminal ileum in IBS-C patients (S Taylor, personal communication).

# Chapter 6: Comparison of MRI assessed small bowel dysmotility in irritable bowel syndrome (IBS) and healthy controls

## Author Declaration

The work presented here was led by the thesis author (3 years of experience) including performing the literature review, checking and preparing the datasets for registration, segmenting the datasets, and performing the motility and statistical analysis, under the supervision of Alex Menys, David Atkinson and Stuart Taylor.

Alex Menys and Freddy Odille developed the registration algorithm and GUI (graphical user interface) displaying the dynamic MRI data and motility maps. The thesis author enhanced the functionality of the GUI for data analysis.

Motility data was collected at VO Bild och Function, SUS, Malmö. IBS patient data was acquired from routine clinical scans and healthy controls were recruited separately or taken from clinical scans (see section 6.2.1).

Bodil Ohlsson collected clinical data such as gender, age, symptoms, laboratory data, histopathological examinations, diabetes complications, results from performed clinical investigations and the final diagnosis. Sven Månsson anonymised and made the datasets available to download.

This research has been presented as a conference abstract: **R Gollifer**, A Menys, S Månsson, P Leander, O Ekberg, S Taylor, D Atkinson, B Ohlsson. **"Comparison of MRI assessed small bowel dysmotility in Irritable Bowel Syndrome (IBS) and healthy controls."** The European Society of Neurogastroenterology & Motility, Lisbon, Portugal (2019).

The key components of my work here were:

- Modification of the new computer-based motility metrics (from chapter 5) for analysis of global small bowel motility i.e. the whole small bowel through multiple slices.
- Checking the datasets before and after registration for quality control and preparing the datasets for registration by removing duplicate slices which were acquired in the same anatomical slice position.
- Designing the study to classify IBS patients into subgroups and then comparing these subgroups to each other and healthy controls.
- Performing statistical analysis to compare IBS subgroups and healthy controls through motility analysis and statistical analysis using multivariable linear regression to test combinations of motility features against symptoms from the IBS-SSS questionnaires.

## 6.1 Introduction

As discussed in section 1.3.3, IBS is characterised by a range of gastrointestinal (GI) symptoms such as pain, bloating, constipation and diarrhoea. Therefore, IBS can be subclassified into constipation-predominant (IBS-C), diarrhoea-predominant (IBS-D) and mixed IBS (IBS-M) based on validated patient questionnaires such as IBS-VAS (see section 1.4.2). Another questionnaire, IBS-SSS is commonly

used for assessing the severity of IBS symptoms (see section 1.4.2) and will be used in this chapter for examining the relationship between motility patterns and symptoms.

IBS patients generally have structurally normal bowel and IBS is usually a clinical diagnosis following exclusion of structural disorders such as Crohn's disease (CD).

In Chapters 4 and 5, an association was found between aberrant motility in structurally normal appearing small bowel and GI symptoms in CD patients. As discussed in section 1.3.5, abnormal enteric motility has been hypothesised as a potential cause of IBS symptoms. Quantification of small bowel motility using MRI therefore potentially may give further insights into the pathophysiology of IBS, and its various subtypes.

The purpose of this study was to investigate if differences exist in MRI quantified small bowel motility patterns, using the metrics described in chapter 5, between IBS patients and healthy controls (see section 6.3.3). Motility patterns were also compared between IBS subgroups (see section 6.3.4). Finally, an association between motility patterns and symptoms from the IBS-SSS questionnaire was tested (see section 6.3.5).

## 6.2 Methods

The current study was approved by the relevant medical ethics committees and all patients and subjects gave written informed consent.

### 6.2.1 Patient Selection

All subject data was collected at the VO Bild och Function, SUS, Malmö; all consecutive patients referred for MRE, independently of the reason, were invited to take part in a larger study evaluating motility differences in Crohn's disease, Ulcerative colitis, IBS, dysmotility and healthy controls. Healthy controls were recruited separately, specifically for this study. Clinical scans included Crohn's disease, Ulcerative colitis, IBS and dysmotility patients as well as additional healthy subjects without GI symptoms who were investigated for iron deficiency and were concluded to have normal gastrointestinal investigations.

Subjects taking part in the study were asked to complete symptoms questionnaires for Irritable Bowel Syndrome-Symptom Severity Score (IBS-SSS) and Visual Analog Scale for IBS (VAS-IBS) as described in section 1.4.2. Both questionnaires have been widely used for non-English speaking Swedish patients [248].

VAS-IBS was used for categorising IBS subjects as IBS-C, IBS-D or IBS-M and the IBS-SSS score was used as an outcome measure for testing motility patterns against symptoms.

Patients were subclassified as IBS-C if the VAS-IBS score for constipation was above 22 (out of 100), IBS-D if the VAS-IBS score for diarrhoea was above 10 (out of 100) and IBS-M if both the constipation and diarrhoea VAS-IBS criteria were met. These VAS-IBS thresholds were based on the highest absolute score found for healthy controls in a previous study [94].

For the purposes of this study, the IBS inclusion criteria were patients who had a final diagnosis of IBS based on GI symptoms and exclusion of other GI related disease. The physician, a specialist in gastroenterology, confirmed the diagnosis of IBS for each patient,

based on Rome criteria IV, when all other examinations were normal, and thus organic disease was excluded. VAS-IBS and IBS-SSS symptom questionnaires were also used as confirmation that GI symptoms were present in these patients.

The IBS exclusion criteria were contraindications to undergo MRI, history of abdominal surgery, gastrointestinal diseases other than IBS and the use of medication with known direct effects on motility such as prokinetic agents (e.g. neostigmine), anti-spasmodics (e.g. buscopan) and opioid analgesics.

Heathy controls were recruited by means of advertisement (n=11) and from clinical scans (n=9). The first subset of controls (n=11) had to complete VAS-IBS and IBS-SSS to confirm they were healthy and had no GI symptom complaints. The second subset of controls (n=9), were patients typically seen in the clinic, for the investigation of iron deficiency or anaemia and/or GI bleeding. If they were deemed clinically not to have a GI disorder based on normal investigations (including MRE, and where performed, scintigraphy and/or duodenal manometry) together with no self-reported intestinal symptoms from the VAS-IBS questionnaire then they were included in the study. This was because there were low healthy control recruitment numbers by means of advertisement (n=11) so additional healthy control datasets from clinical scans were used where possible so that the sample sizes between IBS and HCs were as close as possible.

The inclusion criteria for the healthy controls were subjects willing to undergo minimal bowel preparation and MRI and no diagnosis of any gastrointestinal disorder. The exclusion criteria were contraindications to undergo MRI, history of abdominal surgery, gastrointestinal diseases or current gastrointestinal symptoms (from VAS-IBS questionnaire) and use of medication with known direct effects on motility such as prokinetic agents (e.g. neostigmine) and anti-spasmodics (e.g. buscopan).

A total of 225 datasets were available for this study including patients (CD, IBS, Ulcerative colitis etc.) and healthy controls.

Subjects were excluded from the study if they failed to undergo an adequate dynamic MRI sequence through the whole small bowel volume (greater than 3 slices and complete time series with sufficient registration quality – see MRI protocol detail in section 6.2.2 below).

For the comparison of IBS subgroups and HCs, IBS patients were excluded if they either did not complete the VAS-IBS symptom questionnaire to allow IBS subclassification or did not meet the criteria for any of the subgroups of IBS-C, IBS-D or IBS-D.

For the investigation between motility metrics and IBS symptoms, patients were excluded if they did not complete an IBS-SSS questionnaire. These exclusions were confirmed before the final data analysis.

Demographic data pertaining to age, sex, disease duration (presence of IBS) and surgical history was also collected.

### 6.2.2 MRI Protocol

Subjects underwent magnetic resonance enterography (MRE) at SUS, Malmö after ingesting 1 litre of macrogol 3350 solution (LaxabonVR, maximal 1800 mL, BioPhausia, Stockholm, Sweden), 45 minutes prior to the scan to distend the small bowel. They were instructed to stop opioid treatment 7 days prior to scanning and to stop the use of laxatives and motility-affecting drugs 2 days before MRE.

Subjects were scanned in the prone position on a 1.5T unit (Siemens Magnetom Symphony TIM, Siemens Medical Systems, Erlangen, Germany).

The MRE protocol included a free breathing (minimum of 50 frames in 20 seconds) dynamic “cine motility” sequence acquired prior to the administration of the anti-spasmodic butylscopolamin (BuscopanVR, 20mg/mL, dosage 40 mg, Boehringer-Ingelheim, Stockholm, Sweden) using a 2D coronal, true FISP sequence.

The scan parameters were as follows: flip angle 50$^{o}$, time between pulse sequences = 409.5ms, repetition time = 3.2ms, TE = 1.6ms, 192x135 matrix filling, zero-filling to 192x192, 1.8x2.5mm in-plane resolution, temporal resolution = 2.5 images per second, slice thickness = 8mm.

These coronal blocks were repeated from the ventral to dorsal aspect of the abdomen to encompass the whole small bowel volume with the number of acquisitions ranging from 10 to 14 depending on the size of the patient.

### 6.2.3 Motility Assessment

Motility data visualisation and analysis were performed in MATLAB 2018 (The MathWorks, Natick, MA). This included a graphical user interface (described previously in sections 3.2.3, 4.2.3 and 5.2.3), where anonymised datasets are displayed, as both a static reference image and as a “cine” movie. This allowed for inspection of all the MRI data (as well as ROI placement and automated MRI metric measurement).

The motility and temporal variations maps were generated as described previously in section 5.2.4. However, an extended version

of the previously described registration algorithm (see sections 2.3.2 and 2.3.3) called Dual Registration of Abdominal Motion (DRAM) [226] was implemented to register the free breathing datasets. In brief, there is an additional processing step prior to the generation of motility maps called Robust Data Decomposition Registration (RDDR). This involves registering and removing the respiratory component of motion, whilst preserving peristaltic motion in the data. RDDR is a technique using Robust Principal Component Analysis (RPCA) to separate the (sparse) intensity changes from the (low rank) motion [226].

For each patient, the thesis author used the motility analysis GUI to place ROIs over the small bowel on the reference image, with the cine motility movies available to aid ROI placement. The ROIs were validated by a research fellow with over 5 years MRE experience (Menys).

In detail, for each of the motility datasets, ROIs were placed in morphologically normal appearing small bowel on all the coronal motility acquisition slices.

The motility and distension metrics described in section 5.2.4 were derived from the ROIs and summed across multiple slices in the whole patient to provide global small bowel motility metrics:

1. mean motility
2. spatial variation
3. temporal variation
4. area of motile bowel
5. intestinal distension (the threshold was different for each slice since it was based on 50% of the median intensity within the ROIs for each slice)

### 6.2.4 Statistical analysis

All statistical analysis was performed in MATLAB 2018 (MathWorks, Natick, MA). All data was checked for normality using a Shapiro-Wilk test (alpha = 0.05).

If both the healthy control group and IBS patient group were normally distributed, an independent two sample t-test was performed for comparing the two groups. If one of the groups was not normally distributed, the Mann-Whitney test was performed instead.

Either a two-sample t-test (for normal data) or the Mann-Whitney test (for non-normal data) was performed to compare healthy controls and IBS patients, with $p < 0.05$ being taken as statistically significant.

*MATLAB function used: [h,p,ci,stats]=ttest2(current HCs,current IBS); [p_ranksum,h_ranksum,stats]=ranksum(current HCs,current IBS);*

The comparison between HCs and IBS patient was performed independently for the five motility and distension metrics: 1) mean motility, 2) spatial variation of motility, 3) temporal variation of motility, 4) area of motile bowel and 5) distension.

For each of the five metrics, the Kruskal-Wallis test was performed to see if there were differences between IBS subgroups (IBS-C, IBS-D, IBS-M) and HCs, followed by Tukey-Kramer (or Tukey's Honestly Significant Difference) test to determine which groups showed differences. Tukey-Kramer has been proven to be conservative for Kruskal-Wallis with different sample sizes, which is the case with the data in this chapter.

Furthermore, Kruskal-Wallis test was performed to see if there were differences between only the IBS subgroups, followed by Tukey-Kramer test to determine which groups showed differences.

*MATLAB function used: [p, tbl, stats]= kruskalwallis (Data_IBS_MDC_HCs(:,metricno), Names_IBS_MDC_HCs, 'off'); figure, c=multcompare(stats, 'CType', 'hsd');*

Univariate and multivariable regression models were tested to assess the relationship between global small bowel motility metrics and IBS-SSS patient symptoms by a similar scheme as described in section 5.2.6. Thirty combinations of the five independent variables metric 1 – mean motility, metric 2 – spatial variation, metric 3 – temporal variation, metric 4 – area of motile bowel, metric 5 – intestinal distension) tested against the dependent variable or outcome measure of IBS-SSS.

*MATLAB function used: mdl_glm = fitglm (Metrics_Used, IBS_SSS, 'linear', 'Distribution', Normal, 'Link', 'identity');*

In brief, models with different combinations of the motility metrics would be accepted if they met the following criteria (see more details in section 5.2.6):

- Low multicollinearity i.e. all independent variables in the model had a low variance inflation factor (VIF<5) [243]
- F-statistic for the model significant ($P < 0.05$)
- R2 (adjusted) value for the model positive ($R2 > 0$)
- Standardised coefficient estimates for all variables in the model significant ($P < 0.05$)

## 6.3 Results

### 6.3.1 Cohort Demographics

The full study cohort consisted of 225 subjects (34 IBS, 11 recruited healthy controls, 9 subjects investigated for iron deficiency with normal gastrointestinal investigations and without GI symptoms, 152 Crohn’s disease, 15 Ulcerative colitis, 4 dysmotility).

For this study, 34 IBS patients (mean age, 36; age range, 18-67 years; 26 females) and 20 healthy controls (mean age, 37; age

range, 19-75 years; 9 females) were included. Data was available for disease duration in 19 IBS patients (13 patients with a diagnosis within the last 5 years, 1 patient between 5-10 years and 5 patients with a diagnosis over 10 years ago). No patients had undergone enteric surgery i.e. gut resection.

All these subjects had MRI data of sufficient quality available.

For testing the motility metrics against symptoms, 7 IBS patients were excluded due to a lack of a completed IBS-SSS questionnaire.

For testing the motility metrics in different IBS subgroups, 10 IBS patients were excluded either because a VAS-IBS score was not obtained, or because they did not fulfil the criteria for any subgroup classification.

### 6.3.2 IBS-SSS, VAS-IBS and Motility Metrics

A summary of automated motility metrics and scores from symptoms questionnaires (VAS-IBS and IBS-SSS) for the IBS patients is shown in table 16.

| **IBS motility metrics (n = 34)** | Median | Range | |
|---|---|---|---|
| | | Minimum | Maximum |
| **Mean motility** | 0.330 | 0.223 | 0.379 |
| **Spatial variation** | 0.026 | 0.014 | 0.035 |
| **Temporal variation** | 0.018 | 0.008 | 0.024 |

| | | | |
|---|---|---|---|
| **Area of motile bowel (% of ROI)** | 95.7 | 81.4 | 99.5 |
| **Intestinal distension (% of ROI)** | 75.7 | 53.3 | 87.1 |
| **IBS-SSS (n = 27)** | | | |
| *Total* | 317 | 100 | 433 |
| *Pain Intensity* | 71 | 0 | 100 |
| *Pain Frequency* | 64.3 | 0 | 100 |
| *Bloating* | 51 | 0 | 98 |
| *Dissatisfaction with bowel habits* | 52 | 0 | 100 |
| *Interference in daily life* | 77 | 19 | 100 |
| **VAS-IBS (n = 24)** | | | |
| *Diarrhoea* | 70 | 0 | 100 |
| *Constipation* | 61 | 0 | 93 |

**Table 16: Median, minimum and maximum IBS-SSS, VAS-IBS and automated motility metric values for IBS patients.**

A summary of the automated motility metrics and scores from IBS-SSS symptoms questionnaires for the healthy controls is shown in table 17. In Appendix 3 (section 9.3), a summary of the automated motility metrics is shown separately for the two subsets of healthy controls (described in section 6.2.1).

| **Healthy Controls (n = 20)** | Median | Range | |
|---|---|---|---|
| | | Minimum | Maximum |
| **Mean motility** | 0.325 | 0.264 | 0.382 |
| **Spatial variation** | 0.028 | 0.014 | 0.036 |
| **Temporal variation** | 0.018 | 0.011 | 0.025 |
| **Area of motile bowel (% of ROI)** | 97.2 | 84.5 | 99.5 |
| **Intestinal distension (% of ROI)** | 78.1 | 48.4 | 89.5 |
| **IBS-SSS** | | | |
| *Total* | 17 | 0 | 121 |
| *Pain Intensity* | 0 | 0 | 6 |
| *Pain Frequency* | 0 | 0 | 14.2 |
| *Bloating* | 0 | 0 | 45 |
| *Dissatisfaction with bowel habits* | 12 | 0 | 65 |
| *Interference in daily life* | 5 | 0 | 56 |

**Table 17: Median, minimum and maximum IBS-SSS and automated motility metric values for healthy controls.**

### 6.3.3 Motility metrics IBS or IBS subgroups vs Healthy Controls

No significant differences in motility metrics were found between IBS patients (n = 34) and healthy controls (n=20) (see figure 34 And Appendix 4 in section 9.4) or between IBS subgroups; IBS-C (n = 3), IBS-D (n = 9), IBS-M (n = 12) and healthy controls (n=20) (see figure 35 and Appendix 5 in section 9.5). There were also no differences when comparisons were limited to the 11 healthy recruited volunteers only (see table 18).

| **P values** | **IBS (n = 34) & HCs (n = 20)** | **IBS subgroups (n = 24) & HCs (n=20)** | **IBS subgroups (n = 24) & recruited HCs (n=11)** |
|---|---|---|---|
| **Type of statistical test** | Two sample t-test or Mann-Whitney test | Kruskal-Wallis | Kruskal-Wallis |
| **Mean motility** | 0.69 | 0.10 | 0.15 |
| **Spatial variation** | 0.33 | 0.16 | 0.15 |
| **Temporal variation** | 0.55 | 0.14 | 0.23 |
| **Area of motile bowel** | 0.51 | 0.15 | 0.09 |
| **Intestinal distension** | 0.73 | 0.16 | 0.14 |

**Table 18: P values for statistical tests comparing IBS and HCs for each of the five motility and distension metrics.**

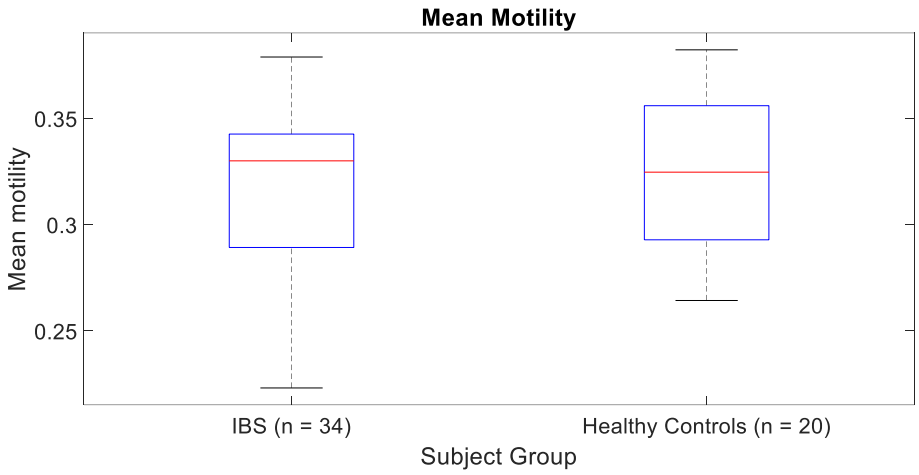


**Figure 34: Boxplot of mean motility metric for an example comparison of IBS patients (n = 34) and healthy controls (n=20). Boxplots for spatial variation of motility, temporal variation of motility, area of motile bowel and intestinal distension are in the Appendix 4 (section 9.4).**

### 6.3.4 Motility metrics IBS subgroups comparison

When differences between only the IBS subgroups were tested, there were differences found between IBS subgroups for temporal variation of motility (P = 0.0497) and area of motile bowel (P = 0.04) using the Kruskal-Wallis test.

The subgroups showing differences for these metrics were interrogated further using the Mann-Whitney U test. Significant differences were found between IBS-M (n = 12) and IBS-C (n = 3) with a decreased temporal variation of motility (P < 0.001) and area of motile bowel (P < 0.001) for IBS-C as shown in figure 35.

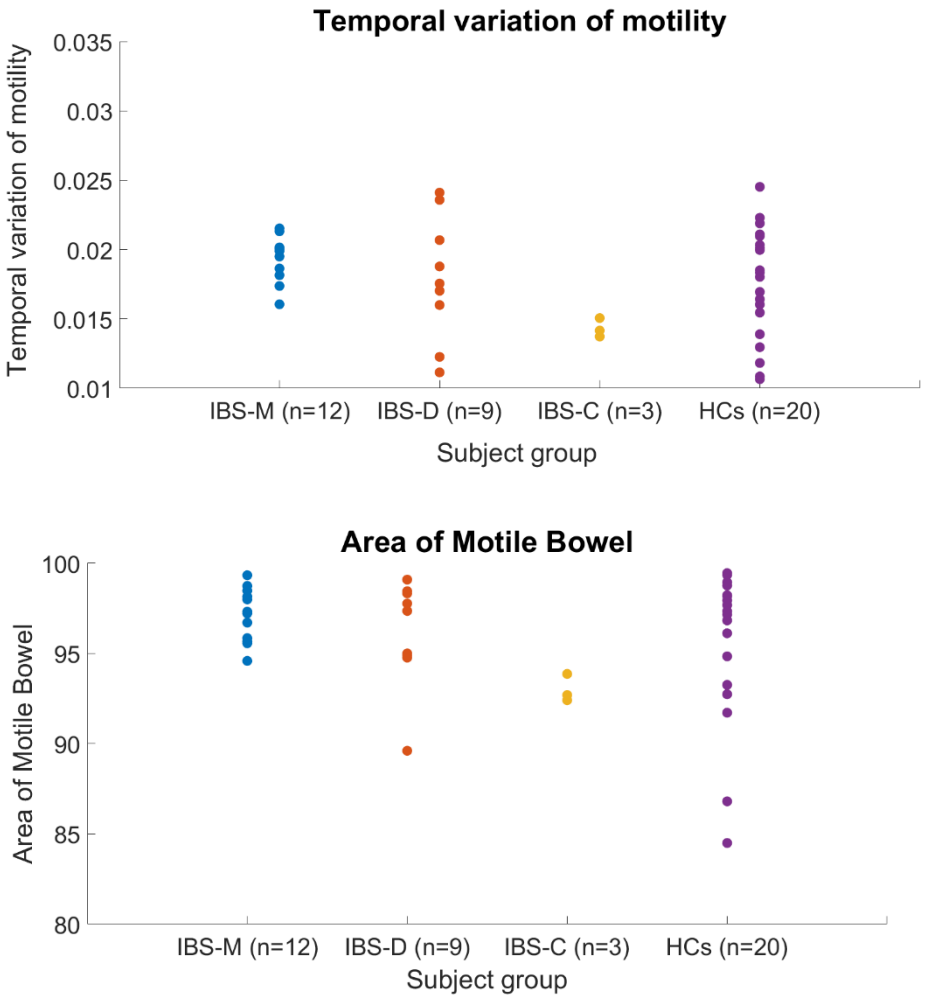


**Figure 35: Scatterplots of temporal variation of motility (top) and area of motile bowel (bottom) metrics for a comparison of IBS subgroups; IBS-C (n = 3), IBS-D (n = 9), IBS-M (n = 12) and healthy controls (n=20). Boxplots for mean motility, spatial variation of motility and intestinal distension are in the Appendix 5 (section 9.5).**

### 6.3.5 Multivariable regression of IBS motility metrics vs symptoms (IBS-SSS)

None of the motility metrics correlated individually with either the total IBS-SSS or any of the IBS-SSS components (Appendix 6 in section 9.6).

None of the multivariable models with different combination of motility metrics demonstrated an association with the total IBS-SSS (Appendix 7 in section 9.7).

## 6.4 Discussion

This preliminary study suggests that, whilst there were no differences in global small bowel motility metrics between IBS patients and healthy controls (HCs), there may potentially be differences between IBS subgroups, notably between IBS-C and IBS-M patients.

Specifically, a lower temporal variation of motility and lower area of motile bowel was demonstrated in IBS-C patients compared to IBS-M patients. However, no significant differences were found between HCs and any of the IBS subgroups for any of the motility metrics.

Previously, Akerman et al. (2016) [198] found no segmental small bowel motility differences in the terminal ileum, jejunum or ileum between IBS and HCs using dynamic MRI.

In the current study IBS patients were subclassified into IBS-C, IBS-D and IBS-M and the global or whole small bowel motility was analysed (as opposed to segmental). In chapter 5, the quantitative motility and distension metrics were applied in a single slice using 20 second breath-hold data in CD patients. In this chapter, the previously described metrics (from chapter 5) were modified to quantify global small bowel motility, through multiple slices, and applied in IBS patients, using 20 second free breathing datasets, for the first time.

The advantage of free breathing protocols is that they reduce patient discomfort compared to breath-holding (see section 3.4.2). A previously developed algorithm called DRAM, validated against breath-hold data, allows free breathing datasets to be registered and therefore motility to be quantified [226]. In a study comparing DRAM to the original optic flow-based registration algorithm (without respiratory motion correction), described in sections 2.3.2 and 2.3.3, the differences between the two algorithms based on the global mean SD Jacobian were found to be minimal. In a cohort of 20

healthy controls, the mean SD Jacobian values ranged from 0.181-0.422 (mean value of 0.340) for the original algorithm and from 0.189-0.430 (mean value of 0.335) for DRAM [226].

In keeping with previous data [161], the motility metrics were found to be highly variable in health. Menys et al. (2013) [161] reported that the mean global small bowel motility of 21 healthy controls had a mean score of 0.34 ranging from 0.28 to 0.39. The cohort of 20 HCs in this chapter were similar with a mean score of 0.35 ranging from 0.26 to 0.38.

In the current study however, there was also a large range of mean motility values within IBS patients (mean score, 0.32; range 0.22-0.38) which was not significantly different from healthy controls, suggesting that global motility is not useful for identifying IBS as a whole. It is however clear that IBS is a heterogenous disease with patients suffering a range of differing symptoms, which underlies the clinical usefulness of subclassifying patients into subgroups of IBS-C, IBS-D and IBS-M. It is therefore perhaps not unexpected that a heterogeneous group of IBS patients showed overall no difference in motility metrics, compared to healthy controls and that subclassifying patients in future research will perhaps be more fruitful.

Indeed, the normal variability found in healthy controls appears to be reduced in IBS-M and IBS-C subtypes. There were differences found between IBS-M and IBS-C subgroups for temporal variability of motility ($P < 0.001$) and area of motile bowel ($P < 0.001$). The range in the temporal variation was narrower for both subtypes than healthy controls, indicating that motility could be used to better characterise the underlying symptoms of these specific subtypes.

In terms of an explanation for the findings, it can be hypothesised that in IBS-C, transit of contents through the small bowel into the colon is affected by a lack of coordination (low temporal variation) and low motility (low area of motile bowel). Patients with constipation have previously been shown to have a longer transit time than those

without constipation symptoms using radiopaque marker data [249]. IBS-C patients have been found to have slower transit than HCs based on scintigraphy data [132]. Additionally, differences have been found between IBS-C and IBS-D patients with migrating motor complex intervals measured from manometry data longer in IBS-C [128].

High variation of small bowel motility appears to be a marker of gut well-being [65], [241], [250] (see chapters 4 and 5) and previously greater terminal ileum mean motility has been shown in healthy controls compared to Crohn's disease patients [198]. Hence, a lack of variation in motility and low area of motile bowel may contribute to constipation in IBS-C patients. Abnormal motility will be explored again in IBS-C in chapter 7.

Conversely, IBS-M patients were seen to exhibit high temporal variation of motility and high area of motile bowel. Patients often experience changing bowel habits alternating between diarrhoea and constipation. The symptomology is therefore less defined. The motility is varied and active which would suggest normal small bowel motility as seen in healthy individuals. It is possible that transit through the small bowel is normal but there is abnormal transit through the colon. It may therefore be useful to study colonic motility and retrograde sigmoid contractions. The data here though is of insufficient length to analyse motility in the colon since colonic contractions occur much less frequently than in the small bowel and so 20 seconds is not long enough to capture colon motility.

It would be expected that IBS-M patients would exhibit motility values in between IBS-C and IBS-D. However, these results do not support this hypothesis. It appears that the temporal variation of motility is similar between IBS-M and IBS-D patients, which could possibly be explained by IBS-M patients, with mixed bowel habits, were experiencing more diarrhoeal symptoms than constipation symptoms at the time of the scan.

It should be noted that the data can only be considered preliminary as only a small number of IBS-C patients (n = 3) were available for this study. This reflects recruitment of patients undergoing MRE as part of usual clinical practice when exclusion of Crohn's disease is the major indication in patients presenting with abdominal symptoms. As such patients suffering predominantly diarrhoeal symptoms (such as IBS-D and IBS-M) are much more likely to be suspected of having Crohn's disease compared to patients presenting with constipation. Despite the low number of IBS-C patients, the clustered values for temporal variation and area of motile bowel are indicative of a potential characteristic pattern and in future studies this could be analysed with greater numbers. The symptomatology for IBS-M is less well defined generally than the other IBS subgroups so perhaps recruiting IBS-C and IBS-D patients would be a better approach especially considering the low numbers in this study and the similarities between the IBS-M and IBS-D patients. Additionally, functional constipation patients could be recruited and grouped together with IBS-C patients for a larger subset of constipated patients.

A potential limitation of this study is that the VAS-IBS questionnaire was used to subclassify patients. The VAS-IBS thresholds used in this study were based on the highest absolute scores found for healthy controls. However alternate thresholds could have been used. For example, patients were classified as having IBS-D if they had a diarrhoea score of 10 or above out of 100 which could mean patients with relatively mild diarrhoea symptoms were considered as having IBS-D. However, to ensure that healthy individuals were excluded, the thresholds were set to be the maximum score seen in 52 healthy controls [94]. Even if using a conventional threshold of 17 [94], only one patient would have been reclassified from IBS-D patient to unspecified IBS with pain and bloating.

Another potential limitation of this study was the inclusion of patients who were being investigated for bleeding and/or anaemia (n = 9).

Although they were ruled out from having any organic disease based on normal investigations including MRE and in some cases scintigraphy and/or duodenal manometry they were not necessarily completely healthy. They did appear to have slightly higher symptoms scores than the healthy volunteers who were recruited (n = 11), but their symptoms were still well below the scores achieved by the IBS patients. It would be preferable to only include healthy volunteers recruited and not patients undergoing investigations for other health issues. However, when the analysis was performed with and without these patients, who were defined as having no GI symptoms, the results remained unchanged with no differences seen between IBS patients and healthy controls.

Previous associations between small bowel motility and symptoms have been shown in Crohn's disease, but often these correlations are weak or only moderately strong. For example, reduced global spatial variation of motility has been linked to the severity of diarrhoea in Crohn's disease patients [65], [241], [250] as described in chapter 4. In this study, there was a large variation in the values for both spatial and temporal variation in IBS-D. Indeed, IBS-D was more closely matched with healthy controls than with other IBS subgroups for all of the motility metrics. Therefore, perhaps only differences can be seen between IBS-D patients and other IBS subgroups in those IBS-D patients with more severe diarrhoea.

As discussed in section 1.4, not all of the HBI components are strictly related to symptoms as HBI was originally designed to assess Crohn's disease activity and does not include a score for symptoms such as constipation and bloating. In this study, IBS-SSS was used to assess the severity of IBS with more focus on pain, bloating and quality of life issues such as dissatisfaction with bowel habit and disruption to daily life.

However, there was no association found between any combination of motility metrics and symptoms from the IBS-SSS questionnaire.

The lack of correlation could therefore be due to the subjective nature of these particular symptoms and suggests that global small bowel motility is not related to pain or bloating.

## 6.5 Summary

In summary, this study found no association between small bowel motility in IBS patients and symptoms from IBS-SSS questionnaire. Furthermore, no differences were found between IBS patients and healthy controls where there was a large range of motility values in both groups. However, IBS-C and IBS-M subtypes exhibited reduced variability in motility metric values, especially for temporal variation and area of motile bowel. This could be indicative of characteristic motility patterns for these symptom groups.

Throughout this thesis, the focus has been mainly on global motility patterns. In chapter 7, segmental motility, in the terminal ileum (TI), and its relationship to bloating symptoms in IBS-C patients will be investigated further, along with ascending colon diameter and texture analysis measures. Specifically, the hypothesis that a potential reflux of caecal contents from the colon back into the terminal ileum is caused by abnormal TI motility and contributes to symptoms will be explored. With a greater emphasis on a specific mechanism that may be characteristic to a particular IBS subgroup (IBS-C), these MRI measures may show promise as biomarkers to aide understanding of the pathophysiology of bloating symptoms in IBS-C patients.

# Chapter 7: MRI assessed dysmotility and texture analysis in the terminal ileum and small bowel: a pilot study comparison between irritable bowel syndrome (IBS) patients with bloating and healthy controls

## Author Declaration

The work presented here was led by the thesis author (3 years of experience) including performing the literature review, downloading, anonymising, registering and segmenting the UCLH datasets, designing the study for ROI placement, and performing the texture analysis, motility, colon diameter and statistical analysis, under the supervision of Alex Menys, David Atkinson and Stuart Taylor.

Alex Menys and Freddy Odille developed the registration algorithm and GUI (graphical user interface) displaying the dynamic MRI data and motility maps. The thesis author enhanced the functionality of the main GUI for data analysis and created a separate texture analysis GUI.

Both anatomical and motility data was collected at UCLH; for IBS-C patients from routine clinical scans and for healthy controls recruited as part of another study.

Anton Emmanuel, Natalia Zarate-Lopez and Dave Chatoor were involved in discussions regarding the clinical problem of IBS-C patients with abdominal boating and the planning of the analysis as well as providing datasets used in the study from UCLH.

This research has been presented as a conference abstract: **R Gollifer**, A Menys, N Zarate-Lopez, D Chatoor, F Vos, A Emmanuel, S Taylor, D Atkinson. **"MRI assessed dysmotility and texture analysis in the terminal ileum and small bowel: A pilot study comparison between Irritable Bowel Syndrome (IBS) patients with bloating and healthy controls."** Proceedings of the 27th meeting of ISMRM, Montreal, Canada (2019). Oral presentation (Power Pitch)

The key components of my work here were:

- Designing the study to compare IBS-C patients and healthy controls through texture and motility analysis in specific localised regions of the small bowel and colon.
- Development of a new, separate GUI to allow anatomical datasets to be viewed and to perform texture analysis and colon diameter measurements
- Development of new computer-based texture analysis summary measures applied to IBS patients and healthy controls
- Performing statistical analysis to compare IBS-C patients and HCs

## 7.1 Introduction

As previously discussed in sections 1.3 and 6.1, IBS manifests with recurrent gastrointestinal symptoms including abdominal pain, bloating, constipation and/or diarrhoea in the absence of any demonstrable structural or functional gut abnormality [89].

These patients can be subclassified into IBS-C, IBS-D and IBS-M (see sections 1.3.3 and 1.4.2 and chapter 6), and as discussed in section 1.3.5 and chapter 6, abnormal enteric motility has been hypothesised as a potential cause of IBS symptoms.

Additionally, IBS-C patients with bloating often present in clinic with a large, distended abdomen which could potentially be caused by an enlarged colon diameter due to colonic distension (see section 1.3.3 for more details).

Differences in enteric motility and terminal ileum (TI) luminal content have not previously been investigated in IBS-C patients using MRI. MRI may therefore provide a useful biomarker of IBS-C, aide in phenotyping these patients more accurately and increase the understanding of its pathophysiology. Previously, in chapter 6, differences in global motility measures were found between IBS-C and IBS-M subgroups, but not between IBS-C and healthy controls. Here, in this study abnormal TI motility, texture analysis measures and ascending colon diameter in IBS-C patients with bloating are investigated and compared to HCs.

Anecdotally, radiologists report “faecalisation” of terminal ileum luminal content on MRI performed in patients with IBS-C (S Taylor, personal communication). This is hypothesised to be reflux of caecal contents into the terminal ileum with altered motility postulated as a potential cause (see sections 1.3.5 and 2.4).

As discussed in section 2.1.7, it is standard clinical practice for patients to ingest oral contrast such as mannitol prior to undergoing

MR enterography to distend the small bowel and colon, allowing better visualisation of the bowel wall by increasing contrast with the luminal contents, which appear brighter on the image.

Chyme food particles are reduced in size and altered in composition by time they reach the end of the small bowel. Remaining food material is passed into the first part of the large intestine (caecum) where bacteria begin to break down any remaining proteins and carbohydrates. The remaining nutrients and water are extracted during transit through the colon and the remaining semi-solid material is passed as faeces. “Faecalisation” is considered to be the appearance of a semi solid content in the TI caused by a mixture of liquid (brighter image intensity from chyme mannitol contrast solution) and solid content (darker image intensity from solid right sided colonic contents i.e. faeces).

The hypothesis is that in the healthy controls there will be no movement of contents back and forth between the terminal ileum of the small bowel and the colon. Therefore, the contents within the small bowel, including the terminal ileum, and the caecum and the first part of the ascending colon will have a bright, homogenous appearance with a smooth texture (see figure 40C-D in section 7.3.2).

Conversely, it is expected that there will be a variety of intensity values in the terminal ileum of IBS-C patients i.e. the texture will be heterogeneous due to the reflux of caecal contents moving back into the terminal ileum (see figure 40A-B in section 7.3.2). This could be because of slow transit time through the rest of the colon. The slow transit may also lead to distension and therefore an increased ascending colon diameter. As discussed in section 1.3.3, bloating and abdominal distension, in this context increased abdominal girth, is frequently reported in IBS-C patients and those with associated slow colonic transit.

The purpose of this study was to investigate whether MRI can demonstrate differences in terminal ileum luminal content, TI motility, and ascending colon diameter between IBS patients with abdominal bloating (IBS-C) and healthy controls.

Specifically, texture analysis, motility and colon diameter derived measures were investigated. For texture analysis summary measures, ratios were calculated between the contents of the TI and 1) the small bowel and 2) the ascending colon. Since the mannitol was expected to travel through the small bowel and terminal ileum into the ascending colon with no reflux, it would be expected that both the ratios would be around 1 for the healthy controls (since all the regions would have a similar textural appearance) and to be higher or lower than 1 for the IBS-C patients due to the different appearance of the contents within the TI.

The TI motility and the ascending colon diameter would be compared between IBS-C patients and healthy controls.

## 7.2 Methods

This study was approved by the relevant medical ethics committees with all IBS-C patient data covered by data sharing ethics and all healthy controls giving written informed consent.

### 7.2.1 Patient Selection

IBS-C patient data was collected at University College London hospital (UCLH) from MRI scans performed as part of usual clinical care between December 2012 and June 2018. Healthy control data from volunteers recruited over an 18-month period was included from a prior study designed to assess the repeatability in human

volunteers of software-quantified MRI small bowel motility, and to test the ability to detect motility changes induced by pharmacologic agents [161].

A total of 38 datasets were available for this study (18 IBS-C patients and 20 healthy controls).

IBS-C patients were included if they had a diagnosis of IBS-C with bloating and MRI data was available. All patients included had severe objective abdominal distension unresponsive to routine clinical management, including the low FODMAP diet and standard laxative regime. All patients had a negative glucose breath test, excluding small intestinal bacterial overgrowth.

The IBS exclusion criteria were contraindications to undergo MRI, history of abdominal surgery, gastrointestinal diseases other than IBS and the use of medication with known direct effects on motility such as prokinetic agents (e.g. neostigmine), anti-spasmodics (e.g. buscopan) and opioid analgesics.

Healthy controls were included if they were willing to undergo minimal bowel preparation and MRI, were non-smokers and abstained from caffeinated and alcoholic drinks on the day of the scan and were excluded if they had any known chronic intestinal disease, self-reported gastrointestinal (GI) symptoms, history of GI surgery or were using any long-term medication excluding the oral contraceptive.

There were three parts to the study with texture analysis, motility analysis and ascending colon diameter comparison. Tagging was not used since this data is not readily available clinically, dedicated software is necessary for analysing tagging data and the taglines only last in the order of T1. Additionally, taglines are particularly obtrusive for small structures i.e. the small bowel so are more suitable for analysing motility in the colon. Subjects were excluded

from the motility analysis if they failed to undergo an adequate dynamic MRI sequence, i.e. data was unavailable, or the terminal ileum was not able to be identified on any of the available slices. Subjects were excluded from the texture analysis if the terminal ileum was unable to be identified or if the size of the TI ROI was under 50 pixels. This was set empirically through a homogenous area of small bowel being analysed in a small subset of the datasets by testing the texture analysis measures for different sized ROIs in the same region. The texture analysis measures were consistent in ROIs above 50 pixels, but the TA contrast, for instance, was inflated in smaller ROIs.

These exclusions were confirmed prior to the final data analysis.

### 7.2.2 MRI Protocol

Healthy controls fasted for 4 hours before slowly ingesting 1 litre of 2% mannitol solution, starting 50 minutes prior to the start of the scan to distend the small bowel. They were instructed to avoid alcohol and caffeinated drinks on the day of imaging and medication, potentially influencing motility, 1 week before imaging.

IBS patients fasted for 4 hours before slowly ingesting 1-1.5 litres of 2% mannitol solution (100ml mannitol with 800ml of water), starting 40 minutes to an hour prior to the start of the scan.

Healthy controls were scanned in the prone position on a 3T unit (Achieva; Philips Healthcare, Best, the Netherlands) using the manufacturer’s torso coil (XL-TORSO, Philips Healthcare) and IBS patients were scanned in the prone position on either a 1.5T (Avanto, Siemens, Medical Systems, Erlangen, Germany) or 3T (Achieva, Philips Healthcare) unit.

A dynamic “cine motility” sequence was acquired during a 20 second breath-hold with a temporal resolution of 1 image (or volume) per second prior to the administration of the anti-spasmodic butylscopolamine (20mg/mL, dosage 40mg) which allowed anatomical images to be acquired. The anatomical images were acquired using balanced sequences at a higher spatial resolution than the motility data, as part of a routine clinical MRE protocol (table 19).

The healthy control data was acquired using a 2D balanced turbo field-echo sequence and the IBS patient data was acquired using a 2D coronal, balanced steady-state free precession sequence. These coronal blocks were repeated to encompass the whole small bowel volume. The scan parameters are detailed in table 19.

| | **Motility** | | |
|---|---|---|---|
| **MR Parameter** | Healthy Control (Achieva) | IBS (Achieva) | IBS (Avanto) |
| Scan Type | Dynamic | Dynamic | Dynamic |
| Field Strength | 3T | 3T | 1.5T |
| TR (ms) | 3.5 | 3.7 | 3.6-4.3 |
| TE (ms) | 1.7 | 1.8 | 1.8-2.2 |
| Flip Angle | 20 | 20 | 47-64 |
| Field of View (mm) | 420x420 | Variable | Variable |
| Spatial Resolution (mm) | 2.5x2.5 | 2.5x2.5 | 2.5x2.5 |
| Slice Thickness (mm) | 10 | 5 | 10 |

| | **Anatomical** | | |
|---|---|---|---|
| **MR Parameter** | Healthy Control (Achieva) | IBS (Achieva) | IBS (Avanto) |
| Scan Type | BTFE | BTFE | FISP |
| Field Strength | 3T | 3T | 1.5T |
| TR (ms) | 2.5 | 2.5 | 3.5-4.3 |
| TE (ms) | 1.2 | 1.2-1.3 | 1.5-1.9 |
| Flip Angle | 45 | 45 | 46 |
| Field of View (mm) | 400x400 | 268x224 | 256x166 |
| Spatial Resolution (mm) | 1.5x2 | 1.5x2 | 1.5x2 |
| Slice Thickness (mm) | 5 | 5 | 4 |

**Table 19: Balanced sequence parameters for motility and anatomical MRI data on two scanners at UCLH.**

## 7.2.3 Texture Analysis (TA)

All texture analysis was performed in MATLAB 2018 (The MathWorks, Natick, MA) using anatomical data in a newly developed "Texture analysis" GUI, which allowed for ROI placement.

*MATLAB function used: [glcms_offset, SI] = graycomatrix (Image_ROIonly, 'Offset', offsets, 'NumLevels', 32, 'GrayLimits', [0,1], 'Symmetric', true);*
*glcms_offset_NaN_stats=graycoprops(glcms_offset);*

*offsets = [ 0 1; 0 2; 0 3; 0 4;... %0 degrees*

*-1 1; -2 2; -3 3; -4 4;... %45 degrees*

*-1 0; -2 0; -3 0; -4 0;... %90 degrees*

*-1 -1; -2 -2; -3 -3; -4 -4]; %135 degrees*

*Step 1: ROI placement*

Three ROIs of identical shape and size were placed on anatomical images: 1) in the terminal ileum (TI), 2) in an oral contrast filled region of small bowel (SB), and 3) in the ascending colon. A ROI would be drawn in the smallest of the three regions and then copied to the other two locations.

The ROI in the TI was placed in the anatomical datasets in a single slice where the TI was most visible. Texture analysis measures are affected by the shape and size of the region being analysed.

Therefore, the TI ROI was copied and transferred to a region of SB with good oral contrast filling. The location of the SB ROI was selected based on visual assessment and was placed in a region distant from the terminal ileum. The intention was to select a SB region which appeared bright and well distended i.e. filled with oral contrast and not collapsed. If possible, the SB ROI was placed within 3 slices of the TI ROI so the both ROIs were located in a similar slice location, but this was not always possible.

The ROI in the ascending colon was placed away from a proximal part of the colon wall (5-10cm horizontally above the ileocaecal valve) in the centre of the colon, in order to be as near to the TI ROI as possible, but at a standard distance apart.

The ROIs were placed carefully to avoid the bowel wall and only include the contents of the bowel.

Where the TI was large it was often difficult to select a SB ROI of the same shape and size without including the bowel wall. Therefore, the

TI ROI was only drawn in part of the TI visible in the image in order to draw a SB ROI of equivalent shape and size.

*Step 2: Input image creation through intensity scaling*

Each slice containing a ROI was rescaled to intensities in the range [0 98$^{th}$ percentile] i.e. between a minimum intensity of 0 and a maximum intensity of the 98$^{th}$ percentile value of the whole image, eliminating outliers.

The newly calculated intensity values were then rescaled again, in the range between 0 and 1 for the purposes of texture analysis calculations.

Finally, a mask was created where only the pixel values within the ROIs were kept and the rest of the image was set to NaN (not a number). Therefore, any pixels outside the ROI would not be included in the texture analysis.

This input image was used to calculate the GLCM in step 3 below.

*Step 3: Grey level co-occurrence matrix calculation*

Grey level co-occurrence matrices (GLCMs) were calculated in four directions (0$^o$, 45$^o$, 90$^o$, 135$^o$) for pixel distances from 1-4 (distance between the pixel of interest and its neighbour) using 32 grey levels. More details about the calculation of the GLCM is in section 2.4.2.

32 grey levels were chosen as a compromise between resolution (fewer grey levels means lower contrast resolution) and the computational intensity (too many grey levels would make the calculation more computationally expensive). This generated 16 GLCMs of size 32x32 from an input image with a range of intensity values from 0 to 1 (mapped to grey levels from 1 to 32).

In more detail, the input image (created in step 2) has its' image intensity values (ranging from 0 to 1) mapped to a single grey level

i.e. 1 to 32 [222] grey levels by dividing the intensity values into 32 equal width bins. For example, an intensity value between 0 and 1/32 would be mapped to the grey level 1 and a value between 31/32 and 1 would be mapped to the grey level 32.

A count is then made between pairs of pixels separated by the defined pixel distance in the given direction for the distribution of grey level values. This allowed comparison of pixel pairs with similar grey levels within the ROI indicating smooth, homogenous texture whereas several different grey levels within the ROI would indicate rough, heterogeneous texture.

*Step 4: Summary measures of the GLCM and ratio between TI & SB*

Three summary measures were derived for each GLCM: 1) TA contrast (texture analysis contrast, not to be confused with oral contrast), 2) TA energy and 3) TA homogeneity. Since directionality was not a concern in regards to the texture (and in some cases the ROIs were rotated to fit within the bowel lumen), measures from the 4 directions were averaged [221] which provided, for each ROI, 12 texture analysis measures per subject i.e. 3 summary measures each at 4 pixel distances.

More details about the GLCM summary measures can be found in section 2.4.3. In brief, TA contrast is higher for heterogenous texture whereas TA energy and TA homogeneity are higher for homogenous texture.

Finally, for each summary measure, the ratio was calculated between the TI and 1) a distal part of the SB and 2) the colon at each of the 4 pixel distances.

### 7.2.4 Motility Analysis

Motility data visualisation and analysis were performed in MATLAB 2018 (The MathWorks, Natick, MA). This included a graphical user interface (GUI) (described previously in sections 3.2.3, 4.2.3, 5.2.3 and 6.2.3), where anonymised datasets are displayed, as both a static reference image and as a “cine” movie. This allowed for inspection of all the MRI data (as well as ROI placement and automated MRI metric measurement).

For each patient, the thesis author used the “Motility analysis” GUI to place a ROI on the reference image, in a single slice where the terminal ileum was most visible, with the cine motility movies available to aid ROI placement. The ROIs were validated by a research fellow with over 5 years MRE experience (Menys).

The motility metrics described in section 5.2.4 were derived from the single TI ROI:

1) mean motility

2) spatial variation

3) temporal variation

4) area of motile bowel

### 7.2.5 Colon Diameter Assessment

All analysis was performed in MATLAB 2018 (The MathWorks, Natick, MA) using anatomical data in the same newly developed “Texture analysis” viewer (see section 7.2.3).

The colon diameter was measured from a position on the ascending colon wall 5-10cm horizontally above the ileocaecal valve to the opposite ascending colon wall and along a line perpendicular to the long, vertical axis of the ascending colon (see figure 36).

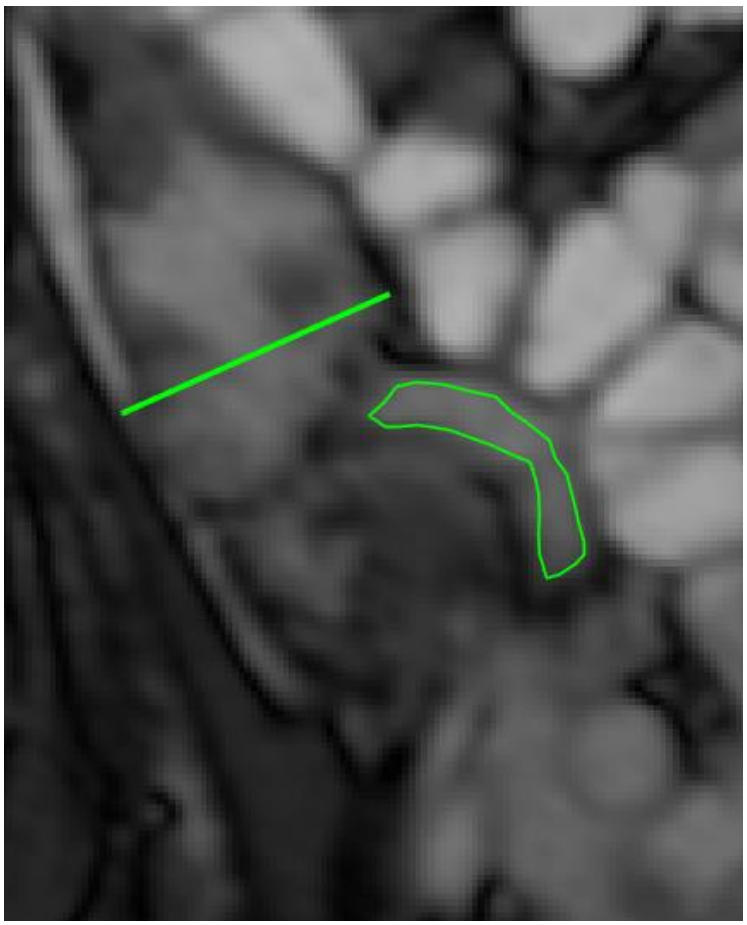

**Figure 36: The colon diameter (line ROI) was measured along a line perpendicular to the long, vertical axis of the ascending colon and above the ileocaecal valve which joins the colon and the terminal ileum (polygon ROI).**

### 7.2.6 Statistical analysis

All statistical analysis was performed in MATLAB 2018 (MathWorks, Natick, MA). All data was checked for normality using a Shapiro-Wilk test (alpha = 0.05).

If both the healthy control group and IBS patient group were normally distributed, an independent two sample t-test was performed for comparing the two groups. If one of the groups was not normally distributed, the Mann-Whitney test was performed instead.

*MATLAB function used: [h,p,ci,stats]=ttest2(current HCs,current IBS); [p_ranksum,h_ranksum,stats]=ranksum(current HCs,current IBS);*

Either a two-sample t-test (for normal data) or the Mann-Whitney test (for non-normal data) was performed to compare healthy controls and IBS patients, with $p < 0.05$ being taken as statistically significant.

The comparison between HCs and IBS patients was performed independently for: 1) each of the three texture analysis summary measures at the four pixel distances (see sections 2.4.3 and 7.2.3), 2) each of the four motility metrics (described in section 5.2.4) and 3) the ascending colon diameter (see section 7.2.5).

An additional texture analysis was performed comparing only subjects imaged using BTFE anatomical sequences i.e. acquired on a 3T Achieva scanner and not including the 1.5T Avanto scanner data. The BTFE images only analysis was performed since the texture analysis measures may be affected by the sequences/scanner used to acquire the data and all the healthy control data was acquired using BTFE sequences.

Intra-observer variability of the colon diameter was assessed using Bland-Altman plots. Mean absolute differences, 95% limits of agreement (LOA) and coefficient of variation (CV) were calculated. A low CV would be considered good and a high CV considered poor.

Mean absolute differences give an idea of the systematic bias between repeat measurements for the same observer.

LOA gives an indication of the repeatability of the measurement and is calculated by 1.96 times the standard deviation of the measurements.

CV assesses the variability of the measurement and is calculated by the ratio of the standard deviation between measurements to the overall mean of measurements.

## 7.3 Results

### 7.3.1 Cohort Demographics

The full study cohort consisted of 38 subjects (18 IBS-C patients and 20 healthy controls) (figure 37).

From the entire study 4 IBS-C patients were excluded due to MRI data being unavailable (n=3) and a diagnosis of CIPO instead of IBS-C (n=1).

There were 14 IBS-C patients (mean age, 39; age range, 21-56 years; 13 females) and 20 healthy controls (mean age, 28; age range, 22-48 years; 14 males) available for analysis

From the texture analysis component of the study, 2 subjects (1 IBS-C and 1 HC) were excluded due to a BTFE or true FISP anatomical data not being available (n=1) and the terminal ileum not being visible (n=1).

From the motility analysis component of the study, 4 healthy controls were excluded due to dynamic MRI data not being available.

From the colon diameter component of the study, 1 IBS-C patient was excluded due to BTFE or true FISP anatomical data not being available.

There were 32 subjects remaining for texture analysis (13 IBS-C patients and 19 healthy controls). For the BTFE only texture analysis, there were 22 subjects (3 IBS-C patients and 19 healthy controls).

There were 30 subjects remaining for motility analysis (14 IBS-C patients and 16 healthy controls) and 33 subjects remaining for measuring ascending colon diameter (13 IBS-C patients and 20 healthy controls).

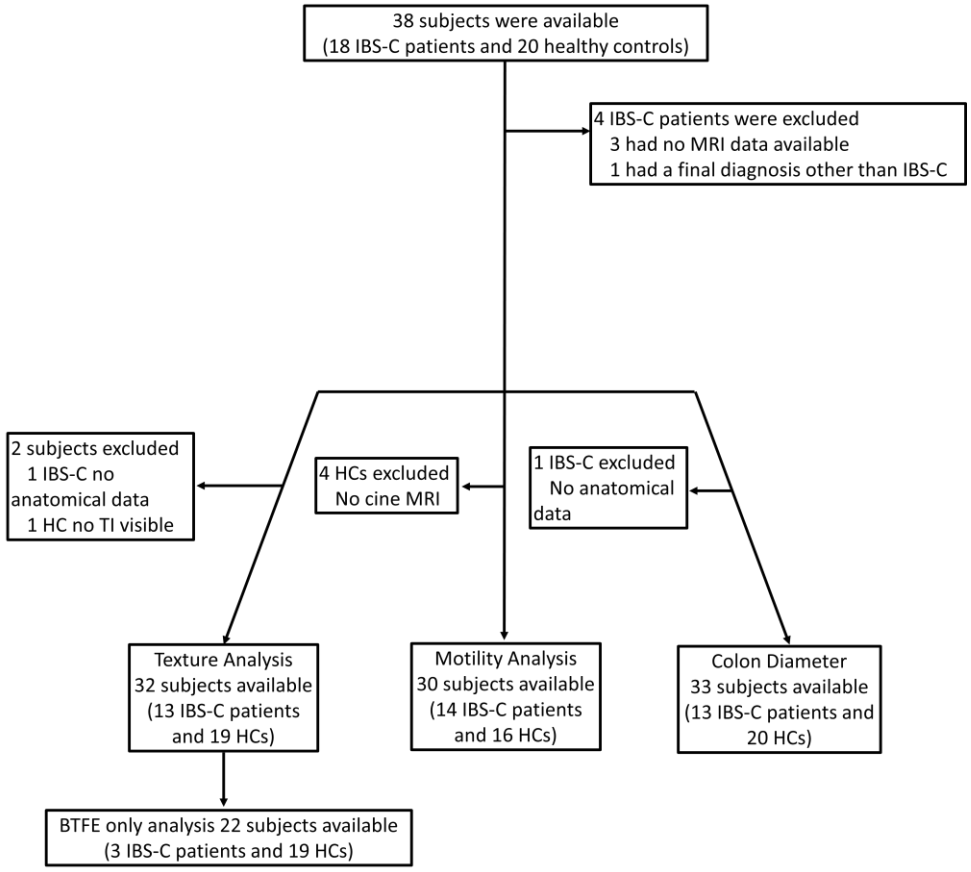


**Figure 37: Flow chart demonstrating patient inclusions and exclusions for texture analysis, motility analysis and colon diameter comparison.**

## 7.3.2 Texture Analysis

*TI/SB Ratio comparison of IBS-C v HCs using Texture Analysis measures (Full Datasets)*

The best texture analysis measure to discriminate between the two subject groups for the TI to SB ratio (TI/SB ratio) was TA contrast at a pixel distance of 2 pixels (or 5mm). The TI/SB ratio was similar in IBS-C patients (mean TI/SB ratio = 2.32, n = 13) and in HCs (mean TI/SB ratio = 1.94, n = 19) so there was no significant difference (P = 0.38) (figure 38).

There were also no significant differences between IBS-C and HCs for the TI/SB ratio for TA energy or TA homogeneity measures.

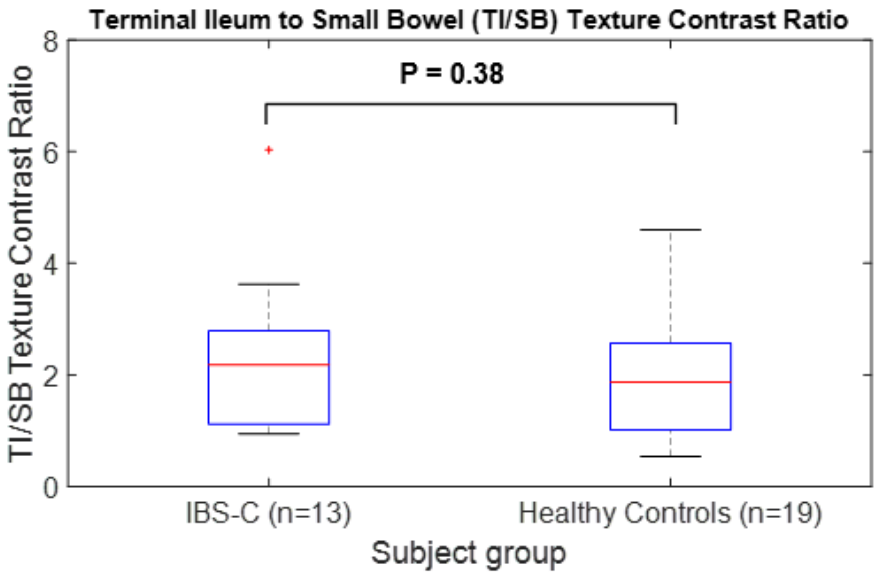


**Figure 38: Boxplot of terminal ileum to small bowel (TI/SB) Texture Contrast Ratio at a pixel distance of 2 pixels for IBS-C patients vs healthy controls.**

*TI/SB Ratio comparison of IBS-C v HCs using Texture Analysis measures (BTFE images only)*

A significant difference was found between the two subject groups for TA contrast at a pixel distance of 2 pixels when analysing only BTFE anatomical images acquired from the same scanner (P = 0.04). The TI/SB ratio was significantly higher in IBS-C patients (mean TI/SB ratio = 3.63, n = 3) than in HCs (mean TI/SB ratio = 1.94, n = 19) (figure 39).

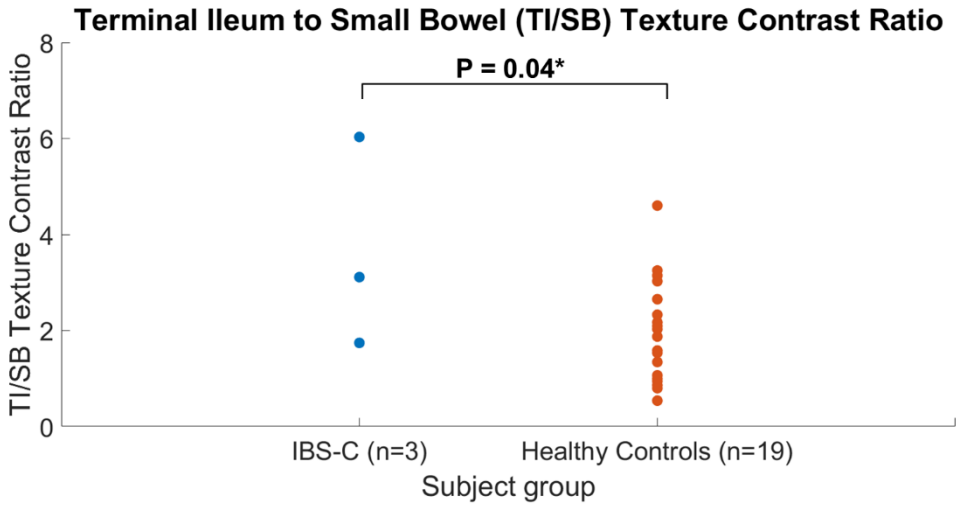


**Figure 39: Scatterplot of terminal ileum to small bowel (TI/SB) Texture Contrast Ratio at a pixel distance of 2 pixels for IBS-C patients vs healthy controls, only in BTFE datasets. *indicates significant result**

An IBS-C patient with a heterogenous TI and homogenous SB, resulting in a high TI/SB TA Contrast ratio of 4.4 (figure 40A-B) and a healthy control with homogenous TI and SB, resulting in a TI/SB TA Contrast ratio of 1.68, much closer to 1 (figure 40C-D) is shown below in figure 40.

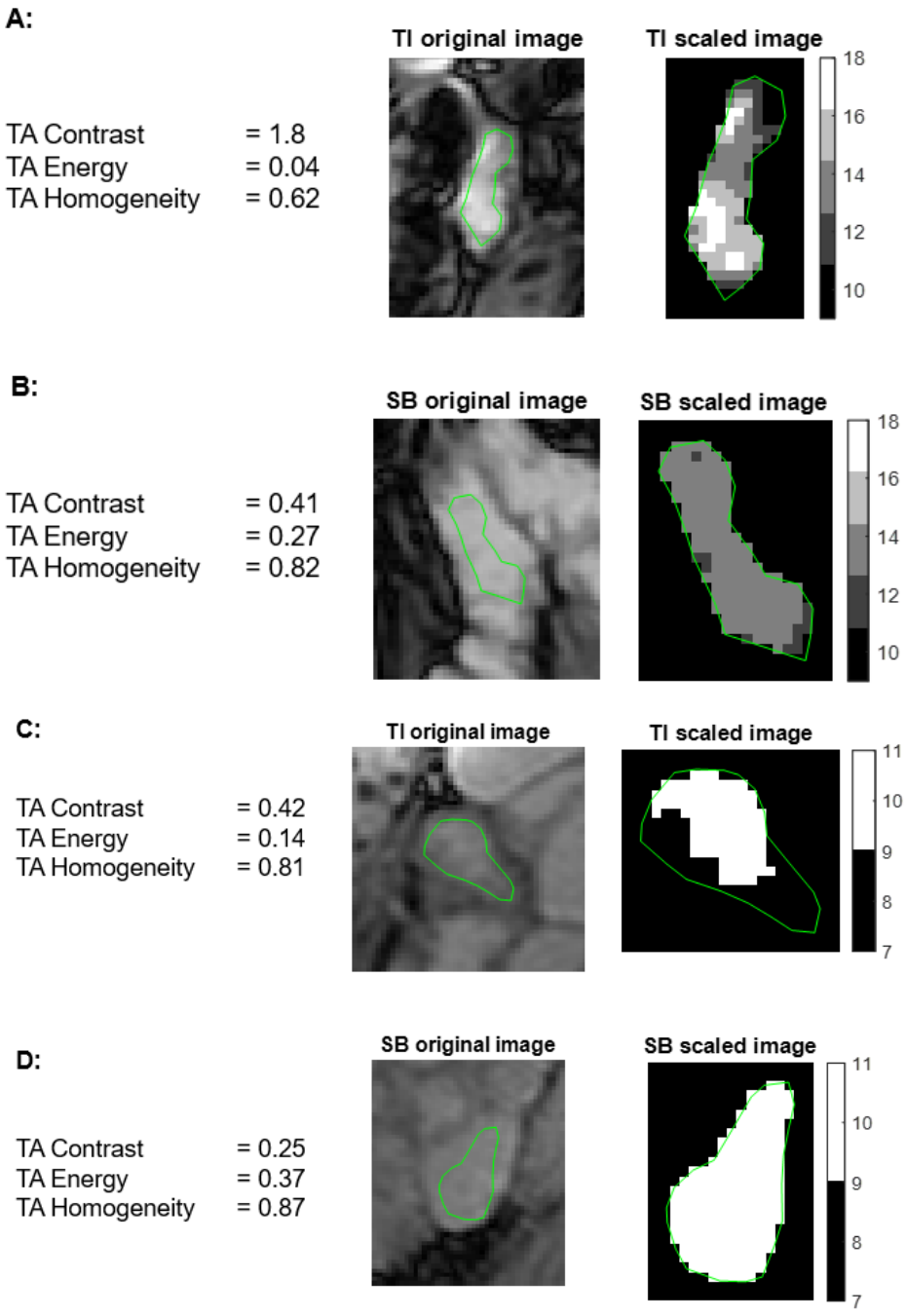


**Figure 40: An ROI is drawn on the original MRI image (left column) and this ROI is scaled between 0-32 grey levels (right column). Shown here is a representative IBS-C patient with the TI which is patchy/heterogenous with a large variation in grey level values as indicated by a TA contrast of 1.8 (A) and the SB which is homogenous with fewer grey level values as indicated by a TA contrast of 0.41 (B). A representative HC with homogenous luminal contents throughout the SB is shown with a low number of grey levels in both ROIs and similar TA contrasts of 0.42 (C) and 0.25 (D).**

*TI/Colon Ratio comparison of IBS-C v HCs using Texture Analysis measures (Full Datasets)*

The best texture analysis measure to discriminate between the two subject groups for the TI to colon ratio (TI/Colon ratio) was TA contrast at a pixel distance of 2 pixels. The TI/Colon ratio was significantly higher (P = 0.005) in IBS-C patients (mean TI/Colon ratio = 3.2, n = 13) than in HCs (mean TI/Colon ratio = 0.9, n = 19) (figure 41).

There were also significant differences found between the two subject groups for TA contrast at pixel distances of 1 (P = 0.007), 3 (P = 0.008) and 4 (P = 0.02).

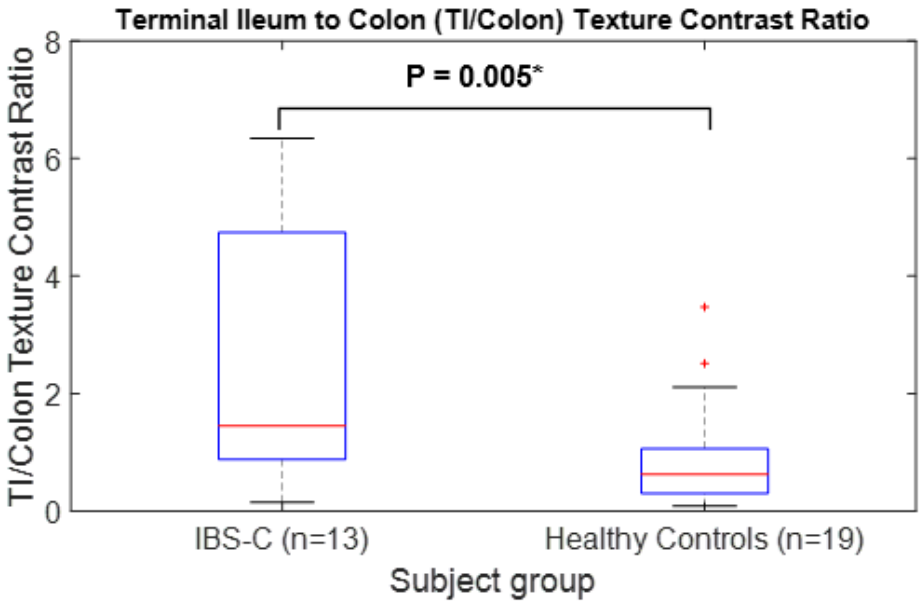


**Figure 41: Boxplot of terminal ileum to colon (TI/Colon) Texture Contrast Ratio at a pixel distance of 2 pixels for IBS-C patients vs healthy controls. *indicates significant result**

There were significant differences between IBS-C and HCs for the TI/Colon ratio for TA energy at pixel distances of 1 (P = 0.03) and 2 (P = 0.05). The TI/Colon ratio was significantly lower in IBS-C patients (mean TI/Colon ratio = 1.1) than in HCs (mean TI/Colon ratio = 2.7) for a pixel distance of 1 (figure 42).

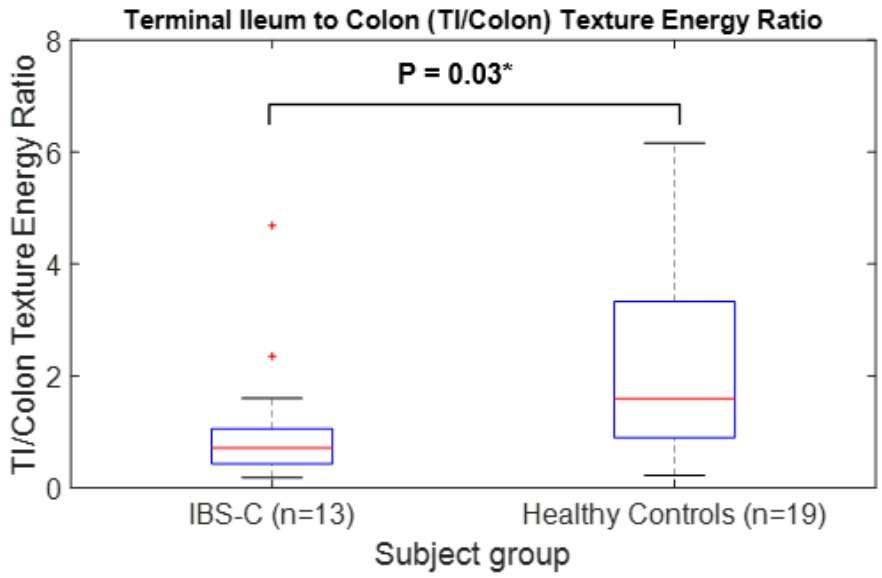


**Figure 42: Boxplot of terminal ileum to colon (TI/Colon) Texture Energy Ratio at a pixel distance of 1 pixel for IBS-C patients vs healthy controls. *indicates significant result**

There were significant differences between IBS-C and HCs for the TI/Colon ratio for TA homogeneity at pixel distances of 1 (P = 0.005) (figure 43) and 2 (P = 0.03).

The TI/Colon ratio was significantly lower in IBS-C patients (mean TI/Colon ratio = 0.95) than in HCs (mean TI/Colon ratio = 1.1).

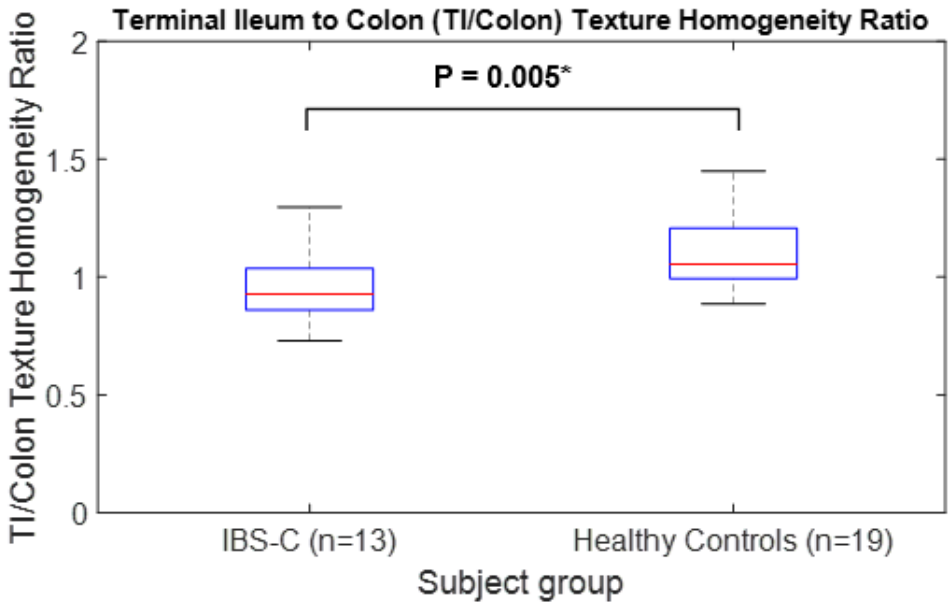


**Figure 43: Boxplot of terminal ileum to colon (TI/Colon) Texture Homogeneity Ratio at a pixel distance of 1 pixel for IBS-C patients vs healthy controls. *indicates significant result**

An IBS-C patient with a heterogenous TI and homogenous colon, resulting in a high TI/Colon TA Contrast ratio of 6.1, a TI/Colon TA Energy ratio < 1 (0.17) and a TI/Colon TA homogeneity ratio < 1 (0.72) is shown below in figure 44.

*TI/Colon Ratio comparison of IBS-C v HCs using Texture Analysis measures (BTFE images only)*

There were no significant differences between IBS-C and HCs for the TI/Colon ratio for TA contrast, TA energy or TA homogeneity measures when analysing only BTFE anatomical images acquired from the same scanner.

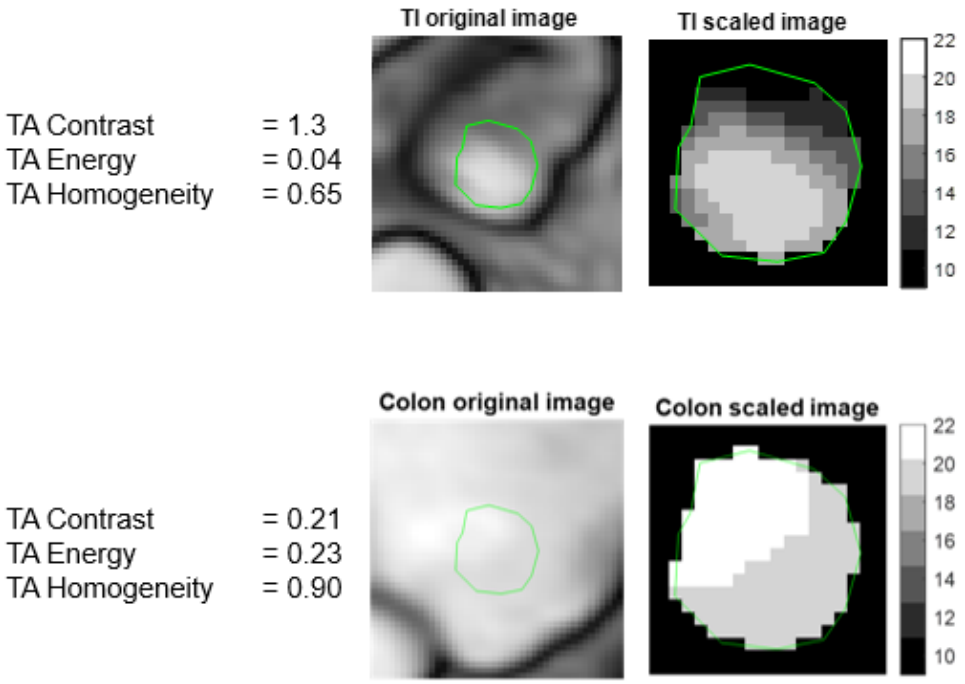


**Figure 44: The heterogeneous texture in the TI ROI is represented well by the scaled texture image (top) where there is a range of grey level values seen. Conversely, the homogenous texture in the colon ROI is represented by a homogenous scaled texture image (bottom) with much fewer grey level values. The summary measures accurately represent the heterogeneity/homogeneity of the texture seen in the image with over a fivefold increase in TA contrast for the heterogeneous ROI (0.21 to 1.3) and over a fivefold increase in TA energy for the homogeneous ROI (0.04 to 0.21).**

### 7.3.3 Terminal Ileum (TI) Single Slice Motility Analysis

The TI temporal variation (metric 3) was higher in HCs (mean = 0.024, n = 16) than IBS-C patients (mean = 0.009, n = 14), but only achieved borderline significance (P = 0.05) (figure 45).

There were no significant differences between the two subject groups for mean motility (P = 0.07) with a lower mean motility in IBS-C (mean = 0.24) compared to HCs (mean = 0.33), spatial variation of motility (P = 0.20) and area of motile bowel (P = 0.06).

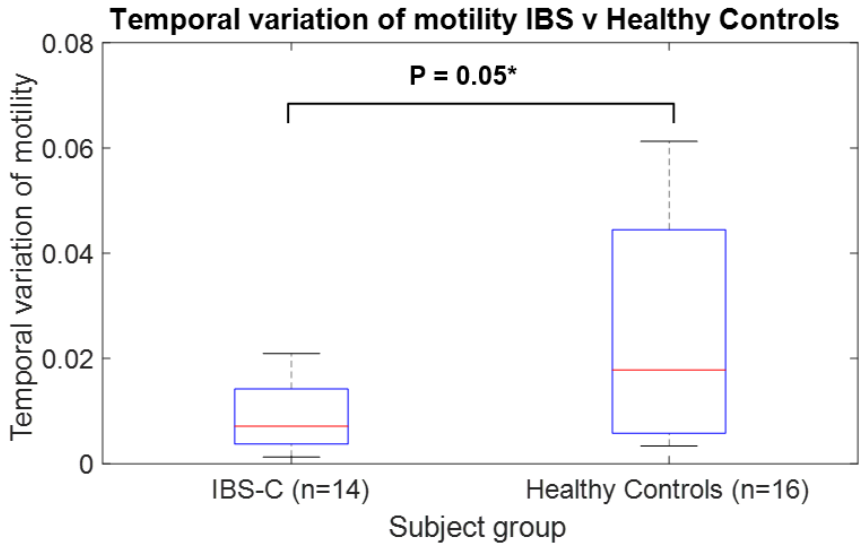


**Figure 45: Boxplot of temporal variation of motility for IBS-C patients vs healthy controls. *indicates borderline significance.**

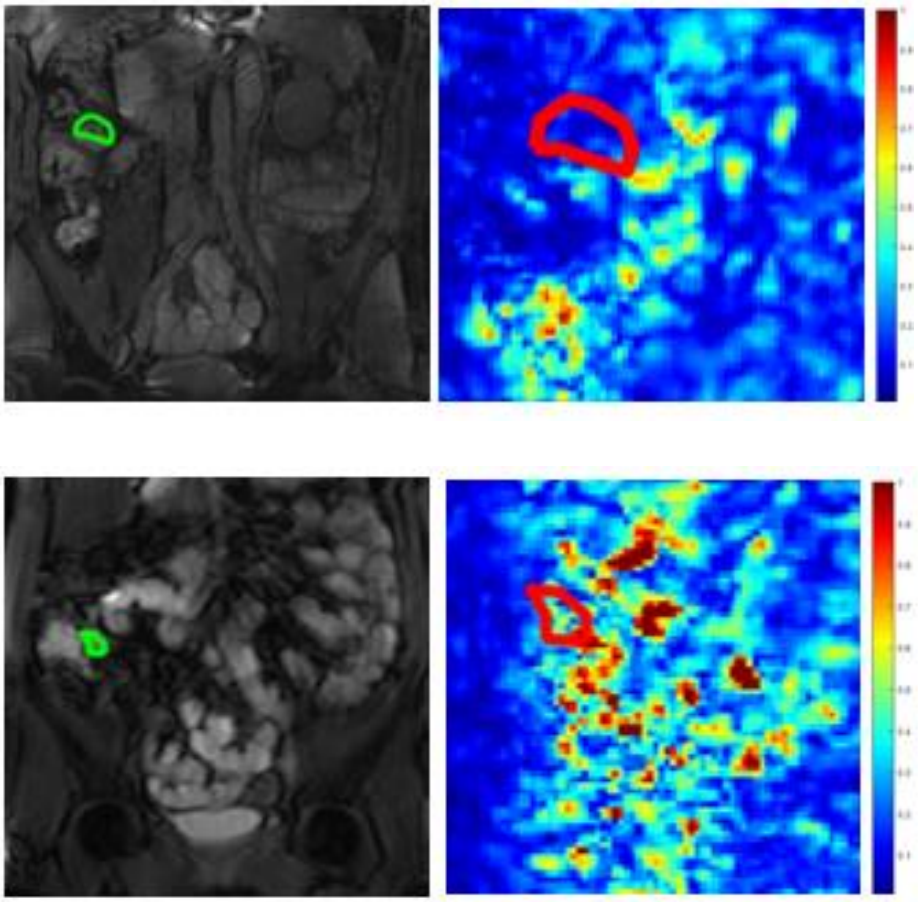

**Figure 46: Two examples of coronal temporal variation maps based on the standard deviation of the Jacobian determinant with colourbar showing low (blue) to high (red) temporal variation of motility. A region of interest was drawn in the terminal ileum with a low temporal variation seen in the IBS-C patient (top) and a high temporal variation seen in the healthy control (bottom).**

A summary of automated motility metrics for the IBS-C patients and healthy controls is shown in table 20.

| **Subject group** | **Motility metrics** | Median | Range | |
|---|---|---|---|---|
| | | | Minimum | Maximum |
| **IBS-C patients (n = 14)** | **Mean motility** | 0.224 | 0.122 | 0.433 |
| | **Spatial variation** | 0.092 | 0.041 | 0.198 |
| | **Temporal variation** | 0.007 | 0.001 | 0.021 |
| | **Area of motile bowel (% of ROI)** | 92.1 | 48.9 | 100.0 |
| **Healthy Controls (n = 16)** | **Mean motility** | 0.311 | 0.136 | 0.629 |
| | **Spatial variation** | 0.107 | 0.045 | 0.350 |
| | **Temporal variation** | 0.018 | 0.003 | 0.061 |
| | **Area of motile bowel (% of ROI)** | 98.7 | 46.3 | 100.0 |

**Table 20: Median, minimum and maximum automated motility metric values for IBS-C patients and healthy controls.**

## 7.3.4 Colon Diameter

There were significant differences between IBS-C and HCs for the ascending colon diameter (P = 0.005) (figure 47).

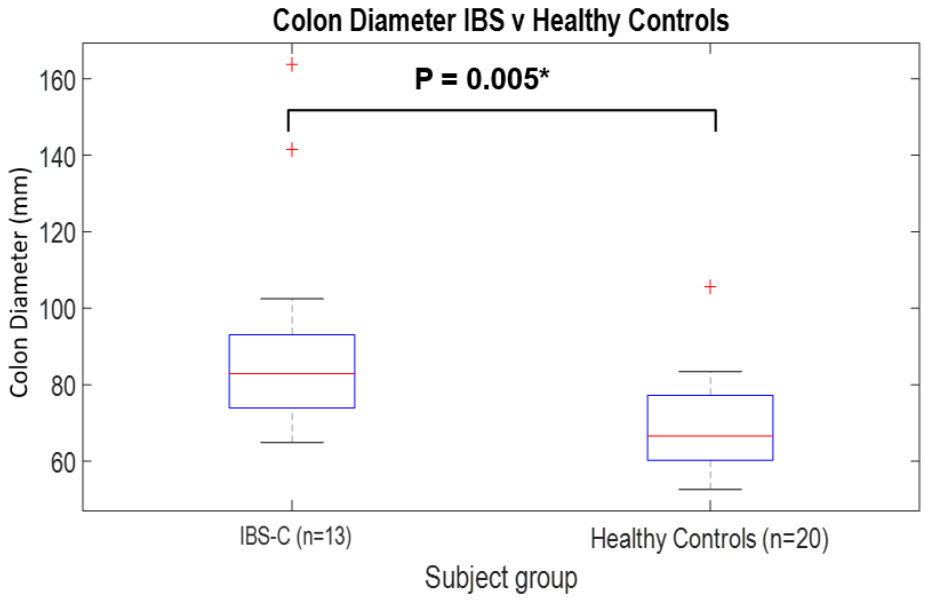


**Figure 47: Boxplot of ascending colon diameter for IBS-C patients vs healthy controls.**

The CV was 17%, the absolute mean difference was 7.7mm and the 95% LOA ranged from -19mm to +35mm (figure 48).

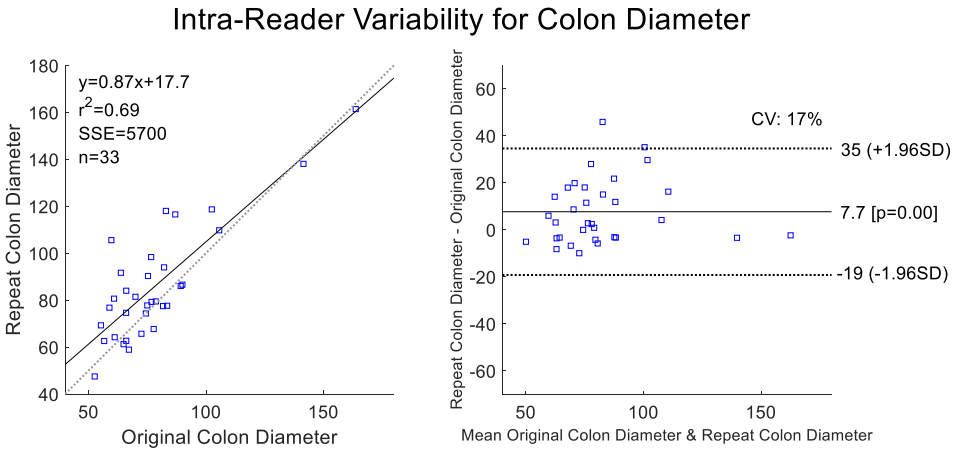


**Figure 48: The colon diameter measurement is displayed on a simple correlation plot (left) and a Bland-Altman plot (right). The absolute mean difference was 7.7mm, the 95% LOA ranged from -19mm to +35mm and the coefficient of variation (CV) was 17% on the Bland-Altman plot.**

## 7.4 Discussion

This pilot study suggests that MRI can potentially be used to differentiate between IBS-C patients with abdominal bloating and distension and healthy controls. The study provides potential explanation into the mechanisms leading to patients' clinical complaint, supporting altered gut motility as contributing factor to patients' clinical presentation.

Here, it was demonstrated that texture analysis summary measures such as TA contrast, TA energy and TA homogeneity were able to differentiate between IBS-C patients and healthy controls for the TI to SB ratio and the TI to colon ratio. An increased ascending colon diameter was shown for IBS-C patients compared to healthy controls. In addition, a higher temporal variability of motility in healthy controls was seen compared to IBS-C patients, although this only achieved borderline significance.

It should be acknowledged as a limitation of the study that the thesis author was not blinded to these analyses due to collating and processing the datasets prior to analysis.

### 7.4.1 Texture Analysis

Significant differences were found between HCs and IBS-C for the TI/Colon TA contrast, TA energy and TA homogeneity.

For instance, there was a higher TI/Colon contrast ratio in IBS-C patients (mean TI/Colon ratio = 3.2) than in HCs (mean TI/Colon ratio = 0.9) at a pixel distance of 2 pixels (P = 0.005). The range of TI/Colon contrast ratios was narrow in the HCs meaning that the TA contrast was similar between the TI and the colon ROIs. Most of the IBS-C patients had TI/Colon ratios > 1 which suggests that the TA contrast within the TI was much higher than in the colon.

There was a lower TI/Colon energy ratio in IBS-C patients (mean TI/Colon ratio = 1.1) than in HCs (mean TI/Colon ratio = 2.7) for a pixel distance of 1 (P = 0.03). Most of the IBS-C patients had TI/Colon energy ratios lower than 1 (10 out of 13 patients) meaning that the TA energy was higher in the colon than in the TI. A higher TA energy represents a more homogenous texture appearance, so this suggests that the texture within the TI is more heterogenous and the colon texture is more homogenous. The range of TI/Colon energy ratios was large in the HCs with a TI/Colon energy ratio > 1. This suggests that the TA energy within the TI was much higher i.e. more homogenous than in the colon.

In this small pilot study, a significant difference was unable to be detected between HCs and IBS-C for the TI/SB ratio with the best texture analysis measure being TA contrast at a pixel distance of 2 pixels (P = 0.38). However, imaging data was acquired from multiple scanners and a significant TA contrast TI/SB ratio (at a pixel distance of 2 pixels) difference was observed in a sub-set of 3 patients from one scanner using a BTFE sequence (P = 0.04). The TI/SB ratio was higher in IBS-C patients (mean TI/SB ratio = 3.63) than in HCs (mean TI/SB ratio = 1.94). Therefore, the non-significance in the full dataset might be due to scanner variation which could affect the texture analysis measurements. Due to the small number of IBS patients (n=3) in this BTFE only subset, this result can only be tentatively stated as being significant, especially considering the lack of multiple comparison correction i.e. the full dataset and the smaller subset BTFE only analysis.

Considering both the TI/Colon TA energy ratio < 1 and the TI/Colon TA contrast ratio > 1 in the IBS-C patients, this suggests that the texture within the TI of IBS-C patients is much more heterogenous when compared to the colon texture which seems more homogenous. Since each pixel equates to 2.5mm in these images

and the TA energy and TA contrast best demonstrated differences between IBS-C patients and HCs at pixel distances between each pixel and its' neighbour of 1 and 2 pixels respectively, this could indicate that the differing contents within the TI are 2.5-5mm or less in size.

A better discrimination between IBS-C and HCs using the TI/Colon ratio compared to the TI/SB ratio could be due to a more consistent anatomical location of the colon ROIs compared to the variable placement of the SB ROIs. Additionally, a better and more homogenous oral contrast content in both the TI and ascending colon in HCs, due to normal transit, could also in part explain the differences between IBS-C and HCs. Due to the difficulty of the SB ROI placement without including bowel wall, it was not possible to always place the ROIs in the same part of the small bowel i.e. the ileum or the jejunum across all patients so therefore there could be texture differences between different parts of the small bowel before the TI.

A limitation in this study was the placement and size of the ROIs. ROIs of the same size and shape were selected for texture analysis rather than analysing the entire image, which kept the GLCM summary measures consistent for comparison of different regions i.e. TI to small bowel. This also had the added benefit of more efficient computation of the GLCM. However, ROI placement, size and shape was not trivial for this application. Since GLCMs are calculated from the distribution of grey levels between pairs of pixels then the size and shape of the area being analysed greatly affects the value of the texture analysis summary measure. For example, if the ROI is too small then not only would a pixel distance of 4 be too high meaning the pixels would often be out of bounds, but the TA contrast would be much higher since there are less combinations of pairs of pixels available. Whereas a large ROI would mean that there would be a smoothing effect of the grey level distribution of the pairs of pixels.

The TI was the most important consideration in this study, so all the ROIs were set to the same shape and size as the TI ROI. This is often a fairly small region so to account for this, subjects were excluded from the analysis if their TI ROIs were below 100 pixels in size (n = 1).

Additionally, the placement of the SB ROI was subjectively based on visual assessment of a convenient area of oral contrast filled small bowel. This means that the choice of SB placement could greatly affect the TI/SB ratio calculated and could potentially explain the lack of significant difference found between HCs and IBS-C. Several SB ROIs could be placed in different parts of the SB and the calculated TI/SB ratios could be averaged, but this would be time consuming due to the difficulty in placing ROIs within the bowel walls in several different locations.

### 7.4.2 TI Motility Analysis

Lower temporal variability of motility in IBS-C patients (mean = 0.009) compared to healthy controls (mean = 0.24) suggests that bloated symptoms could be in part caused by aberrant terminal ileum motility, being either consistently switched “on” or “off”. Low temporal variability of motility can either indicate high mean motility (motility consistently “on”) or low mean motility (motility consistently “off”). Lower mean motility was found in IBS-C patients (mean = 0.24) compared to HCs (mean = 0.33), but this did not reach significance (P = 0.07). This suggests that the TI was mainly exhibiting low motility in IBS-C patients.

There did appear to be a slight overlap in the TI temporal variation of motility values between IBS-C patients and HCs, perhaps explaining the borderline significance (P = 0.05) with a large range in the temporal variation of the healthy controls. However, the range in the temporal variation was much narrower for the IBS-C patients

suggesting that these patients could have a characteristically low temporal variation.

As discussed in section 1.3.5, colonic transit time has been shown to be slower in IBS-C patients compared to healthy controls [132]. Altered motility, in addition to total and segmental colonic transit time, was shown to be linked to IBS symptoms i.e. altered bowel habits [133]. Postprandial motor activity is shorter in IBS patients compared to HCs and migrating motor complexes were longer in IBS-C compared to IBS-D [128].

Previously, differences in motility have been demonstrated between inflamed and non-inflamed TI in Crohn's disease patients using MRI with lower mean motility in inflamed TI compared to non-inflamed TI [199].

In this study, there was a suggestion of low motility in the TI of the IBS-C patients. This would likely affect transit of luminal contents from the terminal ileum into the colon. Altered motility and TI filling may cause aberrant viscero-somatic reflexes, resulting in abdominal bloating. This study provides another example of TI motility as a potential biomarker in a GI related disease or condition perhaps suggesting that this is important region when concerning GI symptoms.

As previously discussed in section 2.5, there are limitations with the motility MRI data such as the preparation (using oral contrast or not) which could affect transit time, scan duration (20 seconds breath-hold or longer free breathing scans) potentially affecting the measure of motility (see chapter 3) and slice position (only selecting one slice where the TI is most visible).

Another potential limitation in the study is that the low range of temporal variation of motility and mean motility values in the TI of IBS-C patients may be due to slow transit causing the oral contrast not to reach the TI. Therefore, low TI motility could indicate

unprepared bowel in fasted state, rather than inherent abnormally low motility in IBS-C. However, this could also explain the borderline significance between IBS-C and HCs if the wide range of motility values in HCs was caused by HCs exhibiting low motility due to sub-optimal TI filling.

Additionally, the inability of the oral contrast to reach the TI in some patients could affect the TI/SB and the TI/Colon texture ratios. Particularly for the TI/Colon ratio, the hypothesised reflux of caecal contents back into the terminal ileum would be more difficult to observe. Subjectively, through visual inspection, there were a low number of subjects where the TI was not filled effectively.

### 7.4.3 Colon Diameter

Previously, a decreased ascending colon diameter has been found in IBS-D patients compared to healthy controls [100].

This study finds an increased colon diameter ($P = 0.005$) in IBS-C patients (mean colon diameter = 91.7mm) compared to healthy controls (mean colon diameter = 69.7mm).

This was not surprising since bloated patients often appear in clinic with a distended abdomen and constipation. It would be expected that a large ascending colon diameter caused by excessive distension and a lack of movement of the oral contrast through the rest of the colon would be seen.

Bloating, a subjective sensation of abdominal fullness, and distension, an objective increase in abdominal girth, are common symptoms in IBS-C patients and are associated with slow transit [99] which is potentially caused by abnormal motility.

In IBS-C patients, there is a feedback loop starting with increased luminal contents after the ingestion of food. Impaired intestinal transit and emptying leads to constipation with the retention of gas

associated with an increased abdominal girth [101]. Additionally, a postprandial reduction of colonic tone is associated with distension in IBS-C patients [251].

An increased perception to the feeling of bloating is associated with gas retention and increased abdominal girth with visceral hypersensitivity postulated to be the cause [101]. Abdomino-phrenic dyssnergia is a mechanism which is hypothesised to act in response to meals and/or constipation with diaphragm descent and reduced abdominal wall tone leading to an exaggerated enlargement in the abdominal region [252].

There was a limitation in where to measure the colon diameter. The measurement was always taken along the lateral axis where possible i.e. normally a horizontal line if the ascending colon was directly vertical. To keep as consistent as possible, the colon diameter was always measured from 5-10cm above the terminal ileum.

However, in some cases this meant that the colon diameter slices location away from the slice where the terminal ileum was visible so the distances away from the terminal ileum may have varied from subject to subject. Furthermore, it was clear that for some subjects there was a much larger colon diameter in different slices and positions than where the diameter was actually measured. Despite these limitations, the main advantage was that there was at least a consistent methodology for the measurement of the colon diameter.

Intra-reader variability was assessed to study the repeatability of the colon diameter measurement. The coefficient of variation was low at 17%. The bias between the original and the repeat measurement was 7.7mm which is fairly low considering the colon diameter measurements ranged from 52.6mm to 143.6mm. The 95% limits of agreement ranged from -19mm to +35mm, which indicates that the measurements were moderately repeatable.

## 7.5 Summary

In summary, this study has demonstrated that texture analysis measures between the TI and the colon or the small bowel, increased ascending colon diameter and low motility temporal variation in the terminal ileum are MRI measures which could increase the understanding of the pathophysiology of bloated IBS-C patients. The IBS-C data was acquired during standard clinical scan protocol so was therefore representative of data seen in daily clinical practice. The “faecalisation” seen in IBS-C patients is likely to be relevant to any functionally constipated patient, not simply IBS-C patients due to it not being specific and diagnostic of IBS-C.

Texture analysis shows promise in its ability to differentiate between various luminal contents in IBS-C, especially when comparing heterogenous TI contents to more homogenous colon contents. Optimisation of sequences and scan parameters to increase sensitivity to luminal contents may lead to a more robust detection of differences using texture analysis in the comparison of TI contents to a distal part of the SB. Differences were only found between HCs and IBS-C for the TI/SB ratio when analysing BTFE images from the same scanner. Additionally, IBS-C patients showed an increased ascending colon diameter and a decreased temporal variation of motility.

A summary table is shown in table 21.

| **Measure** | Motility | TA Contrast (TI/SB ratio) | TA Contrast/Energy (TI/Colon ratio) | Ascending Colon diameter |
|---|---|---|---|---|
| **Finding** | Temporal variation of motility and mean motility lower in IBS-C | Significant differences only from 1 scanner with higher TI/SB ratio in IBS-C | Significant differences with TI/Colon ratio higher for contrast and lower for energy in IBS-C | Larger diameter in IBS-C |

| | | | | |
|---|---|---|---|---|
| **Interpretation** | Motility consistently switched “on” or “off” indicated by low temporal variation. Additionally, low mean motility would indicate motility consistently “off” so transit of luminal contents from TI to colon affected in IBS-C | Potentially higher TI/SB ratio in IBS-C indicating a potential reflux of contents from the colon back into the TI due to a heterogenous TI, but SB varies in texture so possibly affecting the measurement since the SB would be expected to be homogenous | TI/Colon energy ratio < 1 and TI/Colon contrast ratio > 1 in IBS-C indicates TI of IBS-C patients more heterogenous (high contrast, low energy) when compared to the homogenous colon texture (low contrast, high energy). More consistent anatomical location for colon ROI gives improved results for TI/Colon ratio compared to TI/SB ratio | IBS-C patients have constipation and therefore transit through the colon is affected with large distended ascending colon potentially contributing to the bloated feeling they experience so larger diameter would be expected from the symptoms |

**Table 21: A summary of texture analysis (TI/SB and TI/Colon ratio), ascending colon diameter and TI motility findings and interpretation of the results for IBS-C patients compared to HCs.**

# Section E: Conclusions and Future Work

# Chapter 8: Discussion of Results and Future Perspectives

In this final chapter, there is a discussion of the original research chapters (chapters 3-7) and interpretation of the results in the context of the thesis as a whole.

## 8.1 Discussion of results

Small bowel motility has an important role to play in both health and disease, particularly Crohn's disease (CD) and Irritable Bowel Syndrome (IBS). Ideally, a test that can assess both global and segmental motility patterns under physiological conditions is desired. Traditionally, as described in **chapter 1**, motility assessment has been carried out in specialised centres by non-MRI techniques such as manometry, providing pressure measurements to represent contractile activity, and scintigraphy, to measure transit time. These techniques are expensive, and the results are difficult to interpret meaning they are still not widely applicable. Furthermore, there is radiation exposure from scintigraphy and manometry is highly invasive due to the insertion of catheters that can only reach regions of the small bowel proximal to the colon or to the stomach. MRI offers advantages over these techniques as it is non-invasive and non-ionising and allows the whole small bowel to be visualised, and therefore assessment of both global and segmental bowel motility is possible.

Throughout this thesis, small bowel motility in dynamic MRI has been quantified using the optic flow registration technique described in **chapter 2**. One of the quantitative MRI motility metrics, most widely used in research, is mean motility (also referred to as the mean SD Jacobian and the motility index in the literature). This has been used in several research studies and an ongoing multi-centre clinical trial,

being run by two consultant radiologists, called MOTILITY. The trial is using MRI for early response prediction to anti-TNF therapy in Crohn's disease, by scanning patients before treatment and then at 3 and 6 months after treatment. In **chapter 3**, the minimum scan acquisition parameters necessary for robust measurements of bowel motility from MRI, through mean motility, was investigated. The assumptions, regarding acquisition protocols, were tested for scan duration and temporal resolution, using healthy volunteers. The results demonstrated that a scan duration of 15 seconds, in breath-hold, with a temporal resolution of 1 image per second was sufficient for quantified MRI small bowel motility analysis. This is in line with most previous research studies and all the breath-hold datasets analysed in this thesis.

Having established the standard dynamic MRI acquisition protocol parameters, the utility of quantitative motility measures in candidate diseases such as CD and IBS was explored in the rest of this thesis. It is thought that abnormal small bowel motility may be linked to patient symptoms. Previously, a single-centre study found an association between reduced spatial variation of motility and abdominal symptoms in 53 CD patients. In **chapter 4**, a two-centre validation study was performed in 82 CD patients. The results partly reproduce the findings from the original study. Spatial variation of motility was again negatively associated with symptoms, particularly with diarrhoea. Motility did not significantly correlate with individual scores of pain and well-being, indicating that diarrhoea is a major contributor to the observed association between motility and symptoms. A possible explanation for these results is that impaired coordination of bowel motility (low spatial variation) rather than absolute levels of motility (mean motility) leads to worsening of patient symptoms, particularly diarrhoea. Conversely, variation in small bowel motility appears to be a marker of gut health as it is a normal finding in healthy individuals.

The utility of motility metrics in the future may therefore be greatest in patients with moderate and severe abdominal symptoms. The

MOTILITY trial is currently investigating the effects of Crohn's disease medication on motility metrics and patient symptoms. Patients who retain a high symptom scores despite being in apparent clinical remission, with reduced levels of inflammation, may exhibit aberrant motility. This patient group could be a suitable target for pharmacological intervention.

Motility patterns are complex and therefore a combination of metrics, rather than a single metric, may provide better insight into aberrant motility and the relationship with symptoms in CD. In **chapter 5**, new motility metrics were developed to investigate several different motility features. The performance of these computer-based metrics was compared to subjective radiological scoring of the equivalent features through testing the association between motility and symptoms. Clinically, radiologists assess motility in a binary manner determining whether motility is "active" or "inactive". Beyond this, the ability of radiologists to subjectively assess motility was not previously assessed. This study showed that inter- and intra-observer variation was lowest for area of motile bowel. Additionally, low intra-observer variation was seen for mean motility and intestinal distension. However, computer-based motility metrics outperformed visual scoring by radiologists when tested against symptoms. Spatial and temporal variation of motility were the most difficult features to visually assess, with high intra- and inter-observer variation, yet they appear to have the strongest relationship to symptoms. Therefore, subjective grading cannot capture aberrant global motility in CD and objective quantitative motility metrics are required (see section 8.2.4).

Having investigated the motility metrics in CD, another candidate disease for assessing the relationship between motility and symptoms was explored with IBS. In IBS, symptoms are present in patients with structurally normal bowel. In **chapter 6**, it was shown that there was no relationship between a combination of the global motility metrics and symptoms, assessed using IBS-SSS, in IBS patients. Similarly, to the CD work, using symptoms scores as an outcome measure can make it difficult to make definitive conclusions

about the role of motility in contributing to symptoms. In CD, the HBI symptom questionnaire was used and it would be interesting to test the motility metrics against more complex questionnaires such as IBDQ to see if the associations between global motility and symptoms are stronger. However, symptoms are subjective in nature and although there are limitations with HBI as a symptoms questionnaire, the symptoms patients experience such as diarrhoea, pain and wellbeing are clearly important. IBS-SSS also assess pain and wellbeing, in addition to bloating, dissatisfaction with bowel habits and interference in daily life.

It was clear that a symptom which showed a strong association with motility was diarrhoea. It could be said that diarrhoea is an objective symptom and the utility of motility metrics could be in providing an explanation for objective symptoms. Another symptom that could be considered as being more objective is constipation. In **chapter 6**, global motility metrics were compared in healthy controls and in IBS, where patients were categorised into constipation-predominant (IBS-C), diarrhoea-predominant (IBS-D) and mixed IBS (IBS-M). This data suggested there were no differences in global bowel motility between IBS patients and healthy controls. A large variation in motility values has previously been shown in healthy controls. In this study, this was found to be the case in both HCs and IBS. However, IBS is a heterogenous patient group so perhaps this is not surprising and suggests that subclassifying IBS patients would be a helpful step towards better understanding the condition. Indeed, a significantly lower temporal variation of motility and lower area of motile bowel was demonstrated in IBS-C patients compared to IBS-M patients. This could be indicative of characteristic motility patterns in these diseases, especially considering the clustered values for temporal variation of motility and area of motile bowel. It can be hypothesised that, in IBS-C, the transit of contents through the small bowel into the colon is affected by a lack of coordination (low temporal variation) and low motility (low area of motile bowel). Conversely, IBS-M patients often experience changing bowel habits, alternating between diarrhoea and constipation so the symptomology is less defined. The

motility is varied and active which would suggest normal small bowel motility as seen in healthy individuals. It is possible that transit is normal in the small bowel and abnormal in the colon. Since colonic motility involves contractions which are much less frequent than in the small bowel, it was not possible to capture colonic motility with 20 second datasets. It would be interesting in further studies to acquire longer, free breathing datasets to analyse colonic motility (see section 8.2.1).

There were only a small number of IBS-C patients (n=3) available due to the datasets being acquired as part of usual clinical practice, where IBS diagnosis is confirmed normally due to exclusion of CD. Patients are much more likely to be suspected of having CD if they are suffering diarrhoeal symptoms such as those seen in IBS-D and IBS-M. In **chapter 7,** the link between motility and IBS-C symptoms was explored further with greater numbers of IBS-C patients analysed, using clinical data, and switching focus from global motility patterns to segmental motility analysis. The terminal ileum motility, along with ascending colon diameter and texture analysis, were used to investigate the mechanisms related to bloating symptoms in IBS-C patients. Anecdotally, “faecalisation” of the terminal ileum in IBS-C patients with bloating has been reported by radiologists. The hypothesis was that a contributing factor to bloated symptoms could be the reflux of caecal contents from the colon back into the terminal ileum, possibly caused by abnormal TI motility.

Temporal variation of motility and mean motility was shown to be lower in IBS-C patients with bloating than HCs. This suggests that motility is consistently switched “on” or “off”, indicated by low temporal variation, and this is likely to be inactive motility, indicated by low mean motility. These results point towards the transit of luminal contents from the TI to the colon being affected in IBS-C. The texture analysis demonstrated that the texture in the TI was heterogenous, compared to the more homogeneous texture seen in both the small bowel and colon. The results were stronger for the TI/colon ratio than for the TI/SB ratio. This is likely due to the more

consistent anatomical location of the colon ROI. Reflux of caecal contents back into the TI is a possible explanation for the heterogenous texture seen in the TI. An increased ascending colon diameter was seen in IBS-C patients compared to HCs. Transit of contents through the colon is affected in patients with constipation. This likely contributes to the bloated feeling patients experience and could provide an explanation for the reflux back into the TI. If the contents cannot move forward through the ascending colon into the transverse colon then the perhaps the ascending colon reaches capacity and some contents move back into the TI.

This thesis has demonstrated the utility of MRI motility metrics in understanding GI symptoms in CD and IBS. It was important to establish that the MRI acquisition was adequate for motility to be quantified (chapter 3) and to show that similar results have been found between motility and symptoms in two different CD study cohorts (chapters 4 and 5). Another key result was that automated motility metrics perform better than radiologist visual scoring for features such as spatial and temporal variation of motility that are difficult to visually assess (chapter 5).

An interesting point to note is that the temporal variation of motility has been shown to be one of the most important motility metrics in several of the studies in this thesis (chapters 5-7). A limitation of the standard motility map with the SD Jacobian is that it is blind to time. If a bowel loop undergoes multiple rapid contractions of equal amplitude, the same SD Jacobian would be recorded as if it only underwent one large contraction. An advantage of the temporal variation of motility map is that it incorporates temporal information into the metric through analysing the motility in 5 second sliding windows. Thus, a bowel loop with long gaps between contractions will provide a different temporal variation of motility value than a bowel loop where there are regular contractions. In the future, the motility metrics used and developed in this thesis can complement the work of the radiologist in evaluating more complicated motility patterns.

Another important aspect of this work is that promising results have already been demonstrated in IBS patients analysed using clinical data (chapters 6 and 7). Magnetic Resonance Enterography, including dynamic MRI, has become clinically routine at UCLH and other hospitals worldwide for diagnostic purposes such as evaluating Crohn's disease and irritable bowel syndrome. This has generated a substantial amount of clinical data that has been largely ignored by research, and this offers the opportunity for future analysis. For example, the potential of these large datasets to be used in machine learning is an interesting prospect, particularly concerning faster acquisition, segmentation of the small bowel and inference of the optimal treatment from motility data.

## 8.2 Future Perspectives

Overall, the research questions raised and addressed from this thesis could lead to future developments in the treatment and management of GI conditions such as CD and functional constipation and/or IBS-C. For future studies, there needs to be careful consideration of the protocol chosen for data acquisition including bowel preparation (section 8.2.2), breath-hold or free breathing protocol, 2D or 3D slice acquisition and parameters such as scan duration and temporal resolution. Study design for the analysis including how to apply the motility metrics i.e. in combination or individually, globally or in a specific region such as the terminal ileum and the patient symptom questionnaire used needs to be planned carefully. Incorporation of motility alongside other MRI biomarkers such as volume and transit time would also be useful moving forward.

### 8.2.1 Acquisition

For dynamic MRI acquisition, there is a compromise between spatial resolution, temporal resolution and coverage. As shown in chapter 3, a temporal resolution of 1 image per second is sufficient for global motility analysis. If acceleration techniques such as compressed sensing were used, then this could improve the temporal and spatial resolution. Generally, data is acquired with multiple 2D slices. This poses a few issues such as temporal incoherence between slices for global motility measures throughout the whole small bowel volume and slice positioning if only one slice is used for analysis. Another emerging acceleration technique is simultaneous multislice (see section 2.1.7). Since two or more slices are excited simultaneously then not only could this speed up the acquisition, but it could also overcome the temporal incoherence and slice positioning problems.

To expand on the work in chapter 3, the optimal scan duration and temporal resolution could be assessed in longer free breathing datasets, since this protocol is likely to be used more often than breath hold in the clinic moving forward. The quantitative motility maps would be generated using an extended version registration algorithm, which accounts for respiratory motion (discussed in chapter 6). It would also be useful to assess aberrant motility in CD in these longer datasets as potentially they may capture a more complete picture of motility. For example, the 5 second sliding windows used in the temporal variation of motility measurement in 20 second breath hold datasets could be modified. Perhaps a different duration of the sliding windows would capture the motility better in these free breathing datasets. Another aspect of longer datasets would be the ability to apply the motility metrics developed in this thesis in the colon where contractions occur much less frequently (discussed in chapter 1).

Another consideration is whether subjects should be scanned supine or prone. Supine data was acquired for temporal resolution and scan duration analysis (chapter 3) and Crohn’s disease datasets (chapters

4 and 5) whereas prone data was acquired for IBS and HC datasets (chapters 6 and 7). The bowel is flattened out and allows for better visualisation in prone so there may be differences in supine and prone data. If two different patient groups are being compared directly then there should be consistency in supine or prone positioning in the scanner.

### 8.2.2 Oral contrast bowel preparation

In this thesis, mannitol solution was ingested as oral contrast which is thought to stimulate motility (see section 2.1.7). However, the motility could be stretch-induced i.e. the large volume of fluid ingested distends the bowel and the bowel wall contains stretch receptors which trigger motility [253]. Determining that the motility is stretch-induced due to a large volume being ingested would suggest that natural food stuffs could be used instead of mannitol in stimulating motility, but visualisation of the bowel would be difficult so it is unlikely that food would entirely replace mannitol [228]. Different types of food generate different motility responses, and this is especially interesting in IBS. For example, the low FODMAP diet has been used as dietary intervention in IBS, where it is thought to reduce symptoms in some patients [254]. Kiwi fruit has also been shown to decrease transit time, increase defecation frequency and improve bowel function in IBS-C patients [255]. The potential differences in motility if the patients were scanned before (baseline scan), during and after a dietary intervention could be tracked. This is essentially measuring the transition from fasted to fed state. Currently, manometry is used to measure the fasted state, but measurements are taken over several hours and therefore it is unlikely that MRI will be able to replicate this for the fasted state. The best use of MRI is likely to be found in stimulating motility with different types of food or drugs and measuring the motility response [256].

### 8.2.3 Patient subgrouping

Due to the large amount of clinical data available, this opens up opportunities for machine learning to be implemented. The data used in chapter 6 was from a larger cohort of IBS, CD and HCs. It would be interesting to compare all these different patient groups for global small bowel motility measures throughout multiple slices. This would be a useful step in establishing standard ranges of motility metric values in several patient groups. Neural networks could also be trained to identify the patient groups based on the motility to determine if there are characteristic motility patterns associated with disease and health. Furthermore, the outcome measure could be a particular symptom score rather than the patient group the dataset belongs to. This could be especially useful in IBS where it would be useful to identify IBS subgroups through motility patterns. For instance, the standard IBS-D, IBS-C and IBS-M subgroups may be subclassified further or the data could lead us to subclassify IBS patients differently. This could provide more insight into the underlying pathophysiology of the symptoms.

It would be desirable to recruit higher numbers for each IBS subgroup to determine whether motility is a useful indication of symptoms as it is difficult to make definitive conclusions from the small numbers in each subgroup analysed in this thesis. In addition to global motility, it would be interesting to analyse motility segmentally, particularly in the terminal ileum. In CD, the terminal ileum is the most common area affected. In IBS, it was terminal ileum motility, rather than global motility, which demonstrated differences between IBS-C patients and healthy controls. Although, in future studies, the texture analysis measures from chapter 7 could be utilised more as a biomarker of faecalisation linked to functional constipation as opposed to simply IBS-C.

### 8.2.4 Automation and clinical applicability

A large obstacle to analysing large datasets is the lack of an automated segmentation tool for the small bowel. In neuroimaging, a common approach to automatic segmentation is to generate a brain atlas from hundreds of datasets and use this as a template to perform the segmentation [257]. Due to the diversity in the shape and size of the small bowel from individual to individual, it is extremely difficult to segment the bowel in this way. A neural network could be trained, using manual ROIs as the “ground truth” database, to segment the whole small bowel. There are a few MRI features that are commonly seen in patients who have ingested mannitol as an oral contrast agent. For instance, the contents in the lumen are generally brighter than the surrounding tissue and even in cases of low motility, the SD Jacobian values are higher in the small bowel than elsewhere in the abdomen. Additionally, the texture measure absolute gradient could be used since there is a large difference in intensity values between the bright lumen content and the darker bowel walls. Absolute gradient would therefore, in theory, highlight the bowel walls. A combination of these features could also be used for segmentation.

An automatic or semi-automatic segmentation tool would greatly improve the analysis of global small bowel motility since manually drawing ROIs in several slices is time consuming and is a major reason limitation in the motility metrics discussed in this thesis being widely applicable in large datasets. Furthermore, if a solution to the ROI problem was found, then introducing objective motility metrics in the clinic could improve the efficiency of the clinical workflow. The objective MRI measurements could complement the work of the radiologist. For example, highlighting extremely low or high motility in patients that need closer examination and thus introducing a time-saving measure for radiologists. If a “normal” motility pattern could be established for healthy individuals, then this would mean the radiologists would only need to visually assess motility datasets that

have been judged abnormal by the motility metrics. Additionally, more complex motility patterns that are difficult to visually assess such as spatial and temporal variation of motility would be useful for the radiologist and potentially enhance their ability to assess motility effectively. Ideally, MRI would be able to provide a summary of computer-based metrics such as motility, transit time and volume throughout the GI tract. This would provide radiologists with more useful information to guide clinical decision making and improve the management and treatment of conditions such as CD and IBS.

# 9 Appendices

## 9.1 Appendix 1: Radiologist viewer/GUI (Chapter 5)

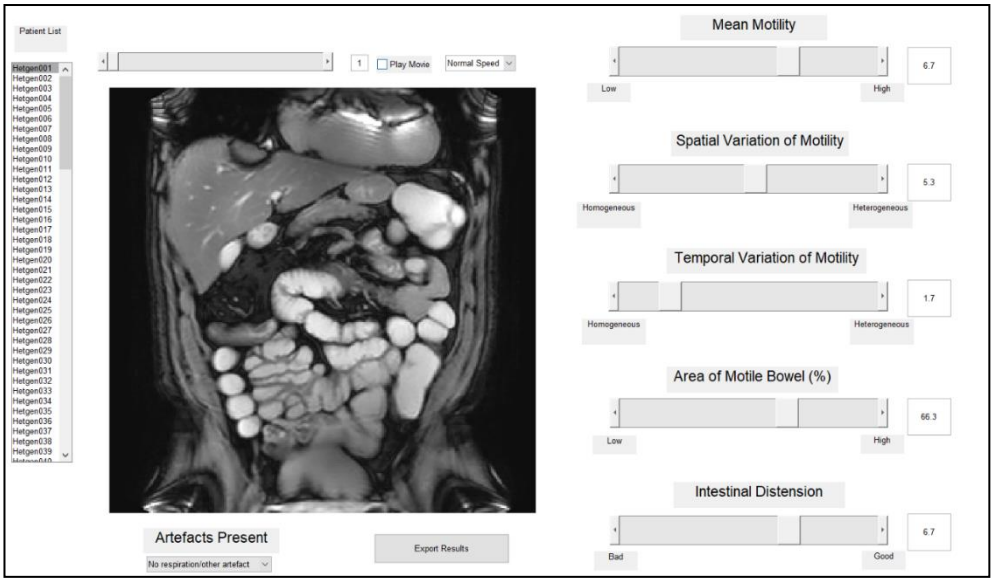


**Appendix 1:** Layout of the “radiologist viewer” for the visual grading of the five metrics by the study radiologists. The “cine” movie would be viewed as a repeated loop and the sliding bars to the right-hand side would be used by the radiologists to grade on a 0-10 scale (% scale for area of motile bowel) as explained in section 5.2.5.

## 9.2 Appendix 2: Subjective models for combined observer motility scores v HBI (Chapter 5)

| **Metrics/Predictors included in the model** | **P values for F-statistic** |
|---|---|
| 1 | 0.50 |
| [1,2] | 0.42 |
| [1,2,3] | 0.33 |
| [1,2,3,4] | 0.32 |
| [1,2,3,4,5] | 0.44 |
| [1,2,3,5] | 0.43 |
| [1,2,4] | 0.41 |
| [1,2,4,5] | 0.54 |
| [1,2,5] | 0.51 |
| [1,3] | 0.44 |
| [1,3,4] | 0.60 |
| [1,3,4,5] | 0.74 |
| [1,3,5] | 0.61 |
| [1,4] | 0.67 |
| [1,4,5] | 0.81 |
| [1,5] | 0.67 |
| 2 | 0.44 |
| [2,3] | 0.27 |
| [2,3,4] | 0.19 |

| | |
|---|---|
| [2,3,4,5] | 0.30 |
| [2,3,5] | 0.35 |
| [2,4] | 0.23 |
| [2,4,5] | 0.37 |
| [2,5] | 0.47 |
| 3 | 0.23 |
| [3,4] | 0.39 |
| [3,4,5] | 0.58 |
| [3,5] | 0.42 |
| 4 | 0.37 |
| [4,5] | 0.61 |

**Appendix 2:** P values for insignificant F-statistic for subjective radiological models vs HBI (see section 5.3.4).

## 9.3 Appendix 3: Motility metrics in two subsets of the healthy control datasets (Chapter 6)

| Subject Type | Metric | Median | Range | |
|---|---|---|---|---|
| | | | Minimum | Maximum |
| **Healthy Controls recruited by advertisement (n = 11)** | **Mean motility** | 0.354 | 0.264 | 0.382 |
| | **Spatial variation** | 0.029 | 0.014 | 0.034 |
| | **Temporal variation** | 0.020 | 0.011 | 0.025 |
| | **Area of motile bowel (% of ROI)** | 97.7 | 86.8 | 99.5 |
| | **Intestinal distension (% of ROI)** | 78.5 | 63.8 | 86.3 |
| **Healthy Controls recruited from clinical scans with no GI symptoms present** | **Mean motility** | 0.320 | 0.282 | 0.346 |
| | **Spatial variation** | 0.026 | 0.020 | 0.036 |

| | | | | |
|---|---|---|---|---|
| **(n = 9)** | **Temporal variation** | 0.017 | 0.012 | 0.020 |
| | **Area of motile bowel (% of ROI)** | 94.8 | 84.5 | 98.2 |
| | **Intestinal distension (% of ROI)** | 74.4 | 48.4 | 89.5 |

**Appendix 3:** Median, minimum and maximum automated motility metric values for healthy controls split into two subsets based on recruitment by advertisement (n = 11) and recruitment from clinical scans with no GI symptoms (details in section 6.3.2).

# 9.4 Appendix 4: Motility metrics for IBS vs Healthy Controls (Chapter 6)

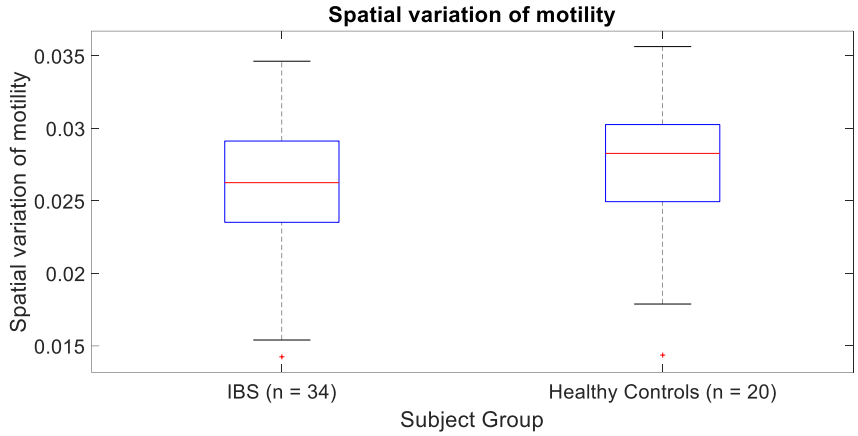


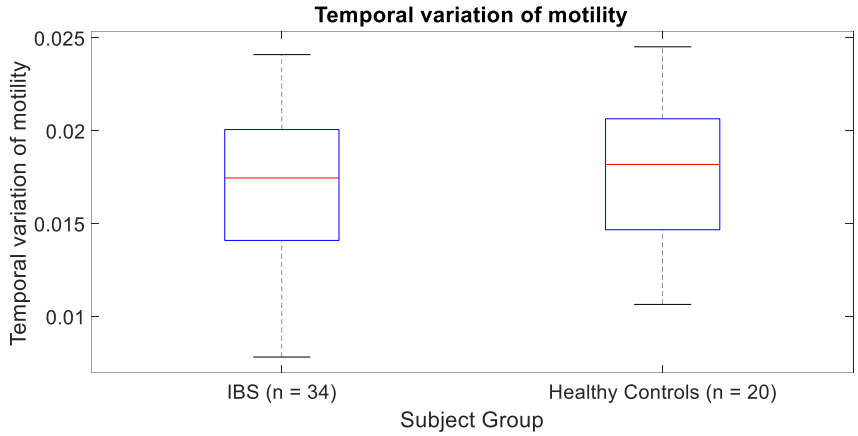


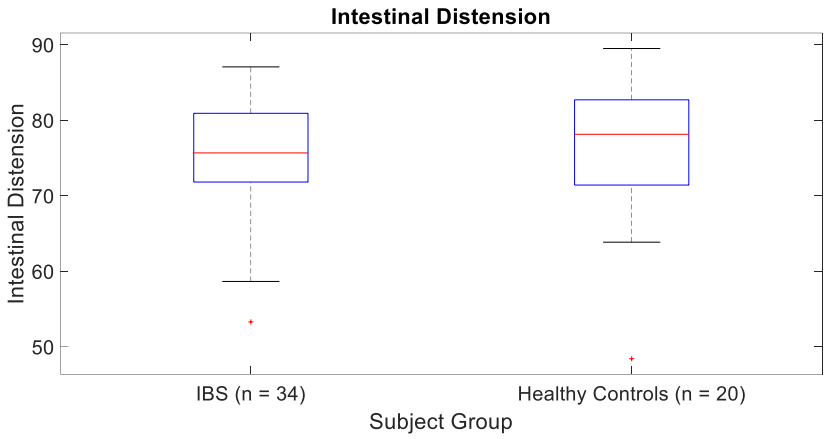


**Appendix 4:** Boxplots for spatial variation of motility, temporal variation of motility, area of motile bowel and intestinal distension comparing IBS patients (n = 34) and healthy controls (n = 20). No significant differences were found between IBS and healthy controls for these metrics.

# 9.5 Appendix 5: Motility metrics for IBS subgroups vs Healthy Controls (Chapter 6)

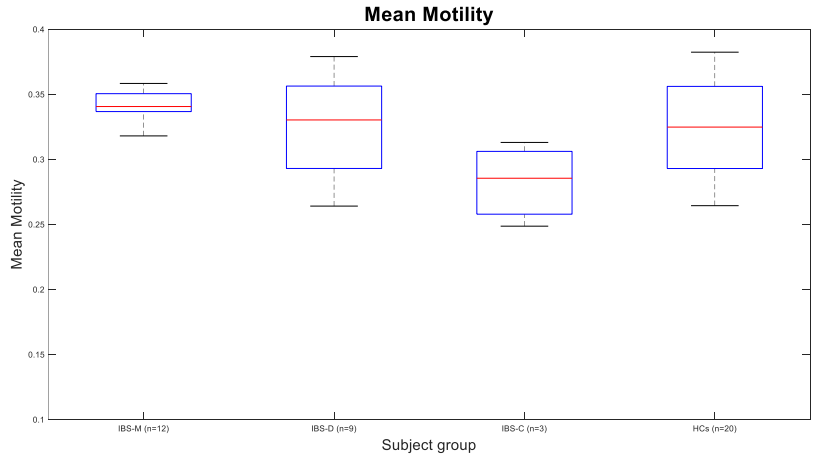


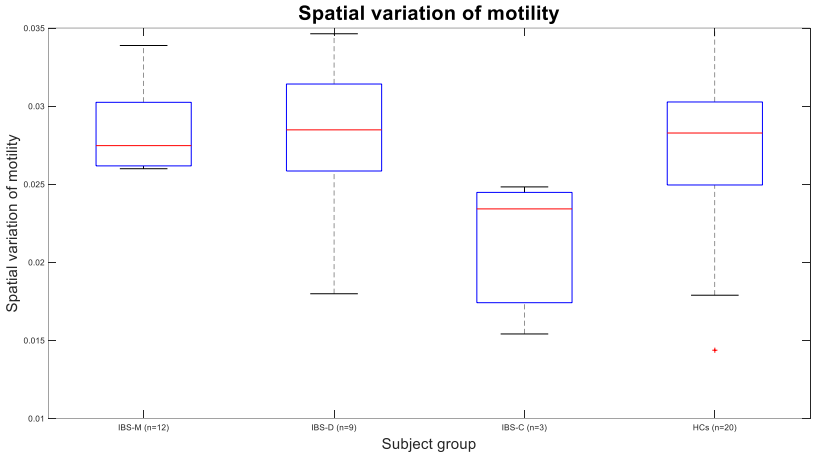


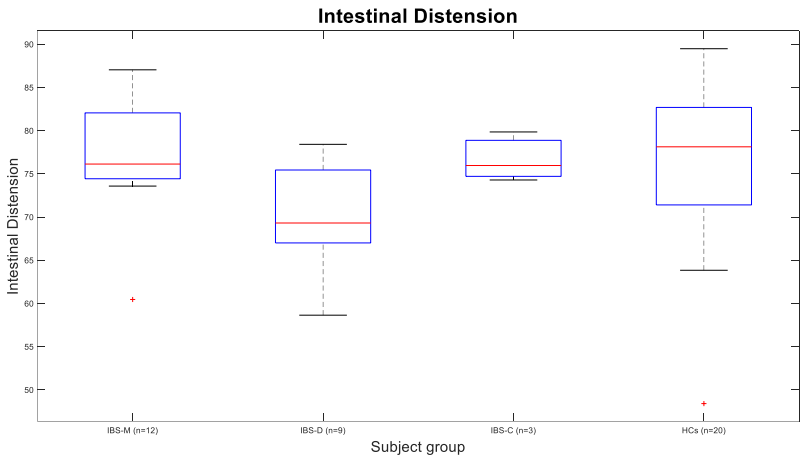


**Appendix 5:** Boxplots for mean motility, spatial variation of motility and intestinal distension metrics comparing IBS subgroups; IBS-C (n = 3), IBS-D (n = 9), IBS-M (n = 12) and healthy controls (n=20). No significant differences were found between IBS subgroups and healthy controls for these metrics.

# 9.6 Appendix 6: Correlation of IBS motility metrics vs symptoms (IBS-SSS) (Chapter 6)

| **Component motility correlated against** | **Mean motility** | **Spatial variation of motility** | **Temporal variation of motility** | **Area of motile bowel** | **Intestinal distension** |
|---|---|---|---|---|---|
| IBS-SSS Total | Rho value = 0.03 | Rho value = 0.14 | Rho value = 0.09 | Rho value = - 0.08 | Rho value = 0.14 |
| | P value = 0.87 | P value = 0.48 | P value = 0.65 | P value = 0.68 | P value = 0.49 |
| IBS-SSS Pain Intensity | -0.11 | -0.12 | -0.12 | -0.26 | -0.07 |
| | 0.58 | 0.53 | 0.54 | 0.19 | 0.72 |
| IBS-SSS Pain Frequency | 0.09 | 0.31 | 0.25 | -0.10 | 0.20 |
| | 0.66 | 0.11 | 0.21 | 0.60 | 0.31 |
| IBS-SSS Bloating | -0.15 | -0.05 | -0.26 | -0.07 | 0.00 |
| | 0.46 | 0.80 | 0.20 | 0.72 | 0.99 |
| IBS-SSS Dissatisfaction with bowel habits | 0.03 | 0.17 | 0.09 | 0.02 | -0.04 |
| | 0.87 | 0.40 | 0.65 | 0.91 | 0.84 |

| | | | | | |
|---|---|---|---|---|---|
| IBS-SSS Interference in daily life | 0.17 | -0.02 | 0.20 | 0.01 | 0.18 |
| | 0.38 | 0.90 | 0.33 | 0.95 | 0.37 |

**Appendix 6:** None of the motility metrics correlated individually with either the total IBS-SSS or any of the IBS-SSS components (see section 6.3.5).

## 9.7 Appendix 7: Multivariable regression of IBS motility metrics vs symptoms (IBS-SSS) (Chapter 6)

| | **P values for F-statistic with different IBS-SSS outcome measures** | | | | | |
|---|---|---|---|---|---|---|
| **Metrics included in the model** | IBS-SSS Total | IBS-SSS Pain Intensity | IBS-SSS Pain Freq-uency | IBS-SSS Bloating | IBS-SSS Dissatis-faction with bowel habits | IBS-SSS Inter-ference in daily life |
| 1 | 0.96 | 0.73 | 0.90 | 0.59 | 0.68 | 0.92 |
| [1,2] | 0.33 | 0.94 | 0.27 | 0.46 | 0.46 | 0.98 |
| [1,2,5] | 0.53 | 0.76 | 0.41 | 0.66 | 0.46 | 0.67 |
| [1,4] | 0.64 | 0.61 | 0.41 | 0.86 | 0.85 | 0.55 |
| [1,4,5] | 0.83 | 0.50 | 0.48 | 0.95 | 0.93 | 0.60 |
| [1,5] | 0.93 | 0.61 | 0.53 | 0.84 | 0.83 | 0.57 |
| 2 | 0.45 | 0.79 | 0.32 | 0.87 | 0.32 | 0.99 |
| [2,3] | 0.54 | 0.93 | 0.61 | 0.20 | 0.52 | 0.85 |
| [2,3,5] | 0.75 | 0.78 | 0.59 | 0.35 | 0.58 | 0.59 |
| [2,4] | 0.38 | 0.72 | 0.23 | 0.84 | 0.62 | 0.85 |
| [2,4,5] | 0.59 | 0.56 | 0.37 | 0.95 | 0.71 | 0.77 |
| [2,5] | 0.72 | 0.67 | 0.38 | 0.95 | 0.51 | 0.58 |
| 3 | 0.89 | 0.70 | 0.48 | 0.36 | 0.65 | 0.74 |

| | | | | | | |
|---|---|---|---|---|---|---|
| [3,4] | 0.60 | 0.70 | 0.16 | 0.60 | 0.86 | 0.49 |
| [3,4,5] | 0.80 | 0.57 | 0.24 | 0.77 | 0.93 | 0.56 |
| [3,5] | 0.91 | 0.61 | 0.40 | 0.65 | 0.81 | 0.54 |
| 4 | 0.59 | 0.43 | 0.55 | 0.70 | 0.57 | 0.62 |
| [4,5] | 0.83 | 0.41 | 0.52 | 0.91 | 0.79 | 0.57 |
| 5 | 0.69 | 0.37 | 0.27 | 0.76 | 0.62 | 0.30 |

**Appendix 7:** P values for insignificant F-statistic for multivariable models with different combination of motility metrics vs total IBS-SSS (see section 6.3.5).

# Bibliography


[1] F. Martini, *Fundamentals of Anatomy and Physiology*, 9th ed. Benjamin Cummings, 2012.

[2] D. C. Baumgart and W. J. Sandborn, “Crohn’s disease,” *Lancet*, vol. 380, no. 9853, pp. 1590–1605, 2012.

[3] M. Costa, “Anatomy and physiology of the enteric nervous system,” *Gut*, vol. 47, no. 90004, pp. 15iv--19, Dec. 2000.

[4] J. D. Huizinga and W. J. E. P. Lammers, “Gut peristalsis is governed by a multitude of cooperating mechanisms,” *AJP Gastrointest. Liver Physiol.*, vol. 296, no. 1, pp. G1–G8, 2008.

[5] L. Thomson *et al.*, “Interstitial cells of Cajal generate a rhythmic pacemaker current,” *Nat. Med.*, vol. 4, no. 7, pp. 848–851, Jul. 1998.

[6] L. Ye and R. A. Liddle, “Gastrointestinal hormones and the gut connectome.,” *Curr. Opin. Endocrinol. Diabetes. Obes.*, vol. 24, no. 1, pp. 9–14, Feb. 2017.

[7] R. V Seimon *et al.*, “Effects of varying combinations of intraduodenal lipid and carbohydrate on antropyloroduodenal motility, hormone release, and appetite in healthy males.,” *Am. J. Physiol. Regul. Integr. Comp. Physiol.*, vol. 296, no. 4, pp. R912-20, Apr. 2009.

[8] R. C. Spiller, I. F. Trotman, T. E. Adrian, S. R. Bloom, J. J. Misiewicz, and D. B. Silk, “Further characterisation of the ‘ileal brake’ reflex in man--effect of ileal infusion of partial digests of fat, protein, and starch on jejunal motility and release of neurotensin, enteroglucagon, and peptide YY.,” *Gut*, vol. 29, no. 8, pp. 1042–51, Aug. 1988.

[9] A.-B. Witte *et al.*, “Differential effect of PYY1-36 and PYY3-36 on gastric emptying in man.,” *Regul. Pept.*, vol. 158, no. 1–3, pp. 57–62, Nov. 2009.

[10] R. L. Batterham *et al.*, “Inhibition of food intake in obese subjects by peptide YY3-36.,” *N. Engl. J. Med.*, vol. 349, no. 10, pp. 941–8, Sep. 2003.

[11] J. D. Huizinga, C. M. McKay, and E. J. White, “The many facets of intestinal peristalsis.,” *Am. J. Physiol. Gastrointest. Liver Physiol.*, vol. 290, no. 6, pp. G1347-9; author reply G1348-9, 2006.

[12] J. E. Kellow, T. J. Borody, S. F. Phillips, R. L. Tucker, and A. C. Haddad, “Human interdigestive motility: variations in patterns from esophagus to colon.,” *Gastroenterology*, vol. 91, no. 2, pp. 386–395, Aug. 1986.

[13] E. Husebye, “The patterns of small bowel motility: Physiology and implications in organic disease and functional disorders,” *Neurogastroenterol. Motil.*, vol. 11, no. 3, pp. 141–161, 1999.

[14] H. Seidl, F. Gundling, A. Pfeiffer, C. Pehl, W. Schepp, and T. Schmidt, “Comparison of small-bowel motility of the human jejunum and ileum.,” *Neurogastroenterol. Motil.*, vol. 24, no. 8, pp. e373--80, Aug. 2012.

[15] A. Dive, M. Moulart, P. Jonard, J. Jamart, and P. Mahieu, “Gastroduodenal motility in mechanically ventilated critically ill patients: a manometric study.,” *Crit. Care Med.*, vol. 22, no. 3, pp. 441–7, Mar. 1994.

[16] E. M. Quigley, “Gastric and small intestinal motility in health and disease.,” *Gastroenterol. Clin. North Am.*, vol. 25, no. 1, pp. 113–45, Mar. 1996.

[17] A. B. Thomson, M. Keelan, A. Thiesen, M. T. Clandinin, M. Ropeleski, and G. E. Wild, “Small bowel review: normal physiology part 1.,” *Dig. Dis. Sci.*, vol. 46, no. 12, pp. 2567–2587, Dec. 2001.

[18] A. B. Thomson, M. Keelan, A. Thiesen, M. T. Clandinin, M. Ropeleski, and G. E. Wild, “Small bowel review: normal physiology part 2.,” *Dig. Dis. Sci.*, vol. 46, no. 12, pp. 2588–2607, Dec. 2001.

[19] S. M. C. Edwin E. Daniel, *Comprehensive Physiology*. Hoboken, NJ, USA: John Wiley {&} Sons, Inc., 2010.

[20] G. Bassotti, M. Clementi, E. Antonelli, M. A. Pelli, and M. Tonini, "Low-amplitude propagated contractile waves: a relevant propulsive mechanism of human colon," *Dig. Liver Dis.*, vol. 33, no. 1, pp. 36–40, Feb. 2001.

[21] G. Bassotti and M. Gaburri, "Manometric investigation of high-amplitude propagated contractile activity of the human colon.," *Am. J. Physiol.*, vol. 255, no. 5 Pt 1, pp. G660-4, Nov. 1988.

[22] G. Basilisco and A. E. Bharucha, "High-resolution anorectal manometry: An expensive hobby or worth every penny?," *Neurogastroenterol. Motil.*, vol. 29, no. 8, p. e13125, Aug. 2017.

[23] l. kloetzer *et al.*, "Motility of the antroduodenum in healthy and gastroparetics characterized by wireless motility capsule," *Neurogastroenterol. Motil.*, vol. 22, no. 5, pp. 527-e117, Jan. 2010.

[24] D. Grønlund *et al.*, "Established and emerging methods for assessment of small and large intestinal motility," *Neurogastroenterol. Motil.*, vol. 29, no. 7, p. e13008, Jul. 2017.

[25] L. A. Szarka and M. Camilleri, "Methods for measurement of gastric motility," *AJP Gastrointest. Liver Physiol.*, vol. 296, no. 3, pp. G461--G475, Jan. 2009.

[26] L. A. Szarka and M. Camilleri, "Methods for the assessment of small-bowel and colonic transit.," *Semin. Nucl. Med.*, vol. 42, no. 2, pp. 113–123, Mar. 2012.

[27] A. E. Bharucha, M. Camilleri, E. Veil, D. Burton, and A. R. Zinsmeister, "Comprehensive assessment of gastric emptying with a stable isotope breath test.," *Neurogastroenterol. Motil.*, vol. 25, no. 1, pp. e60--9, Jan. 2013.

[28] A. Rezaie *et al.*, "Hydrogen and Methane-Based Breath Testing in Gastrointestinal Disorders: The North American Consensus," *Am. J. Gastroenterol.*, vol. 112, no. 5, pp. 775–784, May 2017.

[29] C. S. Yuan, J. F. Foss, J. Osinski, A. Toledano, M. F. Roizen, and J. Moss, "The safety and efficacy of oral methylnaltrexone in preventing morphine-induced delay in oral-cecal transit time.," *Clin. Pharmacol. Ther.*, vol. 61, no. 4, pp. 467–75, Apr. 1997.

[30] M. Hirakawa, M. Iida, N. Kohrogi, and M. Fujishima, "Hydrogen breath test assessment of orocecal transit time: comparison with barium meal study.," *Am. J. Gastroenterol.*, vol. 83, no. 12, pp. 1361–3, Dec. 1988.

[31] A. M. Metcalf, S. F. Phillips, A. R. Zinsmeister, R. L. MacCarty, R. W. Beart, and B. G. Wolff, "Simplified assessment of segmental colonic transit," *Gastroenterology*, vol. 92, no. 1, pp. 40–47, Jan. 1987.

[32] H. Abrahamsson, S. Antov, and I. Bosaeus, "Gastrointestinal and Colonic Segmental Transit Time Evaluated by a Single Abdominal X-ray in Healthy Subjects and Constipated Patients," *Scand. J. Gastroenterol.*, vol. 23, no. sup152, pp. 72–80, Jan. 1988.

[33] P. Grybäck, H. Jacobsson, L. Blomquist, P. O. Schnell, and P. M. Hellström, "Scintigraphy of the small intestine: a simplified standard for study of transit with reference to normal values.," *Eur. J. Nucl. Med. Mol. Imaging*, vol. 29, no. 1, pp. 39–45, Jan. 2002.

[34] M. R. von der Ohe, M. Camilleri, L. K. Kvols, and G. M. Thomforde, "Motor dysfunction of the small bowel and colon in patients with the carcinoid syndrome and diarrhea.," *N. Engl. J. Med.*, vol. 329, no. 15, pp. 1073–8, Oct. 1993.

[35] D. Carter, R. Eliakim, O. Har-Noy, S. Goldstein, E. Derazne, and E. Bardan, "PillCam small bowel capsule endoscopy gastric passage interval

association with patient's complaints and pathological findings," *Eur. J. Gastroenterol. Hepatol.*, vol. 26, no. 1, pp. 47–51, Jan. 2014.

[36] H. O. Diaz Tartera *et al.*, "Validation of SmartPill ® wireless motility capsule for gastrointestinal transit time: Intra-subject variability, software accuracy and comparison with video capsule endoscopy," *Neurogastroenterol. Motil.*, vol. 29, no. 10, p. e13107, Oct. 2017.

[37] S. Maqbool, H. P. Parkman, and F. K. Friedenberg, "Wireless Capsule Motility: Comparison of the SmartPill® GI Monitoring System with Scintigraphy for Measuring Whole Gut Transit," *Dig. Dis. Sci.*, vol. 54, no. 10, pp. 2167–2174, Oct. 2009.

[38] C. Malagelada *et al.*, "Functional gut disorders or disordered gut function? Small bowel dysmotility evidenced by an original technique," *Neurogastroenterol. Motil.*, vol. 24, no. 3, pp. 223-e105, Mar. 2012.

[39] L. Liu, S. Towfighian, and A. Hila, "A Review of Locomotion Systems for Capsule Endoscopy," *IEEE Rev. Biomed. Eng.*, vol. 8, pp. 138–151, 2015.

[40] M. Drozdzal, S. Seguí, J. Vitrià, C. Malagelada, F. Azpiroz, and P. Radeva, "Adaptable image cuts for motility inspection using WCE.," *Comput. Med. Imaging Graph.*, vol. 37, no. 1, pp. 72–80, Jan. 2013.

[41] W. L. Hasler, "The use of SmartPill for gastric monitoring," *Expert Rev. Gastroenterol. Hepatol.*, vol. 8, no. 6, pp. 587–600, Aug. 2014.

[42] R. J. Saad, "The Wireless Motility Capsule: a One-Stop Shop for the Evaluation of GI Motility Disorders.," *Curr. Gastroenterol. Rep.*, vol. 18, no. 3, p. 14, Mar. 2016.

[43] S. S. C. Rao *et al.*, "Investigation of colonic and whole-gut transit with wireless motility capsule and radiopaque markers in constipation.," *Clin. Gastroenterol. Hepatol.*, vol. 7, no. 5, pp. 537–44, May 2009.

[44] A. M. Haase *et al.*, "Pilot study trialling a new ambulatory method for the clinical assessment of regional gastrointestinal transit using multiple electromagnetic capsules," *Neurogastroenterol. Motil.*, vol. 26, no. 12, pp. 1783–1791, Dec. 2014.

[45] A.-M. Haase, S. Fallet, M. Otto, S. M. Scott, V. Schlageter, and K. Krogh, "Gastrointestinal motility during sleep assessed by tracking of telemetric capsules combined with polysomnography - a pilot study.," *Clin. Exp. Gastroenterol.*, vol. 8, pp. 327–32, 2015.

[46] J. L. Poulsen, M. Nilsson, C. Brock, T. H. Sandberg, K. Krogh, and A. M. Drewes, "The Impact of Opioid Treatment on Regional Gastrointestinal Transit.," *J. Neurogastroenterol. Motil.*, vol. 22, no. 2, pp. 282–91, Apr. 2016.

[47] T. Gregersen, A.-M. Haase, V. Schlageter, H. Gronbaek, and K. Krogh, "Regional Gastrointestinal Transit Times in Patients With Carcinoid Diarrhea: Assessment With the Novel 3D-Transit System.," *J. Neurogastroenterol. Motil.*, vol. 21, no. 3, pp. 423–32, Jul. 2015.

[48] A. M. Haase *et al.*, "Regional gastrointestinal transit times in severe ulcerative colitis," *Neurogastroenterol. Motil.*, vol. 28, no. 2, pp. 217–224, Feb. 2016.

[49] P. G. Dinning *et al.*, "Quantification of in vivo colonic motor patterns in healthy humans before and after a meal revealed by high-resolution fiber-optic manometry.," *Neurogastroenterol. Motil.*, vol. 26, no. 10, pp. 1443–1457, Oct. 2014.

[50] P. G. Dinning *et al.*, "Colonic motor abnormalities in slow transit constipation defined by high resolution, fibre-optic manometry.," *Neurogastroenterol. Motil.*, vol. 27, no. 3, pp. 379–388, Mar. 2015.

[51] J. S. Soh *et al.*, "The Diagnostic Value of a Digital Rectal Examination Compared With High-Resolution Anorectal Manometry in Patients With

Chronic Constipation and Fecal Incontinence," *Am. J. Gastroenterol.*, vol. 110, no. 8, pp. 1197–1204, Aug. 2015.

[52] S. N. Reddy *et al.*, "Colonic motility and transit in health and ulcerative colitis," *Gastroenterology*, vol. 101, no. 5, pp. 1289–1297, Nov. 1991.

[53] A. Panarese *et al.*, "Chronic functional constipation is strongly linked to vitamin D deficiency.," *World J. Gastroenterol.*, vol. 25, no. 14, pp. 1729–1740, Apr. 2019.

[54] A. Menys *et al.*, "A magnetic resonance imaging study of gastric motor function in patients with dyspepsia associated with Ehlers-Danlos Syndrome-Hypermobility Type: A feasibility study," *Neurogastroenterol. Motil.*, vol. 29, no. 9, p. e13090, Sep. 2017.

[55] R. De Giorgio, G. Sarnelli, R. Corinaldesi, and V. Stanghellini, "Advances in our understanding of the pathology of chronic intestinal pseudo-obstruction.," *Gut*, vol. 53, no. 11, pp. 1549–1552, Nov. 2004.

[56] G. Lindberg, H. Törnblom, M. Iwarzon, B. Nyberg, J. E. Martin, and B. Veress, "Full-thickness biopsy findings in chronic intestinal pseudo-obstruction and enteric dysmotility.," *Gut*, vol. 58, no. 8, pp. 1084–1090, Aug. 2009.

[57] A. Menys *et al.*, "Comparative quantitative assessment of global small bowel motility using magnetic resonance imaging in chronic intestinal pseudo-obstruction and healthy controls," *Neurogastroenterol. Motil.*, vol. 28, no. 3, pp. 376–383, Mar. 2016.

[58] H. Ohkubo *et al.*, "Assessment of small bowel motility in patients with chronic intestinal pseudo-obstruction using cine-MRI.," *Am. J. Gastroenterol.*, vol. 108, no. 7, pp. 1130–1139, Jul. 2013.

[59] A. Fuyuki *et al.*, "Clinical importance of cine-MRI assessment of small bowel motility in patients with chronic intestinal pseudo-obstruction: a retrospective study of 33 patients," *J. Gastroenterol.*, vol. 52, no. 5, pp. 577–584, May 2017.

[60] S. H. W. van Bree *et al.*, "Identification of clinical outcome measures for recovery of gastrointestinal motility in postoperative ileus.," *Ann. Surg.*, vol. 259, no. 4, pp. 708–714, Apr. 2014.

[61] P. Barone *et al.*, "The PRIAMO study: A multicenter assessment of nonmotor symptoms and their impact on quality of life in Parkinson's disease.," *Mov. Disord.*, vol. 24, no. 11, pp. 1641–1649, Aug. 2009.

[62] C. H. Hawkes, K. Del Tredici, and H. Braak, "Parkinson's disease: a dual-hit hypothesis.," *Neuropathol. Appl. Neurobiol.*, vol. 33, no. 6, pp. 599–614, Dec. 2007.

[63] H. Reichmann, A. D. Korczyn, and W. H. Jost, "Gastrointestinal dysfunction in Parkinson's Disease," *J. Neurol. Sci.*, vol. 289, no. 1, pp. 69–73, 2010.

[64] R. Savica *et al.*, "Medical records documentation of constipation preceding Parkinson disease: A case-control study.," *Neurology*, vol. 73, no. 21, pp. 1752–1758, Nov. 2009.

[65] A. Menys *et al.*, "Aberrant Motility in Unaffected Small Bowel is Linked to Inflammatory Burden and Patient Symptoms in Crohn's Disease," *Inflamm. Bowel Dis.*, vol. 22, no. 2, pp. 424–432, 2016.

[66] A. E. M'Koma, "Inflammatory bowel disease: an expanding global health problem.," *Clin. Med. Insights. Gastroenterol.*, vol. 6, pp. 33–47, 2013.

[67] A. Dignass *et al.*, "The second European evidence-based Consensus on the diagnosis and management of Crohn's disease: Current management.," *J. Crohn's {&} colitis*, vol. 4, no. 1, pp. 28–62, Mar. 2010.

[68] H. H. Shim, P. W. Chan, S. W. Chuah, B. J. Schwender, S. C. Kong, and K. L. Ling, "A review of vedolizumab and ustekinumab for the treatment of inflammatory bowel diseases," *JGH Open*, vol. 2, no. 5, pp. 223–234, Oct.

2018.
[69] G. D'Haens *et al.*, "Early combined immunosuppression or conventional management in patients with newly diagnosed Crohn's disease: an open randomised trial," *Lancet*, vol. 371, no. 9613, pp. 660–667, Feb. 2008.
[70] J. F. Colombel *et al.*, "Infliximab, Azathioprine, or Combination Therapy for Crohn's Disease," *N. Engl. J. Med.*, vol. 362, no. 15, pp. 1383–1395, Apr. 2010.
[71] J. Dretzke *et al.*, "A systematic review and economic evaluation of the use of tumour necrosis factor-alpha (TNF-$α$) inhibitors, adalimumab and infliximab, for Crohn's disease.," *Health Technol. Assess.*, vol. 15, no. 6, pp. 1–244, Feb. 2011.
[72] S. Ben-Horin and Y. Chowers, "Review article: loss of response to anti-TNF treatments in Crohn's disease.," *Aliment. Pharmacol. {&} Ther.*, vol. 33, no. 9, pp. 987–995, May 2011.
[73] M. del C. R-Grau *et al.*, "Effectiveness of anti-TNFα drugs in patients with Crohn's disease who do not achieve remission with their first anti-TNFα agent," *Dig. Liver Dis.*, vol. 48, no. 6, pp. 613–619, Jun. 2016.
[74] L. Peyrin-Biroulet, E. V Loftus, J.-F. Colombel, and W. J. Sandborn, "The natural history of adult Crohn's disease in population-based cohorts.," *Am. J. Gastroenterol.*, vol. 105, no. 2, pp. 289–297, Mar. 2010.
[75] E. F. Stange *et al.*, "European evidence based consensus on the diagnosis and management of Crohn's disease: definitions and diagnosis.," *Gut*, vol. 55 Suppl 1, pp. i1--15, Mar. 2006.
[76] P. Molander *et al.*, "Fecal calprotectin concentration predicts outcome in inflammatory bowel disease after induction therapy with TNFα blocking agents.," *Inflamm. Bowel Dis.*, vol. 18, no. 11, pp. 2011–7, Nov. 2012.
[77] R. J. Saad and W. L. Hasler, "A technical review and clinical assessment of the wireless motility capsule.," *Gastroenterol. {&} Hepatol.*, vol. 7, no. 12, pp. 795–804, Dec. 2011.
[78] D. J. M. Tolan, R. Greenhalgh, I. a Zealley, S. Halligan, and S. a Taylor, "MR enterographic manifestations of small bowel Crohn disease.," *Radiographics*, vol. 30, pp. 367–384, 2010.
[79] J. W. Berrill, J. T. Green, K. Hood, and A. K. Campbell, "Symptoms of irritable bowel syndrome in patients with inflammatory bowel disease: examining the role of sub-clinical inflammation and the impact on clinical assessment of disease activity," *Aliment. Pharmacol. Ther.*, vol. 38, no. 1, pp. 44–51, 2013.
[80] F. Farrokhyar, J. K. Marshall, B. Easterbrook, and E. J. Irvine, "Functional gastrointestinal disorders and mood disorders in patients with inactive inflammatory bowel disease: prevalence and impact on health.," *Inflamm. Bowel Dis.*, vol. 12, no. 1, pp. 38–46, Jan. 2006.
[81] A. C. M. Nóbrega *et al.*, "Dyspeptic symptoms and delayed gastric emptying of solids in patients with inactive Crohn's disease.," *BMC Gastroenterol.*, vol. 12, no. 1, p. 175, Jan. 2012.
[82] V. Annese *et al.*, "Gastric Emptying of Solids in Patients with Nonobstructive Crohn's Disease Is Sometimes Delayed," *J. Clin. Gastroenterol.*, vol. 21, no. 4, pp. 279–282, Dec. 1995.
[83] J. Keller, C. Beglinger, J. J. Holst, V. Andresen, and P. Layer, "Mechanisms of gastric emptying disturbances in chronic and acute inflammation of the distal gastrointestinal tract," *AJP Gastrointest. Liver Physiol.*, vol. 297, no. 5, pp. G861--G868, Aug. 2009.
[84] A. Tursi, G. Brandimarte, G. Giorgetti, and G. Nasi, "Assessment of orocaecal transit time in different localization of Crohn's disease and its possible influence on clinical response to therapy.," *Eur. J. Gastroenterol.*

*{&} Hepatol.*, vol. 15, no. 1, pp. 69–74, Jan. 2003.

[85] F. Castiglione *et al.*, "Orocecal Transit Time and Bacterial Overgrowth in Patients with Crohn's Disease," *J. Clin. Gastroenterol.*, vol. 31, no. 1, pp. 63–66, Jul. 2000.

[86] V. Annese, G. Bassotti, G. Napolitano, P. Usai, A. Andriulli, and G. Vantrappen, "Gastrointestinal Motility Disorders in Patients with Inactive Crohn's Disease," *Scand. J. Gastroenterol.*, vol. 32, no. 11, pp. 1107–1117, Jan. 1997.

[87] G. W. Moran, J. Pennock, and J. T. McLaughlin, "Enteroendocrine cells in terminal ileal Crohn's disease," *J. Crohn's Colitis*, vol. 6, no. 9, pp. 871–880, Oct. 2012.

[88] G. W. Moran, F. C. Leslie, and J. T. McLaughlin, "Crohn's disease affecting the small bowel is associated with reduced appetite and elevated levels of circulating gut peptides," *Clin. Nutr.*, vol. 32, no. 3, pp. 404–411, Jun. 2013.

[89] D. A. Drossman, "Functional Gastrointestinal Disorders: History, Pathophysiology, Clinical Features, and Rome IV," *Gastroenterology*, vol. 150, no. 6, pp. 1262-1279.e2, May 2016.

[90] S. J. Halpin and A. C. Ford, "Prevalence of Symptoms Meeting Criteria for Irritable Bowel Syndrome in Inflammatory Bowel Disease: Systematic Review and Meta-Analysis," *Am. J. Gastroenterol.*, vol. 107, no. 10, pp. 1474–1482, Oct. 2012.

[91] B. M. R. Spiegel *et al.*, "Measuring symptoms in the irritable bowel syndrome: development of a framework for clinical trials.," *Aliment. Pharmacol. {&} Ther.*, vol. 32, no. 10, pp. 1275–1291, Nov. 2010.

[92] D. A. Andrae, D. L. Patrick, D. A. Drossman, and P. S. Covington, "Evaluation of the Irritable Bowel Syndrome Quality of Life ( IBS-QOL ) questionnaire in diarrheal-predominant irritable bowel syndrome patients," pp. 1–12, 2013.

[93] M. Bengtsson, B. Ohlsson, and K. Ulander, "Development and psychometric testing of the Visual Analogue Scale for Irritable Bowel Syndrome (VAS-IBS)," *BMC Gastroenterol.*, vol. 7, no. 1, p. 16, Dec. 2007.

[94] M. Bengtsson, O. Hammar, T. Mandl, and B. Ohlsson, "Evaluation of gastrointestinal symptoms in different patient groups using the visual analogue scale for irritable bowel syndrome (VAS-IBS)," *BMC Gastroenterol.*, vol. 11, no. 1, p. 122, Dec. 2011.

[95] D. A. Drossman, "The Functional Gastrointestinal Disorders and the Rome III Process," *Gastroenterology*, vol. 130, no. 5, pp. 1377–1390, Apr. 2006.

[96] C. J. Bijkerk, N. J. de Wit, W. A. Stalman, J. A. Knottnerus, A. W. Hoes, and J. W. Muris, "Irritable Bowel Syndrome in Primary Care: The Patients' and Doctors' Views on Symptoms, Etiology and Management," *Can. J. Gastroenterol.*, vol. 17, no. 6, pp. 363–368, Jun. 2003.

[97] M. Dapoigny *et al.*, "Irritable bowel syndrome in France: a common, debilitating and costly disorder.," *Eur. J. Gastroenterol. Hepatol.*, vol. 16, no. 10, pp. 995–1001, Oct. 2004.

[98] G. R. Locke, B. P. Yawn, P. C. Wollan, L. J. Melton, E. Lydick, and N. J. Talley, "Incidence of a clinical diagnosis of the irritable bowel syndrome in a United States population," *Aliment. Pharmacol. Ther.*, vol. 19, no. 9, pp. 1025–1031, May 2004.

[99] A. Agrawal, L. A. Houghton, B. Reilly, J. Morris, and P. J. Whorwell, "Bloating and Distension in Irritable Bowel Syndrome: The Role of Gastrointestinal Transit," *Am. J. Gastroenterol.*, vol. 104, no. 8, pp. 1998–2004, Aug. 2009.

[100] R. Undseth, A. Berstad, N.-E. Kløw, K. Arnljot, K. S. Moi, and J. Valeur, "Abnormal accumulation of intestinal fluid following ingestion of an unabsorbable carbohydrate in patients with irritable bowel syndrome: an

MRI study.," *Neurogastroenterol. Motil.*, vol. 26, no. 12, pp. 1686–93, Dec. 2014.

[101] J. Serra, F. Azpiroz, and J. R. Malagelada, "Impaired transit and tolerance of intestinal gas in the irritable bowel syndrome.," *Gut*, vol. 48, no. 1, pp. 14–9, Jan. 2001.

[102] J. Ritchie, "Pain from distension of the pelvic colon by inflating a balloon in the irritable colon syndrome.," *Gut*, vol. 14, no. 2, pp. 125–32, Feb. 1973.

[103] K. C. Trimble, R. Farouk, A. Pryde, S. Douglas, and R. C. Heading, "Heightened visceral sensation in functional gastrointestinal disease is not site-specific," *Dig. Dis. Sci.*, vol. 40, no. 8, pp. 1607–1613, Aug. 1995.

[104] M. Simrén *et al.*, "Visceral hypersensitivity is associated with GI symptom severity in functional GI disorders: consistent findings from five different patient cohorts," *Gut*, vol. 67, no. 2, pp. 255–262, Feb. 2018.

[105] L. Bueno, J. Fioramonti, M. Delvaux, and J. Frexinos, "Mediators and pharmacology of visceral sensitivity: From basic to clinical investigations," *Gastroenterology*, vol. 112, no. 5, pp. 1714–1743, May 1997.

[106] S. V Coutinho, X. Su, J. N. Sengupta, and G. F. Gebhart, "Role of sensitized pelvic nerve afferents from the inflamed rat colon in the maintenance of visceral hyperalgesia.," *Prog. Brain Res.*, vol. 129, pp. 375–87, 2000.

[107] H. E. Torebjörk, L. E. Lundberg, and R. H. LaMotte, "Central changes in processing of mechanoreceptive input in capsaicin-induced secondary hyperalgesia in humans.," *J. Physiol.*, vol. 448, no. 1, pp. 765–80, Mar. 1992.

[108] R. D. Treede, R. A. Meyer, S. N. Raja, and J. N. Campbell, "Peripheral and central mechanisms of cutaneous hyperalgesia.," *Prog. Neurobiol.*, vol. 38, no. 4, pp. 397–421, 1992.

[109] D. Silverman, J. Munakata, H. Ennes, M. Mandelkern, C. Hoh, and E. Mayer, "Regional cerebral activity in normal and pathological perception of visceral pain," *Gastroenterology*, vol. 112, no. 1, pp. 64–72, Jan. 1997.

[110] H. Mertz *et al.*, "Regional cerebral activation in irritable bowel syndrome and control subjects with painful and nonpainful rectal distention," *Gastroenterology*, vol. 118, no. 5, pp. 842–848, May 2000.

[111] B. Bonaz *et al.*, "Central processing of rectal pain in patients with irritable bowel syndrome: an fMRI study.," *Am. J. Gastroenterol.*, vol. 97, no. 3, pp. 654–61, Mar. 2002.

[112] G. Barbara, R. De Giorgio, V. Stanghellini, C. Cremon, and R. Corinaldesi, "A role for inflammation in irritable bowel syndrome?," *Gut*, vol. 51, no. Supplement 1, pp. i41–i44, Jul. 2002.

[113] G. Barbara *et al.*, "The Immune System in Irritable Bowel Syndrome," *J. Neurogastroenterol. Motil.*, vol. 17, no. 4, pp. 349–359, Oct. 2011.

[114] S. P. Dunlop *et al.*, "Randomized, double-blind, placebo-controlled trial of prednisolone in post-infectious irritable bowel syndrome.," *Aliment. Pharmacol. Ther.*, vol. 18, no. 1, pp. 77–84, Jul. 2003.

[115] G. Barbara *et al.*, "The Intestinal Microenvironment and Functional Gastrointestinal Disorders," *Gastroenterology*, vol. 150, no. 6, pp. 1305-1318.e8, May 2016.

[116] F. Scaldaferri, M. Pizzoferrato, V. Gerardi, L. Lopetuso, and A. Gasbarrini, "The gut barrier: new acquisitions and therapeutic approaches.," *J. Clin. Gastroenterol.*, vol. 46 Suppl, pp. S12-7, Oct. 2012.

[117] L. Öhman, H. Törnblom, and M. Simrén, "Crosstalk at the mucosal border: importance of the gut microenvironment in IBS.," *Nat. Rev. Gastroenterol. Hepatol.*, vol. 12, no. 1, pp. 36–49, Jan. 2015.

[118] m. camilleri and h. gorman, "Intestinal permeability and irritable bowel syndrome," *Neurogastroenterol. Motil.*, vol. 19, no. 7, pp. 545–552, Jul.

2007.
[119] G. Barbara *et al.*, "Mucosal permeability and immune activation as potential therapeutic targets of probiotics in irritable bowel syndrome.," *J. Clin. Gastroenterol.*, vol. 46 Suppl, pp. S52-5, Oct. 2012.
[120] L. Van Oudenhove *et al.*, "Biopsychosocial Aspects of Functional Gastrointestinal Disorders: How Central and Environmental Processes Contribute to the Development and Expression of Functional Gastrointestinal Disorders," *Gastroenterology*, vol. 150, no. 6, pp. 1355-1367.e2, May 2016.
[121] O. Bednarska *et al.*, "Vasoactive Intestinal Polypeptide and Mast Cells Regulate Increased Passage of Colonic Bacteria in Patients With Irritable Bowel Syndrome," *Gastroenterology*, vol. 153, no. 4, pp. 948-960.e3, Oct. 2017.
[122] J. Tap *et al.*, "Identification of an Intestinal Microbiota Signature Associated With Severity of Irritable Bowel Syndrome," *Gastroenterology*, vol. 152, no. 1, pp. 111-123.e8, Jan. 2017.
[123] A. D. Farmer, S. D. Mohammed, G. E. Dukes, S. M. Scott, and A. R. Hobson, "Caecal pH is a biomarker of excessive colonic fermentation.," *World J. Gastroenterol.*, vol. 20, no. 17, pp. 5000–7, May 2014.
[124] T. Ringel-Kulka *et al.*, "Altered Colonic Bacterial Fermentation as a Potential Pathophysiological Factor in Irritable Bowel Syndrome.," *Am. J. Gastroenterol.*, vol. 110, no. 9, pp. 1339–46, Sep. 2015.
[125] J. Keller and P. Layer, "Intestinal and anorectal motility and functional disorders.," *Best Pract. {&} Res. Clin. Gastroenterol.*, vol. 23, no. 3, pp. 407–423, Jan. 2009.
[126] K. Ravi, A. E. Bharucha, M. Camilleri, D. Rhoten, T. Bakken, and A. R. Zinsmeister, "Phenotypic variation of colonic motor functions in chronic constipation.," *Gastroenterology*, vol. 138, no. 1, pp. 89–97, Jan. 2010.
[127] L. Wiklendt, S. D. Mohammed, S. M. Scott, and P. G. Dinning, "Classification of normal and abnormal colonic motility based on cross-correlations of pancolonic manometry data.," *Neurogastroenterol. Motil.*, vol. 25, no. 3, pp. e215--23, Mar. 2013.
[128] J. E. Kellow, R. C. Gill, and D. L. Wingate, "Prolonged ambulant recordings of small bowel motility demonstrate abnormalities in the irritable bowel syndrome.," *Gastroenterology*, vol. 98, no. 5 Pt 1, pp. 1208–1218, May 1990.
[129] H. C. Lin, "Small intestinal bacterial overgrowth: a framework for understanding irritable bowel syndrome.," *JAMA*, vol. 292, no. 7, pp. 852–858, Aug. 2004.
[130] M. Pimentel, E. E. Soffer, E. J. Chow, Y. Kong, and H. C. Lin, "Lower frequency of MMC is found in IBS subjects with abnormal lactulose breath test, suggesting bacterial overgrowth.," *Dig. Dis. Sci.*, vol. 47, no. 12, pp. 2639–2643, Dec. 2002.
[131] J. Serra *et al.*, "Impaired intestinal gas propulsion in manometrically proven dysmotility and in irritable bowel syndrome.," *Neurogastroenterol. Motil.*, vol. 22, no. 4, pp. 401--6, e91--2, Apr. 2010.
[132] n. manabe, b. s. wong, m. camilleri, d. burton, s. mckinzie, and a. r. zinsmeister, "Lower functional gastrointestinal disorders: evidence of abnormal colonic transit in a 287 patient cohort," *Neurogastroenterol. Motil.*, vol. 22, no. 3, pp. 293-e82, Mar. 2010.
[133] H. Törnblom, L. Van Oudenhove, R. Sadik, H. Abrahamsson, J. Tack, and M. Simrén, "Colonic Transit Time and IBS Symptoms: What's the Link?," *Am. J. Gastroenterol.*, vol. 107, no. 5, pp. 754–760, May 2012.
[134] J. C. Makanyanga *et al.*, "Evaluation of Crohn's disease activity: Initial

validation of a magnetic resonance enterography global score (MEGS) against faecal calprotectin," *Eur. Radiol.*, vol. 24, no. 2, pp. 277–287, Feb. 2014.

[135] A. K. Shergill *et al.*, "The role of endoscopy in inflammatory bowel disease," *Gastrointest. Endosc.*, vol. 81, pp. 1101-1121.e13, 2015.

[136] F. Casellas *et al.*, "Mucosal healing restores normal health and quality of life in patients with inflammatory bowel disease.," *Eur. J. Gastroenterol. {&} Hepatol.*, vol. 24, no. 7, pp. 762–769, Jul. 2012.

[137] M. Simrén and J. Tack, "New treatments and therapeutic targets for IBS and other functional bowel disorders," *Nat. Rev. Gastroenterol. Hepatol.*, vol. 15, no. 10, pp. 589–605, Oct. 2018.

[138] R. Harvery and J. Bradshaw, "A simple index of Crohn's-disease activity.," *Lancet*, vol. 315, no. 8167, p. 514, 1980.

[139] "How to do your Harvey Bradshaw Index Information for patients."

[140] C. Y. FRANCIS, J. MORRIS, and P. J. WHORWELL, "The irritable bowel severity scoring system: a simple method of monitoring irritable bowel syndrome and its progress," *Aliment. Pharmacol. {&} Ther.*, vol. 11, no. 2, pp. 395–402, Apr. 1997.

[141] D. W. McRobbie, E. A. Moore, M. J. Graves, and M. R. Prince, *MRI from Picture to Proton*. Cambridge University Press, 2003.

[142] R. K.-S. Kwan, A. C. Evans, and G. B. Pike, "MRI simulation-based evaluation of image-processing and classification methods," *IEEE Trans. Med. Imaging*, vol. 18, no. 11, pp. 1085–1097, 1999.

[143] K. Shmueli, "MRI & Biomedical Optics MRes Lecture series." University College London, London, 2015.

[144] O. Bieri and K. Scheffler, "Fundamentals of balanced steady state free precession MRI," *J. Magn. Reson. Imaging*, vol. 38, no. 1, pp. 2–11, Jul. 2013.

[145] T.-Y. Huang, I.-J. Huang, C.-Y. Chen, K. Scheffler, H.-W. Chung, and H.-C. Cheng, "Are TrueFISP images T2/T1-weighted?," *Magn. Reson. Med.*, vol. 48, no. 4, pp. 684–8, Oct. 2002.

[146] K. Scheffler and J. Hennig, "Is TrueFISP a gradient-echo or a spin-echo sequence?," *Magn. Reson. Med.*, vol. 49, no. 2, pp. 395–397, Feb. 2003.

[147] H. Y. Carr, "Steady-State Free Precession in Nuclear Magnetic Resonance," *Phys. Rev.*, vol. 112, no. 5, pp. 1693–1701, Dec. 1958.

[148] G. B. Chavhan, P. S. Babyn, B. G. Jankharia, H.-L. M. Cheng, and M. M. Shroff, "Steady-state MR imaging sequences: physics, classification, and clinical applications.," *Radiographics*, vol. 28, no. 4, pp. 1147–60, Jul. 2008.

[149] B. Hargreaves, "Rapid gradient-echo imaging," *J. Magn. Reson. Imaging*, vol. 36, no. 6, pp. 1300–1313, Dec. 2012.

[150] E. H. Botvinick, "Current methods of pharmacologic stress testing and the potential advantages of new agents.," *J. Nucl. Med. Technol.*, vol. 37, no. 1, pp. 14–25, Mar. 2009.

[151] C. S. de Jonge, A. Menys, K. L. van Rijn, A. J. Bredenoord, A. J. Nederveen, and J. Stoker, "Detecting the effects of a standardized meal challenge on small bowel motility with MRI in prepared and unprepared bowel," *Neurogastroenterol. Motil.*, vol. 31, no. 2, p. e13506, Feb. 2019.

[152] K. Schunk *et al.*, "Hydro-MRI in Crohn's disease: appraisal of disease activity.," *Invest. Radiol.*, vol. 35, no. 7, pp. 431–437, Jul. 2000.

[153] S. A. Taylor *et al.*, "The first joint ESGAR/ ESPR consensus statement on the technical performance of cross-sectional small bowel and colonic imaging," *Eur. Radiol.*, vol. 27, no. 6, pp. 2570–2582, Jun. 2017.

[154] M. A. Griswold *et al.*, "Generalized autocalibrating partially parallel acquisitions (GRAPPA)," *Magn. Reson. Med.*, vol. 47, no. 6, pp. 1202–1210,

Jun. 2002.
[155] K. P. Pruessmann, M. Weiger, M. B. Scheidegger, and P. Boesiger, “SENSE: sensitivity encoding for fast MRI.,” *Magn. Reson. Med.*, vol. 42, no. 5, pp. 952–62, Nov. 1999.
[156] C. S. de Jonge *et al.*, “Evaluation of compressed sensing MRI for accelerated bowel motility imaging,” *Eur. Radiol. Exp.*, vol. 3, no. 1, p. 7, Dec. 2019.
[157] M. Barth, F. Breuer, P. J. Koopmans, D. G. Norris, and B. A. Poser, “Simultaneous multislice (SMS) imaging techniques,” *Magn. Reson. Med.*, vol. 75, no. 1, pp. 63–81, Jan. 2016.
[158] C. S. de Jonge, A. J. P. M. Smout, A. J. Nederveen, and J. Stoker, “Evaluation of gastrointestinal motility with MRI: Advances, challenges and opportunities,” *Neurogastroenterol. Motil.*, vol. 30, no. 1, p. e13257, Jan. 2018.
[159] A. Menys, A. Plumb, D. Atkinson, and S. A. Taylor, “The challenge of segmental small bowel motility quantitation using MR enterography.,” *Br. J. Radiol.*, vol. 87, no. 1040, Aug. 2014.
[160] P. M. Ghobrial *et al.*, “Cine MR enterography grading of small bowel peristalsis: evaluation of the antiperistaltic effectiveness of sublingual hyoscyamine sulfate.,” *Acad. Radiol.*, vol. 21, no. 1, pp. 86–91, Jan. 2014.
[161] A. Menys *et al.*, “Global Small Bowel Motility: Assessment with Dynamic MR Imaging,” Nov. 2013.
[162] S. E. Pritchard *et al.*, “Assessment of motion of colonic contents in the human colon using MRI tagging,” *Neurogastroenterol. Motil.*, vol. 29, no. 9, p. e13091, Sep. 2017.
[163] F. F. Guglielmo *et al.*, “Identifying decreased peristalsis of abnormal small bowel segments in Crohn’s disease using cine MR enterography: the frozen bowel sign.,” *Abdom. Imaging*, Oct. 2014.
[164] Y. Kitazume, S. Satoh, H. Hosoi, O. Noguchi, and H. Shibuya, “Cine magnetic resonance imaging evaluation of peristalsis of small bowel with longitudinal ulcer in Crohn disease: preliminary results.,” *J. Comput. Assist. Tomogr.*, vol. 31, no. 6, pp. 876–83, Nov. 2007.
[165] T. Heye, D. Stein, D. Antolovic, M. Dueck, H.-U. Kauczor, and W. Hosch, “Evaluation of bowel peristalsis by dynamic cine MRI: detection of relevant functional disturbances--initial experience.,” *J. Magn. Reson. Imaging*, vol. 35, no. 4, pp. 859–867, Apr. 2012.
[166] M. Wakamiya, A. Furukawa, S. Kanasaki, and K. Murata, “Assessment of small bowel motility function with cine-MRI using balanced steady-state free precession sequence.,” *J. Magn. Reson. Imaging*, vol. 33, no. 5, pp. 1235–1240, May 2011.
[167] S. Bickelhaupt *et al.*, “Software-assisted quantitative analysis of small bowel motility compared to manual measurements,” *Clin. Radiol.*, vol. 69, no. 4, pp. 363–371, Apr. 2014.
[168] S. Bickelhaupt *et al.*, “Automatic detection of small bowel contraction frequencies in motility plots using lomb-scargle periodogram and sinus-fitting method-initial experience.,” *Magn. Reson. Med.*, Mar. 2013.
[169] S. Bickelhaupt *et al.*, “Crohn’s disease: small bowel motility impairment correlates with inflammatory-related markers C-reactive protein and calprotectin.,” *Neurogastroenterol. Motil.*, vol. 25, no. 6, pp. 467–473, Jun. 2013.
[170] J. L. Cullmann *et al.*, “MR imaging in Crohn’s disease: correlation of MR motility measurement with histopathology in the terminal ileum.,” *Neurogastroenterol. Motil.*, vol. 25, no. 9, pp. 749--e577, Sep. 2013.
[171] S. Bickelhaupt *et al.*, “Differentiation between active and chronic Crohn’s

disease using MRI small-bowel motility examinations — Initial experience," *Clin. Radiol.*, vol. 68, no. 12, pp. 1247–1253, 2013.

[172] S. Bickelhaupt, M. Wurnig, A. Boss, and M. A. Patak, "Correlation between morphological expansion and impairment of intra- and prelesionary motility in inflammatory small bowel lesions in patients with Crohn's disease - preliminary data.," *Eur. J. Radiol.*, vol. 83, no. 7, pp. 1044–1050, Jul. 2014.

[173] S. Bickelhaupt *et al.*, "Software-supported evaluation of gastric motility in MRI: a feasibility study.," *J. Med. Imaging Radiat. Oncol.*, vol. 58, no. 1, pp. 11–7, Feb. 2014.

[174] M. A. Kwiatek *et al.*, "Quantification of distal antral contractile motility in healthy human stomach with magnetic resonance imaging.," *J. Magn. Reson. Imaging*, vol. 24, no. 5, pp. 1101–9, Nov. 2006.

[175] M. M. Unger *et al.*, "Real-time visualization of altered gastric motility by magnetic resonance imaging in patients with Parkinson's disease.," *Mov. Disord.*, vol. 25, no. 5, pp. 623–628, Apr. 2010.

[176] S. Kirchhoff, M. Nicolaus, J. Schirra, M. F. Reiser, B. Göke, and A. Lienemann, "Assessment of colon motility using simultaneous manometric and functional cine-MRI analysis: preliminary results.," *Abdom. Imaging*, vol. 36, no. 1, pp. 24–30, Feb. 2011.

[177] J. M. Froehlich, M. Daenzer, C. von Weymarn, S. M. Erturk, C. L. Zollikofer, and M. A. Patak, "Aperistaltic effect of hyoscine N-butylbromide versus glucagon on the small bowel assessed by magnetic resonance imaging.," *Eur. Radiol.*, vol. 19, no. 6, pp. 1387–1393, Jun. 2009.

[178] A. Gutzeit *et al.*, "Evaluation of the anti-peristaltic effect of glucagon and hyoscine on the small bowel: comparison of intravenous and intramuscular drug administration.," *Eur. Radiol.*, vol. 22, no. 6, pp. 1186–1194, Jun. 2012.

[179] A. Menys *et al.*, "Spatio-temporal motility MRI analysis of the stomach and colon," *Neurogastroenterol. Motil.*, vol. 31, no. 5, p. e13557, May 2019.

[180] A. M. J. Sprengers *et al.*, "Use of continuously MR tagged imaging for automated motion assessment in the abdomen: A feasibility study.," *J. Magn. Reson. Imaging*, vol. 36, no. 2, pp. 492–497, 2012.

[181] M. P. van der Paardt, A. M. J. Sprengers, F. M. Zijta, R. Lamerichs, A. J. Nederveen, and J. Stoker, "Noninvasive automated motion assessment of intestinal motility by continuously tagged MR imaging.," *J. Magn. Reson. Imaging*, vol. 39, no. 1, pp. 9–16, Jan. 2014.

[182] J. V. Hajnal, D. L. G. Hill, and D. L. G. Hill, *Medical Image Registration*. CRC Press, 2001.

[183] J. B. A. Maintz and M. A. Viergever, "A survey of medical image registration," *Med. Image Anal.*, vol. 2, no. 1, pp. 1–36, Mar. 1998.

[184] B. Zitová and J. Flusser, "Image registration methods: a survey," *Image Vis. Comput.*, vol. 21, no. 11, pp. 977–1000, Oct. 2003.

[185] W. R. Crum, T. Hartkens, and D. L. G. Hill, "Non-rigid image registration: theory and practice," *Br. J. Radiol.*, vol. 77, no. suppl{_}2, pp. S140--S153, Dec. 2004.

[186] W. M. Wells, P. Viola, H. Atsumi, S. Nakajima, and R. Kikinis, "Multi-modal volume registration by maximization of mutual information," *Med. Image Anal.*, vol. 1, no. 1, pp. 35–51, Mar. 1996.

[187] J. P. W. Pluim, J. B. A. Maintz, and M. A. Viergever, "Mutual-information-based registration of medical images: a survey.," *IEEE Trans. Med. Imaging*, vol. 22, no. 8, pp. 986–1004, Aug. 2003.

[188] C. Studholme, D. L. G. Hill, and D. J. Hawkes, "An overlap invariant entropy measure of 3D medical image alignment," *Pattern Recognit.*, vol. 32, no. 1,

pp. 71–86, Jan. 1999.
[189] D. Rueckert, L. I. Sonoda, C. Hayes, D. L. G. Hill, M. O. Leach, and D. J. Hawkes, “Nonrigid registration using free-form deformations: application to breast MR images,” *IEEE Trans. Med. Imaging*, vol. 18, no. 8, pp. 712–721, Aug. 1999.
[190] B. K. P. Horn and B. G. Schunck, “Determining optical flow,” *Artif. Intell.*, vol. 17, no. 1–3, pp. 185–203, Aug. 1981.
[191] G. Hermosillo, C. Chefd’Hotel, and O. Faugeras, “Variational Methods for Multimodal Image Matching,” *Int. J. Comput. Vis.*, vol. 50, no. 3, pp. 329–343, 2002.
[192] F. Odille, A. Menys, A. Ahmed, S. Punwani, S. A. Taylor, and D. Atkinson, “Quantitative assessment of small bowel motility by nonrigid registration of dynamic MR images.,” *Magn. Reson. Med.*, vol. 68, no. 3, pp. 783–793, Sep. 2012.
[193] C. Studholme, C. Drapaca, B. Iordanova, and V. Cardenas, “Deformation-based mapping of volume change from serial brain MRI in the presence of local tissue contrast change.,” *IEEE Trans. Med. Imaging*, vol. 25, no. 5, pp. 626–39, May 2006.
[194] S. Klein, U. A. van der Heide, I. M. Lips, M. van Vulpen, M. Staring, and J. P. W. Pluim, “Automatic segmentation of the prostate in 3D MR images by atlas matching using localized mutual information.,” *Med. Phys.*, vol. 35, no. 4, pp. 1407–17, Apr. 2008.
[195] D. Loeckx, P. Slagmolen, F. Maes, D. Vandermeulen, and P. Suetens, “Nonrigid Image Registration Using Conditional Mutual Information,” *IEEE Trans. Med. Imaging*, vol. 29, no. 1, pp. 19–29, Jan. 2010.
[196] X. Zhuang, S. Arridge, D. J. Hawkes, and S. Ourselin, “A nonrigid registration framework using spatially encoded mutual information and free-form deformations.,” *IEEE Trans. Med. Imaging*, vol. 30, no. 10, pp. 1819–28, Oct. 2011.
[197] G. Hermosillo and O. Faugeras, “Dense image matching with global and local statistical criteria: a variational approach,” in *Proceedings of the 2001 IEEE Computer Society Conference on Computer Vision and Pattern Recognition. CVPR 2001*, vol. 1, pp. I-73-I–78.
[198] A. Åkerman *et al.*, “Computational postprocessing quantification of small bowel motility using magnetic resonance images in clinical practice: An initial experience.,” *J. Magn. Reson. Imaging*, Jan. 2016.
[199] A. Menys *et al.*, “Quantified terminal ileal motility during MR enterography as a potential biomarker of Crohn’s disease activity: a preliminary study.,” *Eur. Radiol.*, vol. 22, no. 11, pp. 2494–2501, Nov. 2012.
[200] N. Saeed and B. K. Puri, “Cerebellum segmentation employing texture properties and knowledge based image processing: applied to normal adult controls and patients.,” *Magn. Reson. Imaging*, vol. 20, no. 5, pp. 425–9, Jun. 2002.
[201] R. Pérez de Alejo *et al.*, “Computer-assisted enhanced volumetric segmentation magnetic resonance imaging data using a mixture of artificial neural networks.,” *Magn. Reson. Imaging*, vol. 21, no. 8, pp. 901–12, Oct. 2003.
[202] G. Castellano, L. Bonilha, L. M. Li, and F. Cendes, “Texture analysis of medical images,” *Clin. Radiol.*, vol. 59, no. 12, pp. 1061–1069, Dec. 2004.
[203] S. Herlidou, Y. Rolland, J. Y. Bansard, E. Le Rumeur, and J. D. de Certaines, “Comparison of automated and visual texture analysis in MRI: characterization of normal and diseased skeletal muscle.,” *Magn. Reson. Imaging*, vol. 17, no. 9, pp. 1393–7, Nov. 1999.
[204] J. M. Mathias, P. S. Tofts, and N. A. Losseff, “Texture analysis of spinal cord

pathology in multiple sclerosis.," *Magn. Reson. Med.*, vol. 42, no. 5, pp. 929–35, Nov. 1999.
[205] V. A. Kovalev, M. Petrou, and Y. S. Bondar, "Texture anisotropy in 3-D images," *IEEE Trans. Image Process.*, vol. 8, no. 3, pp. 346–360, Mar. 1999.
[206] S. Herlidou-Même *et al.*, "MRI texture analysis on texture test objects, normal brain and intracranial tumors.," *Magn. Reson. Imaging*, vol. 21, no. 9, pp. 989–93, Nov. 2003.
[207] D. Mahmoud-Ghoneim, G. Toussaint, J. M. Constans, and J. D. de Certaines, "Three dimensional texture analysis in MRI: a preliminary evaluation in gliomas.," *Magn. Reson. Imaging*, vol. 21, no. 9, pp. 983–7, Nov. 2003.
[208] V. A. Kovalev, F. Kruggel, H.-J. Gertz, and D. Y. von Cramon, "Three-dimensional texture analysis of MRI brain datasets," *IEEE Trans. Med. Imaging*, vol. 20, no. 5, pp. 424–433, May 2001.
[209] A. Bernasconi *et al.*, "Texture analysis and morphological processing of magnetic resonance imaging assist detection of focal cortical dysplasia in extra-temporal partial epilepsy.," *Ann. Neurol.*, vol. 49, no. 6, pp. 770–5, Jun. 2001.
[210] S. B. Antel *et al.*, "Computational models of MRI characteristics of focal cortical dysplasia improve lesion detection.," *Neuroimage*, vol. 17, no. 4, pp. 1755–60, Dec. 2002.
[211] S. B. Antel *et al.*, "Automated detection of focal cortical dysplasia lesions using computational models of their MRI characteristics and texture analysis.," *Neuroimage*, vol. 19, no. 4, pp. 1748–59, Aug. 2003.
[212] L. Bonilha *et al.*, "Texture Analysis of Hippocampal Sclerosis," *Epilepsia*, vol. 44, no. 12, pp. 1546–1550, Dec. 2003.
[213] G. R. C. Caselato *et al.*, "Hippocampal texture analysis in patients with familial mesial temporal lobe epilepsy.," *Arq. Neuropsiquiatr.*, vol. 61 Suppl 1, pp. 83–7, Sep. 2003.
[214] O. Yu, Y. Mauss, I. J. Namer, and J. Chambron, "Existence of contralateral abnormalities revealed by texture analysis in unilateral intractable hippocampal epilepsy.," *Magn. Reson. Imaging*, vol. 19, no. 10, pp. 1305–10, Dec. 2001.
[215] K. Jafari-Khouzani, M.-R. Siadat, H. Soltanian-Zadeh, and K. Elisevich, "Texture analysis of hippocampus for epilepsy," 2003, vol. 5031, p. 279.
[216] Q. Ji, J. Engel, and E. Craine, "Texture analysis for classification of cervix lesions," *IEEE Trans. Med. Imaging*, vol. 19, no. 11, pp. 1144–1149, Nov. 2000.
[217] F. Chabat, G.-Z. Yang, and D. M. Hansell, "Obstructive lung diseases: texture classification for differentiation at CT.," *Radiology*, vol. 228, no. 3, pp. 871–7, Sep. 2003.
[218] M. Hall-Beyer, "GLCM texture: A tutorial v. 3.0 March 2017," 2017.
[219] M. M. Galloway and M. M., "Texture analysis using grey level run lengths," *Unknown*, vol. 75, 1974.
[220] R. M. Haralick, K. Shanmugam, and I. Dinstein, "Textural Features for Image Classification," *IEEE Trans. Syst. Man. Cybern.*, vol. SMC-3, no. 6, pp. 610–621, Nov. 1973.
[221] R. P. Kruger, W. B. Thompson, and A. F. Turner, "Computer Diagnosis of Pneumoconiosis," *IEEE Trans. Syst. Man. Cybern.*, vol. SMC-4, no. 1, pp. 40–49, 1974.
[222] MATLAB, "Texture Analysis - MATLAB {&} Simulink." 2016.
[223] J. M. Froehlich, C. Waldherr, C. Stoupis, S. M. Erturk, and M. A. Patak, "MR motility imaging in Crohn's disease improves lesion detection compared with standard MR imaging.," *Eur. Radiol.*, vol. 20, no. 8, pp. 1945–1951,

Aug. 2010.
[224] A. M. J. Sprengers *et al.*, “Use of continuously MR tagged imaging for automated motion assessment in the abdomen: a feasibility study.,” *J. Magn. Reson. Imaging*, vol. 36, no. 2, pp. 492–497, Aug. 2012.
[225] M. L. Hahnemann *et al.*, “Quantitative assessment of small bowel motility in patients with Crohn’s disease using dynamic MRI.,” *Neurogastroenterol. Motil.*, vol. 27, no. 6, pp. 841–848, Jun. 2015.
[226] A. Menys *et al.*, “Dual registration of abdominal motion for motility assessment in free-breathing data sets acquired using dynamic MRI.,” *Phys. Med. Biol.*, vol. 59, no. 16, pp. 4603–4619, Aug. 2014.
[227] V. Hamy *et al.*, “Respiratory motion correction in dynamic MRI using robust data decomposition registration - application to DCE-MRI.,” *Med. Image Anal.*, vol. 18, no. 2, pp. 301–313, Feb. 2014.
[228] A. Khalaf *et al.*, “Cine MRI assessment of motility in the unprepared small bowel in the fasting and fed state: Beyond the breath-hold,” *Neurogastroenterol. Motil.*, p. e13466, Sep. 2018.
[229] C. S. de Jonge, A. Menys, K. L. van Rijn, A. J. Bredenoord, A. J. Nederveen, and J. Stoker, “Detecting the effects of a standardized meal challenge on small bowel motility with MRI in prepared and unprepared bowel.,” *Neurogastroenterol. Motil.*, vol. 31, no. 2, p. e13506, Feb. 2019.
[230] A. Khalaf *et al.*, “MRI assessment of the postprandial gastrointestinal motility and peptide response in healthy humans,” *Neurogastroenterol. Motil.*, vol. 30, no. 1, p. e13182, Jan. 2018.
[231] W. J. Sandborn *et al.*, “A review of activity indices and efficacy endpoints for clinical trials of medical therapy in adults with Crohn’s disease.,” *Gastroenterology*, vol. 122, no. 2, pp. 512–530, Feb. 2002.
[232] C. A. J. Puylaert *et al.*, “Semiautomatic Assessment of the Terminal Ileum and Colon in Patients with Crohn Disease Using MRI (the VIGOR++ Project),” *Acad. Radiol.*, vol. 25, no. 8, pp. 1038–1045, Aug. 2018.
[233] S. K. Sarna *et al.*, “Spatial and temporal patterns of human jejunal contractions.,” *Am. J. Physiol.*, vol. 257, no. 3 Pt 1, pp. G423--32, Sep. 1989.
[234] E. E. Soffer and T. E. Adrian, “Effect of meal composition and sham feeding on duodenojejunal motility in humans.,” *Dig. Dis. Sci.*, vol. 37, no. 7, pp. 1009–1014, Jul. 1992.
[235] N. Qvist, E. Oster-Jørgensen, L. Rasmussen, K. Kraglund, and S. A. Pedersen, “The relationship between gallbladder dynamics and the migrating motor complex in fasting healthy subjects.,” *Scand. J. Gastroenterol.*, vol. 23, no. 5, pp. 562–566, Jun. 1988.
[236] D. Smith, B. Waldron, and F. C. Campbell, “Response of migrating motor complex to variation of fasting intraluminal content.,” *Am. J. Physiol.*, vol. 263, no. 4 Pt 1, pp. G533--7, Oct. 1992.
[237] M. J. Steward *et al.*, “Non-perforating small bowel Crohn’s disease assessed by MRI enterography: derivation and histopathological validation of an MR-based activity index.,” *Eur. J. Radiol.*, vol. 81, no. 9, pp. 2080–2088, Sep. 2012.
[238] T. Sipponen *et al.*, “Fecal calprotectin and S100A12 have low utility in prediction of small bowel Crohn’s disease detected by wireless capsule endoscopy,” *Scand. J. Gastroenterol.*, vol. 47, no. 7, pp. 778–784, Jul. 2012.
[239] C. Dobrzanski, N. Pedersen, J. Burisch, V. Voxen Hansen, H. Fuglsang, and P. Munkholm, “P643 Faecal calprotectin: correlation with the Harvey–Bradshaw Index in patients with Crohn’s disease,” *J. Crohn’s Colitis*, vol. 7, no. Supplement_1, p. S268, Feb. 2013.
[240] G. Guyatt *et al.*, “A new measure of health status for clinical trials in inflammatory bowel disease.,” *Gastroenterology*, vol. 96, no. 3, pp. 804–

10, Mar. 1989.
[241] R. M. Gollifer *et al.*, “Relationship between MRI quantified small bowel motility and abdominal symptoms in Crohn’s disease patients—a validation study,” *Br. J. Radiol.*, p. 20170914, Jun. 2018.
[242] T. A. Craney and J. G. Surles, “Model-Dependent Variance Inflation Factor Cutoff Values,” *Qual. Eng.*, vol. 14, no. 3, pp. 391–403, Mar. 2002.
[243] S. Menard, *Applied Logistic Regression Analysis: Sage University Series on Quantitative Applications in the Social Sciences. Thousand Oaks, CA: Sage.* 1995.
[244] T. Ohama *et al.*, “Intestinal inflammation downregulates smooth muscle CPI-17 through induction of TNF-α and causes motility disorders,” *Am. J. Physiol. Liver Physiol.*, vol. 292, no. 5, pp. G1429–G1438, May 2007.
[245] B. Stoffels, J. Schmidt, A. Nakao, A. Nazir, R. S. Chanthaphavong, and A. J. Bauer, “Role of interleukin 10 in murine postoperative ileus,” *Gut*, vol. 58, no. 5, pp. 648–660, May 2009.
[246] A. Menys *et al.*, “Quantified terminal ileal motility as a biomarker of Crohn’s Disease activity assessed using Magnetic Resonance Enterography: A prospective study,” in *Quantified terminal ileal motility as a biomarker of Crohn’s Disease activity assessed using Magnetic Resonance Enterography: A prospective study*, 2015, p. 1.
[247] A. A. Plumb *et al.*, “Magnetic resonance imaging-quantified small bowel motility is a sensitive marker of response to medical therapy in Crohn’s disease.,” *Aliment. Pharmacol. Ther.*, Jun. 2015.
[248] M. Simrén, O. S. Palsson, S. Heymen, A. Bajor, H. Törnblom, and W. E. Whitehead, “Fecal incontinence in irritable bowel syndrome: Prevalence and associated factors in Swedish and American patients.,” *Neurogastroenterol. Motil.*, vol. 29, no. 2, Feb. 2017.
[249] J. Bohlin, E. Dahlin, J. Dreja, B. Roth, O. Ekberg, and B. Ohlsson, “Longer colonic transit time is associated with laxative and drug use, lifestyle factors, and symptoms of constipation.,” *Acta Radiol. open*, vol. 7, no. 10, p. 2058460118807232, Sep. 2018.
[250] R. M. Gollifer *et al.*, “Automated versus subjective assessment of spatial and temporal MRI small bowel motility in Crohn’s disease,” *Clin. Radiol.*, Jul. 2019.
[251] M. Di Stefano, M. Bergonzi, E. Miceli, C. Klersy, E. Pagani, and G. R. Corazza, “In irritable bowel syndrome, postprandial abdominal distention is associated with a reduction of intestinal tone,” *Neurogastroenterol. Motil.*, vol. 29, no. 10, p. e13098, Oct. 2017.
[252] A. Accarino, F. Perez, F. Azpiroz, S. Quiroga, and J. Malagelada, “Abdominal Distention Results From Caudo-ventral Redistribution of Contents,” *Gastroenterology*, vol. 136, no. 5, pp. 1544–1551, May 2009.
[253] X.-Z. Shi, Y.-M. Lin, D. W. Powell, and S. K. Sarna, “Pathophysiology of motility dysfunction in bowel obstruction: role of stretch-induced COX-2.,” *Am. J. Physiol. Gastrointest. Liver Physiol.*, vol. 300, no. 1, pp. G99--G108, Jan. 2011.
[254] E. P. Halmos, V. A. Power, S. J. Shepherd, P. R. Gibson, and J. G. Muir, “A Diet Low in FODMAPs Reduces Symptoms of Irritable Bowel Syndrome,” *Gastroenterology*, vol. 146, no. 1, pp. 67-75.e5, Jan. 2014.
[255] C.-C. Chang, Y.-T. Lin, Y.-T. Lu, Y.-S. Liu, and J.-F. Liu, “Kiwifruit improves bowel function in patients with irritable bowel syndrome with constipation.,” *Asia Pac. J. Clin. Nutr.*, vol. 19, no. 4, pp. 451–7, 2010.
[256] A. Khalaf *et al.*, “MRI assessment of the postprandial gastrointestinal motility and peptide response in healthy humans,” *Neurogastroenterol. Motil.*, vol. 30, no. 1, 2018.

[257] B. Fischl *et al.*, “Whole Brain Segmentation: Automated Labeling of Neuroanatomical Structures in the Human Brain,” *Neuron*, vol. 33, no. 3, pp. 341–355, Jan. 2002.